UNIVERSITAT DE BARCELONA

The influence of Mediterranean riparian zones on stream nitrogen dynamics: A catchment approach

Anna Lupón i Navazo

Anna Lupon Navazo
Doctoral Thesis 2015

The influence of Mediterranean riparian zones on stream nitrogen dynamics
A catchment approach

THE INFLUENCE OF MEDITERRANEAN RIPARIAN ZONES ON STREAM NITROGEN DYNAMICS

A CATCHMENT APPROACH

Anna Lupon Navazo
Doctoral Thesis 2015

Universitat de Barcelona

Centre d'Estudis Avançats de Blanes

CSIC

TESI DOCTORAL

Universitat de Barcelona
Facultat de Biologia — Departament d'Ecologia
Programa de Doctorat en Ecologia Fonamental i Aplicada

THE INFLUENCE OF MEDITERRANEAN RIPARIAN ZONES ON STREAM NITROGEN DYNAMICS

A CATCHMENT APPROACH

La influència dels boscos de ribera mediterranis en la dinàmica del nitrogen dels rius

Una aproximació a escala de conca

Memòria presentada per Anna Lupon i Navazo
per optar al grau de doctora per la Universitat de Barcelona

ANNA LUPON i NAVAZO

Barcelona, Setembre de 2015

Vist-i-plau dels directors de la tesi:

Dra. Susana Bernal i Berenguer
Científica Associada
CEAB-CSIC

Dr. Francesc Sabater i Comas
Professor Titular
Departament Ecologia UB

A mis avis,
als meus pares,
i a tu, per llegir-me.

Temblé escuchando casi dormido
lo que el dulce río me contaba.
Yo no sé lo que dicen
los cuadros ni los libros
(no todos los cuadros ni todos los libros,
sólo algunos),
pero sé lo que dicen
todos los ríos.
Tienen el mismo idioma que yo tengo.

Fragment del poema *El Río*
Pablo Neruda (1904-1973)

AGRAÏMENTS

Són moltes les persones que, d'una manera o altra, han posat el seu granet de sorra perquè aquesta tesi fos possible. A tots ells, anomenats o no: moltíssimes gràcies!

Sens dubte, els que més han "patit" aquesta tesi són els meus directors, el Quico i la Susana. Quico, moltes gràcies per obrir-me les portes de l'ecologia, per confiar cegament en mi i per animar-me a seguir fent ciència en aquests temps difícils. Susana, són tantes coses a agrair-te! Milions de gràcies per treure hores d'on no n'hi havia, per acompanyar-me en els plors del "rejected" i "accepted", per comptar incondicionalment amb mi i, sobretot, per ser la directora més pera-punyetes però amb més passió, energia, sinceritat, coratge, seny i cor del món. Com tu, n'hi ha poques.

Infinites gràcies també a les Quico's Girls, ara repartides pel món, a qui dec molt més del que mai admetré. A la Sílvia, per ser una gran companya i una fonamental amiga. Juntes hem après, somiat i també crescut, però sobretot, hem creat records indelebles que mai passaran a l'oblit. T'enyoraré; ja t'enyoro ara. A l'Ada, per donar sempre més i més, no perdre mai l'optimisme i animar-me cada divendres amb MaximaFM. I a la Lídia, per fer trivials els obstacles del laboratori, ensenyar-me els trucs que s'amaguen darrera el Technicon & Co i escoltar pacientment els meus monòlegs rondinaires. També a les noves incorporacions, Astrid, Marta i Myrto, qui amb el temps descobriran que juntes, som un gran equip. No ho oblideu!

No em puc oblidar tampoc, de tots aquells que han viscut les penúries i entrebancs del camp amb mi. A "los del río" del CEAB, per fer de les campanyes, una festa. Marc, Miquel, Edu, Clara, Steffi i Elliot, mil gràcies! I especialment a l'Eugènia, per acollir-me al grup i fer-me sentir com si fos una "del río" més. També a la gent del CREAF, però sobretot a la Eli, per compartir infinites picades de mosquit a la parcel·la del Regàs. I finalment a la Marta, la Sara, l'Alfons i la Rosa, per ajudar-me gratuïtament en els mesos més difícils.

Al Departament, he trobat l'esperança que una millor ciència és possible; que junts, podem canviar el món. Milions de gràcies a tots per ensenyar-me que la tesi no és tan important com la happy hour, les reunions al voltant de la cafetera, les festes majors dels barris, les manifestacions revolucionàries, les pelis del Phenomena o, simplement,

l'amistat. Gràcies al Pablo (soy fan tuya, y lo sabes), al Pau (ànims!) i la de Castro (pixurriii), amb qui vaig començar el màster, i amb qui seguim compartint penes i alegries des d'aleshores. També als altres EcoRics (si més no, de cor) que s'han anat sumant al llarg del temps: Pol (infinites gràcies), Lluís, Txell, Max, Auro, Eneko, Alba, Pol 2, Txell B i Laura. I als sèniors: Catalán, Dani, Patri, Bet, Esther, Mari, Isis, Eusebi i Jaime; se us troba tant a faltar!!! Moltes gràcies per ensenyar-me que la vida segueix, apassionant, després de la tesi. També a tots els fans de les tertúlies al galliner o la peixera de FEM, però especialment al Pau, la Núria S. i la Sandra, per alegrar-me cada matí i cada vespre. I finalment, a tots aquells que lluny d'odiar-me, encara em somriuen quan crido a "Seminari".

Moltíssimes gràcies als que em van acollir amb els braços oberts a l'altra punta del món. Stefan: thank you for your generosity, your eternal patience, your optimism, and your invaluable help with the models. Cindy, Leila, and Jay: thanks for being my family in Gainesville, for staying at my side during my best and worst days, and for the best pool parties ever. I miss you guys! Thanks as well to all the other people that make me love the sunny Florida: Yuang, Stuart, Julius, Andrea, Kenny, and Mike. I want to also thank Martin Earlandson and Andrew Wade for helping me with the PERSiST model and bring me the chance to spend four great weeks at the University of Reading. Thanks as well to all the PhD students for welcoming me, but especially to Sonia and Kasia, for all the dinners, pubs, trips, and parties.

Gràcies també a tots aquells que, tot i no tenir res a veure amb la ciència, heu sofert les hores baixes de la tesi. Aquells qui, sense haver vist mai la Font del Regàs, us la sentiu vostra. Als que m'heu arrencat un somriure quan més ho necessitava. A les tuppers, que després 10 anys, segueixen al meu costat compartint riures, somnis, tristors, felicitat, records, més riures i esperances. Alba, Lucia, Mar i Núria: sou les meves prefes, la meva segona família. Als S'Agaronins, per fer-me oblidar la tesi a base d'estius a la platja, boletades pixapines i esquiades a Andorra. Als Escaladors & Co, les Uecarres de SAME i les meves princeses, per la muntanya, les birres de divendres, els sopars i les vivències viscudes. A les bruixes, per seguir lluitant pels vostres somnis arreu del món. Al grup de running "faig el que puc", per ajudar-me a fer mudances i ensenyar-me a no defallir quan el camí fa pujada. I a les que malgrat tenir abandonades, sempre (sempre) esteu allà, disposades a donar-ho tot: la Vinacua, l'Adaia i la Neus. I finalment, a totes les compis del piset de Legalitat; però sobretot a la Mar per cuidar-me, suportar-me, cuinar-me, animar-me, i ser una companya de sofà i vida incondicional. Et trobo a faltar.

Els últims agraïments, els més íntims, són per a la meva família. Als meus cosins i tiets reals i adoptius (sobretot a la Maria i al Pol), per ensenyar-me que "les coses, o es fan bé, o no es fan". Als meus avis, referents de vida i savis de paraula, de qui espero haver heretat la tossuderia (avi), la sinceritat (abuela), el sentit del humor (trucho) i la bondat (iaia). Als meus pares, per demostrar-me diàriament el seu amor sense demanar res a canvi. Al meu germà, per ser el meu pilar i agafar-me ben fort quan tot s'ensorrava. Et dec tant! I finalment al Jordi, per no deixar-me oblidar que les coses importants a la vida estan més enllà de les parets del galliner, potser en un piset modest de Calàbria.

Barcelona, 11 de Setembre 2015

He tingut el suport econòmic d'una Beca FPU del Ministerio de Educación, Cultura y Deporte (AP-2009-3711) i actualment de la prestació per desocupació. Part de la meva recerca ha estat finançada per dos projectes del Plan Nacional del Ministerio de Ciencia e Innovación: MONTES-CONSOLIDER i MED_FORESTREAM. A més, he disposat de tres beques de mobilitat de la Facultat de Biologia per assistir a congressos i de dues ajudes per estades breus, associades a la beca FPU.

INFORME DELS DIRECTORS

La Dra. Susana Bernal Berenguer, del Centre d'Estudis Avançats de Blanes (CEAB-CSIC) i el Dr. Francesc Sabater Comas, de la Universitat de Barcelona, directors de la Tesi Doctoral elaborada per la candidata Anna Lupon i Navazo, i que porta per títol "The influence of Mediterranean riparian zones on stream nitrogen dynamics: A catchment approach",

INFORMEN

Que els treballs de recerca portats a terme per Anna Lupon i Navazo com a part de la seva formació pre-doctoral i inclosos a la seva Tesi Doctoral han donat lloc a tres articles publicats, un article enviat que està en procés de revisió, i un manuscrit que està a punt de ser enviat a una revista d'àmbit internacional. A continuació, es detalla la llista d'articles, així com els índex d'impacte (segons el CSI i la ISI Web of Knowledge) de les revistes on han estat publicats o bé s'han enviat els treballs.

1. Lupon, A., F. Sabater and S. Bernal. Contribution of soil nitrogen mineralization and nitrification pulses to soil nitrogen availability in three Mediterranean forests. *European Journal of Soil Science* (en revisió).

   L' índex d'impacte de la revista *European Journal of Soil Science* l'any 2014 va ser de 2.649. Aquesta revista està situada en el primer quartil de la categoria "Soil Science". Aquesta categoria té una mediana d'índex d'impacte de 1.462 i inclou un total de 34 revistes. Tenint en compte l'índex d'impacte d' *European Journal of Soil Science*, aquesta revista ocupa el 7è lloc de la seva categoria.

2. Lupon, A., S. Gerber, F.Sabater and S. Bernal. 2015. Climate response of the soil nitrogen cycle in three forest types of a headwater Mediterranean catchment. *Journal of Geophysical Research – Biogeosciences*, 120: 859-875.

   L'índex d'impacte de la revista *Journal of Geophysical Research – Biogeosciences* l'any 2014 va ser de 3.426. Aquesta revista està situada en el primer quartil de la categoria "Geosciences/Multidisciplinary". Aquesta categoria té una mediana d'índex d'impacte de 1.605 i inclou un total de 175 revistes. Tenint en compte l'índex

d'impacte de *Journal of Geophysical Research – Biogeosciences*, aquesta revista ocupa el 19è lloc de la seva categoria.

3. Lupon, A., E. Martí, F. Sabater and S. Bernal. 2015. Green light: Gross primary production influences seasonal stream nitrogen exports by controlling fine-scale nitrogen dynamics, *Ecology* (in press).

   L'índex d'impacte de la revista *Ecology* l'any 2014 va ser de 5.000. Aquesta revista està situada en el primer quartil de la categoria "Ecology". Aquesta categoria té una mediana d'índex d'impacte de 1.844 i inclou un total de 144 revistes. Tenint en compte l'índex d'impacte de *Ecology*, aquesta revista ocupa el 17è lloc de la seva categoria.

4. Bernal, S., A. Lupon, M. Ribot, F. Sabater and E. Martí. 2015. Riparian and in-stream controls on nutrient concentrations and fluxes in a headwater forested stream. *Biogeosciences* 12:1941–1954.

   L'índex d'impacte de la revista *Biogeosciences* l'any 2014 va ser de 3.978. Aquesta revista està situada en el primer quartil de la categoria "Geosciences/Multidisciplinary". Aquesta categoria té una mediana d'índex d'impacte de 1.605 i inclou un total de 175 revistes. Tenint en compte l'índex d'impacte de *Biogeosciences*, aquesta revista ocupa el 10è lloc de la seva categoria.

Alhora CERTIFIQUEN

Que la Srta. Anna Lupon i Navazo ha participat activament en el desenvolupament del treball de recerca associat a cadascun d'aquests articles, així com en la seva elaboració. En concret, la seva participació en cadascun dels articles ha estat la següent:

- Participació en el plantejament inicial dels objectius de cadascun dels capítols, els quals estaven emmarcats en dos projectes del Plan Nacional del Ministerio de Ciencia e Innovación (MONTES-CONSOLIDER i MED_FORESTREAM).

- Participació en el disseny i desenvolupament de la part experimental de cada estudi, i posada a punt de les metodologies de camp i de laboratori associades a cadascun dels experiments.

- Processat i anàlisi de totes les mostres obtingudes, càlcul de resultats, anàlisi de dades i realització de models matemàtics de tots els capítols (exceptuant el setè, on va processar totes les mostres, però només va col·laborar en el anàlisis de dades). Part d'aquesta tasca va comportar dues estades al Soil and Water Department de la University of Florida amb el grup del Dr. Stefan Gerber, per l'aprenentatge de la parametrització i avaluació dels models basats en processos empírics.

- Redacció dels articles i seguiment del procés de revisió de tots els capítols (exceptuant el setè, en el qual va tenir una col·laboració activa).

Finalment, certifiquem que cap dels coautors dels articles abans esmentats i que formen part de la Tesi Doctoral de la Srta. Anna Lupon i Navazo han utilitzat, ni tenen previst utilitzar, implícita o explícitament aquests treballs per a l'elaboració d'una altra Tesi Doctoral.

Barcelona, 9 de setembre de 2015

Dra. Susana Bernal i Berenguer
Científica Associada
CEAB-CSIC

Dr. Francesc Sabater i Comas
Professor Titular
Departament Ecologia UB

ABSTRACT

During last decade, anthropogenic activities have doubled the available nitrogen (N) in catchments, leading to several environmental problems such as eutrophication, toxicity, or reduced biodiversity. Within catchments, riparian areas are recognized to be natural filters of N because they can substantially diminish the delivery of this essential nutrient from terrestrial to aquatic ecosystems. However, understanding the influence of riparian zones on regulating N export from catchments still remains a challenge, mainly because stream water chemistry integrates biogeochemical processes co-occurring within upland, riparian, and fluvial ecosystems. The present dissertation aims to explore the influence of Mediterranean riparian zones on regulating both stream hydrology and catchment N exports by combining empirical and modelling approaches at different temporal and spatial scales.

The findings obtained from plot experiments show that the studied Mediterranean riparian soils acted as hot spots of soil microbial N supply within the catchment because riparian soils exhibited higher net N mineralization (NNM) and net nitrification (NN) rates than upland oak and beech soils (NNM = 1.3 vs. 0.4 mg N kg^{-1} d^{-1}; NN = 1.2 vs. 0.1 mg N kg^{-1} d^{-1}). We attributed this difference between forest soils to larger stocks of N-rich leaf litter and permanent moist conditions in the riparian soils. Furthermore, soil microbial processes in the riparian site showed a distinct climatic sensitivity than in upland sites, which ultimately led to different temporal patterns of soil N cycling. Soil moisture was the major driver of NNM and NN in upland forests, while both temperature and precipitation shaped soil N dynamics in the riparian forest. Therefore, both upland and riparian soils exhibited pulses of NNM and NN following spring rewetting events, though summer temperatures only stimulate microbial activity at the riparian site. Riparian microbial pulses contributed > 25% to annual rates of riparian NNM and NN; and coincided with increases in stream N loads. Together, these results suggest that Mediterranean riparian soils may become important sources of nitrate (NO_3^-) to streams under future warming scenarios.

Additionally, the findings obtained from catchment-scale studies show that Mediterranean riparian zones can exert a strong control on stream hydrology during the vegetative period. In the studied catchment, riparian evapotranspiration (ET) influenced the temporal pattern of stream discharge and riparian groundwater elevation across daily and seasonal scales. Moreover, the influence of riparian ET on stream hydrology increased

from headwaters to the valley bottom, where stream hydrological retention was prominent in summer. Stream hydrological retention was accompanied by increases rather than by decreases in stream N export from the catchment, likely because low flow conditions, relatively warm conditions, and large stocks of N-rich leaf litter within the streambed enhanced in-stream NO_3^- release. Conversely, in-stream photoautotrophic NO_3^- uptake was the major controlling factor of diel patterns of stream N concentration in spring, when high light inputs favored gross primary productivity (GPP) prior to riparian canopy closure. As it occurred for summer nitrification, the influence of GPP on stream N dynamics increased along the stream continuum. At the valley bottom, in-stream photoautotrophic activity drop midday stream NO_3^- concentration by 13% and reduced catchment spring NO_3^- exports by 10%. Finally, we found no clear evidence of either NO_3^- uptake or release within the riparian zone during the dormant period. Mass balance calculations at the whole-reach scale showed that both in-stream processes and riparian groundwater inputs contributed to longitudinal changes in stream NO_3^- concentrations, and thus, both sources of variation were necessary to understand stream water chemistry along the stream. Together, these results suggest that the high bioreactivity of streams ecosystems can influence stream N dynamics at the catchment scale, and even screen the potential buffer capacity of riparian zones as observed for this Mediterranean catchment.

Overall, findings gathered in the present dissertation question the well-established idea that riparian zones are efficient N buffers, at least for Mediterranean regions, and stress that an integrated view of upland, riparian, and stream ecosystems is essential for advancing our understanding of catchment hydrology and biogeochemistry.

RESUM

Durant l'última dècada, les activitats antropogèniques han doblat el nitrogen (N) disponible als ecosistemes terrestres, provocant nombrosos problemes ambientals tals com l'eutrofització dels rius, la toxicitat de l'aigua o la reducció de la biodiversitat. En aquest context, un gran nombre d'estudis han conclòs que les zones de ribera tenen la capacitat de reduir els excessos de N que els hi arriben dels ecosistemes adjacents i, per tant, poden jugar un paper fonamental en la regulació de la concentració de N al riu i l'exportació d'aquest nutrient aigües avall. Tanmateix, entendre la influència de les zones de ribera sobre les exportacions de N de les conques encara suposa un gran repte, ja que l'aigua del riu integra tots els processos biogeoquímics que ocorren als ecosistemes forestals, a la zona de ribera i als ecosistemes fluvials. L'objectiu d'aquesta tesi és explorar la influència de les zones de ribera mediterrànies sobre els recursos hídrics i la dinàmica del N a escala de conca, mitjançant la combinació d'aproximacions empíriques i models matemàtics a diferents escales temporals i espacials.

Els resultats obtinguts a escala de parcel·la indiquen que els sòls de ribera poden ser punts calents d'activitat microbiana dintre de les conques, perquè el bosc de ribera estudiat exhibí unes taxes de mineralització neta del N (MNN) i nitrificació neta (NN) considerablement més altes que els sòls dels boscos de capçalera (alzinars i fagedes) (MNN = 1.3 vs. 0.4 mg N kg^{-1} d^{-1}; NN = 1.2 vs. 0.1 mg N kg^{-1} d^{-1}). Aquesta gran diferència en l'activitat microbiana fou atribuïda als estocs de fullaraca dipositats sobre els sòls riparians, així com a les permanents condicions d'humitat que caracteritzen aquests ecosistemes. A més, els processos microbians mostraren una sensitivitat climàtica diferent pels boscos de ribera i pels ubicats a la capçalera de la conca, resultant en una diferent dinàmica temporal del cicle del N al sòl. Així, la humitat del sòl fou el factor determinant dels patrons temporals de MNN i NN en els boscos de capçalera, mentre la temperatura i la precipitació controlaren les dinàmiques de N en el sòl de ribera. Conseqüentment, tant els sòls de boscos de capçalera com els de ribera exhibiren pics d'activitat microbiana durant les pluges de primavera, mentre que la calor pròpia de l'estiu només estimulà la MNN i NN en els sòls de ribera. Als sòls de ribera, els pics d'activitat microbiana contribuïren > 20% a les taxes anuals de MNN i NN; coincidint amb períodes d'elevada càrrega de N al riu. Aquests resultats suggereixen que la disponibilitat i exportació de nitrat (NO_3^-) des dels sòls de ribera podria incrementar en el futur en les regions mediterrànies com a conseqüència de l'escalfament global.

D'altra banda, els resultats obtinguts a escala de conca mostren que les zones de ribera poden controlar de forma significativa els recursos hídrics en conques mediterrànies durant el període vegetatiu. Per exemple, en la conca estudiada, l'evapotranspiració (ET) de ribera influencià la dinàmica temporal del cabal fluvial, així com del nivell freàtic de ribera, tant a escala diària com estacional. A més, la influència de la ET de ribera sobre els recursos hídrics i la retenció hidràulica incrementaren al llarg del curs fluvial, sent més prominents en el fons de vall durant els mesos d'estiu. L'increment en la retenció hidràulica fou acompanyat per un increment en les concentracions de N del riu, segurament a conseqüència del poc cabal fluvial, les altes temperatures i els estocs de fullaraca dipositats sobre la llera del riu, els quals podrien afavorir la mineralització i nitrificació dintre el canal fluvial. En canvi, l'activitat fotoautotròfica dins del riu fou el principal factor responsable de les variacions diàries de la concentració de N al riu durant la primavera, quan l'entrada de llum afavorí la producció primària bruta (PPB). De la mateixa manera que succeí per la nitrificació, la influència de la PPB sobre la dinàmica del N incrementà al llarg del curs fluvial. Així doncs, l'activitat fotosintètica disminuí un 13% la concentració de NO_3^- de l'aigua del riu al migdia, i reduí un 10% les exportacions de NO_3^- aigües avall durant la primavera. Finalment, els resultats obtinguts pel període no vegetatiu no ens van permetre determinar de forma clara si l'activitat biogeoquímica dins la ribera pot donar lloc a canvis en la concentració de N del riu. El balanç de masses a escala de tram fluvial, revelà que tant les aportacions d'aigua del freàtic de ribera, com els processos que ocorren dins del riu, contribueixen als canvis longitudinals en les concentracions de NO_3^- al llarg del curs fluvial. Per tant, totes dues fonts de N són necessàries per entendre la dinàmica d'aquest nutrient a escala de conca. Conjuntament, aquests resultats suggereixen que l'alta bio-reactivitat dels rius pot influir substancialment la dinàmica del N a escala de conca, i fins i tot emmascarar la capacitat dels boscos de ribera per filtrar els nutrients que els hi arriben.

Els resultats d'aquesta tesi qüestionen doncs la idea que les zones de ribera són filtres naturals de N en zones mediterrànies, i posen de manifest la importància d'una visió integrada del funcionament dels boscos de capçalera, la zona de ribera i els sistemes fluvials per tal d'avançar en el nostre coneixement sobre la hidrologia i la biogeoquímica a escala de conca.

CONTENTS

LIST OF FIGURES

LIST OF TABLES

PART I

CHAPTER 1

General Introduction and Objectives

Riparian zones, those transitional areas between terrestrial and aquatic ecosystems, are responsible for > 25% of the terrestrial ecosystem services, functioning as biological corridors and natural filters for pollutants, pathogens, organic matter, and nutrients (especially nitrogen) arriving from adjacent terrestrial ecosystems. However, and despite the wide body of studies performed at plot scale, our understanding of the potential and limitation of riparian ecosystems as drivers of water and nutrient fluxes at catchment scale is still limited. This dissertation aims to contribute to fill this gap of knowledge by exploring the influence of Mediterranean riparian zones on stream hydrology and stream nitrogen dynamics at catchment scale.

In this first chapter, a brief introduction to riparian zones is provided, placing riparian systems in a broader context within catchment hydrology and nitrogen biogeochemistry. Furthermore, this chapter includes the overarching aim of the present dissertation, as well as the specific objectives of each of the following chapters.

1.1 RIPARIAN ZONES

Riparian zones are those ecosystems lying at the border of stream channels, and they constitute a unique ecotone between terrestrial and aquatic environments. As true boundaries, riparian areas usually extend from the edges of aquatic ecosystems to the edges of upland terraces, and therefore, they often exhibit strong vertical and horizontal gradients of temperature and humidity (Naiman et al. 2005, Sabater et al. 2013). These pronounced environmental gradients enable an extremely high biodiversity, as well as the establishment of unique plant communities that cannot inhabit elsewhere in the catchment (Sabater and Bernal 2011).

Although riparian ecosystems represent only 1.4% of the world surface land area, they are responsible for > 25% of the terrestrial ecosystem services as a whole, being essential for human and wildlife welfare (Tockner and Stanford 2002). Indeed, riparian zones are among the most productive ecosystems of the world, and they act as biological corridors by providing shelter for diverse animal species and favoring seed dispersion along the longitudinal axis (Sabater and Bernal 2011). Moreover, in water limited regions, riparian zones are critical habitats for fauna because they provide essential resources that lack in the dry surrounding upland areas (Sabater and Bernal 2011).

Riparian areas can regulate energy and elemental fluxes between terrestrial and aquatic environments, playing a fundamental role in keeping healthy the adjacent fluvial ecosystems. First, riparian tree canopy buffers stream temperature and light inputs by shading the stream channel, which is particularly important for regulating stream primary productivity and for ensuring the survival of some fish species (Hill and Dimick 2002, Sabater and Bernal 2011). Second, riparian tree roots and large woody debris accumulated in streamside areas dissipate the energy associated with floods by stabilizing stream banks, and by lowering down water and sediment inputs from uplands (McGlynn and Seibert 2003, Naiman et al. 2005). Third, riparian forests supply large amounts of high quality leaf litter and coarse woody debris to stream ecosystems, which diversifies stream habitats, enhances hydrological retention, and ultimately increases in-stream nutrient retention and stream productivity (Dobson et al. 2004, Mineau et al. 2011). Finally, riparian zones influence stream chemistry because they can effectively remove (i) pollutants by enhancing sediment filtration and (ii) excessive nutrients, especially nitrogen (N), by favoring biological assimilation (Hill 1996, Vidon et al. 2010). Despite the impressive body of knowledge highlighting the potential of riparian zones as biodiversity reservoirs and natural filters of water, these ecosystems

are still not in the spotlight of the European Water Framework Directive (WFD) (200/960/EC). Therefore, riparian zones can be extremely vulnerable to anthropogenic impacts and climate change if these ecosystems are not integrated in landscape management strategies ensuring their good status in the future.

Riparian areas can be found under a wide range of climatic, hydrologic, and ecological environments; including high elevation montane forests, intermediate elevation woodlands, low elevation shrublands, and desert grasslands. Hence, the vegetation community constituting riparian zones can vary widely among biomes, as well as along the stream network (Naiman et al. 2005, Sabater et al. 2013) (Figure 1.1).

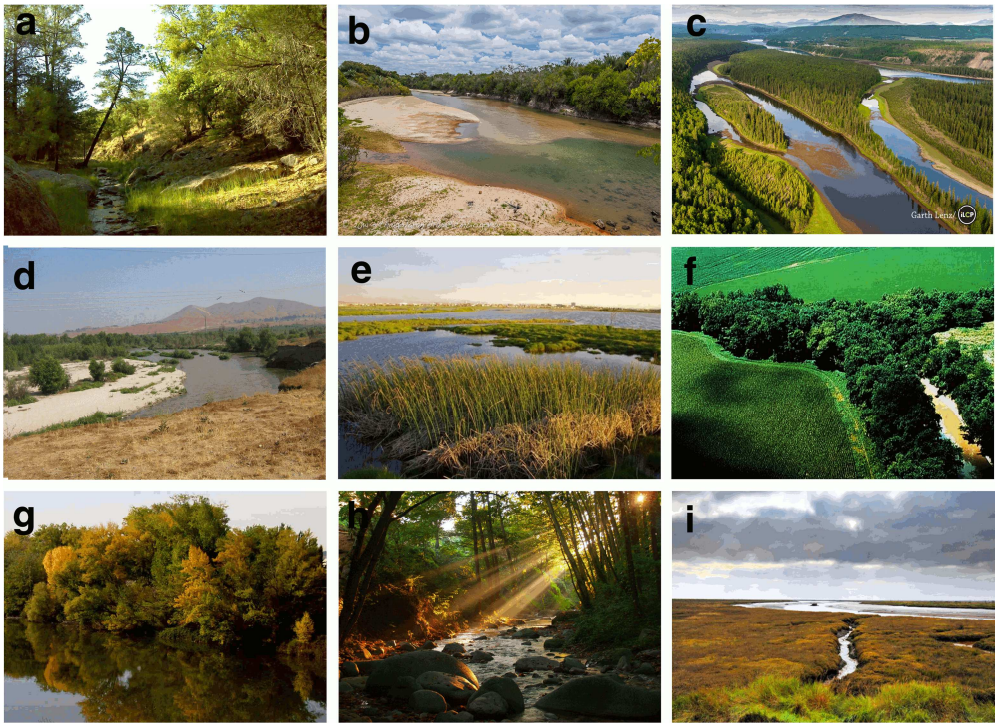

Figure 1.1 Photographs of riparian zones worldwide; (a) alpine riparian forest of Cave Creek, NY, USA (public domain), (b) riparian woodland along the Cauamé River, Brasil (author: Thiago Orsi), (c) dense riparian forest along Peace River, Canada (author: Garth Lenz) (d) desert grassland along Santa Ana river, CA, USA (public domain), (e) natural wetland in Cape Town, South Africa (author: Abu Shawka), (f) riparian gallery along a Lake Erie tributary, OH, USA (public domain), (g) riparian deciduous woodland in Pisuerga river, Spain (author: Guillermo Martínez), (h) montane riparian forest in Montseny, Spain (author: Francesc Nogueres) and (i) riparian grassland in Wallasea Island, UK (author: Timon Singh).

In mountainous environments, such as the one studied in this dissertation, riparian zones are generally poorly developed in steep and constrained headwater streams (orders 1-2), being often constituted by narrow strips (< 5 m) of alders, cottonwoods, and willows adjacent to the channel (Dimopoulos and Zogaris 2008, Sabater et al. 2013). In mid-order steams (orders 3-5), with flatter topography and wider streams, riparian zones became larger (10-100 m). Further, the riparian vegetation is more diverse, with distinct bands determined by lateral variations in topography, water availability, and soil type (Naiman et al. 2005). Typically, a narrow band of phreatophyll species (alder, cottonwood and willow) overlies on alluvial deposits near the stream, while ashes and poplars dominated in places where the groundwater table is far from the surface and soils are consolidated (Tabacchi et al. 1998, Dimopoulos and Zogaris 2008). Finally, in the lowest part of the river network (orders > 5), riparian zones are characterized by extensive (> 100 m wide) and geomorphically complex floodplains, with different vegetation communities in areas near the stream (alder, cottonwood and willow) and faraway (ash, elm and even oak) (Naiman and Décamps 1997, Dimopoulos and Zogaris 2008, Sabater et al. 2013).

These longitudinal gradients in riparian size, topography, and vegetation communities can influence stream structure, chemistry, and functioning along the longitudinal axis. The River Continuum Concept (Vannote et al. 1980), a theoretical framework based on perspectives from fluvial geomorphology, already postulated the potential influence of riparian ecosystems on regulating stream functioning along the stream network, though it did not deepen into the potential mechanisms involved. Later on, other studies have suggested that the interaction between catchment hydrology and riparian biological processes can have a strong influence on the amount and fate of nutrients, sediments and pollutants entering to streams (Covino and McGlynn 2007, Jencso et al. 2009, Burt et al. 2010). Therefore, a more integrated view of riparian zones within catchments and along the stream continuum could be essential for advancing our understanding of the potential and limitations of these ecosystems as drivers of catchment and stream biogeochemistry. This perspective may be especially important for Mediterranean and other regions with some degree of water limitation, for which riparian ecosystems could play a disproportionally large influence on catchment hydrology and biogeochemistry.

1.2 HYDROLOGICAL LINKAGES IN RIPARIAN ZONES

Water can arrive to riparian zones by different flow paths, including direct rainfall (after excluding interception) and inflows from adjacent uplands and aquatic ecosystems (Figure 1.2) (Pinay et al. 2000, Tabacchi et al. 2000, Burt et al. 2002). Water inputs from uplands flow laterally and longitudinally across riparian zones, and drain into streams via quick surface flow paths during storms and through more slow moving water pools, such as unsaturated subsurface soil and groundwater (Pinay et al. 2000, Tabacchi et al. 2000). In turn, stream water can enter to the riparian zone via overbank flow during floods, or else, through subsurface zones, which promotes hydrological retention, i.e., the transitory storage of water within the stream-riparian interface (Dent et al. 2007, Covino et al. 2010). During the vegetative period, stream water, soil water, and groundwater can be intercepted by riparian tree roots, and arrive to the atmosphere via evapotranspiration (Scott et al. 2008, Brooks et al. 2009).

The relative magnitude of these water flow paths vary widely depending on the climatic regime. As such, the influence of riparian tree evapotranspiration on groundwater table

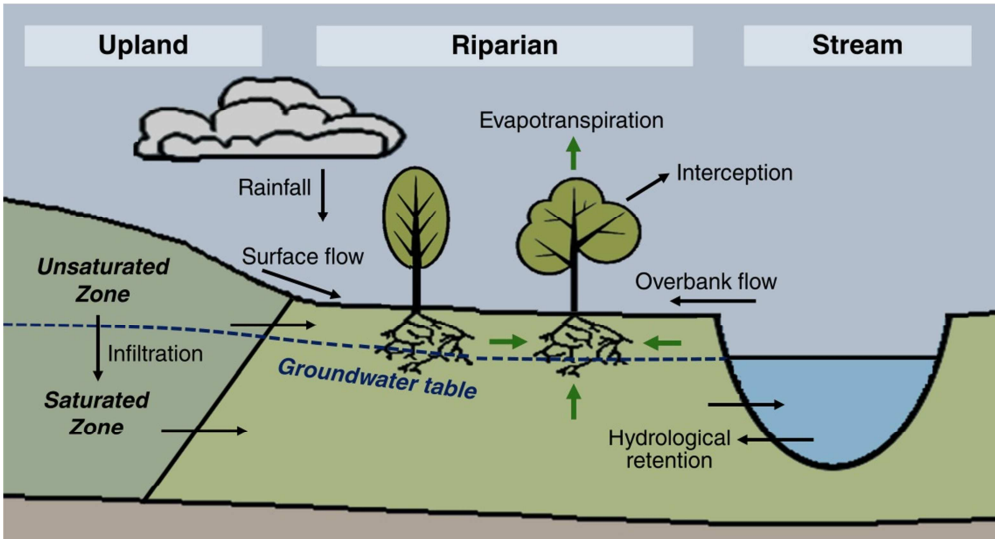

Figure 1.2 Conceptual model of input and output water fluxes to and from the riparian compartment. Hydrological inputs are rainfall, inflow from upland systems (via surface, unsaturated subsurface and groundwater flow paths) and inflow from the stream via hydrological retention and overbank flow. Hydrological outputs from the riparian compartment are riparian tree evapotranspiration from both unsaturated and saturated zones (green arrows), and groundwater inputs to the stream.

elevation and soil moisture content differs greatly between temperate and more water limited regions (Burt et al. 2002, Vidon and Hill 2004a). In temperate systems, riparian soils are generally close to saturation because elevated groundwater tables maintain waterlogged conditions despite the impressive evapotranspiration rates achieved by riparian vegetation (up to 4.5 mm d^{-1}) (Tabacchi et al. 2000). Nevertheless, strong declines in groundwater level associated with riparian tree evapotranspiration have been reported, which can decrease groundwater inputs to the receiving streams by 30-80% (Schilling 2007, Kellogg et al. 2008).

The effect of water demand by riparian trees on riparian and stream hydrology is especially noticeable in water limited regions. For instance, Dahm et al. (2002) showed that riparian evapotranspiration can be a massive component of catchment water budgets, accounting for 20-35% of the annual water budget in a lowland floodplain in New Mexico, USA. In its turn, the summer peak of riparian evapotranspiration promoted the abrupt decline of the groundwater table (54 cm in few days) in a Mediterranean headwater catchment, which led to premature abscission of riparian tree leafs (Bernal et al. 2003, Sabater and Bernal 2011) and to sustained hydrological retention until the complete desiccation of the stream channel (Butturini et al. 2003).

Together, these studies suggest that riparian evapotranspiration can influence the exchange of water between uplands and fluvial ecosystems. Therefore, hydrological processes at the upland-riparian-stream interface can be critical to understand the temporal pattern of stream discharge, especially in mid-order streams (orders 3-5) (Kellogg et al. 2008) and lowland rivers (orders > 5) (Dahm et al. 2002, Scott et al. 2008). However, the interactions between riparian evapotranspiration, groundwater dynamics, and stream hydrological retention still remain largely unknown for hydrologists. As a result, the riparian compartment is not considered in most of the up-to-date catchment hydrological models (but see Medici et al. 2008, Futter et al. 2013).

1.3 NITROGEN TRANSFORMATIONS IN RIPARIAN ZONES

Since the 80s, riparian buffer strips have been considered as an economically and environmentally efficient tool for protecting freshwaters from diffuse N pollution originated in farm and agricultural lands. The use of riparian buffer strips as a restoration strategy may likely grow in the future, given that chronic N fertilization is becoming a widespread environmental issue, leading to problems of eutrophication, acidification, water toxicity and biodiversity declines (Galloway et al. 2004, Dise 2009). Moreover,

environmental issues derived from N excesses may likely be intensified in the future, because increased warming and dryness would probably reduce water availability, as well as the dilution capacity of fluvial ecosystems (Martí et al. 2010, Cooper et al. 2013).

Several biogeochemical processes are responsible for the transformation and retention of N in riparian zones. Dissolved inorganic nitrogen (DIN) arriving from uplands to the riparian zone can be transitorily or permanently removed from the system via denitrification and biological uptake (Figure 1.3). Microbial denitrification, i.e., the transformation of nitrate (NO_3^-) to nitrogen gas (N_2), is a permanent sink for N (Pinay et al. 2000, Vidon et al. 2010). In turn, riparian vegetation and soil microbes can uptake large amounts of ammonium (NH_4^+) and NO_3^- from groundwater, especially when upland water flows through the organic soil layers and the rhizosphere (Clément et al. 2003, Mayer et al. 2007). However, biological assimilatory uptake by plants and microbes only provides a transitory storage of N because a fraction of the assimilated N may return to the soil in the form of leaf litter and exudates, becoming part of the soil organic matter pool (SOM) (Dosskey et al. 2010). The high quality of leaf litter and root exudates from riparian trees, and especially from N_2-fixing species, can enhance microbial N mineralization and nitrification, i.e., the transformation of NH_4^+ to NO_3^-, and thus, increase NO_3^- storage in riparian surface soils (Helfield and Naiman 2002). A fraction of this NO_3^- pool can undergo biogeochemical cycling, while another fraction may be infiltrated to groundwater (Pinay et al. 1998) or leached towards the stream via surface and subsurface flows (Butturini et al. 2003, Harms and Grimm 2010).

Noteworthy, the biogeochemical processes involved in the soil N cycle depend primarily on moisture conditions (Hefting et al. 2004). SOM can be mineralized to NH_4^+ under either oxic or anoxic conditions, nitrification can only occur in aerated soils (water filled pore space (WFPS) < 80%), and both denitrification and dissimilatory nitrate reduction require saturated soils (WFPS > 60%) (Linn and Doran 1984). Therefore, the soil moisture regime and water table elevation controls to a great extent the end products of the soil N cycling in riparian zones, and ultimately, their buffer capacity. For instance, denitrification has been identified as the primary mechanism for groundwater NO_3^- removal (> 90%) in regions with elevated riparian groundwater tables such in North Europe and North America (Vidon and Hill 2004b, Pinay et al. 2007). In water limited regions, however, soil dryness and deep groundwater tables limits denitrification but encourages nitrification, and, as a result, NO_3^- tends to accumulate in the soil pool (Hefting et al. 2004, Bernal et al. 2007, Harms et al. 2009). Therefore, the N buffer capacity of riparian zones in these regions mostly relies on assimilatory N uptake by plants and microbes (Butturini et al. 2003, Jacobs et al. 2007). Assimilatory N uptake can be especially relevant during periods of stream hydrological

retention, because the transitorily retention of water in the stream-riparian interface enhances nutrient and organic carbon exchange between these two ecosystems, and increases the residence time of water in the hyporheic and rhizosphere environments (Martí et al. 2000, Schade et al. 2002, 2005).

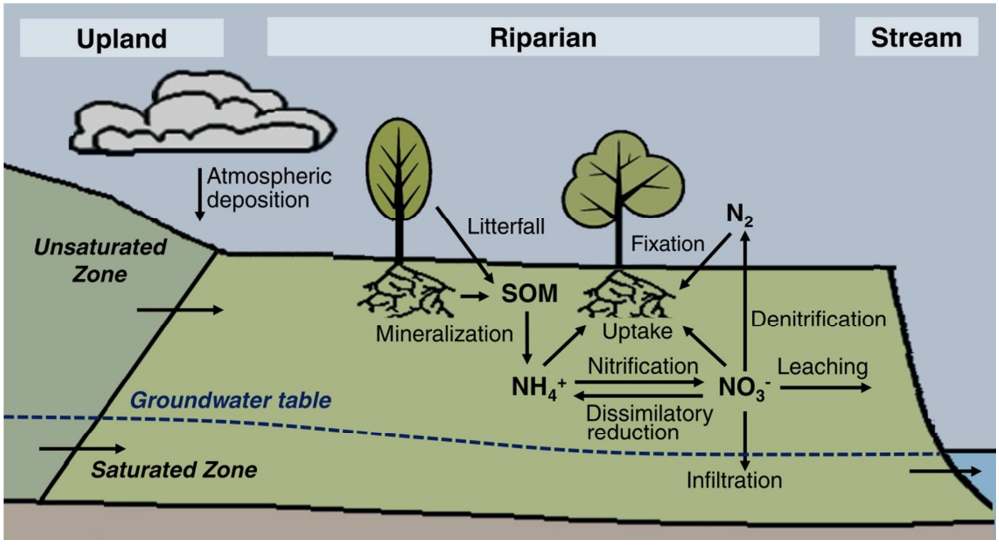

Figure 1.3 Cycle of nitrogen (N) in the riparian surface soil. Inorganic N enters to the soil pool via lateral inputs from upland sources, atmospheric deposition, N_2 fixation and N mineralization of soil organic matter (SOM). The SOM pool depends mainly on litterfall inputs. The proportion of ammonium (NH_4^+) and nitrate (NO_3^-) in the soil depends on nitrification and dissimilatory nitrate reduction. Outputs of dissolved inorganic nitrogen (DIN) from the surface soil layer assimilatory uptake by biota, infiltration to groundwater, leaching towards the stream, and denitrification (the latter, only for nitrate).

Previous studies highlight that riparian zones often exhibit disproportionately high reaction rates relative to the surrounding areas, and thus, they can be considered *hot spots* of N cycling at catchment scale (McClain et al. 2003, Pinay et al. 2015). However, the capability of these hot spots to modify stream N dynamics is still not well understood. For instance, Gold et al. (2001) found that alluvial deposits acted as hot spots for denitrification in a forested riparian zone of Rhode Island, but that their contribution to NO_3^- removal at the landscape scale was minimal despite denitrification rates were locally high. Dent et al. (2007) showed that the capacity of riparian zones to remove N from an arid stream in Arizona varied strongly (from 7-67%) depending on the volume of stream water that was lost toward the riparian zone, and on the degree of interaction between the two water bodies. Therefore, extrapolating the N buffering capacity found in riparian plots to larger scales can be extremely difficult, limiting our

ability for an integrated conservation and management of ecosystems within landscapes (Strayer et al. 2003, Pinay et al. 2015).

In addition, the delivery of DIN from upland forests as well as the soil moisture conditions prevailing in riparian zones can vary highly over time (Butturini et al. 2003, Bernal et al. 2007). As a result, N biogeochemistry in riparian zones can also be 'hot' in the temporal dimension, which implies that the impact of these ecosystems on catchment N exports may be restricted to specific time windows during the year (Burt et al. 2010, Vidon et al. 2010). *Hot moments*, or periods during which biogeochemical processes are enhanced (*sensu* McClain et al. 2003), are common in regions experiencing some degree of water limitation. In arid riparian zones, for instance, severe drought periods followed by intense rainfall events fuels soil microbial mineralization, immobilization and denitrification (Jacobs et al. 2007, Harms and Grimm 2008). However, some authors have suggested that the alleviation of water limitation is a necessary but not always sufficient condition for N transformation in arid riparian soils (Harms and Grimm 2008, Borken and Matzner 2009). Hence, our understanding of the microbial pulse behavior still remains far from complete (Borken and Matzner 2009). Furthermore, little is known about whether hot moments of microbial activity could affect nutrient budgets and exports at relevant time scales.

1.4 RIPARIAN ZONES AND CATCHMENT NITROGEN EXPORTS

Traditionally, most of the studies analyzing patterns of catchment N export have assumed that the assimilation and transformation of N occurs primarily in upland ecosystems, and, consequently, that stream N concentrations quantitatively reflect upland processes with minimal influence of the N cycling in riparian and stream ecosystems (Hedin et al. 1995, Goodale and Aber 2001, Brookshire et al. 2011). Conversely, recent stream monitoring programs have shown that, despite terrestrial systems strongly determine catchment N exports, spatial and temporal variations in stream N exports can be, at least partially, attributed to changes in riparian vegetation community, riparian hydrology, and/or riparian biogeochemistry. For instance, shifts in dominant riparian tree species (red alder vs. conifer) drove the spatial pattern of stream N concentration in the Salmon basin (Oregon, USA) (Compton et al. 2003). Moreover, net nitrification in riparian soils has been identified as a key factor for explaining stream NO_3^- concentrations and fluxes in both semiarid Mediterranean and temperate headwater catchments (Medici et al. 2010, Ross et al. 2012, Duncan et al. 2015).

Recently, some authors have reported that the capability of riparian zones to regulate catchment nutrient export increases downstream, favored by a decrease in the upland-riparian hydrological connectivity (McGlynn and McDonnell 2003, Jencso et al. 2009, Pacific et al. 2010) as well as by increases in stream hydrological retention (Montreuil et al. 2010, Covino et al. 2010, Bernal and Sabater 2012). Nonetheless, results are not consistent among different studies (Pattison et al. 1998, Pinay et al. 1998, Finlay et al. 2011), suggesting that the potential influence of riparian processes on stream nutrient dynamics at the catchment scale cannot be assessed independently from upland and in-stream processes. In fact, both streams and rivers have a strong capacity to transform and retain N inputs from terrestrial systems at both reach (Peterson et al. 2001, Ensign and Doyle 2006, Mulholland et al. 2008b) and catchment scales (Bernhardt et al. 2005, Alexander et al. 2007, Bernal et al. 2012a), and thus, N cycling within riparian and stream ecosystems may certainly contribute to catchment N exports.

Ultimately, processes occurring in upland, riparian, and stream zones mutually influence each other as a result of the intimate hydrological links between them. Upland ecosystems regulate the amount of water and DIN entering to riparian zones. Hence, these ecosystems play a pivotal role in determining the capability of riparian zones to change N exports from catchments (Vidon et al. 2010, Montreuil et al. 2011). In turn, riparian zones influence in-stream N cycling by modifying the amount and form of N entering to streams, as well as by regulating light and organic matter inputs along the stream network (Hill 1996, Pinay et al. 2000). Finally, streams may influence the N removal at the stream-riparian interface during periods of stream hydrological retention by supplying DIN and carbon to riparian vegetation and microbial population (Martí et al. 2000, Dent et al. 2007).

Overall, these interactions highlight the need of investigating riparian zones within a wider context, integrating the upland-riparian-stream continuum (Bormann and Likens 1967). However, and paradoxically, most catchment studies focused exclusively on upland ecosystems (Goodale et al. 2009, Brookshire et al. 2011), while studies assessing in-stream nutrient cycling do not consider the interaction between the stream and riparian groundwater (Roberts and Mulholland 2007, von Schiller et al. 2011). Aforementioned sort of simplifications are helpful for understanding the main patterns and drivers of complex systems such forest, riparian, and stream ecosystems. Nonetheless, we believe that integrating the different "slices" into the "whole pie" is a must if we are to understand the capacity of riparian ecosystems on shaping N dynamics at ecological relevant scales. This is a true challenge and, at the same time, an essential exercise, in order to advance catchment biogeochemistry and develop integrated management strategies that successfully mitigate future increments in anthropogenic N inputs.

1.5 DISSERTATION OBJECTIVES

The overarching goal of the present dissertation is to explore the potential role of riparian zones on regulating stream hydrology and stream N dynamics in headwater Mediterranean catchments. In particular, we aim (i) to understand the underlying mechanisms by which Mediterranean riparian forests control catchment N exports and (ii) to distinguish riparian processes from those occurring in other parts of the catchment, i.e., upland and in-stream processes.

The suite of studies included in this dissertation are articulated in two parts (*Part II* and *Part III*), each one addressing one of the two main objectives mentioned above. The chapters included within each part are written as independent publications and all of them explore to some extend the relation between riparian processes and stream N dynamics, though at different spatial and temporal scales.

The *Part II* of this dissertation aims to compare patterns and controls of the soil N cycle between riparian zones and upland forests in order to understand the potential effect of these two catchment pools on catchment N exports. The two chapters included in this part were designed from a terrestrial perspective, and they include both empirical (Chapter 3) and modelling (Chapter 4) approaches. Specifically:

In Chapter 3, we investigated (i) differences in the magnitude and in the temporal pattern of soil net N mineralization (NNM) and net nitrification (NN) between riparian and upland soils, (ii) the contribution of pulses of NNM and NN to annual rates, and (iii) the influence of NN in riparian and upland soils on soil NO_3^- availability, soil NO_3^- concentrations, and stream NO_3^- exports from the catchment.

In Chapter 4, we used a simple process based model to explore (i) the differential climatic sensitivity of the soil N cycle in riparian and upland soils, and (ii) the implications of such different response for future climate scenarios.

The *Part III* of this dissertation aims to elucidate the mechanisms by which Mediterranean riparian forests regulate stream N dynamics, and to distinguish riparian processes from in-stream processes. This part is articulated in three chapters conducted at the catchment scale, which explore changes in stream N concentrations and N fluxes along the stream continuum at different time scales. Specifically:

In Chapter 5, we analyzed (i) the influence of riparian tree evapotranspiration on stream hydrology and stream hydrological retention at both short (diel variation) and

large (seasonal variation) time scales, and (ii) whether stream hydrological retention increased the N buffer capacity of the riparian zone.

In Chapter 6, we investigated (i) the potential influence of riparian and in-stream processes on regulating the temporal pattern of diel variations in stream NO_3^- concentration along the stream continuum, and (ii) the extent to which diel variations in stream NO_3^- concentrations influence stream N exports at seasonal and annual scales.

In Chapter 7, we explored (i) the longitudinal pattern of stream nutrient concentrations along a Mediterranean catchment, and (ii) the relative contribution of net riparian groundwater inputs and in-stream biogeochemical processing to stream NO_3^-, NH_4^+, and phosphorous fluxes at the whole-reach scale.

CHAPTER 2

Study Site and Field Design

The experiments included in this dissertation were carried out during a three year period in the Font del Regàs, a subhumid Mediterranean catchment located within the Montseny Mountains Range (NE Spain). The selected catchment was relatively small and undisturbed, and it had a well preserved riparian zone that increased in size from the headwaters to the valley bottom, thus offering optimal conditions and an excellent study scenario to address the objectives of this dissertation.

In this chapter, we describe the Montseny Mountains Range, characterize the Font del Regàs catchment, and explain in detail the plot and catchment experiments conducted during the development of the present dissertation.

2.1 THE MONTSENY MOUNTAINS RANGE

Research for this dissertation was carried out in Font del Regàs, a catchment located within the Montseny Mountains, UNESCO's Biosphere Reserve since 1978, which was declared Natural Park by the Spanish Government 17 years later (in 1995). Located at approximately 50 km NE of Barcelona (NE Spain) and 20 km inland from the Mediterranean Sea, the Montseny Natural Park occupies 30.000 ha and its altitude ranges from 300 to 1700 m above the sea level (a.s.l.) (Figure 2.1).

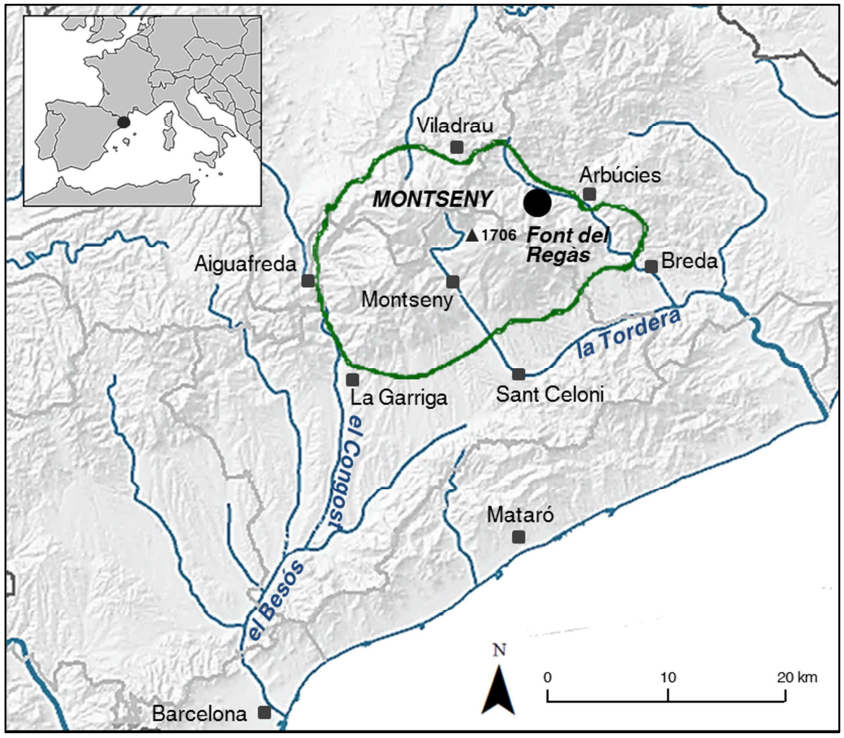

Figure 2.1 Location of the Montseny Mountains Range (NE Spain). The studied catchment (Font del Regàs) is depicted with a black dot.

The altitudinal gradient that characterizes the Montseny Mountains is essential for understanding its unique climate, that ranges from dry Mediterranean at lowland areas (300-1000 m a.s.l.) to humid temperate and cold subalpine at the highest altitudes (1000-1700 m a.s.l.). The altitudinal zonation of humidity and temperature makes the Montseny Natural Park a mosaic of Mediterranean and central-European landscapes with an extraordinary floristic diversity. The lowland areas are typically dominated by

Mediterranean vegetation such as pine forests (*Pinus sp.*) and oak woods (*Quercus sp.*). This Mediterranean landscape is replaced by temperate forests of beech (*Fagus sp.*) and fir trees (*Abies sp.*) as one moves up toward intermediate and high altitudes (> 1000 m a.s.l.) (Bolós 1983, Peñuelas and Boada 2003). Grasslands, heathlands, and alpine meadows cover the peaks of the massif, while well-developed riparian forests flank the large number of mountainous headwater streams (orders < 3) draining to the Congost and Tordera basins. As it occurs with the flora, several Mediterranean and central-European animal species coexist in the Montseny Mountains. Common Mediterranean species that inhabit in evergreen oak (*Q. ilex*) and cork oak *(Q. suber*) forests are the tawny owl (*Strix aluco*), the common genet (*Genetta genetta*) or the blackbird (*Turdus merula*), whereas the European robin (*Erithacus rubecula*), the long-eared owl (*Asio otus*) or the beech marten (*Martes foina*) can be found at high altitudes. In addition, the isolation of this massif has led to the evolution of endemic species, such as the Montseny salamander (*Calotriton arnoldi*) and the Sant Segimon herb (*Saxifraga vayredana*).

The climatic characteristics of the Montseny Mountains Range determine the stream hydrological regime, which shares characteristics with both temperate (i.e., permanent flow) and semi-arid streams (i.e., flow seasonality and episodic flood events). This wide range of hydrological conditions makes of the Montseny Mountains a unique natural laboratory for terrestrial and stream ecology. A probe of that is the fact that these mountains have been the focus of > 300 scientific studies, including hydrological, ecological and biogeochemical perspectives (e.g. Àvila et al. 2002, von Schiller et al. 2007, Àvila and Rodà 2012, Bernal et al. 2013, Pastor et al. 2014). These studies provide a wealth of extremely valuable background information for this dissertation, such as data on atmospheric N deposition, groundwater residence time, upland and riparian evapotranspiration, and in-stream N uptake rates.

2.2 THE FONT DEL REGÀS CATCHMENT

At the NE part of the Montseny Natural Park, close to the Arbúcies town, it is located the Font del Regàs stream, a small tributary of the Tordera river (41°50'N, 2°30'E, 500-1500 m a.s.l.) (Figure 2.1). The Font del Regàs catchment is relatively small (14.2 km^2) and it has a low population density (< 1 person km^{-2}) (Figure 2.2). The climate is subhumid Mediterranean and the catchment can be considered as a temperate island surrounded by a semiarid landscape. At the Arbúcies town, the mean annual temperature is 12.1 ± 2.5ºC and the annual precipitation averages 925 ± 151 mm (mean ± SD, period: 1940-2000, Catalan Meteorological Service). Total inorganic

atmospheric N deposition in the Montseny Mountains Range oscillates between 15-30 kg N ha^{-1} yr^{-1} (period: 1983-2007, Àvila and Rodà 2012).

The catchment is dominated by biotitic granite and it has steep slopes (slope ~ 28%). Mediterranean evergreen oak (*Q. ilex*) and temperate European beech (*F. sylvatica*) forests cover the major part of the catchment, while heathlands and grasslands can be found at higher altitudes (Cartographic and Geological Institute of Catalonia) (Figure 2.2). The catchment is drained by a perennial stream that increases in order along the reach (from 1 to 3) and that has two major tributaries. At the top of the catchment, the streambed is composed by rocks and cobbles, while sands and gravels predominate at the valley bottom. The stream channel is flanked by a relatively flat (slope < 10%) riparian forest which occupies the 6% of the catchment area. Common riparian tree species are black alder (*Alnus glutinosa*), black poplar (*Pupolus nigra*) European ash (*Fraxinus excelsior*), black locust (*Robinia pseudoacacia*), and hybrid sycamore (*Platanus hybrid*) (the latter two only at the valley bottom). The longitudinal gradients in topography, stream channel morphology, and riparian forest size make of the Font del Regàs catchment the perfect site to explore the effect of riparian forests on stream hydrology and N dynamics along the stream continuum.

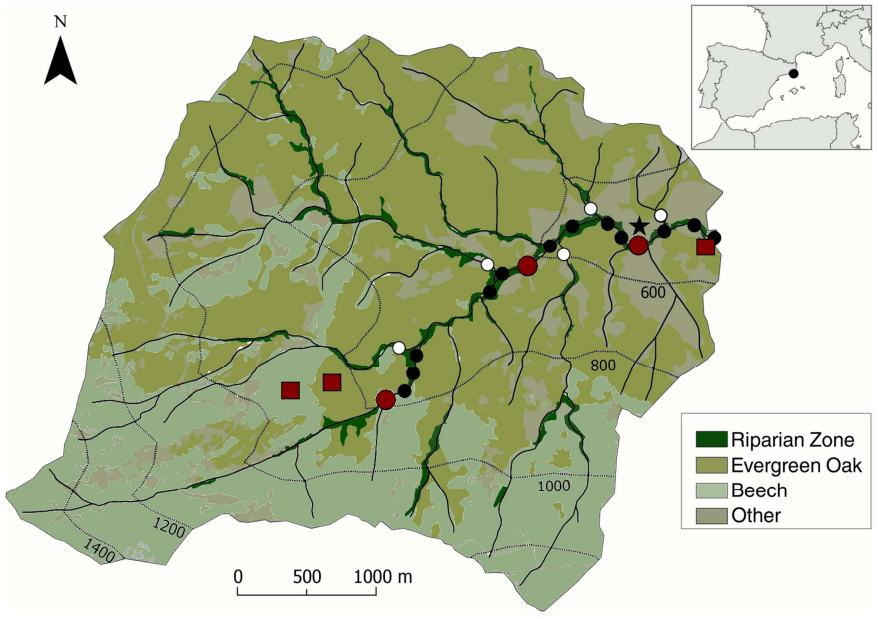

Figure 2.2 Map of the Font del Regàs catchment. The map indicates the location of the three forest sites (red squares), the three intensively sampled stream sites (red circles), the extensively sampled stream sites (black circles), the permanent tributaries (white circles), and the meteorological station (black star).

2.3 EXPERIMENTAL FIELD DESIGN

During the last decades, both plot and catchment scale studies have been widely used for investigating the potential of riparian ecosystems to transform upland N inputs (Binkley and Hart 1989, Sabater et al. 2003, Mayer et al. 2007). Field plots (or sites) are of tractable size and allow experimental manipulation (Binkley et al. 1992, Likens et al. 1994). Conversely, experimental catchment approaches consider all the ecosystems embedded within a catchment as a single unit, integrating the net effect of riparian zones on the N cycle within the entire system (Bormann and Likens 1967). For the present dissertation, we combined both plot and catchment approaches: *Part II* was performed at the plot scale, while *Part III* was based on a nested catchment design in order to gradually integrate processes occurring at upland, riparian, and in-stream ecosystems.

For conducting the *Part II* of this dissertation, we selected three forest sites, one for each of the dominant forests that coexist in the Montseny Mountain Range. The three forest sites were: a monospecific evergreen oak forest (the oak site), a monospecific European beech forest (the beech site), and a mixed riparian forest (the riparian site) of *R. pseudoacacia*, *P. nigra*, *A. glutinosa*, and *F. excelsior* (75%, 13%, 8%, and 4% of the site total basal area, respectively) (Figure 2.3). The oak and beech sites faced south (850 m a.s.l., slope = 21%) and east (900 m a.s.l., slope = 24%) respectively, while the riparian site (600 m a.s.l., slope = 2%) was located at the valley bottom of the catchment (Figure 2.2, red squares). We measured essential soil physicochemical properties (soil moisture, soil temperature, SOM content, and C:N ratio) and microbial N processes (NNM and NN) every two weeks during a calendar year (Table 2.1 and Table 2.2). Further, instantaneous stream discharge and stream water chemistry (chloride (Cl^-) and DIN concentrations) were measured at the catchment outlet, coinciding with the beginning and the end of each incubation period.

For conducting the *Part III* of this dissertation, we selected three stream sampling sites along a 4 km stream reach with increasing stream discharge, riparian coverage (from 0.1 to 4 m^2 of total basal area), and channel width (from 1.5 to 3 m) (Figure 2.4). The up-stream site (800 m a.s.l.) was a second-order stream (1.7 m wide) with a poorly developed riparian forest composed by evergreen oak and beech trees (Figure 2.3d). The mid-stream site (650 m a.s.l.) was a third-order stream (2.5 m wide) flanked by a mixed forest of typically riparian tree species such as black alder and European ash (Figure 2.3e). The down-stream site (500 m a.s.l.) was also a third-order stream (3.1 m wide) and it had a well-developed riparian forest (~30 m wide) consisting mainly of black locust, black poplar and black alder (Figure 2.3f).

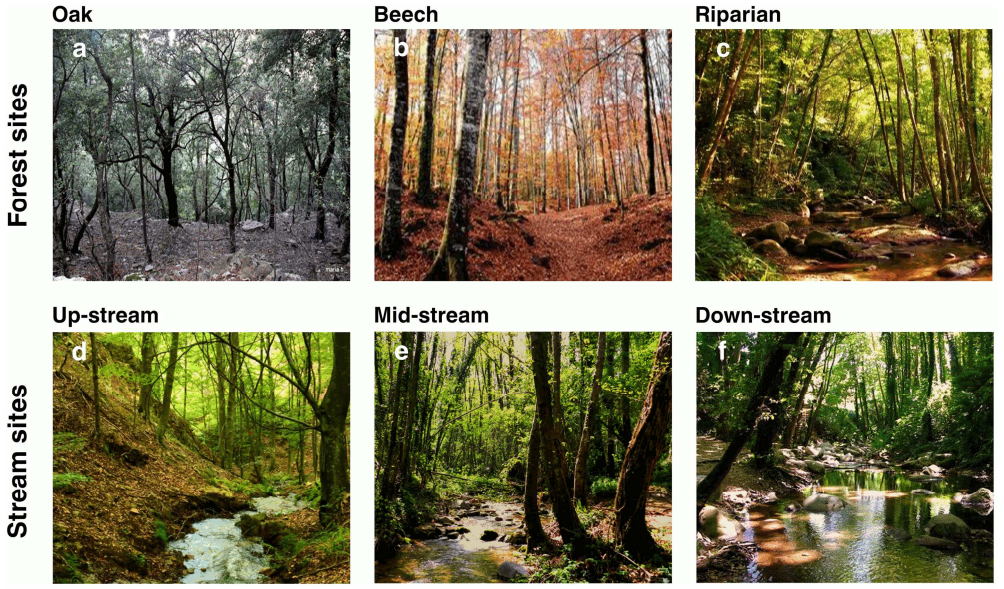

Figure 2.3 The studied forest plots and intensive-sampling stream sampling sites. In order from left to right, and from above to below: (a) oak site, (b) beech site, (c) riparian site, (d) up-stream site, (e) mid-stream site and (f) down-stream site. Source: Anna Lupon.

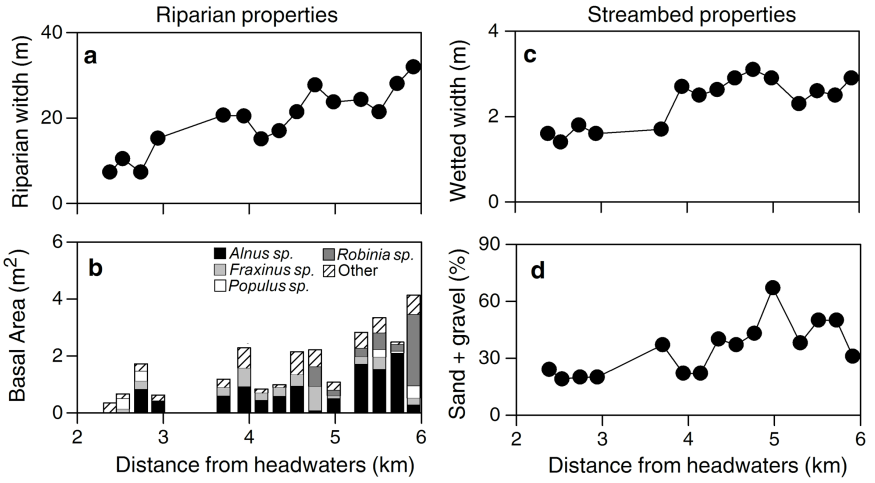

Figure 2.4 (a) Riparian width, (b) total basal area of riparian trees, (c) stream wetted width, and (d) percentage of fine sediments (sand + gravel) in streambed along the Font del Regàs catchment.

For conducting Chapter 5 and Chapter 6, we measured daily stream discharge and stream water chemistry (Cl^- and DIN concentrations) during two water years at the three stream sampling sites (Table 2.1 and Table 2.2). Additionally, groundwater level was measured at 15 minute intervals at the down-stream site. Finally, stream metabolism and high-frequency chemistry monitoring of both stream and groundwater (Cl^- and NO_3^-) were also measured at the down-stream site during spring 2012 (Chapter 6).

Table 2.1 Field scale, field data, number of sampling sites, and frequency and duration of the field work used for each chapter of this dissertation. For field data: SP (soil properties), Inc (soil and resin bags incubation), Q_{sw} (stream discharge), C_{sw} (stream chemistry), h_{gw} (groundwater level), Met (stream metabolism), C_{gw} (groundwater chemistry), Inv (riparian forest inventories), SC (soil characterization), Meteo (meteorological data), and C_{lix} (liviates chemistry). For sites: Oak (oak site), beech (beech site), rip (riparian site), Up (up-stream site), Mid (mid-stream site), Down (down-stream site), and Reach (whole 4 km reach).

Chapter	Scale	Field data	Sites	Frequency	Duration
3 & 4	Plot	SP	Oak, Beech & Rip	2 weeks / 1 month	12 months
		Inc	Oak, Beech & Rip	2 weeks / 1 month	12 months
		Q_{sw}, C_{sw}	Down	2 weeks / 1 month	12 months
5	Catchment	Q_{sw}	Up, Mid & Down	15 minutes	24 months
		C_{sw}	Up, Mid & Down	daily	24 months
		H_{gw}	Down	15 minutes	24 months
6	Catchment	Q_{sw}	Up, Mid & Down	15 minutes	12 months
	& Reach	C_{sw}	Up, Mid & Down	2 times x day	12 months
		C_{sw}	Down	4 times x day	4 months
		Met	Down	30 minutes	4 months
		C_{gw}	Down	2 times x day	4 months
7	Catchment	Q_{sw}	Reach	2 months	18 months
		C_{sw}	Reach	2 months	18 months
		h_{gw}	Reach	2 months	18 months
		C_{gw}	Reach	2 months	18 months
Other		Inv	Reach	---	---
		SC	Oak, Beech & Rip	---	---
		Springs	Reach	seasonal	12 months
		Meteo	Down	15 minutes	24 months
		C_{lix}	Oak, Beech & Rip	2 weeks	30 months

For Chapter 7, twelve additional sampling sites were selected along the 4 km reach (Figure 2.2, black circles). At each sampling site, we measured stream discharge and stream and riparian groundwater chemistry (Cl^-, DIN, and soluble reactive phosphorus (SRP) concentrations) every two months (Table 2.1 and Table 2.2). Stream discharge and water chemistry of the permanent tributaries were also measured during each field campaign (Figure 2.2, white circles).

Overall, we designed a fine sampling strategy, including not only soil plots for the different forest types and the major end members contributing to stream runoff (springs, riparian groundwater, tributaries, and soil lixiviates), but also 15 nested catchments for monitoring stream and riparian groundwater along a 4 km reach with increasing riparian area. Moreover, we did an extraordinary sampling effort in order to monitor water and nutrient fluxes at the highest possible sampling frequency given the field equipment we had.

Table 2.2 Time line of the field sampling periods for each chapter of this dissertation. Field measurements are as in Table 2.1. For chapters: Chapter 3 (orange), Chapter 4 (yellow), Chapter 5 (blue), Chapter 6 (green), and Chapter 7 (red).

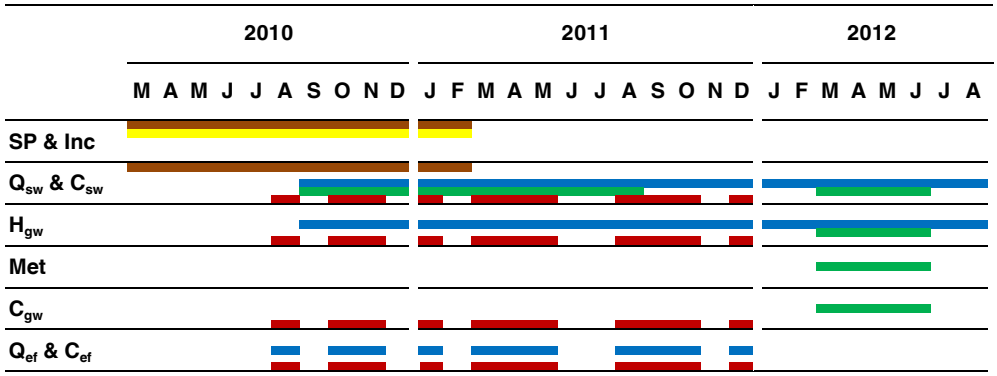

PART II

CHAPTER 3

Contribution of Soil Nitrogen Mineralization and Nitrification Pulses to Soil Nitrogen Availability in Three Mediterranean Forests

Pulses of microbial nitrogen (N) supply often occur during storms in Mediterranean regions, but their contribution to soil N availability and catchment N exports is still unknown. We investigated patterns and controls on net N mineralization (NNM) and nitrification (NN) pulses in three forests (riparian, evergreen oak and beech) coexisting within a Mediterranean headwater catchment, and examined the influence of these on soil N availability and stream N loads. For a year, we measured NNM, NN, precipitation, moisture and temperature within each forest type. Median NNM and NN rates varied widely among forest sites (NNM = 1.30, 0.46, and 0.38 mg N kg^{-1} d^{-1}; NN = 1.19, 0.13, and 0.06 mg N kg^{-1} d^{-1} for riparian, oak and beech, respectively). Generally, NNM and NN pulses occurred in spring, immediately after large rainfall events (> 20 mm). High soil temperatures (> 16ºC) promoted microbial pulses in summer at the riparian site, and no pulses of NN were found at the beech site. Although pulses of microbial activity were infrequent, they could contribute between 26-42% of the annual rates of NNM and NN. However, only NN pulses in the riparian site lead to disproportional increases in soil N availability and stream N loads. These results suggest that upland Mediterranean forests are sinks of N even after storms, while riparian soils can be critical sources of nitrate to the stream. Our study highlights the relevance of intensive monitoring on evaluating the effect of microbial pulses on soil N biogeochemistry in Mediterranean catchments.

Original Work: Lupon, A., F. Sabater and S. Bernal. 2015. Contribution of soil nitrogen mineralization and nitrification pulses to soil nitrogen availability in three Mediterranean forests. European Journal of Soil Science, in review.

3.1 INTRODUCTION

Future changes in climate are expected to alter soil nitrogen (N) dynamics in terrestrial ecosystems worldwide because precipitation and temperature exert a strong influence on microbial and plant activities (Pendall et al. 2008). In water-limited regions, precipitation events can lead to disproportionally high rates of soil microbial activity compared to the surrounding periods (Sponseller 2007, Austin 2011). This typical pulse behavior (*sensu* McClain et al. 2003) generally results from complex microbial responses to an increase in water availability, showing non-linear interactions between temperature, antecedent soil moisture conditions and substrate availability (Collins et al. 2008). Moreover, microbial responses to pulses of water availability are modulated by other abiotic and biotic factors, such as soil texture (McIntyre et al. 2009), aboveground vegetation (Borken and Matzner 2009), and microbial community composition (Schimel et al. 2007). Therefore, the influence of changes in water availability on pulses of soil microbial activity is often difficult to predict and still remains a major challenge for ecological research (Borken and Matzner 2009, Austin 2011).

In Mediterranean regions, temperature and precipitation exhibit a strong seasonal pattern, with mild winters, wet springs and warm dry summers. This marked seasonality in climate typically results in very high rates of soil microbial activity immediately after rainfall events, and low rates during summer and winter (Serrasolses 1999). Based on these observations, some authors have proposed that pulses of soil mineralization that follow rewetting episodes may dominate annual inorganic C and N production in Mediterranean regions (Rey et al. 2002, Miller et al. 2005). However, little is known about their real contribution to annual rates because most experiments have been either performed in the laboratory or in the field, while focusing on just single or few rainfall events (Miller et al. 2005, Sponseller 2007, Borken and Matzner 2009). The fact that environmental variables and vegetation can also vary widely within short distances in Mediterranean systems (Lucas-Borja et al. 2012) means that the occurrence of microbial pulses following rainfall events, as well as their contribution to annual soil N budgets can be highly ecosystem specific. Consequently, more intensive field samplings are needed in order to quantify the microbial pulse dynamics in different forest types and to understand their contribution to temporal variations in soil N availability in Mediterranean catchments.

A better assessment of pulses of soil N mineralization and nitrification is also of paramount importance in helping understand the soil N cycle because these two

processes mediate plant N uptake, N gas losses and leaching. Manipulative studies indicate that the rewetting of soils promotes pulses of soil N mineralization and leaching, which can have a direct impact on ecosystem N pools (Borken and Matzner 2009). However, rain events can also induce pulses of microbial immobilization (Dijkstra et al. 2012), denitrification (Tiemann and Billings 2012) and plant uptake (Jongen et al. 2013). Therefore, the contribution of soil N mineralization pulses to N leaching would ultimately depend on the coupling between inorganic N production and assimilation within the surface soil layers. In addition, N can be posteriorly transformed and retained by biota in its route towards the stream (Harms and Grimm 2010); and, thus, the impact of such pulses on soil N production and stream N export will depend on how quickly water is transferred from upland soils to streams (Welter et al. 2005, Lohse et al. 2013). While a positive relationship between soil nitrification and stream N loads has been reported in temperate regions (Goodale et al. 2009, Ross et al. 2012), the extent to which pulses of soil N mineralization contribute to soil N availability and the increase in stream N export in Mediterranean systems still remains poorly understood.

In this study, soil net N mineralization (NNM) and net nitrification (NN) were measured over the course of a year under three common Mediterranean forest types that coexist within the same catchment: evergreen oak (*Quercus ilex*), European beech (*Fagus sylvatica*) and riparian forests composed by black alder (*Alnus glutinosa*), European ash (*Fraxinus excelsior*), black poplar (*Populus nigra*) and black locust (*Robinia pseudoacacia*). Specifically, these field observations were used to: (i) investigate the temporal pattern of NNM and NN pulses in each forest type, (ii) evaluate their contribution to annual rates of NNM and NN and (iii) explore their influence on soil N availability, soil N pools and stream N export. We hypothesized that soil N processing rates would differ between forest types because water and substrate availability are typically higher in riparian than in upland forests (oak and beech) (McClain et al. 2003). However, we expected that pulses of NNM and NN would follow a similar temporal pattern in the three forest types, and be strongly linked to the seasonality of rainfall events. Moreover, we hypothesized that microbial N pulses would be infrequent but contribute substantially to annual rates of NNM and NN in the three forest types. Finally, we hypothesized that pulses of NN would lead to disproportional increases in soil N availability and stream N export because they occur during periods of high water transport through the catchment.

3.2 MATERIALS AND METHODS

3.2.1 Study Site

The research was conducted in the Font del Regàs catchment (14.2 km^2), located in the Montseny Natural Park, NE Spain (41º50'N, 2º30'E, 500-1500 m above the sea level (a.s.l.)). The climate is subhumid Mediterranean; with annual precipitation of 925 ± 151 mm and annual temperature of 12.1 ± 2.5ºC (mean ± SD, period: 1940-2000, Catalan Meteorological Service). Total inorganic N deposition in this region oscillates between 15-30 kg N ha^{-1} yr^{-1} (period 1983-2010, Àvila and Rodà 2012).

The catchment is dominated by biotitic granite and it has steep slopes (mean slope is 28%) (Cartographic and Geological Institute of Catalonia). The lower part of the catchment (400-1000 m a.s.l.) is covered by evergreen oak forests (54% of the catchment area), whereas the upper part of the catchment (800-1500 m a.s.l.) is covered mainly by European beech forests and heathlands (38% and 2% of the catchment area, respectively) (Figure 3.1). Both *Q. ilex* and *F. sylvatica* (sclerophyll and deciduous tree species, respectively) have high foliar C:N ratio (C:N ~ 40-60, averaged from 5 leaf samples collected in summer 2010). Upland soils are sandy and contain a 4 cm deep O horizon and a 5 to 23 cm deep A horizon. In upland soils, groundwater flows at least 0.5 m below the soil surface and rapidly percolates through the soil towards the stream via preferential flow paths (Àvila et al. 1995).

At the valley's bottom (400-750 m a.s.l.), there is a well-developed riparian forest (~30 m wide) consisting mainly of *A. glutinosa*, *F. excelsior*, *P. nigra*, and *R. pseudoacacia*. All four species have low foliar C:N ratios (C:N ~ 25-35; averaged from 5 leaf samples collected in summer 2010). The riparian zone covers 6% of the catchment area and it is almost flat (slope < 10%). Riparian soils are sandy-loams and contain a 5 cm deep O horizon and a 30 cm deep A horizon. Near-stream riparian groundwater flows at least 0.5 m below the soil surface (see Chapter 5).

We selected three forest sites (~1 ha each) with different vegetation cover: a monospecific evergreen oak forest (the oak site), a monospecific European beech forest (the beech site), and a mixed riparian forest (the riparian site) of *R. pseudoacacia*, *P. nigra*, *A. glutinosa*, and *F. excelsior* (75%, 13%, 8%, and 4% of the site total basal area, respectively). The oak and beech sites faced south (850 m a.s.l., slope = 21%) and east (900 m a.s.l., slope = 24%), respectively (Figure 3.1). The surface soil layer (0-10 cm) of the two upland soils had a pH ~ 6, was dominated by sand and gravel (66% and 34%

of soil mass) and had bulk densities of 1.40 g cm^{-3} and 1.35 g cm^{-3} for the oak and beech sites, respectively (averaged from 5 soil profiles). The riparian site (600 m a.s.l., slope = 2%) was located at the valley bottom of the catchment, where the riparian zone was well developed (Figure 3.1). The surface soil layer of the riparian soil had a pH ~ 7, was dominated by sand and silt (59% and 28% of soil mass) and had a bulk density of 1.09 g cm^{-3} (averaged from 5 soil profiles). The characterization of the surface soil layer was performed in summer 2010 following standard procedures (Page et al. 1982, Klute 1986).

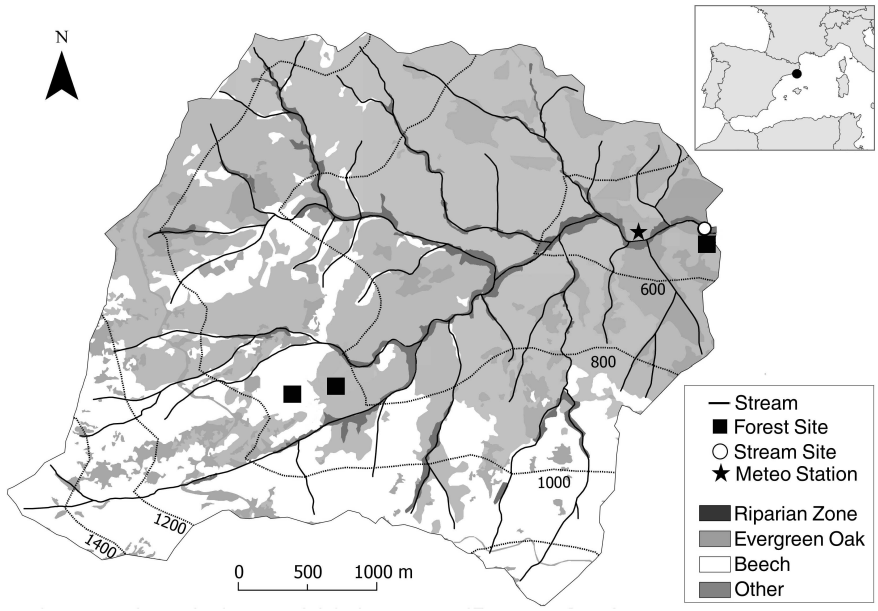

Figure 3.1 Map of the Font del Regàs catchment (Montseny Natural Park, NE Spain). The location of the three studied forest sites (squares), the stream sampling point (white circle) and the meteorological station (star) is shown.

3.2.2 Field Sampling

We delimitated 12 plots (7 x 10 m) within each forest site (riparian, oak and beech). During the period 2010-2011 (18 sampling dates), soil physicochemical properties, net N mineralization and nitrification rates, soil N availability, and environmental parameters were measured at each site in order to analyze patterns and controls of microbial N activity (see below). Further, stream discharge and chemistry were measured at the catchment outlet to investigate whether soil microbial N supply influenced the temporal

pattern of stream N export. We sampled every two weeks from March 2010 to August 2010, and on a monthly basis from September 2010 to February 2011. This field sampling encompassed 8 out of the 13 large rainfall events (> 20 mm) occurring during the course of the study, as well as dry periods (0 mm) within each calendar season.

To analyze soil physicochemical properties, one soil sample was randomly collected from each plot. Soil samples (0-10 cm, including O and A horizons) were taken with a 5 cm diameter core sampler and placed gently into plastic bags after carefully removing the litter layer. Moreover, we performed in situ soil incubations for estimating soil N processes by using the buried polyethylene bag technique (Eno 1960). For this purpose, a second soil core (0-10 cm) was collected from each plot close to the first soil sample, placed relatively undisturbed in a polyethylene bag (that allows temperature and gas exchange but prevents leaching), and buried at the same depth. Soil incubation bags were buried for 12-15 days, that is enough time to ensure that biogeochemical processes happen (Hart et al. 1994), and then removed from the soil.

We used ion exchange resins for estimating the amount of inorganic N available in the soil that was susceptible to be either leached or taken up by vegetation during each incubation period. Amberlite IR-120 and Amberlite IRA-400 resins were used to adsorb either ammonium (NH_4^+) or nitrate (NO_3^-), respectively. A small amount of ion exchange resin (5 g) was inserted into a 3 cm diameter nylon bag (100 μm grid). On each sampling date, a pair of anion-cation resin bags were buried at 10 cm depth, close to each incubation polyethylene bag, and they were removed from the soil at the end of each incubation period. In addition to resin bags, one soil sample was collected from each plot at the beginning and at the end of each incubation period to analyze the instantaneous soil N concentration.

Precipitation was continuously recorded at the meteorological station located close (< 1 km) to the riparian site (Figure 3.1). Precipitation accumulated during the 4 days prior to each sampling date (ΣP4d, mm) was used to characterize the rewetting events. On each sampling date, we measured the soil volumetric moisture content of each plot (4 replicates each time) at 10 cm depth using a time domain reflectometry sensor (HH2 Delta-T Devices Meter). Following standard procedures, the soil volumetric moisture was used for calculating the Water-Filled Pore Space (WFPS, %), a more appropriate measure of soil moisture than volumetric moisture when comparing soils with different porosity (Klute 1986, McIntyre et al. 2009). For each plot, soil temperature (Tsoil, ºC) was recorded at 10 cm depth (2 replicates each time) using a temperature sensor (CRISON 25) (only from June 2010 to February 2011). To infer soil temperature for

the March-May 2010 period we used the linear regression between air temperature and mean soil temperature measured in each site for the period June 2010-February 2011 (R^2 = 0.65, 0.72, and 0.69 for the riparian, oak, and beech sites, respectively; in all cases: n = 14, $p < 0.01$).

Finally, on each sampling date, we collected stream water from the catchment outlet by using pre-acid washed polyethylene bottles after double-rinsing them with stream water. Stream water samples were filtered (Whatman GF/F) immediately after collection. From September 2010 to August 2012, we measured stream discharge with the "slug" chloride addition technique (Gordon et al. 1992). We used the log-log regression between measured discharge and stream chloride concentration to infer stream discharge for the March-August 2010 period (R^2 = 0.76, n = 648, $p < 0.001$) (Walling and Webb 1986). All the soil, resin, and stream water samples were kept cold (< 4ºC) until laboratory analysis (< 24 h after collection).

3.2.3 Laboratory Analysis

Pre-incubation soil samples were sieved in the laboratory, and the fraction < 2 mm was used for measuring the relative soil organic matter content (SOM, %) by ignition (450ºC, 4 h). Soil C and N contents were determined on a gas chromatograph coupled to a TCD detector after combustion at 1000ºC at the Scientific Technical Service of the Universitat de Barcelona.

For estimating microbial N processes from *in situ* soil incubations, we extracted 5 g of field-moist pre- and post-incubation soil core samples with 50 ml of 2 M KCl (1 g: 10 ml; ww:v) (Keeney and Nelson 1982). The supernatant was filtered (Whatman GF/F) and analyzed for NH_4^+ and NO_3^-. For each pair of samples, net N mineralization (NNM; mg N kg^{-1} d^{-1}) and net nitrification (NN; mg N kg^{-1} d^{-1}) were calculated by subtracting, respectively, pre-incubation inorganic N (NH_4^+ + NO_3^-) and NO_3^- from post-incubation values (Eno 1960). Finally, we calculated the net nitrification fraction (i.e., NN/NNM), that is the fraction of ammonium in the soil pool consumed by nitrifiers (Booth et al. 2005).

Resin bags were rinsed with deionized water to remove the soil adhered to the outside of the bag. The inorganic N captured by the resins was extracted with 30 ml of 2 M KCl (5.00 g resin: 30 ml KCl, dw:v) and the extraction filtered (Whatman GF/F) and analyzed for NH_4^+ and NO_3^-. The amount of NH_4^+ and NO_3^- captured by the resin

bags was expressed as mg N kg resin^{-1} to provide a time-integrated index of the overall soil N availability during each incubation period (Jongen et al. 2013).

The inorganic N concentration of soil and stream water as well as from the resin extractions was analyzed by standard colorimetric analysis. NH_4^+ was analyzed by the salicilate-nitropruside method (Baethgen and Alley 1989) using a spectrophotometer (PharmaSpec UV-1700 SHIMADZU). NO_3^- was analyzed by the cadmium reduction method (Keeney and Nelson 1982) using a Technicon Autoanalyzer (Technicon 1976). Chloride was analyzed by ion chromatography (Compact IC-761, Methrom).

3.2.4 Data Analysis

Soil properties and microbial rates

To investigate differences in physicochemical soil properties (WFPS, Tsoil, SOM, and C:N ratio) among forests, we used a Friedman rank sum test (Zar 2010). Forest type (riparian, oak or beech) was used as the between-subjects factor and time as the repeated measure. If differences between sites were significant for a particular variable, we applied a Wilcoxon signed-rank test for assessing which forests were significantly different (Zar 2010). We applied the same statistical procedure to investigate differences in soil N availability (N in resin bags) and microbial N processing rates (NNM and NN) between the three forest types.

Temporal patterns of environmental conditions and soil microbial rates

To avoid the confounding effects of spatial heterogeneity within each site, the temporal pattern of the studied variables was explored using the site-median value for each incubation period, which accurately represents the central tendency of the data (Zar 2010). The seasonality of environmental conditions (ΣP4d, WFPS and Tsoil), and soil microbial N processes (NNM and NN) was explored with a Friedman rank sum test followed by a Wilcoxon signed-rank test to determine which seasons were significantly different. For each forest type, calendar seasons were used as the between-subjects factor and sampling dates as the repeated measure. Further, we performed Spearman correlations to investigate if the temporal pattern of microbial N processes differed among sites. Spearman correlations were also used to analyze the relationship between the temporal pattern of (i) soil moisture and rewetting (WFPS vs. ΣP4d) and (ii) NNM and NN within each site. We considered that a positive and strong correlation between NNM and NN was an indication that NN was substrate limited (Booth et al. 2005).

We determined pulses of NNM and NN by calculating a pulse cut-off (C_p) upon which values were considered disproportionately larger than the median value (Darrouzet-Nardi and Bowman 2011). For each site and microbial process, the C_p was calculated as:

$$C_p = \left(\text{med}\ \left(\frac{x_i^{n}}{x_{rrms}}\right) + F_{99}^{-1}\right) \times x_{rrms} \quad (3.1)$$

where *med* is the median of x values from i to n after being standardized by x_{rrms}, which is a robust version of the root mean square (Darrouzet-Nardi and Bowman 2011). F_{99}^{-1} is a statistical threshold upon which empirical values are considered pulses of soil N cycling and it is defined as the inverse of the 0.99 quantile of the t-distribution function. In contrast to the more standard fix-percentile approach, the C_p approach takes into account the dispersion of the data around the median value (Darrouzet-Nardi and Bowman 2011). When all values for a given distribution are close to the median, the calculated C_p may be larger than the maximum empirical value and no pulses will be identified. As the empirical distribution becomes flatter, an increasing number of values may fall beyond C_p, thus resulting in a larger proportion of pulses.

For each forest site, we calculated the frequency and the annual contribution of microbial pulses. To calculate the frequency of NNM and NN pulses over the year (F_p), we divided the number of incubations that lead to a pulse of soil N cycling by the total number of incubations. In turn, the relative contribution of pulses of either NNM or NN to annual rates (AC_p) was calculated as:

$$AC_p = \frac{\Sigma_1^{p} \text{NNM} \times d}{\widehat{\text{NNM}} \times 365} \quad (3.2)$$

where p corresponds to the incubation periods leading to a NNM (or NN) pulse, d is the incubation period (in days), and $\widehat{\text{NNM}}$ (or $\widehat{\text{NN}}$) is the median NNM (or NN) for the study period.

Relationship between NN, soil N availability and stream N export

We examined the influence of NN pulses on soil N availability by exploring the relationship between NN, resin NO_3^- concentration and soil NO_3^- concentration (Booth et al. 2005). Resin NO_3^- concentration was used as a time-integrated measure of available N in soils during each incubation period, while soil N concentration at the end of each incubation period was considered the result of the net balance between NN and NO_3^- losses (uptake and/or leaching) (Morillas et al. 2013). For each forest site, we built simple

regression models (linear, exponential, potential and logarithmic) between temporal patterns of NN and resin and soil NO_3^- concentration with and without counting pulses of NN. Model selection was performed by ordinary least square and referred only to the best fit model in each case (Zar 2010). A disproportional increase in resin NO_3^- concentration associated with NN pulses was interpreted as an indication that microbial pulses were major contributors to soil N supply. Otherwise, a nil or negative relation between pulses of NN and soil NO_3^- was considered an indication that pulses of NN and NO_3^- losses (uptake and/or leaching) occurred simultaneously.

Similarly, we related NN with stream NO_3^- loads in order to explore the influence of pulses of NN on catchment N exports (Ross et al. 2012). Stream NO_3^- loads were calculated multiplying stream NO_3^- concentrations (in mg L^{-1}) by the specific discharge (in L ha^{-1} d^{-1}) at the catchment outlet. The average of the stream NO_3^- load at the beginning and at the end of each incubation period was used as an integrated measure of the two-week incubation period. We considered that, if the hydrological connectivity between the soil surface and stream is high, there should be a positive relationship between NN and stream NO_3^- loads. A lack of correlation between these two variables was interpreted as an indication of biological and/or hydrological NO_3^- retention within the catchment (Harms and Grimm 2010). Moreover, a disproportional increase in stream NO_3^- loads after NN pulses was interpreted as an indication that the soil available NO_3^- was quickly leached towards the stream (Welter et al. 2005).

All statistical analyses were carried out with R 2.15.1 statistical software (R-project 2012). We chose non-parametric tests because generally data sets did not have a normal distribution (for physicochemical variables, NNM and NN: Shapiro test, $p < 0.01$) (Zar 2010). Differences were considered significant if the Bonferroni adjusted p-value was < 0.05.

3.3 RESULTS

3.3.1 Soil Physicochemical Properties and Microbial N Processes

During the study period, the three forest sites showed distinct physicochemical properties (Table 3.1). For example, the riparian site was the wettest and the beech site the coldest. There were no significant differences in the SOM content between sites, yet soil C:N ratios were significantly lower at the riparian than at the oak and beech sites. There were significant differences in resin NO_3^- concentration between forests

types, being annual median concentrations 2-3 fold higher in the riparian than in the oak and beech sites. In contrast, there were no differences in resin NH_4^+ concentrations between the three forest sites.

The NNM rates varied between forest types, being annual median values 3 fold higher in the riparian than in the oak and beech sites (Table 3.1). The NN rates differed widely with forest type, being annual median values 8 and 23 fold higher in the riparian than in the oak and the beech sites, respectively. The annual median nitrification fraction varied among forest types, being ca. 0.9, 0.3, and 0.1 at the riparian, oak, and beech sites, respectively (Table 3.1).

Table 3.1 Water-Fill Pore Space (WFPS), soil temperature (Tsoil), soil organic matter (SOM), soil C:N ratio, available soil N (NH_4^+ and NO_3^-), soil N processes rates (NNM and NN), and the nitrification fraction for the riparian, oak and beech sites during the study period. Values are medians and the 25th and 75th percentile are shown in brackets. For each variable, different letters indicate statistical significant differences between forest sites (Wilcoxon signed-rank test, p-value < 0.05, df = 1). n = 216 for WFPS, Tsoil, SOM, and C:N. For the remaining variables, n = 199, 165, and 172 for riparian, oak and beech sites, respectively.

	Riparian	Oak	Beech
WFPS (%)	46.2 [35.7, 57.8]^{A}	35.3 [23.1, 50.1]^{B}	39.7 [30.2, 50.2]^{B}
Tsoil (ºC)	11.0 [6.6, 17.0]^{A}	10.7 [7.5, 15.4]^{AB}	9.4 [5.1, 15.0]^{B}
SOM (%)	10.5 [8.7, 12.9]^{A}	9.7 [7.7, 14.2]^{A}	9.5 [7.9, 12.2]^{A}
C:N	12.0 [11.4, 13.5]^{A}	18.3 [16.4, 20.3]^{B}	19.1 [17.9, 12.2]^{B}
NH_4^+ (mg N kg resin^{-1})	0.89 [0.66, 1.22]^{A}	0.73 [0.47, 1.19]^{A}	0.50 [0.25, 0.81]^{A}
NO_3^- (mg N kg resin^{-1})	2.56 [1.65, 3.79]^{A}	1.30 [0.82, 1.80]^{B}	0.80 [0.44, 1.25]^{C}
NNM (mg N kg^{-1} d^{-1})	1.30 [0.80, 1.83]^{A}	0.44 [0.25, 0.83]^{B}	0.38 [0.24, 0.76]^{B}
NN (mg N kg^{-1} d^{-1})	1.19 [0.79,1.57]^{A}	0.13 [0.04, 0.4]^{B}	0.06 [0.01, 0.1]^{C}
Nitrification fraction	0.86 [0.59, 1.30]^{A}	0.33 [0.13, 0.63]^{B}	0.12 [0.03, 0.22]^{C}

3.3.2 Temporal Pattern of Environmental Conditions and Microbial N Processes

During the study period, precipitation showed a marked seasonal pattern (Friedman test, $p < 0.01$, degrees of freedom [df] = 3). Large rainfall events (> 20 mm) occurred mostly in spring, while precipitation was scarce during summer and winter (Wilcoxon test, $p < 0.05$). ΣP4d followed the same seasonal pattern than precipitation (Figure 3.2a). At the oak and beech sites, WFPS showed a spring maxima and a summer minima (Wilcoxon test, $p < 0.05$), and was positively correlated to ΣP4d (oak: $\rho = 0.72$, beech:

$\rho = 0.63$, in both cases: $n = 18$, $p < 0.05$). At the riparian site, WFPS did not significantly differ among seasons (Friedman test, $p > 0.05$, $df = 3$), and there was no correlation between ΣP4d and WFPS (Figure 3.2b). Soil temperature exhibited a clear seasonal pattern at the three forest sites, with a summer maxima and a winter minima (in all cases: Wilcoxon test, $p < 0.05$) (Figure 3.2c).

Rates of NNM and NN showed no seasonal pattern at any of the three forest types (in all cases: Friedman test, $p > 0.05$, $df = 3$) (Figure 3.3). Further, the temporal pattern of NNM and NN was different between forests types (in all cases: Spearman correlation, $\rho < 0.45$, $n = 18$, $p > 0.05$). There was a positive correlation between NNM and NN within each site (riparian: $\rho = 0.82$, oak: $\rho = 0.67$, beech: $\rho = 0.55$, in all cases: $n = 18$, $p < 0.05$).

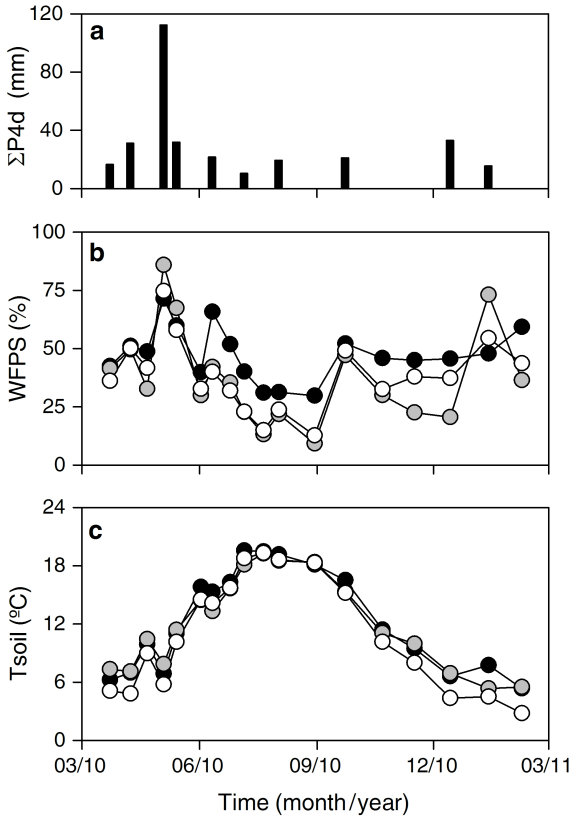

Figure 3.2 Temporal pattern of (a) precipitation accumulated during the 4 days prior to each sampling date, (b) water-filled pore space at 10 cm depth, and (c) soil temperature at 10 cm depth. Data is shown for the riparian (black), oak (gray) and beech (white) forest sites. Circles are median values for each incubation period.

There were NNM pulses at the three forest types, but NN pulses were only detected at the riparian and oak sites. The frequency of pulses (F_p) of NNM and NN (i.e. soil N processing rates > C_p) differed among forest types, being higher at the riparian than at the oak and the beech sites (Table 3.2). The annual contribution of NNM and NN pulses (AC_p) ranged from 0% (beech NN) to 42% (oak NN) (Table 3.2). At the three forest types, pulses of soil N microbial activity occurred in spring (April, May), though they did not occur simultaneously (Figure 3.3). At the riparian site, pulses of NNM and NN also occurred in summer (June, July and August).

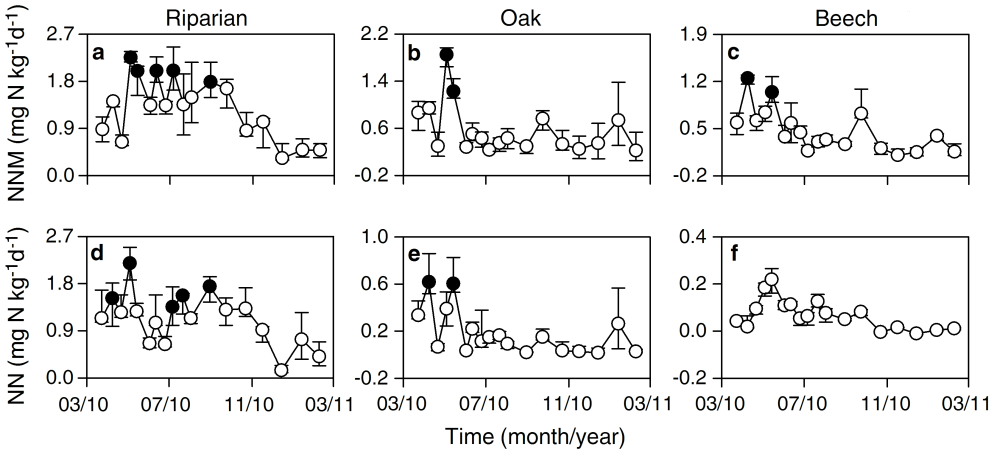

Figure 3.3 Temporal pattern of (a, b, and c) net N mineralization (NNM) and (d, e, and f) net nitrification (NN) at each forest type. Circles are median values for each incubation period and error bars are the 25th and 75th percentiles. Black circles represent pulses of NNM in top panels and NN in bottom panels.

Table 3.2 Pulse cut-off (C_p) for net N mineralization (NNM) and net nitrification (NN), frequency of pulse events relative to the total number of incubation periods (F_p) and contribution of pulse events relative to annual rates (AC_p) at each forest site. In all cases, n = 18.

	C_p (mg N kg^{-1} d^{-1})		F_p (%)		AC_p (%)	
	NNM	**NN**	**NNM**	**NN**	**NNM**	**NN**
Riparian	1.78	1.51	28	22	33	31
Oak	1.14	0.57	11	11	30	42
Beech	1.03	0.47	11	0	26	0

Pulses of both NNM and NN occurred after large rainfall events (ΣP4d > 20 mm) at the three forest types, yet not all large rainfall events led to microbial pulses (Figure 3.4). At the riparian site, both NNM and NN pulses occurred also under warm conditions (Tsoil > 16ºC) (Figures 3.4a and Figure 3.4d).

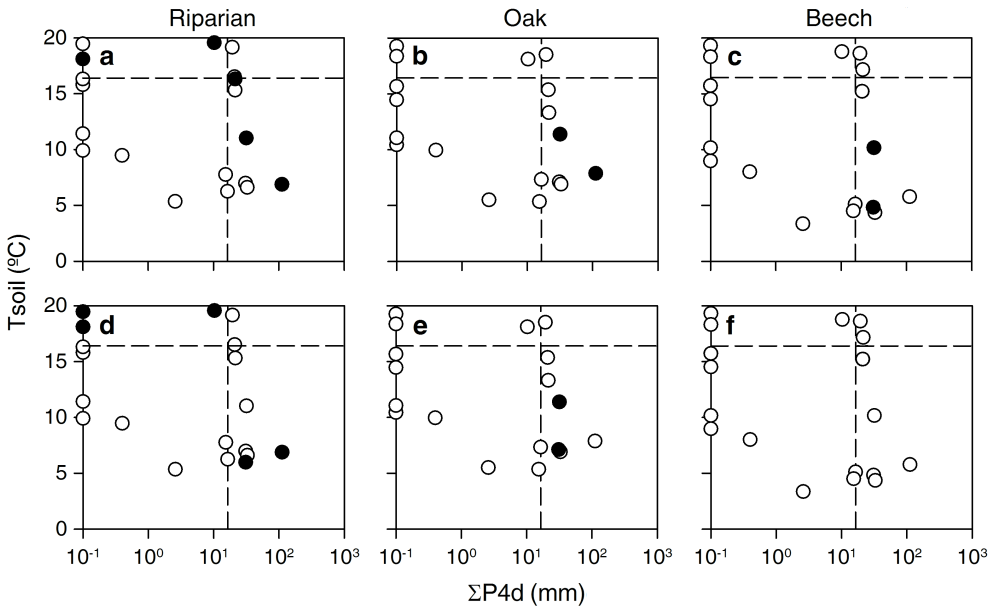

Figure 3.4 Dispersion plots between precipitation accumulated during the 4 days prior to each sampling date (ΣP4d) and soil temperature at 10 cm depth (Tsoil) at each forest type. Data is shown for (a, b, and c) net N mineralization (NNM) and (d, e, and f) net nitrification (NN). Black circles represent pulses of NNM in top panels and NN in bottom panels. Dashed lines are the 75th percentile of ΣP4d (vertical) and Tsoil (horizontal) for each forest site.

3.3.3 Influence of Net Nitrification on Soil N Availability and Stream Nitrate Loads

During the study period, resin NO_3^- concentrations reached a maximum in spring and a minimum in winter at the three forest sites (Figure 3.5a). This temporal pattern was positively related to NN in the riparian (potential reg., $R^2 = 0.63$, $p < 0.01$), oak (linear reg., $R^2 = 0.55$, $p < 0.01$) and beech sites (linear reg., $R^2 = 0.55$, $p < 0.01$) (Figure 3.6). At the riparian site, the relationship between NN and resin NO_3^- concentrations shifted from potential to linear when NN pulses were included (Figure 3.6a), while this relationship was little affected by NN pulses at the oak site (Figure 3.6b).

Soil NO_3^- concentrations showed no clear temporal pattern at any of the three forest sites (Figure 3.5b). There was no relationship between soil NO_3^- concentrations and NN in the riparian and oak sites, while soil NO_3^- concentrations decreased logarithmically with increasing NN in the beech site ($R^2 = 0.51$, $p < 0.01$) (Figure 3.6). Pulses of NN had a small influence on the relationship between NN and soil NO_3^- concentration at the three forest sites.

During the study period, median stream NO_3^- load was 1.12 g N ha^{-1} d^{-1}. The highest values occurred in spring and the lowest in winter (Figure 3.5c). This temporal pattern was positively related to NN in the riparian (potential reg., $R^2 = 0.70$, $p < 0.001$), oak (linear reg., $R^2 = 0.58$, $p < 0.01$) and beech sites (linear reg., $R^2 = 0.53$, $p < 0.01$). Stream NO_3^- loads increased exponentially when pulses of NN were considered at the riparian site (Figure 3.6g), while no disproportional increase in stream NO_3^- loads was associated with oak NN pulses (Figure 3.6h).

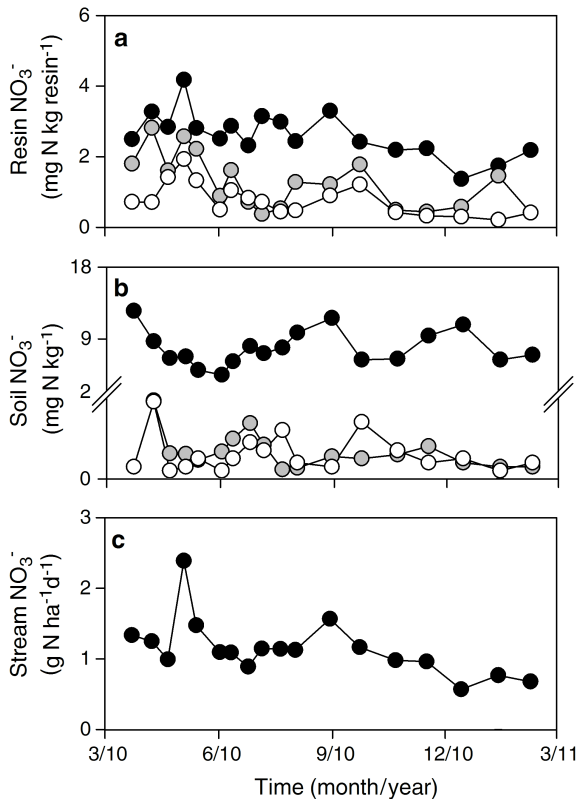

Figure 3.5 Temporal pattern of (a) resin nitrate concentrations, (b) soil nitrate concentrations and (c) area-specific stream nitrate loads. In panels (a) and (b), circles are median values for each incubation period at riparian (black), oak (grey) and beech (white) sites, respectively.

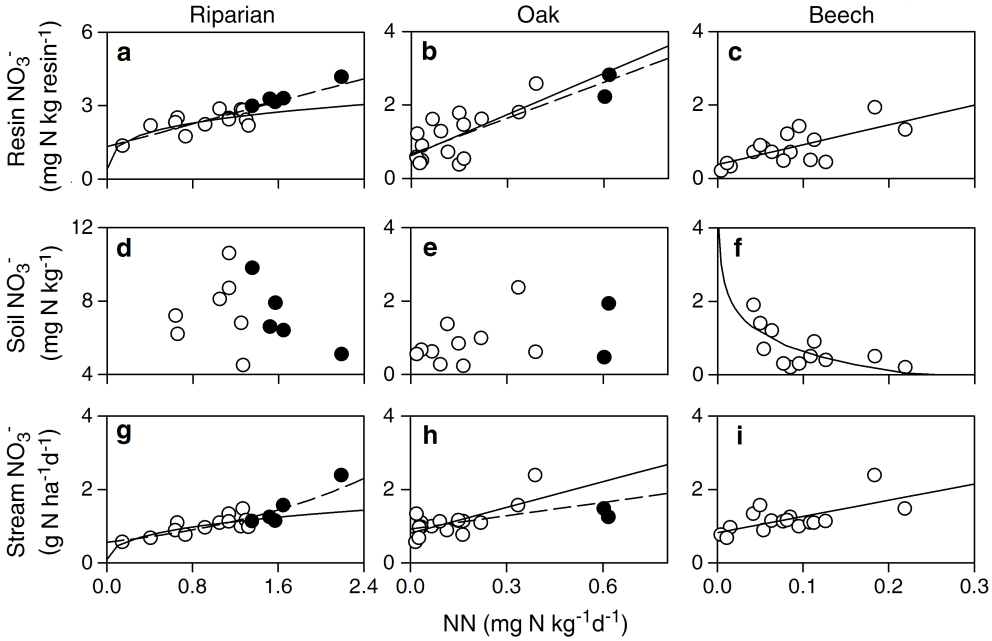

Figure 3.6 Relationship between net nitrification (NN) and (a, b and c) resin nitrate concentrations, (d, e and f) soil nitrate concentrations at the three forest sites, and (g, h and i) area-specific stream nitrate loads at the catchment outlet. Black circles represent pulses of NN. Lines indicate the best fit model with (dashed) and without (solid) including NN pulses (only shown when significant, $p < 0.05$).

3.4 DISCUSSION

3.4.1 Differences in Soil Properties and Microbial Rates among Forests

Our results indicated that differences in topographic features, soil properties and aboveground vegetation were essential to understand different patterns of soil microbial activity among the three forest types. The riparian site, which had the highest soil temperature and moisture, showed multiple fold higher NNM and NN rates than the oak and beech sites. These results are in agreement with previous studies showing high soil N microbial activity in riparian forests as a result of warm, wet and fine-textured soils (Merrill and Benning 2006, McIntyre et al. 2009). Additionally, the abundance of N_2-fixing species (> 80% of the basal area) and low soil C:N ratios (C:N < 20) could further contribute to the high NNM and NN rates measured in the riparian site (Booth et al. 2005, Merrill and Benning 2006).

However, environmental factors driving differences in soil N cycling between the oak and beech sites were difficult to identify. We found that both NN and nitrification factor were 3 fold lower at the beech than at the oak site, despite the fact that the two forests exhibited similar temperature, moisture and soil texture. Low NN values in other forests worldwide have been attributed to strong NH_4^+ demand by heterotrophic microbes, high denitrification rates or poor nitrifier populations (Booth et al. 2005, Guckland et al. 2010, Trap et al. 2011). In the beech site, increased NH_4^+ immobilization and high denitrification seem unlikely because soil NNM, NH_4^+ availability and moisture were similar to the oak site. Instead, the weak correlation between NNM and NN suggests that the nitrifier population at the beech site may have been either poorly developed or inhibited (i.e. by allelopathic compounds) (Trap et al. 2011). Our results indicate that the soil N cycling in this headwater catchment varied widely over relatively small distances, highlighting the fact that the heterogeneity of climatic conditions and associated vegetation inherent to Mediterranean regions can result in marked patterns of soil N availability and potential N leaching (Lucas-Borja et al. 2012).

3.4.2 Temporal Pattern of Net N Mineralization and Net Nitrification

Although precipitation, soil moisture and temperature followed a marked seasonality, NNM and NN rates did not, as previously reported for other Mediterranean forests (Morillas et al. 2013). However, pulses of NNM and NN at the three forest types mainly occurred during spring and were associated with large storm events (ΣP4d > 20 mm). This result concurs with previous studies reporting the highest rates of mineralization during the wettest season in riparian (Harms and Grimm 2010), oak (Serrasolses 1999) and beech forests (Guckland et al. 2010). Several mechanisms have been proposed to explain the stimulation of soil microbial activity during rewetting events, such as the release of intracellular osmolites (Schimel et al. 2007), the increase of available substrate (Collins et al. 2008) or hydrophobicity (Borken and Matzner 2009). These mechanisms often concurred simultaneously and thus, the dominance of one mechanism over the others may result in the final response of microbial activity to storm events. We suggest that the complex combination of the mechanisms underlying rain-induced pulses may explain, in part, the distinct temporal pattern of microbial pulses observed during spring at the three forests types.

No pulses of soil N cycling were detected in summer at the upland soils, not even after large rainfall events, which can be explained by the perpetual dryness of these soils in summer (WFPS < 20%) (see Chapter 4). Conversely, we found summer pulses of NNM and NN at the riparian site, which were associated with high temperatures.

Likely, the stabilizing effect of riparian groundwater contributed to keep riparian soils relatively wet (WFPS > 30%) throughout the year, an idea supported by the lack of correlation between ΣP4d and WFPS at this site. Thus, summer pulses of NNM and NN at the riparian site could result from the combination of both warm temperatures and moderate levels of wetness. In addition, low microbial immobilization and low denitrification in summer may further contribute to increases in soil net mineralization and net nitrification (Bernal et al. 2007). Our findings add novel knowledge to what has been previously reported in Mediterranean regions, by suggesting that the temperature can enhance microbial activity in riparian soils similar to patterns observed in temperate and boreal forests (Goodale et al. 2009, Brookshire et al. 2011).

During the remaining part of the year (autumn and winter), no pulses of NNM and NN were detected in either riparian or upland soil forests. While the lack of soil microbial pulses in winter may be attributed to the absence of precipitation, we expected that rainfall in autumn would have induced pulses in microbial activity (Rey et al. 2002). This result could be explained by a dramatic increase in microbial N demand following large inputs of C from litterfall (Guckland et al. 2010). Consistent with this hypothesis, we found low, or even negative, NNM and NN rates in autumn at the three forest sites. Therefore, our results indicate that rewetting events can have a minimal effect on soil N processing rates when the demand of N is high, further suggesting that the response of the soil microbial community to rainfall events depends of the interplay of a myriad of external drivers and ecosystem internal factors (Collins et al. 2008, Austin 2011).

We found that, despite being relative infrequent, pulses of microbial activity accounted for 26-42% of annual NNM and NN rates (except for NN at the beech site). This value could be even higher because we captured 8 out of the 13 large rainfall events that occurred during the study period. Our results conflict with previous studies carried out in temperate systems, which suggest that the importance of microbial pulses following precipitation events is relatively low (< 10%) on an annual basis (Borken and Matzner 2009). Similarly, Sponseller (2007) reported a minimal contribution (3%) of rewetting pulses on annual C losses in an arid shrub ecosystem. However, these studies encompassed short time periods (days or few months), and thus, they may be underestimating the importance of pulses of soil microbial activity in annual terms. In fact, high temporal resolution data have shown that microbial pulses can be responsible for > 10% of ecosystem annual C losses (Xu et al. 2004, Miller et al. 2005). Similarly, our study indicates that microbial pulses can substantially contribute to NNM and NN on an annual basis, which adds a novel piece of knowledge to our understanding of soil N cycling in Mediterranean forests.

3.4.3 Relationship between Net Nitrification, Soil Nitrate Availability and Stream Nitrate Loads

Our results provide insights into the paramount importance of soil microbial activity in regulating soil N availability in these Mediterranean forests. We found a strong positive relationship between resin NO_3^- concentration and NN at all forest types, which provide evidence for soil organic matter being the main source of inorganic N in these forests, similarly to that reported for other forests worldwide (Kendall et al. 2007). However, the relationship between NN and soil NO_3^- concentration was either nil or negative at the three forest types, suggesting that available NO_3^- was either quickly taken up by plants or leached out (see Chapter 4). As reported in previous studies, we found that the biological demand for NO_3^- was especially noticeable in spring, when N in resin bags was at its maxima and soil NO_3^- concentrations were at their minima (Dijkstra et al. 2012, Jongen et al. 2013).

Furthermore, the positive relationship between stream NO_3^- loads and NN rates found at the three forest types suggests that the terrestrial N cycle strongly influenced the temporal pattern of catchment N exports. Similar patterns have been reported in a variety of temperate catchments (Goodale et al. 2009, Ross et al. 2012), which have been attributed to a large microbial N supply compared to atmospheric N inputs (Kendall et al. 2007). We observed, however, that this relationship was weaker for the upland sites (oak and beech) than for the riparian site, suggesting that NO_3^- was likely hydrological retained and/or biological transformed (via denitrification and/or uptake) while travelling through the catchment (Welter et al. 2005, Lohse et al. 2013). This explanation is supported by previous studies reporting that the water mean travel time is 2-12 weeks in these catchments (Bernal et al. 2013). In addition, stream biota could further modify NO_3^- concentrations arriving from terrestrial ecosystems while travelling from downstream (Bernal et al. 2015).

There is still little research on whether pulses of microbial activity can influence temporal patterns of soil NO_3^- availability and stream NO_3^- loads. Our study shows that pulses of NN did not enhance soil NO_3^- availability, nor increased soil NO_3^- concentration at the oak site, suggesting simultaneous plant N retention during rewetting of the surface soil layers (Dijkstra et al. 2012, Jongen et al. 2013). The fact that stream NO_3^- loads did not disproportionally increase after oak NN pulses further suggests that the produced NO_3^- was retained in soils rather than being quickly flushed towards the stream. In contrast to the oak site, stream NO_3^- loads disproportionally increased after pulses of NN at the riparian site. These results indicate that riparian soils were prone to leach NO_3^-, as reported for N saturated systems with higher N supply than demand

(Compton et al. 2003, Merrill and Benning 2006). Moreover, the proximity and strong hydrological connection likely favored the quick transfer of NO_3^- between the riparian soils and the stream. Riparian zones can remove significant amounts of N from upland soils during subsurface transport (e.g. McClain et al. 2003). However, our study indicates that riparian zones can also act as N sources to streams, likely via surface runoff. Further, these findings suggest that riparian soils may have a disproportionately large influence on the amount and form of N transported to downstream ecosystems compared to other landscape units (Ross et al. 2012); and therefore, pulses of soil N dynamics in riparian areas can be critical to assess both seasonal and annual stream N fluxes in Mediterranean catchments.

3.5 CONCLUSIONS

Our study shows that the magnitude of pulses of NNM and NN differed between the three studied forests, being higher at the riparian than at the oak and the beech sites. Further, rewetting events enhanced pulses of microbial activity in spring, but not in autumn likely due to high microbial N demand. However, high temperatures promoted summer pulses of NNM and NN at the riparian site similarly to more temperate systems. Our results indicate that pulses of microbial activity can contribute substantially (> 25%) to annual rates of NNM and NN in these forests, which highlights the importance of considering pulse events for understanding soil N cycling in Mediterranean systems. Finally, soil N availability and stream NO_3^- loads increased disproportionally after pulses of NN in the riparian site, suggesting that riparian zones can be critical N sources to streams in Mediterranean catchments.

ACKNOWLEDGEMENTS

Financial supported was provided by the Spanish Government through the projects MONTES-Consolider (CSD2008-00040) and MEDFORESTREAM (CGL2011-30590). AL was funded by the Spanish Ministry of Education, Culture and Sport (MECD) with a FPU grant (AP-2009-3711). SB work was funded by the Spanish Research Council (JAE-DOC027) and the Spanish CICT (Juan de la Cierva contract JCI-2008-177). Special thanks are extended to Aitana Oltra for helping us with GIS and Sílvia Poblador for the invaluable field and laboratory assistance. We thank Gary Lovett and two anonymous reviewers for constructive comments on earlier versions of the manuscript. We also thank to Vichy Catalan and the Catalan Water Agency (ACA) for permission to sample at the Font del Regàs catchment.

CHAPTER 4

Climate Response of the Soil Nitrogen Cycle in Three Forest Types of a Headwater Mediterranean Catchment

Future changes in climate may affect soil nitrogen (N) transformations, and consequently, plant nutrition and N losses from terrestrial to stream ecosystems. We investigated the response of soil N cycling to changes in soil moisture, soil temperature and precipitation across three Mediterranean forest types (evergreen oak, European beech and riparian) by fusing a simple process-based model (which included climate modifiers for key soil N processes) with measurements of soil organic N content, mineralization, nitrification, and concentration of ammonium and nitrate. The model describes sources (atmospheric deposition and net N mineralization) and sinks (plant uptake and hydrological losses) of inorganic N from and to the 0-10 cm soil pool as well as net nitrification. For the three forest types, the model successfully recreated the magnitude and temporal pattern of soil N processes and N concentrations (Nash-Sutcliffe coefficient = 0.49-0.96). Changes in soil water availability drove net N mineralization and net nitrification at the oak and beech forests, while temperature and precipitation were the strongest climatic factors for riparian soil N processes. In most cases, net N mineralization and net nitrification showed a different sensitivity to climatic drivers (temperature, soil moisture and precipitation). Our model suggests that future climate change may have a minimal effect on the soil N cycle of these forests (< 10% change in mean annual rates) because positive warming and negative drying effects on the soil N cycle may counterbalance each other.

Original Work: Lupon, A., S. Gerber, F. Sabater and S. Bernal. 2015. Climate response of the soil nitrogen cycle in three forest types of a headwater Mediterranean catchment, Journal of Geophysical Research – Biogeosciences, 120: 859-875.

4.1 INTRODUCTION

Global climate is anticipated to become significantly warmer over the next decades, accompanied with shifts in the water cycle, which in turn, can compromise both terrestrial and aquatic nutrient cycles and budgets (Pendall et al. 2008, Luo et al. 2011). Among other things, climate affects soil nitrogen (N) dynamics through changing soil N mineralization and nitrification rates, influencing plant nutrition and formation of soil organic matter. Furthermore, changes in the terrestrial N cycle could affect N losses from soils to streams, and thus, influence headwater stream N loads, in-stream N retention and downstream water quality (Goodale and Aber 2001, Rogora 2007, Brookshire et al. 2009).

Soil moisture, temperature and precipitation pulses are important drivers of key steps of the soil N cycling (Miller et al. 2007, Bell et al. 2008), although each of these climatic variables may impact differently on the various soil processes. Warming can stimulate soil mineralization and increase soil nutrient availability (Rustad et al. 2001, Emmett et al. 2004), while decreased water availability can reduce mineralization and nutrient availability in the soil pool (Niboyet et al. 2011, Manzoni et al. 2012). The magnitude of this climatic response is likely ecosystem specific. Cold climate ecosystems tend to be more sensitive to changes in temperature than warmer ecosystems (Rustad et al. 2001, Dessureault-Rompré et al. 2010), while arid ecosystems tend to be more sensitive to increases in soil moisture than mesic ecosystems (Borken and Matzner 2009). Less clear is the response of soil nutrient cycles to precipitation pulses, yet most of studies suggest that it increases with dryness and substrate availability (Collins et al. 2008, Borken and Matzner 2009).

Furthermore, changes in water availability and temperature can promote shifts in vegetation, and drive tree species ranges towards higher elevations in headwater catchments (Peñuelas and Boada 2003, Colwell et al. 2008, Chen et al. 2011). The impact of species substitution on the soil N cycle and catchment N losses is difficult to assess empirically, and it is largely unknown. Soil organic matter, litter quality and soil microbial population can vary widely among forest types (Lovett et al. 2004, Booth et al. 2005), and thus, changes in vegetation together with forest type specific climate responses may both contribute to shifts in N cycling patterns at the landscape level. Therefore, understanding the response of the soil N cycle to changes in climate in different forest types coexisting within catchments is central for evaluating present and future characteristics of N cycling in these ecosystems, but it still remains a major challenge of ecological research.

Most of studies analyzing the climate sensitivity of the soil N cycle are based on manipulation experiments (Rustad et al. 2001, Borken and Matzner 2009). However, field observations that consider natural climate variability are complementary tools to add for understanding how ecosystems work, especially when combined with process-based models that allow to explicitly link the response of biogeochemical processes to climate variability (e.g. Ise and Moorcroft 2006, Brookshire et al. 2011). Another appealing feature of process-based models is that they allow testing the sensitivity of ecosystem processes to specific environmental drivers in isolation, and thus, provide the opportunity to separate the simultaneous effect of different environmental drivers on biogeochemical processes (Luo et al. 2011).

The aim of this study was to investigate the response of soil N cycling to changes in soil moisture, soil temperature and precipitation across three forest types (evergreen oak, European beech and riparian) that coexist in Mediterranean catchments by using a simple process-based model. To do so, we analyzed a detailed empirical data set of soil N cycling rates from a headwater catchment in the Montseny Mountains Natural Park (NE Spain) with a simple ad-hoc model that represents the interrelated processes of N mineralization, nitrification and removal of ammonium and nitrate from the soil pool. We hypothesized that the sensitivity of the soil N cycle to climate variables will differ among the three forest types because these forests differ in ecosystem properties (e.g., species composition, and C and N stocks) and microclimatic conditions, which both of them are strong drivers of soil N processes. The evergreen oak (*Quecus ilex*) and European beech (*Fagus sylvatica*) forests are Mediterranean and cold-temperate ecosystems, respectively, which grow in steep upland areas with poorly developed soils and fast water drainage toward the stream channel (Peñuelas and Boada 2003). In contrast, riparian forests are settled in flatter and lower areas with stable groundwater tables, higher moisture content and organic N-rich soils (Bernal et al. 2015). Therefore, we expected that (i) N cycling rates in the oak and beech forests will show strong responses to soil moisture and precipitation compared to the riparian forest because the formers are water-limited ecosystems and (ii) N cycling in the beech forest will be more sensitive to soil temperature than in the oak and riparian forest because beech forests typically grow in colder environments.

Currently, little is known about the combined effect of future changes in temperature and soil water availability on soil N dynamics in seasonally dry forests (Cameron et al. 2013, Bai et al. 2013). In scenarios of medium to severe climate change, Mediterranean regions will experience a year-round decrease in soil moisture and increase in temperature and decreased precipitation in summer (Intergovernmental Panel on Climate Change

(IPCC) 2013). We hypothesized that any positive effect of temperature on the soil N cycle will be reduced by the simultaneous negative effect of dryness, at least in the oak and beech forests, which commonly exhibit severe dry conditions in Mediterranean regions (Peñuelas and Boada 2003). Further, Mediterranean mountains are experiencing a progressive climate-induced beech-by-oak substitution at medium altitudes (800-1400 m) that may result in a complete replacement by the end of this century (Peñuelas and Boada 2003). Thus, we additionally considered the hypothesis that this shift in species composition will affect future soil N cycle in these catchments.

4.2 MATERIALS AND METHODS

4.2.1 Study Site and Empirical Data Set

Font del Regàs is a headwater catchment (14.2 km^2) located in the Montseny Natural Park, NE Spain (41°50'N, 2°30'E). The climate is subhumid Mediterranean, with an annual precipitation of 925 ± 151 mm and a mean annual temperature of 12.1 ± 2.5ºC (mean ± SD, period 1940-2000, Catalan Meteorological Service). Total inorganic N deposition is ~15 kg N ha^{-1} yr^{-1}, with wet and dry deposition fractions being about equally important (45% vs. 55%) (Àvila and Rodà 2012).

The catchment is dominated by biotitic granite and its altitude ranges from 400 to 1500 m above sea level (a.s.l.) (Cartographic and Geological Institute of Catalonia). Oak and beech forests cover 54% (400-1000 m a.s.l.) and 38% (800-1500 m a.s.l.) of the catchment, respectively. Upland soils (pH ~ 6) are sandy and have a 3 cm deep O horizon followed by a 5 to 23 cm deep A horizon. Soil bulk density is 1.40 and 1.35 g cm^{-3} at the oak and beech forests, respectively. The riparian zone covers the remaining 6% of the catchment area and it consists mainly of black alder (*Alnus glutinosa*), black locust (*Robinea pseudoacacia*), European ash (*Fraxinus excelsior*), hybrid sycamore (*Platanus hydrida),* and black poplar (*Populus nigra*). Riparian soils (pH~7) are sandy loam and have a 5 cm deep O horizon followed by a 30 cm deep A horizon. Soil bulk density in the riparian forest is 1.09 g cm^{-3}. During base flow conditions, the riparian groundwater table is located 50 ± 10 cm below the soil surface, and thus, it is disconnected from organic soil layers most of the time (see Chapter 5).

In order to explore the climatic sensitivity of soil microbial N processes, we took advantage of a preexisting empirical data-set of soil N processes and concentrations at

the surface soil layer (0-10 cm depth) collected every 2-4 weeks during the period 2010-2011 (18 sampling dates) at three sites (~1 ha each), one for each dominant forest type (evergreen oak, beech, and riparian). For each forest type, the data set included mean values (from 12 averaged plots, sample size 1 dm^2) of soil organic nitrogen (SON), ammonium (NH_4^+) and nitrate (NO_3^-) concentrations. Moreover, it incorporated mean rates of net N mineralization (NNM) and net nitrification (NN) measured with in situ soil incubations by using the polyethylene bag technique (Eno 1960). At each sampling date, soil was buried into the soil for 12-15 days and then removed from the soil. The polyethylene bags prevented leaching but allowed gas and temperature exchange, and thus, measured NNM and NN were the net result between either gross N mineralization or gross nitrification, and microbial N immobilization and denitrification. In addition, the data set included mean rates of potential NO_3^- losses from the soil pool (PNL, in mg N kg^{-1} d^{-1}) measured with ion exchange resins, which were buried into the soil close to each polyethylene bag during each incubation period (which started at each sampling date). The NO_3^- content in resin bags was used as a proxy of NO_3^- leaching, infiltration and uptake expressed as N content per bag weight (Lovett et al. 2004, Berger et al. 2009). Following Berger et al. (2009), we expressed resin bags data as N content per soil weight by taking into account the bag volume and the soil bulk density. Although this is a rough transformation, it is useful for our purposes because it allows comparing PNL to other soil N processing rates.

The data set further included environmental variables such as mean values of soil moisture (expressed as water-filled pore space (WFPS)) and soil temperature (Tsoil) for each sampling date and forest type (Figures 4.1a and Figure 4.1b). WFPS was calculated from soil volumetric moisture content measured at 10 cm depth (four replicates per plot) with a time domain reflectometry sensor (HH2 Delta-T Devices Moisture Meter). Tsoil was recorded at 10 cm depth (two replicates per plot) by using a temperature sensor (CRISON 25). In addition, we recorded daily precipitation (P) from a meteorological station located at the valley bottom of the catchment, which showed the expected seasonal pattern for this region with higher values in spring than in summer and winter (Figure 4.1c). More details can be found in Chapter 3 (Section 3.2.2).

4.2.2 Model Development and Climatic Modifiers

We developed an ad hoc ecosystem model similar to Brookshire et al. (2011) to evaluate soil N dynamics at the surface soil layer (0-10 cm) over time (Figure 4.2). This model describes sources and sinks of soil inorganic N and therefore incorporates key

mechanisms to link the different measured variables. In our model, inorganic N enters to the system from atmospheric deposition (D_{NH4} and D_{NO3}, in mg N kg^{-1} d^{-1}) and net N mineralization (NNM, in mg N kg^{-1} d^{-1}), which depends on the amount of soil organic N (SON, in mg N kg^{-1}). In turn, inorganic N losses are plant and microbial uptake (U_{NH4} and U_{NO3}, in mg N kg^{-1} d^{-1}) and hydrological leaching (H_{NH4} and H_{NO3}, in mg N kg^{-1} d^{-1}). Simulated concentrations of both ammonium (NH_4^+) and nitrate (NO_3^-) (in mg N kg^{-1}) change over time as a result of changes in input and output fluxes of inorganic N to and from the soil pool, and as a consequence of net nitrification (NN, in mg N kg^{-1} d^{-1}), which transforms NH_4^+ to NO_3^-. For each forest type, changes of soil N concentration over time were described as:

$$dNH_4/dt = SON \times k_{NNM} + D_{NH_4} - NH_4 \times k_{NN} - NH_4 \times k_{UNH_4} - NH_4 \times k_{HNH_4} \quad (4.1)$$

$$dNO_3/dt = NH_4 \times k_{NN} + D_{NO3} - NO_3 \times k_{UNO_3} - NO_3 \times k_{HNO_3} \quad (4.2)$$

where k_{NNM} is the first order rate for net N mineralization, k_{NN} is the rate for net nitrification, and k_U and k_H are first order rates of NH_4^+ and NO_3^- biological uptake and hydrological losses, respectively (all rates in d^{-1}). Following Brookshire et al. (2011), the model assumed that plants are N limited, and thus, plant uptake was scaled to available N. In our case, this assumption can be justified by the strong N limitation usually reported in these Mediterranean forests (Àvila and Rodà 2012). Note that our model considers biological uptake and hydrological losses separately; however, disentangling these two processes is difficult as we do not have independent empirical data to constrain each of them. Thus, we considered that the assumption of N limitation is adequate if there is a fast turnover of mineral N and strong sink strength (high values of $k_U + k_H$) for the inorganic N pool, NH_4^+ and NO_3^-. Finally, the possible nitrogen fixed by symbionts in riparian tree roots is often directly incorporated into biota, and thus, it is implicit in the model in the form of SON mineralization. As such, higher levels of SON and N mineralization in the riparian forest (see below) may be at least partly attributable to N_2 fixation.

We assumed that SON was invariant over time, because soil organic matter changes relatively slowly compared to soil N fluxes and inorganic N concentrations (Lawrence et al. 2000). Our empirical dataset support this assumption because the variation of soil organic matter content and soil C:N ratios (CV < 15%) was consistently lower than the variation of soil microbial processes (CV ~ 50-200%) for the three forests (Chapter 3). Based on available data of soil N content at Font del Regàs soils, SON in the model was fixed to 120, 54 and 60 mg N kg^{-1} for the riparian, oak and beech forests, respectively.

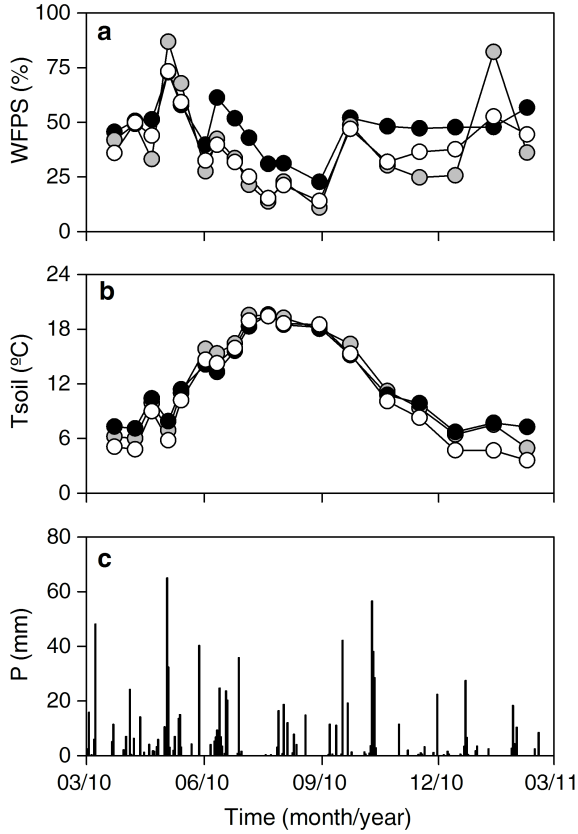

Figure 4.1 Temporal pattern of (a) soil water filled pore space (WFPS) (b) soil temperature (Tsoil) and (c) precipitation (P) during the study period. For both WFPS and Tsoil, mean values for each incubation period are shown for the riparian (black), oak (grey) and beech (white) forest.

D_{NH4} and D_{NO3} were calculated as the sum of wet and dry deposition values for each day by assuming constant dry and wet deposition over time. We used published values of annual N deposition at the Montseny Mountains as a reference (dry deposition: 4.12 and 4.04 kg N ha^{-1} yr^{-1} wet deposition: 3.36 kg N ha^{-1} yr^{-1}, for NH_4^+ and NO_3^-, respectively) (Àvila and Rodà 2012). Deposition rates were divided by soil depth (in cm) and bulk density (in g cm^{-3}) to obtain deposition values per soil weight (mg N kg^{-1} d^{-1}).

Finally, we approximated soil concentrations of NH_4^+ and NO_3^- to be in equilibrium with respect to environmental drivers and inputs from mineralization and deposition. This assumption is based on the observation that turnover times of mineral forms of N in soils are fast (approximately 1 day), and thus, equilibrate rapidly compared to changes in the driving variables (Stark and Hart 1997, Gerber and Brookshire 2014).

For each forest type, we estimated inorganic N concentrations in the soil as (equations 4.1 and 4.2 equal 0):

$$NH_4 = (SON \times k_{NNM} + D_{NH_4}) / (k_{UNH_4} + k_{HNH_4} + k_{NN}) \quad (4.3)$$

$$NO_3 = (NH_4 \times k_{NN} + D_{NO3}) / (k_{UNO_3} + k_{HNO_3}) \quad (4.4)$$

Most of existing models have formulated climate dependency of soil N processes (e.g. Raich et al. 1991, Rastetter et al. 1997, Brookshire et al. 2011). Here the first-order rates k_{NNM}, k_{NN}, k_U and k_H for each forest type were multiplied by factors that parameterize soil moisture (r_θ and r'_θ), soil temperature (r_T) and precipitation (r_P) (Raich et al. 1991, Brookshire et al. 2011), such that:

$$k_n = k_{0,n} \times r_{\theta,n} \times r_{T,n} \times r_{P,n} \quad (4.5)$$

where k_n is the first-order rate for the process n (n = NNM, NN, uptake, or leaching), $k_{0,n}$ is a constant base rate; and $r_{\theta,n}$, $r_{T,n}$ and $r_{P,n}$ are moisture, temperature and rainfall modifier for each process.

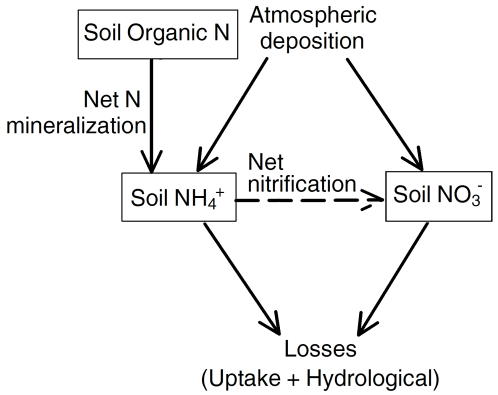

Figure 4.2 The model presented here concerns soil inorganic nitrogen (N) at the surface soil layer (0-10 cm) and the fluxes into and out of this pool (solid arrows). Inputs of soil inorganic N pool are atmospheric deposition and net N mineralization from soil organic matter. The proportion of ammonium (NH_4^+) and nitrate (NO_3^-) in the soil depends on net nitrification (dashed line). Outputs from the soil inorganic N pool are plant and microbial uptake (uptake) and infiltration and leaching (hydrological losses).

The moisture modifier (r_θ) was used as a proxy of the effect of soil water availability on k_{NNM} and k_{NN}, thus relying on the combined effect of precipitation, evapotranspiration and groundwater level. Following Brookshire et al. (2011), r_θ was parameterized as a

Gaussian function for both NNM and NN mimicking moisture limitation at low soil moisture levels and possible oxygen limitation at high levels of soil wetness. Yet rather than inferring soil moisture from stream discharge time series as in Brookshire et al. (2011), we calculated r_θ from empirically measured values of WFPS with:

$$r_\theta = 1 / (\sigma \sqrt{2\pi}) \times e^{-(\mathrm{WFPS} - \mu)^2 / (2\sigma^2)} \quad (4.6)$$

where WFPS is the water-filled pore space in percent measured at the beginning of each incubation period, μ is a parameter indicating the optimal WFPS value for each soil N process and σ is a parameter that indicates the sensitivity to changes in WFPS of each process. Values of μ close to 0 imply an overall negative effect of soil moisture on soil N processes, whereas values close to 100 indicate that soil N processes may be limited by low soil wetness for the measured moisture range. In turn, values of σ close to 0 indicate a narrow range of moisture conditions under which a given soil N process occurs, whereas large values (up to 100) indicate little sensitivity to soil moisture. r_θ is assumed to be 1 for k_U.

The rate of hydrological N losses, k_H, was modified by using a potential function to simulate an increase in leaching and infiltration during high soil moisture conditions.

$$r'_\theta = \mathrm{WFPS}^x \quad (4.7)$$

where x is the exponent representing soil moisture sensitivity. r'_θ replaces r_θ in equation (4.5). Values of x close to 0 indicate that hydrological N losses do not depend on soil moisture, whereas larger values (> 0.5) indicate that leaching and infiltration increase substantially during wet periods.

We used a Q_{10} function to estimate the temperature dependence (r_T) for k_{NNM}, k_{NN} and k_U as:

$$r_T = Q_{10}^{(\mathrm{Tsoil} - \overline{\mathrm{Tsoil}}) / 10} \quad (4.8)$$

where Tsoil is the average of the soil temperature measured empirically at the beginning and at the end of each incubation period, $\overline{\mathrm{Tsoil}}$ is the mean annual soil temperature, and Q_{10} is the factor by which soil N processes are multiplied when temperature increases by 10°C. Typically, Q_{10} values are close to 2, and thus, deviation of Q_{10} values indicates either oversensitivity or undersensitivity of soil N processes to temperature (Emmett et al. 2004). r_T is assumed to be 1 for k_H.

We further explored the influence of hydrological conditions on k_{NNM} and k_{NN}, by considering a precipitation modifier (r_P), that was used to consider the typical pulse behavior reported for microbial activity during rewetting in Mediterranean systems (Borken and Matzner 2009). The r_P was parameterized as a linear function for both NNM and NN, because empirical soil N processes increased linearly with precipitation in our data set.

$$r_P = a \times \mathrm{P} + b \tag{4.9}$$

where P is the precipitation accumulated during 24 h before each incubation period, a is the slope representing precipitation sensitivity and b is the modifier value if no precipitation occurs. Large values of a indicates that soil N processing rates sharply increase after precipitation, whereas a values close to 0 indicate that precipitation affects soil N processes only marginally. In turn, b can be interpreted as the baseline rate in absence of any precipitation pulse in the system. r_P is assumed to be 1 for k_H and k_U.

4.2.3 Model Analysis

The model was fitted to empirical observations obtained at the study site using maximum likelihood estimation (Edwards 1992). According to the present SON and climate data (year 2010), we optimized the parameter set for obtaining the best possible fit between simulated and observed values for NNM, NN and between simulated NO_3^- sinks (uptake + hydrological losses) and empirical PNL on the timeframe of the 18 incubation periods (12 months).

The likelihood (L) for the processes (j) in each incubation period (i) was calculated as follows:

$$L_{(j,i)} = \frac{d_{j,i}^{a_j-1}}{b^{a_j}\,\Gamma(a_j)}\, e^{d_{j,i}/b_j} \tag{4.10}$$

where a_j and b_j are parameters for the gamma function (Γ), which allow for non-normal error distribution (Ise and Moorcroft 2006). $d_{j,i}$ is the absolute difference between the simulated and the observed values of each process (i.e. NNM, NN and PNL) for each incubation period (n=18) ($|\,j_i^{\text{modeled}} - j_i^{\text{observed}}|$). The best model fit is achieved when the sum of the log-transformed likelihoods ($l=\Sigma(log(Lj,i))$ is maximized. To estimate model and gamma distribution parameters for optimization, we used GNU OCTAVE

functions *bfgsmin* and *gamfit*, respectively. Since optimization procedure with GNU OCTAVE depends on the first guess of the parameters, we performed a Monte Carlo simulation with 500 random draws, where the first guess was randomly chosen within a large *a priori* range for the whole suite of parameters (k_n: from 10^{-6} to 100 d^{-1}; σ, μ: from 10^{-6} to 100 %; x: from 0 to 1; Q_{10}: from 10^{-6} to 5; a, b: from 0 to 1).

To investigate the sensitivity of NNM and NN to climate factors at each forest type, base models that included all climatic modifiers were compared with reduced versions, which discount the effect of moisture, temperature or precipitation by setting the relevant modifiers to 1. To quantitatively compare these nested model versions, we used Akaike information criterion (AIC) (Akaike 1974), where $AIC = 2p - 2l$, with p being the number of parameters and l is the sum of the log-transformed likelihoods (see above). Following Burnham and Anderson (2002), we considered that the nested model with minimum AIC was the best one, that is the simplest model minimizing the loss of information. In order to compare the nested models against each other, we rescaled the AIC value ($\Delta_m = AIC_m - AIC_{best}$, where the subscripts m and *best* denote a particular and the best model, respectively) and calculated the relative likelihood ($L_r = L_m/L_{best}$, with L_m and L_{best} being the product of the likelihoods across variables and incubation periods; equation (4.10)) to assess which climatic modifier contributed the most to the best fit of the temporal pattern of either NNM or NN for each forest type (Burnham and Anderson 2002). Large values of Δ_m and small values of L_r indicate that the nested model lost significant information relative to the best model, and thus, it can be interpreted that the discounted climatic variable was a major driver of the temporal dynamics of the soil N cycle.

In order to understand the predictive power of our model, we explored the uncertainty of the parameters by assuming that the more curved the likelihood function is, the more certainty we have that we have estimated the right parameter (Burnham and Anderson 2002). The standard error (S) of each parameter (p_i) was calculated as:

$$S(p_i) = \sqrt{\left[\frac{\partial^2 L}{\partial p_i^2}\right]^{-1}} \tag{4.11}$$

where L again is the product of the likelihoods across incubation periods and variables. Since the analytical form of the likelihood function (L) is not known, we estimated the second derivative by perturbing each parameter by an arbitrary ± 10% to obtain slopes around the maximum likelihood.

Further, we evaluated the goodness of fit between empirical and simulated values of NNM and NN and between empirical PNL and simulated NO_3^- losses (uptake + hydrological) with the Nash-Sutcliffe model efficiency coefficient (*E*), which was calculated as:

$$E = 1 - \frac{\sum_{i=1}^{n}(O_i - M_i)^2}{\sum_{i=1}^{n}(O_i - \bar{O})^2} \quad (4.12)$$

where O_i is the empirical value of a particular process at the incubation period i, M_i is the simulated value and $\bar{O}$ is the mean empirical value over the entire period of length n. The E coefficient is an important determinant of the predictive power of biogeochemical models (Moriasi et al. 2007). An $E = 1$ corresponds to a perfect match of simulated to observed data, whereas an $E = 0$ indicates that the simple mean of the data has the same predictive power as the model. Finally, we validated the performance of our model by comparing an independent empirical data set of soil inorganic N concentration with simulated values. We used mean seasonal concentrations for both NH_4^+ and NO_3^- because soil N concentrations were empirically measured at the beginning of each incubation period, while our model simulated mean soil N concentration between sampling dates (average of 15 days of incubation).

4.2.4 Climate Change Scenarios

In order to understand how climate change may affect soil N dynamics in Mediterranean forests, we calculated future soil N dynamics given the predicted changes in climate for the period 2081-2100. We assumed that climatic conditions during the study period (2010-2011) were representative for the period 1986-2005 because they fall within the annual precipitation and temperature long-term average. We based our simulations on the Representative Concentration Pathway 4.5 (RCP4.5) projections for Mediterranean zones (IPCC 2013), which reported a mean annual decrease in soil moisture of 0.8 mm at 10 cm depth, and an increase in air temperature of 1.25ºC and 2.5ºC from December to May and from June to November, respectively. We considered that soil moisture will decrease equally in the three forest types because we cannot reliably estimate future effects of groundwater level on soil moisture at the riparian site. In turn, we constructed future Tsoil based on the air temperature ICPP projections, and then we inferred Tsoil values from the linear regression between observed mean daily air and soil temperature during the study period ($R^2 > 0.90$, $n = 18$).

According to RCP4.5 projections, future precipitation may not significantly differ from today for winter time (October-March) and may decrease 5% during summer (April-September). Finally, we considered that atmospheric N deposition would not change in the future as both empirical and modelling studies indicate no significant trend for this region (Àvila and Rodà 2012, Lamarque et al. 2013).

Our model is not able of addressing the larger plant-soil cycle, and we therefore do not have the means to predict future levels of soil organic matter and mineralization *per se*. We therefore developed two scenarios which bracket potential alterations of the plant-soil cycle. In our first scenario (i.e., transition), we assumed that due to climate change, the terrestrial N cycle would be in transition towards a future equilibrium, and thus, the SON stock would be similar to the present stock. This transition scenario can be justified by the small temporal variation of soil organic matter stocks over time (Lawrence et al. 2000). In our second scenario (i.e., equilibrium), we assumed that the terrestrial N cycle would be in equilibrium with the new climate regime, and thus, mean annual NNM rate would revert to present mean rates, provided that overall productivity does not change. Clearly, these assumptions are afflicted with uncertainty, but the two scenarios (transition and equilibrium) help bracketing the effects from rapid and long-term adjustments of the N cycle to climate change.

To understand how climate-induced changes in vegetation may affect future soil N budgets and soil N export, we compared the contribution of soil N dynamics of each forest to the overall catchment response according to the areal extent of each forest type for both the present and expected future scenario. Based on Peñuelas and Boada (2003), we considered complete beech-by-oak substitution by the end of this century and that future riparian forest area remains the same.

Future scenarios were based on the same 18 incubation periods as the present-day simulations but with adjusted soil organic N concentrations and climate drivers. In order to compare present and future soil N dynamics among forests, we estimated mean daily rates of both soil N processing rates and soil inorganic N concentrations. The average rates of the simulated soil N dynamics allowed us to explore the central tendency of soil N cycling. We multiplied daily soil N processing rates and mean soil inorganic N concentrations by soil bulk density (in g cm^{-3}) and soil depth (in cm) to obtain areal estimates. We then aggregated the areal values into annual averages and multiplied simulated mean annual soil N processing rates and NO_3^- concentrations of each forest type (and taking into account the changing extent of forest types in the beech-by-oak substitution scenario).

4.3 RESULTS

4.3.1 Data-Model Fusion and Model Evaluation

The empirical data set showed substantial differences in mean daily rates of soil N processing and PNL among forests. At the oak and beech forest, mean daily rates of NNM (0.625 and 0.495 mg N kg^{-1} d^{-1}), NN (0.240 and 0.067 mg N kg^{-1} d^{-1}) and PNL (0.383 and 0.135 mg N kg^{-1} d^{-1}) were low compared to rates measured at the riparian forest (1.352, 1.178 and 0.892 mg N kg^{-1} d^{-1} for NNM, NN and PNL, respectively). Moreover, the oak and beech forests showed minimum soil N processing rates in summer, contrasting with the high rates measured at the riparian forest (Figure 4.3). Consideration of climatic modifiers was essential to model-data agreement (Table 4.1), which allowed the model to capture both the magnitude and the seasonal pattern exhibited by NNM, NN and PNL for the three forest types as indicated by the high Nash-Sutcliffe (*E*) coefficients (Figure 4.3).

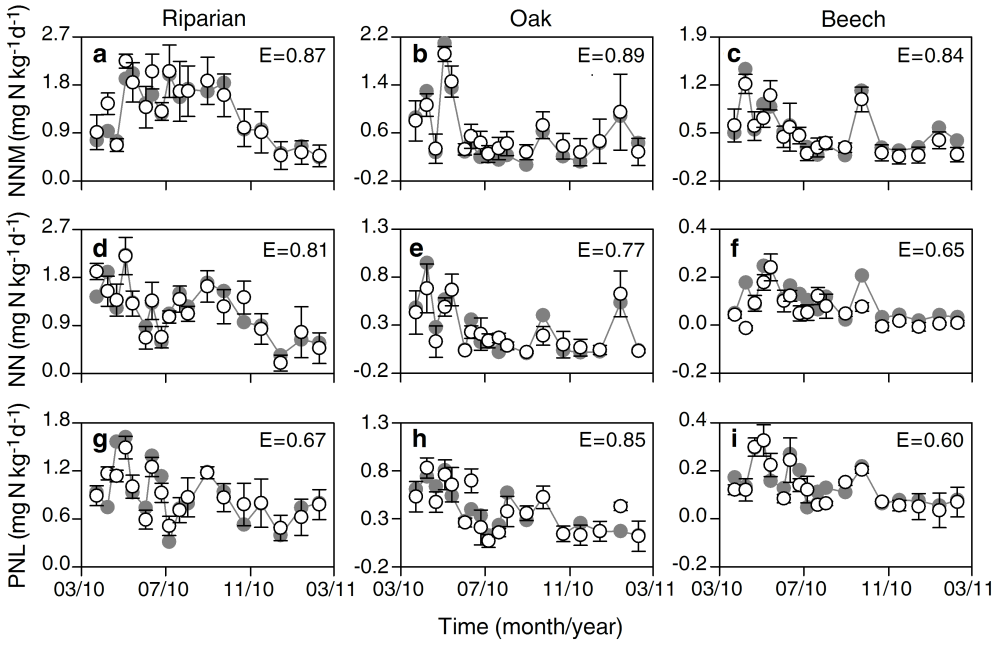

Figure 4.3 Temporal pattern of (a,b, and c) Net N mineralization (NNM), (d,e, and f) net nitrification (NN) and (g,h and i) potential nitrate losses (PNL) at the riparian, oak, and beech forest. Circles are mean values of measured soil N processing rates and error bars standard deviations. Grey circles are simulated values. The Nash-Sutcliffe model efficiency coefficient (*E*) is shown in each panel.

The good fit obtained through the data-model fusion was corroborated by the model validation process because simulated and independently measured soil inorganic N concentrations across seasons and forests yielded a high *E*, except for NH_4^+ at the beech site (Figure 4.4). In all forests, simulated mean daily concentrations differed from empirical data < 10% and < 5% for NH_4^+ and NO_3^-, respectively.

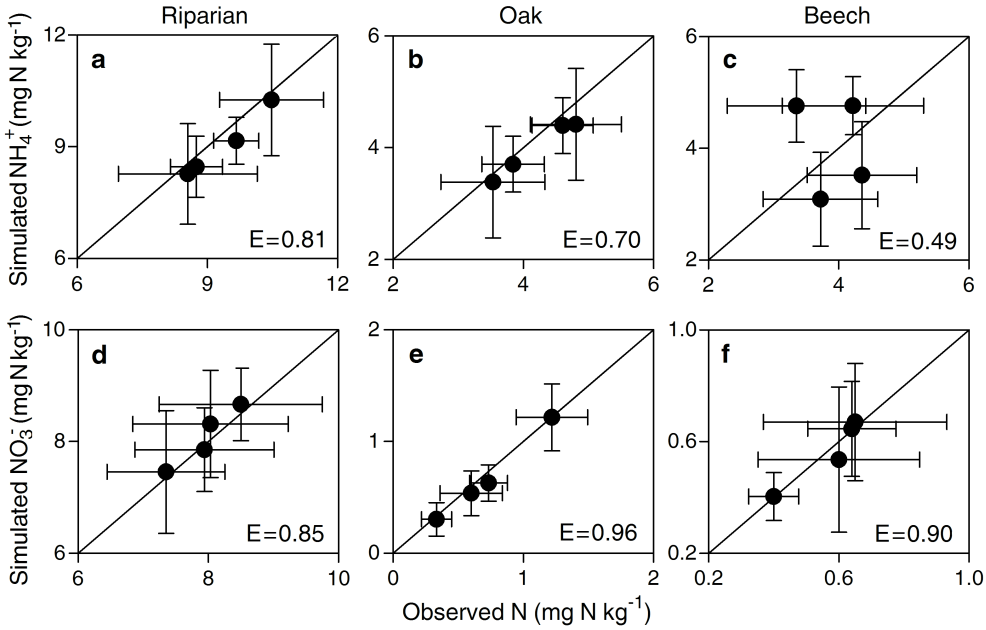

Figure 4.4 Relationship between observed and simulated concentrations of (a, b, and c) ammonium (NH_4^+) and (d, e, and f) nitrate (NO_3^-) at the surface soil layer (0-10 cm) in the riparian, oak, and beech forests. Circles are mean seasonal concentrations and error bars show the standard deviation. The 1:1 relation and the Nash-Sutcliffe model efficiency coefficient (*E*) are shown in each panel.

We calculated mean first-order rates ($\overline{k_n}$) by averaging each k_n over the 18 incubation period (Tables 4.2 and 4.3). The model-data analysis yielded distinct mean first-order rates for NNM ($\overline{k}_{NNM}$) and NN ($\overline{k}_{NN}$) being 10 fold lower for the former than for the latter. Mean $\overline{k}_{NNM}$ and $\overline{k}_{NN}$ were 40-60% lower at the beech than at the oak and riparian forests (Table 4.2). Mean NO_3^- removal rates from the mineral pool ($\overline{k}_U + \overline{k}_H$) showed small differences among forests, and were 3-5 fold higher than those for NH_4^+. In turn, mean $\overline{k}_U + \overline{k}_H$ for NH_4^+ were 15% higher for the beech than for the riparian and oak forests, indicating that NH_4^+ was more efficiently removed from the soil pool at the former than at the latter (Table 4.3).

4.3.2 Climate Sensitivity of Soil N Processes

The AIC model evaluation indicated that climatic modifiers contributed significantly to improve the model fitness (Table 4.1). For the oak and beech forest, the best fit models required all three climatic modifiers (r_θ, r_T and r_P). However, inclusion of soil moisture did not improve riparian NNM and NN to pass the AIC test. We tested the effect of individual climate modifiers by omitting one at a time from the all-inclusive base model (Table 4.1). The optimization of climatic modifiers generally yielded a bigger effect on likelihood estimation (i.e., higher values of Δ_m and lower values of L_m) for NNM than for NN, likely because model errors in NNM propagated into NN. For the riparian forest model, r_T had the strongest effect on NNM, while r_P was the most important environmental driver for NN. For the oak forest, the fitness of the model notably decreased when we excluded r_θ for both NNM and NN, whereas the effect of r_P on NN rates was small. For the beech forest model, r_θ was the dominant driver for NNM, whereas r_T and r_P were critical to improve NN.

Table 4.1 Akaike index criterion (AIC), distance between AIC_m and AIC_{best} (Δ_m) and model likelihood (L_m) for the best model (Best), the null model (no climate sensitivity, Null), the base model including the three climatic modifiers (Base) and, the reduced versions of the base model with no sensitivity to moisture ($r_\theta = 1$), temperature ($r_T = 1$) or precipitation ($r_P = 1$) for net N mineralization (NNM) and net nitrification (NN). Data are shown separately for each forest type.

Model	Riparian			Oak			Beech		
	AIC	Δ_m	L_m	AIC	Δ_m	L_m	AIC	Δ_m	L_m
Best	20.25	0.000	1.000	41.908	0.000	1.000	-17.896	0.000	1.000
Null	41.989	21.742	$<10^{-3}$	49.304	7.396	0.025	-0.844	17.052	$<10^{-3}$
Base model	28.670	8.423	0.015	41.908	0.000	1.000	-17.896	0.000	1.000
Base – r_θ NNM	24.904	4.657	0.097	60.319	18.411	$<10^{-3}$	4.125	22.021	$<10^{-3}$
Base – r_T NNM	52.653	32.406	$<10^{-3}$	50.860	8.952	0.011	-4.847	13.049	0.001
Base – r_P NNM	43.342	23.095	$<10^{-3}$	57.114	15.206	$<10^{-3}$	-5.306	12.590	0.002
Base – r_θ NN	25.343	5.096	0.078	50.842	8.934	0.011	-11.666	6.230	0.044
Base – r_T NN	36.721	16.474	$<10^{-3}$	47.952	6.044	0.049	-7.472	10.424	0.005
Base – r_P NN	49.048	28.801	$<10^{-3}$	45.450	3.542	0.170	-7.410	10.486	0.005

In Figure 4.5, we illustrate the sensitivity of each rate to individual climate variables. The model analysis revealed that the response of soil N processes to changes in WFPS differed between NNM and NN as well as among forest types (Table 4.2). The lack of response of riparian soil N processes to soil moisture contrasted with the pattern exhibited by both NNM and NN at the oak and beech forests, which were sensitive to a narrow range of moisture conditions ($\sigma < 40$) in most cases (Table 4.2). The model-data fusion yielded a sustained increase in oak NNM and beech NN for the whole range of WFPS values. In contrast, oak NN and beech NNM showed a strong reduction at WFPS < 20% and at WFPS > 66% and > 75%, respectively; yet there were only few data points at WFPS < 20% and > 60% (Table 4.2 and Figure 4.5a). Soil moisture had a positive effect on hydrological losses, being higher for NO_3^- ($x > 0.5$) than for NH_4^+ ($x < 0.05$) (Table 4.3).

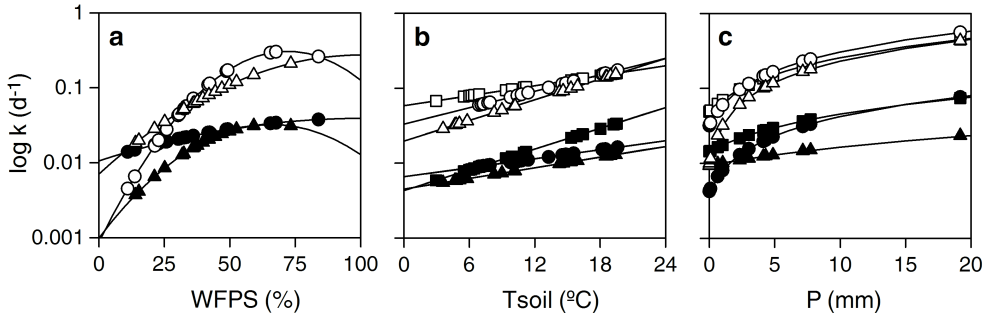

Figure 4.5 Sensitivity of first order rates (k_n) for net mineralization (black) and net nitrification (white) to (a) soil moisture (WFPS), (b) soil temperature (Tsoil) and (c) precipitation (P) at the riparian (squares), oak (circles) and beech (triangles) forests. Symbols are data for each incubation period and lines represent the considered function (Gaussian, Q_{10} and linear for moisture, temperature and precipitation, respectively). Note that first order rates are log transformed. The response of k_n to changes in a particular climatic variable was examined by setting the value of the other two climatic variables to its mean. For example, in (a), Tsoil and P equaled the average of the 18 sampling dates.

The results indicate distinct temperature sensitivity among processes and forest types, being the highest for riparian NNM and for beech NN, which showed a $Q_{10} = 2.9$ (Table 4.2). For the oak and beech forests, NN ($Q_{10} > 2$) was more sensitive to changes in temperature than NNM ($Q_{10} < 2$), whereas Q_{10} values for NN and NNM showed the opposite pattern at the riparian forest (Table 4.2 and slope in Figure 4.5b). The model fit also suggested a stronger effect of temperature on NO_3^- uptake by biota at the riparian forest ($Q_{10} = 2.5$) compared to the oak and beech forests ($Q_{10} \sim 1.8$) (Table 4.3).

Pulses of precipitation had a larger influence on microbial activity at the three forest types but especially for NN at the riparian and oak forests (slope $a > 0.07$) (Table 4.2 and Figure 4.5c). Both oak and beech NNM appeared to be little responsive to rewetting events (slope $a = 0.01$) (Table 4.2). Responses of NNM and NN to rewetting were relatively high at the riparian forest compared to upland forests (Figure 4.5c).

Table 4.2 Best fit model parameters of soil moisture sensitivity (μ, σ), temperature sensitivity (Q_{10}), precipitation sensitivity (a, b) and mean first order rates (k) for net N mineralization (NNM) and net nitrification (NN) for each forest type. Data are mean ± SD.

	Riparian		Oak		Beech	
	NNM	**NN**	**NNM**	**NN**	**NNM**	**NN**
Moisture						
μ (%)	---	---	100±7	72±5	66±4	100±5
σ (%)	---	---	62±13	21±11	25±5	37±8
Temperature						
Q_{10}	2.9±0.3	1.7±0.1	1.6±0.4	2.3±0.3	1.7±0.3	2.9±0.3
Precipitation						
a	0.05±0.01	0.10±0.01	0.01±0.01	0.07±0.02	0.01±0.01	0.05±0.01
b	0.92±0.58	0.94±0.1	0.45±0.32	0.81±1.00	0.56±0.34	0.80±0.1
Constants						
$\bar{k}$ (d^{-1})	0.011±0.007	0.114±0.058	0.012±0.009	0.121±0.024	0.008±0.006	0.077±0.021

Table 4.3 Best fit model parameters of soil moisture sensitivity (x), temperature sensitivity (Q_{10}) and mean first order rates of N losses from the soil pool ($k_U + k_H$) for both ammonium (NH_4^+) and nitrate (NO_3^-) for each forest. N losses are the sum of mean rates of biological uptake and hydrological losses. Data are mean ± SD.

	Riparian		Oak		Beech	
	NH_4^+	NO_3^-	NH_4^+	NO_3^-	NH_4^+	NO_3^-
Moisture						
x	0.01±0.02	0.71±0.4	0.05±0.07	0.80±0.5	0.05±0.04	0.62±0.5
Temperature						
Q_{10}	1.9±0.4	2.5±0.5	1.8±0.4	1.5±0.4	1.5±0.4	1.8±0.3
Constants						
$\bar{k}_U + \bar{k}_H$ (d^{-1})	0.049±0.013	0.223±0.065	0.054±0.022	0.248±0.104	0.059±0.029	0.209±0.072

4.3.3 Soil N Dynamics under Climate Change Scenarios

The application of our model projections of soil N dynamics for the period 2081-2100 revealed a distinct change for NNM and NN because each soil N process showed a different moisture and temperature sensitivity at each forest type. In the transition scenario, where we held SON constant (see Section 4.2.4), changes in mean daily NNM rates were small but differed among forest types (+8%, -12%, and -8% for the riparian, oak and beech forest, respectively) (Table 4.4). Changes in mean daily NN rates were similar or even smaller than for NNM (+6%, -8%, -8% for the riparian, oak and beech forest, respectively). While all forest types experienced the positive effect of warming, the negative effect of drying on soil transformation rates offset the positive effect of temperature in the two upland forest types. In the equilibrium scenario, where mean NNM rate reverts to the present value, the response of NN to climate change became diminishingly small for all forest types (+2%, -4%, -1% for the riparian, oak and beech forest, respectively). In accordance with change in NNM and NN, simulated soil NO_3^- concentration slightly increased by +5% (transition) and +1% (equilibrium) in the riparian forest, while it declined by -11% and -4% at the oak and beech forests, respectively (Table 4.4).

Table 4.4 Simulated mean annual rates of net N mineralization (NNM), net nitrification (NN), and soil nitrate concentration (NO_3) for the present climate, the transition phase (increased mean NNM), and the future equilibrium (mean NNM revert to present value) scenarios. Data are shown as mean ± SD.

	Riparian	Oak	Beech
NNM (mg N kg^{-1} d^{-1})			
Present	1.311 ± 0.460	0.596 ± 0.531	0.502 ± 0.374
Transition	1.421 ± 0.552	0.526 ± 0.633	0.462 ± 0.459
Equilibrium	1.311 ± 0.460	0.596 ± 0.531	0.502 ± 0.374
NN (mg N kg^{-1} d^{-1})			
Present	1.188 ± 0.458	0.264 ± 0.496	0.074 ± 0.242
Transition	1.268 ± 0.476	0.244 ± 0.530	0.068 ± 0.295
Equilibrium	1.208 ± 0.503	0.254 ± 0.586	0.073 ± 0.310
NO_3 (mg N kg^{-1})			
Present	8.10 ± 3.19	0.90 ± 1.66	0.60 ± 1.05
Transition	8.50 ± 3.54	0.80 ± 1.55	0.57 ± 1.10
Equilibrium	8.21 ± 3.85	0.81 ± 1.40	0.58± 1.04

At the catchment scale, our model projections indicated that the expected changes in climate could induce relatively small decreases in mean annual rates of NNM (-8%) and NN (-5%), and minimal changes in the soil NO_3^- pool (-4%) (black bars in Figure 4.6). This reduction is mainly caused by the negative effect of dryness in the upland forests. According to our model results, the beech-by-oak substitution expected by the end of this century could lead to small decreases in mean annual NNM (-4%) but could increase mean annual NN by +13%. As a result, modeled soil NO_3^- concentration increased slightly (+5%, white bars in Figure 4.6). The changes in NN and soil NO_3^- concentrations caused by this species substitution were similar for both the transition and the equilibrium scenarios.

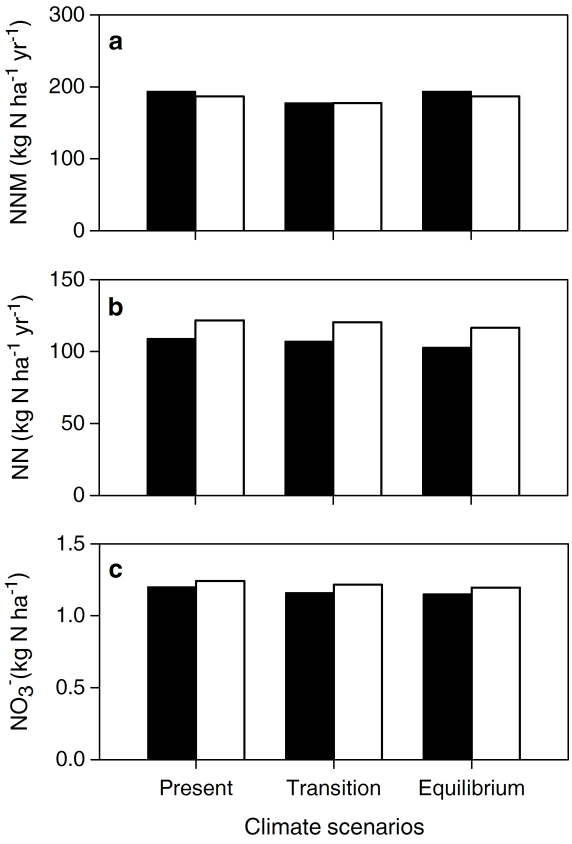

Figure 4.6 Simulated mean annual (a) net nitrogen mineralization (NNM), (b) net nitrification (NN) and (c) soil nitrate concentration (NO_3) in Font del Regàs catchment for the present climate, the transition phase (increased mean NNM), and the future equilibrium (mean NNM reverts to present value). Two vegetation cover scenarios were considered: present tree species composition (black) and a complete beech-by-oak substitution (white).

4.4 DISCUSSION

4.4.1 Data-Model Fusion

This study aimed to understand the impact of climate drivers on crucial steps in the N cycle, which are mineralization, nitrification and removal of bioavailable N (NO_3^- and NH_4^+). To this end, we fused empirical data with a simple mechanistic model of the soil N cycle to evaluate and quantify the sensitivities of Mediterranean forest ecosystems to different environmental drivers simultaneously. Our framework recreated the temporal variation in soil NO_3^- and NH_4^+ concentrations over the course of a year in three forest types. The consideration of climatic modifiers into the model improved the goodness of fit between simulated and empirical data for NNM, NN and PNL during most of the year, which supports the idea that environmental variables are crucial to understand the seasonal behavior of soil N cycling (Miller et al. 2007, Bell et al. 2008). Further, the good fit between simulated and empirical data indicates that our model was able to capture the net result of the main processes determining net rates of mineralization and nitrification. However, mismatches were observed, especially for soil NH_4^+ concentrations and NN rates at the beech forest, which possibly reflect aspects of NH_4^+ uptake not captured in our model such as transient microbial immobilization, biological NN inhibition or sorption-desorption processes (Matschonat and Matzner 1995, Trap et al. 2011). We did not consider denitrification fluxes nor were we able to constrain this process with the available empirical data. Denitrification (and the absence of this process in the model) could skew the empirical estimate of NN rates as incubation bags allow for gas exchange. However, rates of denitrification in these Mediterranean forests are low (by 10 fold or even more) compared to nitrification rates (Bernal et al. 2007), and thus, the effect of denitrification on NN signal is likely small.

Our analysis further supports the idea that processes involved in soil N cycling have a rapid response to climate because the model-data fusion yielded short residence time (~3-4 days) for both NH_4^+ and NO_3^-. This result justifies the equilibrium assumption made for soil N concentrations (Stark and Hart 1997, Gerber and Brookshire 2014). However, our results did not fully justify the assumption of chronic N limitation, at least in the riparian forest, because this forest showed weak sink strength (low $\overline{k}_U + \overline{k}_H$) for soil NH_4^+ and NO_3^- pools compared to upland soils. Such high N availability at the riparian forest could be partially explained by symbiotic N_2 fixation, a process that was not explicitly included in our model conceptualization, but that could supply extra NH_4^+ to riparian trees, increase soil organic nitrogen and ultimately enhance both

riparian NNM and NN (Booth et al. 2005, Rennenberg et al. 2009). Nevertheless, the good matches obtained indicate that the consideration of a first-order N removal rate was not incompatible with the data.

4.4.2 Response of Soil N Dynamics to Climate Variation

As expected, we found that moisture dependence of N processing rates was a key factor for improving the data-model fit at the oak and beech forests. These findings agree with previous empirical studies performed across semiarid biomes, and provide further evidence that the seasonality of soil N dynamics can strongly rely on the temporal pattern of soil moisture (Niboyet et al. 2011, Manzoni et al. 2012). Our results showed increases in soil N processes with increasing water availability, as well as strong decreases during severe dry conditions (i.e., WFPS < 20%), suggesting that extended drought periods may lead to reduced inorganic N turnover in Mediterranean biomes (Larsen et al. 2011). Similar to previous studies, we found that sensitivity to dryness and wetness differed between NNM and NN (Manzoni et al. 2012, Björsne et al. 2014), and further, that high moisture content (> 60%) could reduce soil mineralization in some forest types (Linn and Doran 1984).

In contrast to upland forests, soil moisture did not improve the model fit for the riparian forest, which suggests that water availability was not a limiting factor which was expected for riparian zones (Sleutel et al. 2008). The absence of soil moisture sensitivity was likely due to perennial moist conditions, as riparian soils kept relatively moist even in summer (WFPS > 30%), when precipitation was low and evapotranspiration rates were the highest. At our study site, riparian groundwater usually flowed well below the soil surface, and thus, hydraulic lift by fine roots was likely responsible for keeping top soil layers wet in summer (Tabacchi et al. 2000). As a consequence, riparian systems may be less vulnerable to drought than upland forests. Overall, this contrasting sensitivity to soil moisture highlights that distinct hydrologic dynamics in upland versus riparian sites ultimately lead to marked differences in soil N processing.

Temperature dependence applied for soil NNM and NN was crucial to improve the model's fitness at the three forest types, supporting the well-established idea that warming enhances microbial activity (Emmett et al. 2004, Butler et al. 2012). The obtained Q_{10} values were within the range of other observations carried out in temperate and Mediterranean systems (Emmett et al. 2004, Dessureault-Rompré et al. 2010, Novem Auyeung et al. 2013). Yet our results did not support the hypothesis that microbes adapted to cold climates would be more sensitive to changes in soil temperature

because the highest temperature sensitive ($Q_{10} \sim 3$) was exhibited by both riparian NNM and beech NN. This finding suggests that other site-specific features can influence the temperature sensitivity of soil N cycling. For instance, NNM at the oak and beech forests was less responsive to increases in temperature than riparian NNM, which could be explained by the higher moisture stress experienced by upland forests (Suseela et al. 2012, Novem Auyeung et al. 2013). Additionally, SON availability was 2 fold higher at the riparian than at the upland soils, which could further contribute to enhance riparian soil mineralization during warm periods compared to upland soils that could be substrate limited (von Lützow and Kögel-Knabner 2009, Schütt et al. 2014).

Our results further suggest that the response to changes in temperature can substantially differ between NNM and NN. We found that NN was more responsive to increases in temperature than NNM at the oak and beech forests, in line with previous empirical studies showing that warming enhances NN in forest soils by reducing both NH_4^+ and NO_3^- immobilization (Emmett et al. 2004, Rennenberg et al. 2009, Butler et al. 2012). However, this pattern was not observed in the riparian forest, which showed lower Q_{10} values for NN compared to NNM. Overall, our model supports the idea that the various processes involved in soil N cycling can respond differently to warming (Emmett et al. 2004, Bai et al. 2013). Further, our results point out that interaction between temperature and other site-specific features such as water and substrate availability is essential to understand future responses of ecosystem biogeochemical cycles to warming.

Finally, our results showed that including precipitation pulses into the model improved the goodness of fit at the three forest types. These results support the idea that rewetting episodes are essential to understand soil N cycling likely because they stimulate soil microbial activity through mobilizing soil N, the release of intracellular osmolites and the enhancement of metabolic rates (Schimel et al. 2007, Borken and Matzner 2009). In contrast to our expectation, the highest response to rewetting ($a > 0.5$) was shown by soil N processing rates in the riparian forest, which were expected to be less sensitive to increases in water availability than those in the upland soils. This seemingly counterintuitive result may be partly a modeling artefact and stems from the fact that part of a small but not model-relevant moisture effect has spilled over to a precipitation response in the riparian zone, as moisture and precipitation are somewhat correlated. As observed for soil moisture and temperature, our results point to a differential sensitivity of NNM and NN to rewetting events, being NN more responsive than NNM (as indicated by the steeper a slopes). The higher sensitivity of NN to increases in soil water availability has been previously observed and suggests that soil

NO_3^- availability may be vulnerable to changes in the amount and timing of precipitation (Groffman et al. 2009, Larsen et al. 2011). Our findings showed that rewetting episodes can be crucial to predict temporal patterns of soil N cycling, and thus, the incorporation of water pulse dynamics within terrestrial models could help to our understanding of temporal patterns of nutrient biogeochemistry in Mediterranean systems.

4.4.3 Effect of Climate Change on Soil N Cycling

We developed climate change scenarios for our sites using broad IPCC model evaluations that suggest year-round decrease in soil moisture (-0.8 mm), year-round temperature increase (+2ºC) and decreased precipitation in summer (-5%) when applying the RCP4.5 scenario. While the temperature increase would be similar to or lower than in other systems, Mediterranean forest systems are expected to experience a reduction in precipitation during summer months, which renders these regions more vulnerable to drought compared to other forested regions worldwide (IPCC 2013). Our model approximation allowed us to evaluate the effect of the expected climate change on the overall soil N cycle as the combination of simultaneous changes in the climatic drivers (soil moisture, temperature and precipitation) and the sensitivity of the different soil N processes to these drivers.

Our model calculations were based on seasonal data obtained over 1 year. The model was designed to specifically address the short-term responses of the considered soil N processes to climate variability in presence of soil organic N. Therefore, we cannot predict future levels of soil organic matter, long-term mineralization rates nor future changes in the climatic sensitivity of soil N cycling. However, given the derived sensitivity to climate drivers, the modeling framework allows us to explore how the interactive effect of moisture and temperature could affect soil N cycle in the future. The consideration of two future states of the long-term N cycle (a transition phase with fixed SON versus a steady state equilibrium with fixed mean mineralization fluxes) helps bracketing potential alterations of the long-term plant-soil cycle. Both states showed similar results under future climate scenarios, giving some consistency to the model predictions.

According to our model and our assumptions therein, the climate change projected for later in this century may have a relatively small effect on mean daily rates of soil N cycling. Our results indicate that mean NNM and NN at the riparian forest could increase by up to +8% from today's rates as a consequence of warmer temperatures, as observed for temperate systems (Rustad et al. 2001, Bai et al. 2013). Contrarily, mean

daily NNM and NN in upland forests may slightly decline in the future because the negative effect of decreases in water availability will likely outweigh the positive temperature effect. Our model simulations agree with the hypothesis that future warming and drying may have an antagonistic effect on soil N cycling and ultimately lead to minimal changes in mean NNM, NN and soil NO_3^- concentrations in these Mediterranean upland forests. Similar antagonistic effects between temperature and soil moisture have been recently reported in manipulative warming experiments in grassland systems (Liu et al. 2009, Verburg et al. 2009). Our study adds a novel piece of knowledge to the growing evidence that terrestrial ecosystems can show a complex response to climate change and that the interaction between different climatic drivers can eventually lead to less pronounced responses than previously expected (Rustad et al. 2001, Bai et al. 2013).

When projected to the catchment scale, our results suggest that expected future changes in soil N cycling would not be enough to alter soil N concentration in this Mediterranean system. Moreover, we found that future climate-induced shifts in vegetation would have a relatively small effect on both soil N fluxes and pools because oak and beech forests may respond similar to climate. Our results differ from previous studies in temperate systems that have related long-term increases in hydrological N export to warming-induced increases in mineralization (Rogora 2007, Brookshire et al. 2011). In those mesic regions, extrapolation of past climatic trends did not reveal future changes in soil moisture, and therefore, moisture did not affect function cycling rates. However, our findings revealed that soil water availability can play a pivotal role in driving soil N cycling. Although our results have to be considered with caution, our study and method provide insights into how interaction among direct and indirect climatic drivers affects soil N processing in Mediterranean catchments and stresses that future response of soil N cycle to climate change cannot be generalized among biomes or forest types.

4.5 CONCLUSIONS

Our study adds to the growing evidence demonstrating the effects of changes in climate on soil N cycling in forests ecosystems (Rustad et al. 2001, Larsen et al. 2011). To explore climate sensitivity of key soil N processes, we use a relatively short term data set (18 sampling dates over 1 year) but take advantage of suite of detailed soil N cycle measurements (soil organic and inorganic N concentrations, net N mineralization, net nitrification, and potential N losses from the soil pool). We showed that the

inclusion of climatic modifiers improves the model, supporting the idea that they are important drivers of the dynamics of the N cycle in Mediterranean systems. Soil moisture, temperature and precipitation generally have a positive effect on soil N cycling rates, although sensitivity to climatic factors differed among processes and forests. Soil moisture was the major driver of soil N cycle at oak and beech forests, but temperature and precipitation shifted soil N dynamics at the riparian forest. In most cases, net nitrification was more sensitive to changes in climate than net N mineralization; yet the response of soil N processes to climate change was often masked by antagonistic effects of moisture availability and temperature. As a consequence of this interaction between warming and drying, we found that future climate may have a small influence on mean daily soil N processing rates, which would ultimately lead to minimal variation in mean annual soil NO_3^- concentration in these Mediterranean catchments. Together, our analyses provide mechanistic insights into the sensitivity of the soil N cycle to climate variation and add to our understanding of how future changes in climate may shape soil N cycling in Mediterranean regions.

ACKNOWLEDGMENTS

We thank Sílvia Poblador, Ada Pastor and Lídia Cañas for the invaluable field and laboratory assistance. Financial supported was provided by the Spanish Government through the projects MEDFORESTREAM (CGL2011-30590) and MONTES-Consolider (CSD2008-00040-MONTES). AL was funded by the Spanish Ministry of Education, Culture and Sport (MECD) with a FPU grant (AP-2009-3711). AL received additional funds from the Spanish Government with the grant Estancias Breves FPU. SB was supported by the Spanish Ministry of Economy and Competitiveness (MINECO) with a Juan de la Cierva contract (JCI-2010-594 06397). SB received additional funds from the Spanish Research Council (CSIC) with the contract JAEDOC027. The Vichy Catalan Company, the Regàs family and the Catalan Water Agency (ACA) graciously gave us permission for at the Font del Regàs catchment.

PART III

CHAPTER 5

The Influence of Riparian Evapotranspiration on Stream Hydrology and Nitrogen Retention in a Subhumid Mediterranean Catchment

Riparian evapotranspiration (ET) can influence stream hydrology and nitrogen (N) temporal dynamics, although its relevance at the catchment scale is still poorly understood. To fill this gap of knowledge, we investigated changes in daily discharge, riparian ET, and stream water chloride (Cl^-), nitrate (NO_3^-), and ammonium (NH_4^+) concentrations in two contiguous reaches (headwater and valley) with contrasted riparian forest size in a headwater Mediterranean catchment. Additionally, riparian groundwater level (h_{gw}) was measured at the valley reach. At the two reaches, the temporal pattern of riparian ET showed a strong positive correlation with diel variations in stream discharge (ΔQ_{lost}) ($\rho > 0.95$), and a moderate negative relationship with net riparian groundwater inputs (Q_{gw}) ($\rho < -0.55$) and h_{gw} ($\rho < -0.60$). Net losses of stream water towards the riparian zone (i.e., stream hydrological retention) occurred during the vegetative period, being more frequent at the valley than at the headwater reach (59% vs. 15% of the time, respectively). According to our mass balance calculations, in-stream NO_3^- release and NH_4^+ uptake predominated at the valley reach during periods of high stream hydrological retention. These results suggest that stream hydrological retention at the valley reach was accompanied by in-stream nitrification, which may overwhelm any potential N retention by biota at the stream-riparian interface. When the valley reach was gaining water, measured solute concentrations were similar to those predicted by hydrological mixing, suggesting small differences between the chemical signature of headwater and valley riparian groundwater. Our results highlight that riparian ET was a key driver of the temporal pattern of stream discharge in this Mediterranean headwater catchment, and at the same time, questions the potential of this riparian zone as a natural filter of N loads.

With permission of: S. Poblador, E. Martí, F. Sabater and S. Bernal, who are co-authors of this study.

5.1 INTRODUCTION

The study of riparian zones has been of growing interest during last decades because they are considered hot spots of nitrogen (N) removal within catchments, and thus, they can reduce the pervasive effects of excessive anthropogenic N inputs in forested, agricultural, and urban ecosystems (Hill 1996, Pert et al. 2010). The high capacity of riparian zones for removing groundwater N derives from its unique location at the interface between upland and streams, which favors ammonium (NH_4^+) and nitrate (NO_3^-) biological uptake from shallow groundwater via plant assimilation and microbial denitrification (e.g. Clément et al. 2003, Vidon et al. 2010).

Among other things, the effectiveness of riparian zones for retaining inorganic N critically relays on the residence time of groundwater, which can strongly vary over time depending on the hydrological connectivity between upland, riparian, and stream ecosystems (Pinay et al. 2000, Mayer et al. 2007). During storms periods, the N buffer capacity of riparian zones is limited because water can rapidly move from uplands to the stream via surface runoff (Maître et al. 2003, Meixner and Fenn 2004). Conversely, N removal tends to increase during baseflow conditions because larger residence times favor the contact of groundwater with organic-rich soils (Vidon and Hill 2004a, Ranalli and Macalady 2010). However, little is known about the efficiency of riparian zones to retain upland N inputs during dry conditions, when high water demand by vegetation may reduce the hydrological connectivity between uplands and riparian zones (Ocampo et al. 2006, Covino and McGlynn 2007, Jencso et al. 2009, Detty and McGuire 2010). Some studies have suggested that low or zero water inputs from uplands can drop groundwater down, far below the organic-rich soil layers, and consequently diminish the effectiveness of riparian zones for removing groundwater N (Burt et al. 2002, Hefting et al. 2004). Other authors, however, have concluded that complete hydrological disconnection between uplands and riparian zones can favor the loss of water from the stream toward the riparian aquifer (i.e., stream hydrological retention), which can enhance denitrification of stream nitrate at the stream-riparian interface (Martí et al. 1997, Schade et al. 2002, Rassam et al. 2006). Therefore, stream hydrological retention may play a pivotal role on determining the potential for N removal in riparian zones during periods of low water availability.

Moreover, riparian trees can directly influence groundwater and stream hydrology by consuming high amounts of water during the vegetative period. Previous studies have pointed out that riparian evapotranspiration (ET) drives diel fluctuations of stream discharge and seasonal patterns of riparian groundwater table and soil moisture (Burt et

al. 2002, Brooks et al. 2009, Gribovszki et al. 2010). Thus, riparian ET could be a key element for understanding stream hydrological retention and, as a consequence, the temporal pattern of stream N concentrations and fluxes. Nevertheless, to the best of our knowledge, no studies have explored the effect of riparian ET on stream hydrological retention and its potential to modify stream N dynamics at the catchment scale. A better understanding of the interaction between riparian ET and fluxes of water and nutrients at the stream-riparian interface could be of paramount importance for water resource management, as well as for anticipating how riparian zones and stream water chemistry could respond to a decrease of the water availability induced by climate change.

This study aims to investigate the influence of riparian ET on stream hydrological retention, and its consequences on stream N concentrations and N fluxes in a headwater Mediterranean catchment. To do so, we compared whole-reach riparian tree ET between a reach with limited riparian zone (headwater reach) and a contiguous reach with well-developed riparian forest (valley reach). We expected higher riparian ET, and thus, higher stream hydrological retention at the valley reach and during the vegetative period. Moreover, we expected that stream hydrological retention would promote biological NO_3^- and NH_4^+ uptake at the valley reach, thus lowering stream inorganic N concentrations and N fluxes compared to the headwater reach.

5.2 MATERIALS AND METHODS

5.2.1 Study Site

The Font del Regàs catchment is located in the Montseny Natural Park, NE Spain (41°50'N, 2°30'E). The climate is subhumid Mediterranean, with mild winters, wet springs and dry summers. Annual precipitation is 924.7 ± 151.2 mm, and mean annual temperature averages 12.1 ± 2.5ºC (mean ± SD, period 1940-2000, Catalan Metereologic Service). Atmospheric inorganic N deposition oscillates between 15-30 kg ha^{-1} yr^{-1} (period 1983-2007; Àvila and Rodà 2012).

The catchment area is 14.2 km^2 and its altitude ranges from 500 to 1500 m above the sea level (a.s.l.) (Figure 5.1). The catchment is dominated by biotitic granite (Cartographic and Geological Institute of Catalonia) and it has steep slopes (28%). Evergreen oak (*Quercus ilex*) and European beech (*Fagus sylvatica*) forests cover the 54% and 38% of the catchment, respectively. Upland soils (pH ~ 6) are sandy, with a 4 cm deep O horizon followed by a 5 to 23 cm deep A horizon. The riparian zone covers the 6%

of the catchment area and it is almost flat (slope < 10%). The width of the riparian forest increases from 6 to 28 m along the catchment, while the total basal area of riparian trees increases from 118 to 22776 m^2 ha^{-1}. Black alder (*Alnus glutinosa*), black locust (*Robinea pseudoacacia*), hybrid sycamore (*Platanus hybrid*), European ash (*Fraxinus excelsior*), and black poplar (*Populus nigra)* are the most abundant species. Riparian soils (pH ~ 7) are sandy loam with low rock content (13%) and a 5 cm deep O horizon followed by a 30 cm deep A horizon.

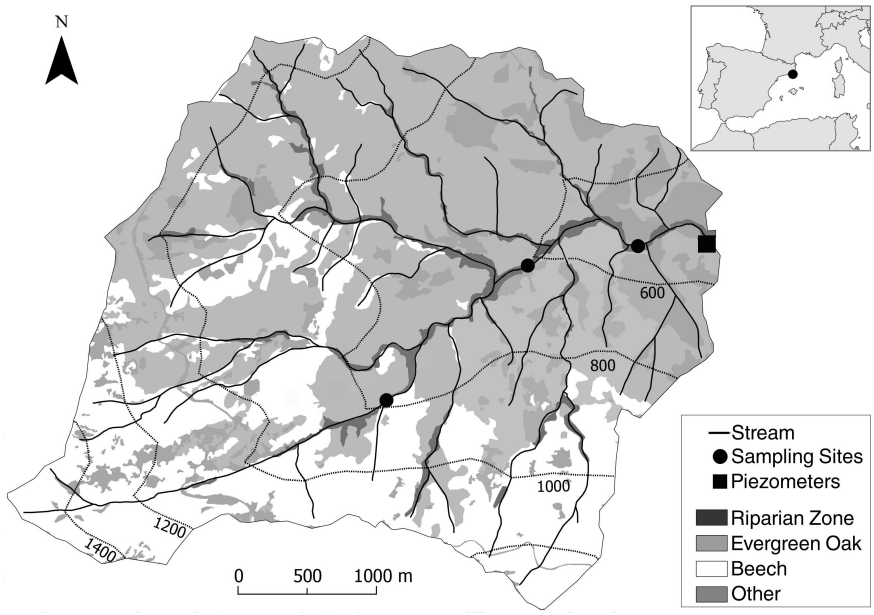

Figure 5.1 Map of the Font del Regàs catchment (Montseny Natural Park, NE Spain). The location of the three sampling sites (circles) and the riparian plot where tree transpiration and groundwater level were measured (square) are shown.

For this study, we selected three sampling sites along a stream section (up-, mid-, and down-stream), which constituted the top and the bottom of two contiguous stream reaches with contrasting riparian zone (the headwater and valley reach) (Figure 5.1). The headwater reach (750-550 m a.s.l.) was 1760 m long and drained 6.74 km^2 (Table 5.1). The reach was flanked by a 5-15 m wide riparian forest that covered 5% of the drainage area. *A. glutinosa*, *F. excelsior*, and *P. nigra* represented 51%, 26%, and 23% of the total basal area, respectively. The valley reach (550-500 m a.s.l.) was 1160 m long and drained 4.42 km^2. The reach was flanked by a 10-25 m wide riparian forest that covered 10% of the drainage area. *A. glutinosa*, *F. excelsior*, *P. nigra*, and *R. pseudoacacia*

represented 53%, 27%, 11%, and 9% of the total basal area, respectively. The two stream reaches showed well preserved channel morphology with a riffle-run structure. The streambed was mainly composed by rock (~30%), cobbles (~25%), and gravel (~15%) at the headwater reach, whereas rock (~25%), cobbles (~30%), and sand (~30%) were the dominant substrates at the valley reach. The stream channel was, on average, 2 and 3 m wide for the headwater and the valley reach, respectively.

Table 5.1 Altitude range, reach length, catchment drainage area, percentage of riparian area, width of the riparian zone, and basal area of riparian trees for the headwater and valley reaches.

	Reach characteristics			Riparian zone characteristics		
	Altitude (m a.s.l.)	Length (m)	Drainage Area (km^2)	Area (%)	Width (m)	Tree Basal Area ($m^2\ ha^{-1}$)
Headwater	733-560	1760	6.74	4.9	5-15	14.68
Valley	560-500	1161	4.42	9.9	10-25	15.76

5.2.2 Field Sampling and Chemical Water Analysis

The three sampling sites (up-, mid-, and down-stream) were monitored during two consecutive water years (from September 2010 to August 2012). Stream water level was recorded at 15 min intervals at the each sampling site with a water pressure (HOBO U20-001-04). Fortnightly, instantaneous stream discharge (Q_i, in L s^{-1}) was measured using the "slug" chloride addition technique (Gordon et al. 1992). At each sampling site, we inferred Q_i from water level measurements by estimating the linear regression between stream water level and empirically measured Q_i (n = 57, 60, and 61 for up-, mid- and down-stream sites, respectively; in all cases: $R^2 > 0.97$). In order to compare stream discharge between the two reaches, we calculated area-specific stream discharge (Q', in mm d^{-1}) by dividing daily Q_i by drainage area.

Riparian groundwater level (h_{gw}, in cm below soil surface) was recorded at 15 min intervals with a water pressure sensor (HOBO U20-001-04) in a 1.8 m long PVC piezometer (3 cm Ø) placed ~3 m from the stream channel at the down-stream site (Figure 5.1). We considered that the riparian groundwater level fluctuations at this piezometer was representative of those at the valley reach because the groundwater level differed < 6% from a set of 7 other piezometers located nearby (Poblador, unpublished data).

Stream water samples were collected daily (at noon) from each sampling site with an auto-sampler (Teledyne Isco Model 1612). From August 2010 to December 2011, stream discharge was measured every 2 months at the four permanent tributaries discharging to Font del Regàs (Figure 5.1). We used pre-acid-washed polyethylene bottles to collect water samples after triple rinsing them with stream water. All water samples were filtered (Whatman GF/F) and kept cold (< 4ºC) until laboratory analysis (< 24 h after collection). Water samples were analyzed for dissolved inorganic N (DIN) (NO_3^- and NH_4^+) and Cl^-, which was used as hydrological tracer (Kirchner et al. 2001). Cl^- was analyzed by ionic chromatography (Compact IC-761, Methrom). NO_3^- was analyzed by the cadmium reduction method (Keeney and Nelson 1982) using a Technicon Autoanalyzer (Technicon 1976). NH_4^+ was manually analyzed by the salicilate-nitropruside method (Baethgen and Alley 1989) using a spectrophotometer (PharmaSpec UV-1700 SHIMADZU).

We inventoried 14 riparian forest plots, 30 m long each (7 plots by reach, ca. 5% of the riparian area). In each plot, we identified each tree individual at species level and measured its diameter at breast height (*DBH*, in cm) and its basal area (*BA*, in cm^2) with $BA = \Pi * (DBH/2)^2$. For each tree species i, we calculated the area-specific *BA* (BA_i, in m^2 of *BA* per ha of riparian area) by dividing the total *BA* for a given species by the total area of the riparian plots of either the headwater (2.3 ha) or valley (2.1 ha) reach, respectively.

5.2.3 Riparian Evapotranspiration

From September 2010 to August 2012, we calculated diel variations in stream discharge at the up-, mid- and down-stream sites (Q_{lost}, in $m^3\ d^{-1}$). For each day, we linearly interpolated and summed up Q_i, and then subtracted this value to the stream discharge obtained by linearly interpolating maxima Q_i (measured between 0:00-3:00 h) between two consecutive days. We used only stream discharge during base flow conditions (i.e., changes in Q_i < 10% in 24 h) to avoid any confounding effect associated with storm events. We attributed Q_{lost} to water withdrawal by riparian tree roots from either the riparian aquifer or directly from the stream channel (Cadol et al. 2012). Furthermore, we considered that Q_{lost} measured at each particular site integrated the riparian ET upstream from that point, and therefore, the area-specific riparian ET (ΔQ_{lost}, in mm d^{-1}) for each reach was estimated as the difference in Q_{lost} measured at the bottom and at the top of the reach divided by the riparian area (33 and 43 ha for the headwater and valley reach, respectively).

To ensure that diel cycles in stream discharge were associated with the activity of riparian trees, we compared ΔQ_{lost} with an independent estimate of riparian ET based on sap flow measurements of the main riparian tree species (*A. glutinosa, F. excelsior*, *P. nigra*, and *R. pseudoacacia*). For each reach, we calculated area-specific riparian ET (ET_{rip}, in mm d^{-1}) with:

$$ET_{rip} = \sum_{i=1}^{n} (ET_i - BA_i) \quad (5.1)$$

where ET_i is monthly mean daily evapotranspiration (in dm^3 of water per m^2 of *BA* and day) and BA_i is the area-specific basal area (in m^2 BA ha^{-1}) of each tree species i. Values of ET for each species i were recorded at the valley of the catchment from January to August 2012 (Nadal-Sala et al., in review) (Figure 5.1). For the valley reach, we compared ΔQ_{lost} values with diel variations in h_{gw} to explore the influence of riparian ET on the riparian groundwater level.

5.2.4 Mass Balance Calculations

Net riparian groundwater inputs

The contribution of net riparian groundwater inputs to stream discharge (Q_{gw}) was estimated with:

$$Q_{gw} = Q_{bot} - Q_{top} - Q_{ef} \quad (5.2)$$

where Q_{top} and Q_{bot}, are mean daily discharge measured at the top and at the bottom of the reach respectively, and Q_{ef} is mean daily discharge at the permanent tributaries (all in L s^{-1}). For the headwater reach, Q_{top} and Q_{bot} were the discharge at the up- and mid-stream sites, respectively; while we used the discharge at the mid- and down-stream sites for the valley reach. For each stream site, mean daily discharge (Q) was the average of Q_i for each day. For estimating mean daily discharge at each tributary, we used the best fit model (log-log) between instantaneous discharge measured at each tributary and at the up-stream site within the same day (for each of the four tributaries: $R^2 > 0.92$, $n = 18$, $p < 0.001$). We considered that the stream reach was net gaining water when $Q_{gw} > 0$, while $Q_{gw} < 0$ was interpreted as a net loss of water from the stream towards the riparian zone. Therefore, $Q_{gw} < 0$ was used as an indicator of stream hydrological retention (Covino et al. 2010).

Chemical signature of riparian groundwater and stream water

We used a mass balance approach to investigate whether differences in stream water Cl^-, NO_3^-, and NH_4^+ concentrations between the headwater and valley reach could be explained by hydrological mixing. For each solute and reach:

$$Q_{bot} \times C_{bot} = Q_{top} \times C_{top} + Q_{gw} \times C_{gw} + Q_{ef} \times C_{ef} \quad (5.3)$$

where Q_{top}, Q_{bot}, Q_{ef}, and Q_{gw} are as in Eq. 5.2 (all in L s^{-1}). C_{top} and C_{bot} are daily solute concentrations measured at the top and at the bottom of the reach, respectively, and C_{gw} is daily solute concentration in riparian groundwater (all in mg L^{-1}). For $Q_{gw} < 0$, we considered that C_{gw} equaled C_{top}. C_{ef} is daily solute concentration at the tributaries, which was estimated by fitting the best fit model (log-log) between solute concentration measured at each tributary and at the up-stream site within the same day (for each of the four tributaries and for the three solute: $R^2 > 0.70$; in all cases: $n = 18$, $p < 0.001$). Although this may be a rough estimation of solute concentrations at the tributaries, it was a useful procedure for inferring riparian groundwater chemistry at daily time steps.

First, we inferred daily riparian groundwater solute concentrations at the headwater reach. To ensure that the estimated riparian groundwater chemistry was within the expected range for this catchment, we compared C_{gw} against solute concentrations measured during the same period at 7 piezometers installed along the headwater reach (< 2 m from the stream) (see Chapter 2). The three solutes showed a good match between predicted and measured concentrations, with median C_{gw} differing < 5%, 7%, and 10% for Cl^-, NO_3^-, and NH_4^+, respectively. Then, we predicted stream solute concentrations at the bottom of the valley reach (down-stream site) assuming similar riparian groundwater chemistry between the headwater and valley reach. For each day, we calculated the ratio between observed and predicted solute concentrations (Obs:Pred ratio) and we interpreted divergences from the 1:1 ratio as an indication of differences in hydrological and/or biogeochemical processes between the two reaches. For Cl^- (hydrological tracer), we expected Obs:Pred ratios close to 1 if there are no additional water sources contributing to stream discharge at the valley reach. For NO_3^- and NH_4^+, Obs:Pred < 1 and $Q_{gw} < 0$ was interpreted as in-stream biological N retention via assimilatory uptake (for NO_3^- and NH_4^+), nitrification (for NH_4^+) and/or denitrification (for NO_3^-). We interpreted Obs:Pred > 1 and $Q_{gw} < 0$ as either in-stream mineralization (for NH_4^+) or nitrification (for NO_3^-). When the stream was gaining water in net terms ($Q_{gw} > 0$), values of Obs:Pred ≠ 1 were interpreted as an indication of differences in riparian groundwater chemistry between the headwater and valley reach. We used the relative difference between measured and predicted C_{gw} at

the headwater reach as a threshold to determine when observed and predicted concentrations differed significantly from each other (±1.05, ±1.07, and ±1.1 for Cl^-, NO_3^-, and NH_4^+ concentrations, respectively).

5.2.5 Statistical Analysis

To investigate the influence of riparian ET on stream discharge and stream water chemistry, we split the data set into vegetative and dormant periods. Based on previous knowledge, we considered that the vegetative period compressed between the onset (April) and offset (October) of riparian tree evapotranspiration (Nadal-Sala et al. 2013).

For each reach, we investigated differences in Q', Q_{gw}, mean daily h_{gw} and stream solute concentrations between the two periods with a Wilcoxon rank sum test (Zar 2010). For each period, the occurrence of stream hydrological retention was calculated by counting the number of days with $Q_{gw} < 0$. For each reach, we further explored the relationship between ΔQ_{lost} and Q_{gw} with a Spearman correlation. Spearman correlation was also used to analyze the relationship between ΔQ_{lost} and mean daily h_{gw} at the valley reach.

To explore whether stream hydrological retention influenced stream NO_3^- and NH_4^+ concentrations at the valley reach, we examined the relationship between Q_{gw} and Obs:Pred ratios measured at the down-stream site with Spearman correlations. For each solute, we further compared the Obs:Pred ratio between days with $Q_{gw} > 0$ and $Q_{gw} < 0$ with a Wilcoxon rank sum test (Zar 2010).

All the statistical analyses were carried out with the R 2.15.1 statistical software (R-project 2012). We chose non-parametric statistical tests because both stream discharge and solute concentrations were not normally distributed (Shapiro test, $p < 0.05$). In all cases, differences were considered statistically significant when $p < 0.01$.

5.3 RESULTS

5.3.1 Seasonal and Diel Patterns of Stream Discharge and Whole-Reach Riparian ET

During the study period, median annual Q_i was 15.9, 53.9 and 62.4 L s^{-1} at the up-, mid- and down-stream sites, respectively. The three sites showed the same seasonal pattern, characterized by a strong decline in Q_i during the vegetative period (Figure 5.2a).

As expressed by catchment area, median annual *Q'* was 0.65, 0.53 and 0.41 mm d^{-1} at the up-, mid- and down-stream sites, respectively. In all sites, *Q'* was significantly higher during the dormant than during the vegetative period (Wilcoxon test, $p < 0.01$).

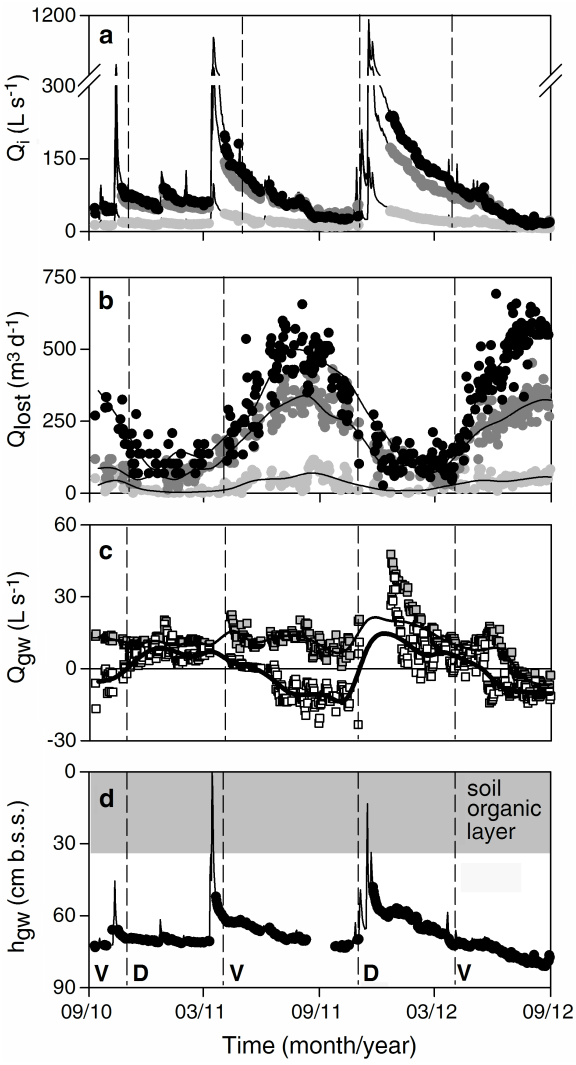

Figure 5.2 Temporal pattern of (a) stream discharge (Q_i), (b) diel cycles in stream discharge (Q_{lost}), (c) daily net riparian groundwater inputs (Q_{gw}) for the headwater and valley reach (white and grey squares, respectively), and (d) groundwater table fluctuation (h_{gw}) at the valley bottom for the period 2010-2012. In panels (a) and (b), light gray, dark gray, and black circles are values during baseflow conditions for the up- mid- and down-stream sites, respectively. In panels (b) and (c), solid lines are the running median (half-window of 7 days). In panel (c), the $Q_{gw} = 0$ line is shown as a reference; $Q_{gw} > 0$ and < 0 indicates when the stream reach was net gaining and net losing water, respectively. In panel (d), the mean soil depth of the O and A horizons is indicated. V: vegetative period, D: dormant period.

During the dormant period, diel variations in stream discharge were relatively small at the three sites, Q_{lost} accounting for < 2% of the mean daily Q_i. In contrast, Q_{lost} was high during the vegetative period, and increased along the stream, being median Q_{lost} values 36, 219 and 340 m^3 d^{-1} at the up-, mid- and down-stream sites, respectively (Figure 5.2b). At the three sites, Q_{lost} increased from April to June, peaked in summer (July-August) and then decreased until November. During the summer peak, Q_{lost} accounted for the 7%, 15% and 19% of mean daily Q_i at the up-, mid- and down-stream sites, respectively. This seasonal pattern was consistent for the two studied water years.

As expressed by riparian area, median annual ΔQ_{lost} was higher at the headwater than at the valley reach (0.52 vs. 0.32 mm d^{-1}), despite the fact that median ET_{rip} was similar in the two reaches (1.33 vs. 1.71 mm d^{-1}) (Figure 5.3a). There was a strong and positive relationship between ET_{rip} and ΔQ_{lost} for both the headwater and valley reach (in the two cases, linear regression [l.r.], $R^2 > 0.95$, $p < 0.001$, $n = 8$) (Figure 5.3a). Both ET_{rip} and ΔQ_{lost} peaked in summer (July-August) and showed minima in winter (January-March). At the valley reach, there was a moderate and positive relationship between ΔQ_{lost} and diel variations in h_{gw} (l.r., $R^2 = 0.53$, $p < 0.001$, $n = 277$).

5.3.2 Net Riparian Groundwater Inputs and Groundwater Table Elevation

During the study period, median annual Q_{gw} was positive at the headwater reach (11.2 L s^{-1}), but negative at the valley reach (-0.5 L s^{-1}). Values of Q_{gw} were lower for the vegetative than for the dormant in the two reaches (Table 5.2), though the valley reach exhibited larger differences in Q_{gw} between periods (Figure 5.2c). The two reaches showed a negative correlation between Q_{gw} and ΔQ_{lost} (headwater: Spearman coefficient [ρ] = -0.57, $p < 0.001$, $n = 273$; valley: $\rho = -0.79$, $p < 0.001$, $n = 286$) (Figure 5.3b).

Stream hydrological retention ($Q_{gw} < 0$) was frequent at the valley reach compared to the headwater reach (27% vs. 4% of the time) (Table 5.2). At the valley reach, $Q_{gw} < 0$ occurred during 59% of the time during the whole vegetative period, while it was detected only during mid-summer (July and August) at the headwater reach (15% of the time). There were no days with $Q_{gw} < 0$ during the dormant period at any of the two reaches.

At the down-stream site, median annual h_{gw} was 70 cm b.s.s., being values lower during the vegetative than during the dormant period (Figure 5.2d and Table 5.2). Moreover, there was a moderate negative correlation between mean daily h_{gw} and ΔQ_{lost} ($\rho = -0.60$, $p < 0.001$, $n = 277$).

Table 5.2 Net groundwater inputs to stream discharge (Q_{gw}), number of days with Q_{gw} < 0 and groundwater depth (h_{gw}) for the vegetative and dormant period, respectively. The number of cases is shown in parentheses for each group. For each variable, the asterisk indicates statistically significant differences between the two periods (Wilcoxon rank sum test, * p < 0.01). For Q_{gw} and h_{gw}, data is shown as median ± interquartile range [25th, 75th].

		Vegetative	Dormant
Q_{gw} (L s^{-1})	Headwater	10.4 [6.9, 13.2] (373)	11.8 [10.4, 15.7] (237)*
	Valley	-5.3 [-10.1, 2.1] (373)	6.0 [3.6, 9.0] (237)*
Q_{gw} < 0 (days)	Headwater	57 (373)	0 (237)
	Valley	219 (373)	0 (237)
h_{gw} (cm b.s.s.)	Headwater	—	—
	Valley	72.3 [68.7, 76.2] (256)	69.6 [65.3, 70.7] (189)*

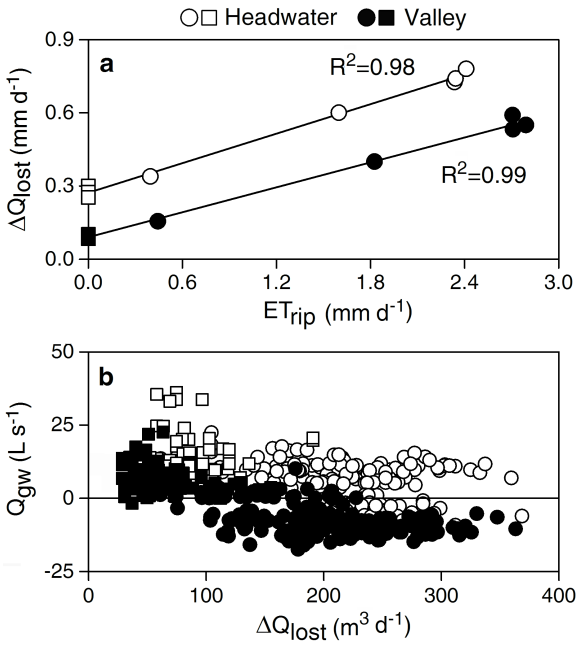

Figure 5.3 Relationship between (a) the monthly mean of daily riparian evapotranspiration estimated from sap-flow data (ET_{rip}) and the difference in diel discharge variation between the top and the bottom of each stream reach (ΔQ_{lost}), and (b) ΔQ_{lost} and daily net riparian groundwater inputs (Q_{gw}) for the headwater (white) and valley (black) reaches. Data is shown separately for the vegetative (circles) and dormant (squares) period. The linear regression and the R^2 are indicated in (a). In (b), the Q_{gw} = 0 line is shown as a reference; Q_{gw} > 0 and < 0 indicates when the stream reach was net gaining and net losing water, respectively.

5.3.3 Stream Solute Concentrations

During the study period, stream Cl^- concentration was lower at the up- than at the mid- and down-stream sites during both the vegetative and dormant periods (Figure 5.4a). The up-stream site showed no differences in stream Cl^- concentration between the two periods, while the mid- and down-stream sites showed lower Cl^- concentration during the dormant than during the vegetative period (Table 5.3). The highest stream NO_3^- concentration was observed at the up-steam site and the lowest at the mid-stream site (Figure 5.4b). Stream NO_3^- concentration was higher during the dormant than during the vegetative period at the up- and mid-stream sites, while no seasonal pattern was observed at the down-stream site (Table 5.3). Stream NH_4^+ concentration tended to decrease from the up- to the down-stream site (Figure 5.4c). The three sites showed higher stream NH_4^+ concentration during the vegetative than during the dormant period (Table 5.3).

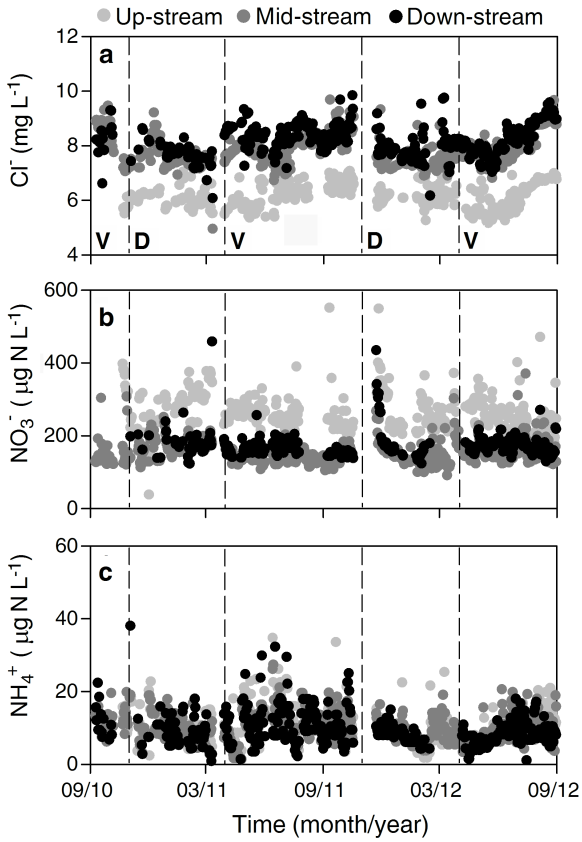

Figure 5.4 Temporal pattern of stream water concentration for (a) chloride, (b) nitrate, and (c) ammonium for the up- (light gray), mid- (dark gray), and down-stream (black) sites for the period 2010-2012. V: vegetative period, D: dormant period.

Table 5.3 Median and interquartile range [25th, 75th] of stream solute concentrations at each sampling site for the vegetative and dormant periods. The number of cases is shown in parentheses for each group. The asterisks indicate statistically significant differences between the two periods (Wilcoxon rank sum test, * $p < 0.01$).

		Vegetative	Dormant
Cl^- (mg L^{-1})	Up-stream	6.1 [5.7, 6.5] (281)	6.0 [5.8, 6.2] (176)
	Mid-stream	8.0 [7.7, 8.4] (333)	7.4 [7.2, 8.6] (220)*
	Down-stream	8.3 [7.9, 8.8] (302)	7.7 [7.5, 7.8] (184)*
NO_3^- (µg N L^{-1})	Up-stream	238 [216, 247] (284)	238[212, 298] (202)*
	Mid-stream	149 [141, 164] (324)	166[152, 190] (234)*
	Down-stream	166 [156, 180] (300)	168 [150, 186] (184)
NH_4^+ (µg N L^{-1})	Up-stream	10.8 [8.2, 14.4] (281)	9.2 [6.8, 10.8] (170)*
	Mid-stream	10.0 [7.2, 13.7] (344)	8.7 [6.6, 10.8] (229)*
	Down-stream	9.2 [6.8, 12.7] (310)	8.0 [6.3, 10.4] (147)*

5.3.4 Comparison between Observed and Predicted Stream Solute Concentrations at the Down-stream Site

During the study period, there was a good match between observed stream Cl^- concentrations at the down-stream site and those predicted by hydrological mixing as indicated by Obs:Pred ratios ~ 1 (Figure 5.5a). For NO_3^-, Obs:Pred ratios were closer to 1 during the dormant period, while increased substantially during the vegetative period (from 1.09 to 1.95) (Figure 5.5b). For NH_4^+, Obs:Pred ratios were higher during the dormant period (~1.15) than during the vegetative period (from 0.29 to 0.87) (Figure 5.5c).

The relationship between Obs:Pred ratios and Q_{gw} was null for Cl^- ($\rho = 0.2$, $p > 0.05$), negative for NO_3^- ($\rho = 0.61$, $p < 0.001$) and positive for NH_4^+ ($\rho = 0.59$, $p < 0.001$) (Figure 5.6). For NO_3^-, Obs:Pred ratios were significantly higher for $Q_{gw} < 0$ than for $Q_{gw} > 0$, while the opposite pattern was observed for NH_4^+ (for the two solutes: Wilcoxon test, $Z > Z_{0.05}$, $p < 0.001$) (Figure 5.6b and Figure 6.5c).

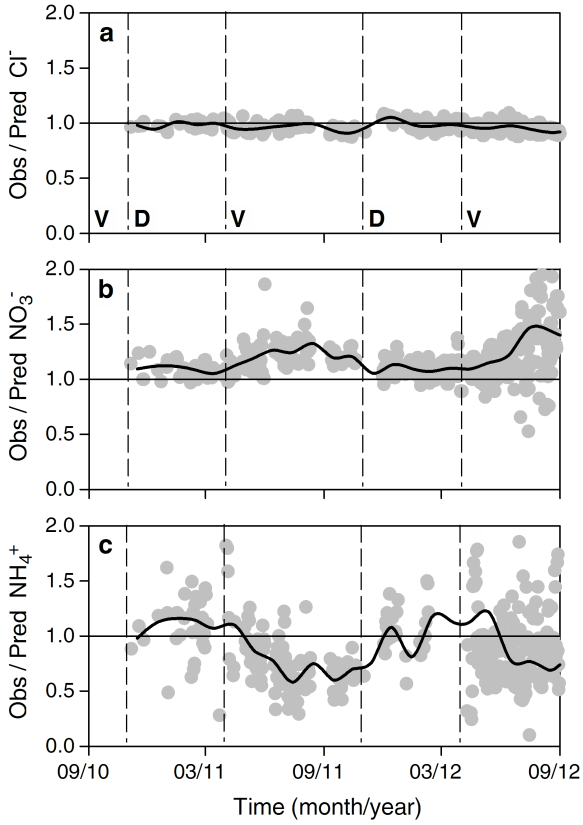

Figure 5.5 Temporal pattern of the ratio between observed stream solute concentration at the bottom of the valley reach (down-stream site) and those predicted from hydrological mixing for (a) chloride, (b) nitrate and (c) ammonium during the period 2010-2012. Bold lines indicate the running median (the half-window is 7 days). The Obs:Pred =1 line is indicated as a reference. V: vegetative period, D: dormant period.

5.4 DISCUSSION

5.4.1 Influence of Riparian ET on Stream and Riparian Groundwater Hydrology

Our results revealed that riparian ET can strongly influence stream and riparian groundwater hydrology, though its influence on catchment hydrology varies depending on the time scale considered. On a sub-daily basis, the strong relationship between ET_{rip}, diel variations in h_{gw}, and ΔQ_{lost} suggests that riparian vegetation was driving diel fluctuations in stream discharge likely by extracting water from the riparian aquifer

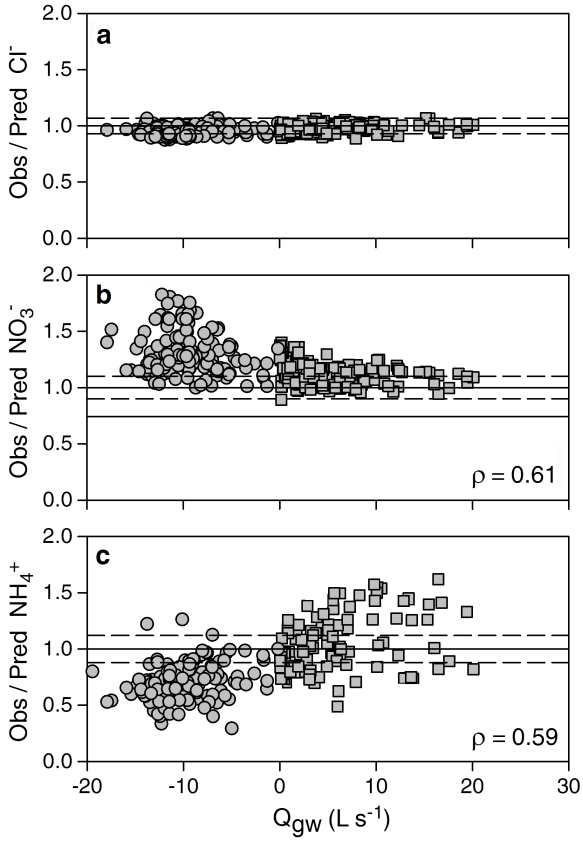

Figure 5.6 Relationship between mean daily net groundwater inputs (Q_{gw}) and the ratio between stream concentrations observed at the bottom of the valley reach (down-stream site) and those predicted from hydrological mixing for (a) chloride, (b) nitrate and (b) ammonium. Data is shown separately for the vegetative (circles) and dormant (squares) period. The Spearman coefficient is shown in each case. The solid line indicates no differences between observed and predicted concentrations, and the dashed lines indicate the uncertainty associated to the zero line as explained in the material and methods section.

Lundquist and Cadol 2002, Gribobski et al. 2010). However, the fact that values of (ΔQ_{lost} were lower than those of ET_{rip} suggest that riparian trees fed also on soil water, which concurs with previous studies showing that some riparian tree species can obtain between 30-90% of their water requirements from the surface soil (0-50 cm depth) (Snyder and Williams 2000, Sánchez-Pérez et al. 2008, Brooks et al. 2009). On a seasonal basis, riparian ET influenced the temporal pattern of both stream and groundwater hydrology because ΔQ_{lost} was negatively related to both Q_{gw} and mean daily h_{gw}. In agreement, previous studies have reported that riparian water demand (0.5-5 mm d^{-1}) can severely diminish the groundwater table (Schilling et al 2007, Sabater and Bernal

2013) and decrease the amount of groundwater entering to streams by 30-100% (Dahm et al. 2002, Kellogg et al. 2008, Folch and Ferrer 2015). On an annual basis, riparian ET (350-450 mm yr^{-1}) was small compared to published values of ET for other riparian forest worldwide (400-1300 mm yr^{-1}; Scott et al. 2008) as well as compared to oak and beech upland forests (600-900 mm yr^{-1}) (Àvila et al. 1996, Llorens and Domingo 2007). These relatively low values, together with the fact that riparian forests occupied a small area of the catchment (6%), resulted in a minimal contribution (4.5%) of riparian ET to the annual catchment water budget.

From a network perspective, we found that the influence of riparian ET on stream hydrology varied along the stream continuum, likely due to changes in the balance between water availability and water demand. At the up-stream site, maxima Q_{lost} values (7% of mean daily Q_i) were similar to those values reported for systems with no water limitation (Bond et al. 2002, Cadol et al. 2012), while maxima Q_{lost} values for the down-stream site (19% of mean daily Q_i) were close to those reported for water-limited systems (Lundquist and Cayan 2002). These differences along the longitudinal pattern are likely resulting from the strong gradient in temperature and moisture that characterizes these mountainous headwater catchments. Moreover, we found that stream hydrological retention occurred mostly at the valley reach, where riparian forest was well developed and riparian water requirements were likely the highest (Covino and McGlynn 2007, Montreuil et al. 2011, Bernal and Sabater 2012). However, the riparian zone at the valley reach was larger and flatter, and the stream was wider compared to the headwater reach. Thus, the increase in stream hydrological retention along the stream could also be favored by other factors such as longitudinal changes in channel geomorphology, riparian topography, upland-riparian hydrological connectivity, and in the hydraulic gradient between the riparian aquifer and the stream (Vidon and Hill 2004a, Duval and Hill 2006, Jencso et al. 2009, Detty and McGuire 2010, Covino et al. 2010). Overall, these results indicate that, despite being insignificant for catchment water budgets, riparian ET can exert a strong influence on diel and seasonal patterns of stream discharge and riparian groundwater due to the proximity and the strong hydrological connectivity between these two ecosystems.

5.4.2 Influence of Stream Hydrological Retention on Stream N Concentrations

In contrast to our expectation, the prevalence of stream hydrological retention during the vegetative period at the valley reach was accompanied by in-stream NO_3^- release rather than by in-stream NO_3^- uptake (Obs:Pred ratios > 1). This pattern conflicts with

previous studies showing that losing reaches tend to promote in-stream NO_3^- uptake (Rassam et al. 2006, Duval and Hill 2007, Bernal and Sabater 2012). Biological NO_3^- uptake associated with the hydrological retention of stream water occurs when a large volume of water flows directly from the stream into the rhizosphere and/or organic-rich soils, and also when stream N remains long time in the anoxic water storage zones within the stream-riparian interface (Martí et al. 1997, Schade et al. 2005). At Font del Regàs, however, there was a permanent disconnection between riparian groundwater and surface soil layers, which may have limited the occurrence of microbial denitrification and plant NO_3^- uptake (Burt et al. 2002, Hefting et al. 2004).

Furthermore, our results suggest that in-stream nitrification prevailed at the valley reach because in-stream NO_3^- release was accompanied by NH_4^+ uptake (Obs:Pred > 1 and < 1 for NO_3^- and NH_4^+, respectively). Previous studies have reported sustained in-stream nitrification either in well-oxygenated, slow water flowing, hyporheic zones (Jones et al. 1995, Dent et al. 2007) or when stored leaf packs are rich in organic N and labile carbon (Starry et al. 2005, Mineau et al. 2011). The two aforementioned explanations suite at Font del Regàs because the valley reach had extra inputs of N-rich leaf litter (Bernal et al. 2015), a well-oxygenated hyporheic zone (~7 mg O_2 L^{-1}, unpublished data), and low discharge during periods of $Q_{gw} < 0$ (< 30 L s^{-1}). Alternatively, differences in NO_3^- and NH_4^+ concentrations between the headwater and the valley reach could be explained by hydrological mixing with unaccounted water sources, such as deeper groundwater (Clément et al. 2003) or riparian N-rich soils (Hill 2011). However, these two explanations were discarded because small mismatches between observed and predicted Cl^- concentrations indicate that the mixing model included the main water sources contributing to stream discharge. Moreover, vertical hydrological disconnection was persistent in the riparian zone, suggesting that leachates from surface organic soils did not likely reached the stream during base flow conditions.

During the dormant season, when the two reaches gained water from the riparian aquifer, observed stream NO_3^- and NH_4^+ concentrations at the down-stream site were similar to those predicted by hydrological mixing, suggesting small differences in the chemical signature of headwater and valley riparian groundwater inputs. This finding does not support the idea that the riparian zone was buffering riparian groundwater N concentrations at the valley reach. This unexpected result could be explained by limited riparian denitrification given that NO_3^- availability was low in groundwater arriving from uplands (< 1 mg L^{-1}; unpublished data) and that groundwater and organic-rich soils were hydrologically disconnected from each other (Bernal et al. 2007, Harms et al. 2009, (Vidon et al. 2010, Montreuil et al. 2010). Alternatively, N removal from riparian

groundwater could be counterbalanced by in-stream N mineralization, an explanation that is not supported by the fact that riparian groundwater and stream NO_3^- concentrations were similar during the dormant period (Bernal et al. 2015).

Ultimately, the potential of in-stream processes to modify N fluxes at the catchment scale depends on the net result of hydrological and biogeochemical processes. For example, during the vegetative period, the median NO_3^- input to and output from the valley reach were practically analogous (8.8 and 8.9 mg N s^{-1} respectively). If instead, one considers no changes in stream NO_3^- concentration along the reach (i.e., no increases in in-stream nitrification at the valley reach compared to the headwater reach), stream NO_3^- flux would have decreased by 15% as a result of the increase in stream hydrological retention. In contrast, there were no changes in stream NO_3^- flux along the valley reach during the dormant period, because input and output stream discharge and NO_3^- concentrations were similar (Q_i = 110 vs. 113 L s^{-1} and NO_3^- = 0.166 vs. 0.168 mg N L^{-1}). These back-of-the-envelope calculations highlight that this headwater stream was acting as a hot spot of nutrient processing during the vegetative period, when in-stream nitrification likely overwhelmed the expected decrease in stream solute fluxes associated with increments in stream hydrological retention.

5.5 CONCLUSIONS

Our study adds to the growing evidence demonstrating that riparian ET is a key process for understanding temporal patterns of stream discharge and hydrological processes at the stream-riparian interface in headwater catchments, despite its modest contribution to annual water budgets (Medici et al. 2008, Folch and Ferrer 2015). Riparian ET exerted a strong control on the temporal pattern of net groundwater inputs and stream discharge across daily and seasonal scales. From a network perspective, the influence of riparian ET on stream hydrology increased along the stream continuum and promoted stream hydrological retention at the valley reach. In contrast to previous studies, high stream hydrological retention was associated with increases in in-stream nitrification likely because of the combined effect of low stream flows, large stocks of N rich leaf litter and well oxygenated hyporheic zones. In addition, we found no clear evidence for the riparian zone acting as a buffer of riparian groundwater N concentrations during the dormant period. This study highlights that riparian ET plays a pivotal role on regulating hydrological processes at the upland-riparian-stream interface and, at the same time, questions the N buffering capacity of this Mediterranean riparian zone.

ACKNOWLEDGMENTS

We are thankful to Ada Pastor and Lídia Cañas for their invaluable assistance in the field, and to Daniel Nadal for providing data on riparian tree evapotranspiration. Financial supported was provided by the Spanish Government through the projects MEDFORESTREAM (CGL2011-30590) and MONTES-Consolider (CSD2008-00040-MONTES). AL was supported by a FPU PhD fellowship from the Spanish Ministry of Education and Science (AP-2009-3711). SB work was funded by the Spanish Research Council (JAE-DOC027), the Spanish CICT (Juan de la Cierva contract JCI-2008-177), European Social Funds (FSE), and the MEDFORESTREAM and NICUS (CGL-2014-55234-JIN) projects. SP was supported by a FPI PhD fellowship from the Spanish Ministry of Economy and Competitiveness (BES-2012-054572). We also thank site cooperators, including Vichy Catalan and the Catalan Water Agency (ACA) for permission to sample at the Font del Regàs catchment.

CHAPTER 6

Green Light: Gross Primary Production Influences Seasonal Stream Nitrogen Exports by Controlling Fine-Scale Nitrogen Dynamics

Monitoring nitrogen (N) concentrations at fine-scale temporal resolution contributes to a better understanding of N cycling in stream ecosystems. However, the mechanisms underlying fine-scale N dynamics and its implications for budget catchment fluxes are still poorly understood. To gain understanding on patterns and controls of fine-scale stream N dynamics, we explored diel variation in stream nitrate (NO_3^-) concentration along a headwater stream with increasing riparian area and channel width. At the down-stream site, the highest day-night variations occurred in early-spring, when stream NO_3^- concentrations were 13% higher at night than at day. Such day-night variations were strongly related to daily light inputs ($R^2 = 0.74$) and they showed an excellent fit with day-night NO_3^- variations predicted from gross primary production (GPP) ($R^2 = 0.85$). These results suggest that diel NO_3^- variations were mainly driven by photoautotrophic N uptake. Terrestrial influences were discarded because no simultaneous diel variations in stream discharge, riparian groundwater level, or riparian solute concentration were observed. In contrast to the down-stream site, no diel NO_3^- variations occurred at the up-stream site likely because water temperature was colder (10 vs. 12 ºC) and light availability was lower (4 vs. 9 mol m^{-2} d^{-1}). Although daily GPP was between 10-100 fold lower than daily respiration, photoautotrophic N uptake contributed to a 10% reduction in spring NO_3^- loads at the down-stream site. Our study clearly shows that the activity of photoautotrophs can substantially change over time and along the stream continuum in response to key environmental drivers such as light and temperature, and further, that its capacity to regulate diel and seasonal N fluxes can be important even in low productivity streams.

Original work: Lupon, A., E. Martí, F. Sabater and S. Bernal. 2015. Green light: Gross primary production influences seasonal stream nitrogen exports by controlling fine-scale nitrogen dynamics, Ecology (in press)

6.1 INTRODUCTION

Human activity has doubled the availability of bioreactive nitrogen (N) worldwide, which compromises the function and biodiversity of terrestrial and freshwater ecosystems, as well as soil and water quality (Schlesinger 2009, Sutton et al. 2011). Nonetheless, biological activity can transform and retain a substantial amount of N inputs, and thus, reduce the pervasive effects of excessive N in ecosystems (Bernhardt et al. 2002, Goodale et al. 2004). Within catchments, biogeochemical processes occurring at upland, riparian and aquatic ecosystems simultaneously contribute to N cycling and retention, and ultimately determine N export downstream (Bernhardt et al. 2005). In particular, there is a growing body of research demonstrating that streams and rivers have a high capacity to transform and retain N (Peterson et al. 2001, Tank et al. 2008), even though their ability to influence N export from catchments to downstream ecosystems is still under debate (Brookshire et al. 2009). This is mostly because water chemistry of stream and rivers integrates biogeochemical processes occurring at different spatial and temporal scales throughout the catchment, which complicates assessing the relative influence of in-stream and terrestrial processes on N exports (Sudduth et al. 2013). A better understanding of the mechanisms and drivers of N dynamics within fluvial ecosystems is critical to evaluate their capacity to modify N inputs from terrestrial sources.

Nitrate (NO_3^-) is the predominant form of dissolved inorganic N (DIN) in fluvial ecosystems, and its uptake is mainly controlled by the metabolic activity of stream biota (Hall and Tank 2003, Mulholland et al. 2008a). Recently, monitoring at fine-scale temporal resolution in streams has provided examples of the close link between gross primary production and NO_3^- uptake (e.g. Johnson et al. 2006, Roberts and Mulholland 2007, Heffernan and Cohen 2010). These studies have found an inverse relationship between fine-scale stream NO_3^- and dissolved oxygen (DO) concentrations, where lower NO_3^- and higher DO were observed during day time compared to night time. This diel pattern of stream NO_3^- concentration has been mainly associated with photoautotrophic activity because the assimilation of NO_3^- by benthic algae needs light energy to reduce this form of DIN to ammonium (Huppe and Turpin 1994). However, diel NO_3^- patterns can also be driven by other processes such as diel fluctuations of riparian groundwater (Flewelling et al. 2013), diurnal in-stream nitrification (Gammons et al. 2011) and nocturnal in-stream denitrification (Baulch et al. 2012). Therefore, elucidating the potential mechanisms controlling diel variations in stream nutrient concentration remains a great challenge in stream ecology (Scholefield et al. 2005, Pellerin et al. 2009). Moreover, the potential of fine-scale N dynamics to vary catchment N fluxes is still

poorly understood because studies so far have been mainly performed during short time periods and within individual reaches.

The goal of this study was to investigate patterns and controls of diel variation in stream NO_3^- concentration and to assess how these diel fluctuations influence N fluxes along a stream continuum with increasing riparian area and channel width. We hypothesized that stream metabolism would drive diel variations in stream NO_3^- concentration. We also expected a positive relationship between daily GPP and diel variations in stream NO_3^- concentration if photoautotrophic activity was the major control of fine-scale N dynamics. In this case, the largest diel NO_3^- variations would be observed during spring and at the downstream-most site, which is the widest site and also the most exposed to light. Conversely, if heterotrophic activity is the main control of fine-scale N dynamics, diel NO_3^- variations would be positively related to ecosystem respiration (ER). Since stream water chemistry integrates processes occurring within the entire catchment, we also considered the alternative hypothesis that terrestrial or riparian processes would control fine-scale N patterns. In this case, we expected a positive relationship between diel variations in NO_3^- concentration in the stream and in riparian groundwater inputs, especially during the vegetative period when water and nutrient uptake by trees is the highest.

To evaluate these hypotheses, we measured diel variations in stream NO_3^- concentration together with stream metabolism, discharge, stream conservative tracer concentration (chloride), and riparian groundwater level and chemistry. Results from this study highlight the relevance of fine-scale temporal nutrient dynamics to understand the mechanisms underlying in-stream nutrient cycling, as well as to assess patterns of in-stream N removal and catchment nutrient fluxes at long-term scales.

6.2 MATERIALS AND METHODS

6.2.1 Study Site

The research was conducted at the Font del Regàs stream, which drains a 14.2 km^2 catchment in the Montseny Natural Park, NE Spain (41°50'N, 2°30'E, 500-1500 m above sea level (a.s.l.)) (Figure 6.1). The catchment is dominated by biotitic granite and it is mainly covered by evergreen oak (*Quercus ilex*) and European beech (*Fagus sylvatica*) forests (Cartographic and Geological Institute of Catalonia). The climate of the area is typical subhumid Mediterranean, with mild winters and warm summers. The meteorological station located at the study catchment recorded a mean annual

precipitation of 972 ± 141 mm (mean ± SD) during the period of study (2010-2012), which falls within the long-term mean for this region (925 ± 151 mm, period: 1940-2000). Similarly, mean annual temperature during the study period (13.0 ± 6.1ºC) was close to the long-term mean (12.1 ± 2.5ºC, period: 1940-2000).

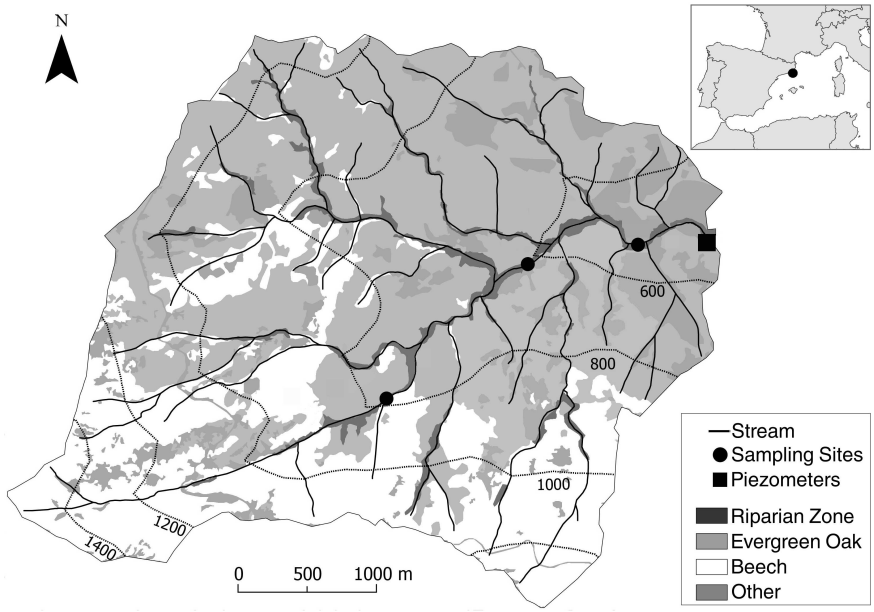

Figure 6.1 Map of the Font del Regàs catchment (Montseny Natural Park, NE Spain). The location of the three sampling sites along the stream continuum is shown with circles. The up-stream site was located 0.6 km upstream of the first tributary discharging to the mainstream. The mid- and down-stream sites were located 1.7 and 2.9 km downstream of the up-stream site, respectively. The piezometer located in the riparian area of the down-stream site is shown with a square.

We selected three sampling sites along 3 km of the Font del Regàs stream (Figure 6.1). The up-stream site (800 m a.s.l., 2.4 km from headwaters) was 1.7 m wide stream with a poorly developed riparian forest composed of *F. sylvatica* and *Q. ilex*. The mid-stream site (650 m a.s.l., 4.1 km from headwaters) was a 2.5 m wide stream flanked by a mixed forest of typically riparian tree species such as *Alnus glutinosa* and *Fraxinus excelsior*. The down-stream site (500 m a.s.l., 5.3 km from headwaters) was the widest (wetted width was 3.1 m) and it had a well-developed riparian forest (~30 m wide) consisting mainly of *Robinea pseudoacacia, Populus nigra* and *A. glutinosa*.

The three sampling sites showed well-preserved channel morphology with a riffle-run structure. The streambed was mainly composed of rock (30%), cobbles (25%) and gravel

(15%) at the up- and mid-stream sites, whereas rock (25%), cobbles (30%) and sand (30%) were the dominant substrates at the down-stream site. During the period of study, instantaneous stream discharge (Q_i) averaged 22.6 ± 18.7 L s^{-1} at the up-stream site, and increased to 78.3 ± 52.9 and 89.4 ± 58.1 L s^{-1} at the mid- and down-stream sites, respectively, that were located downstream of the two main tributaries discharging to the main stem (Figure 6.1). Stream DIN concentration averaged 280 ± 90, 170 ± 70, and 190 ± 80 μg N L^{-1} at the up-, mid- and down-stream sites, respectively, being NO_3^- the predominant form (> 85%). In all the cases, NH_4^+ concentration was low (< 20 μg N L^{-1}) and it represented a small fraction (< 15%) of total DIN. Stream chloride (Cl^-) concentration increased along the stream continuum, from 6.21 ± 1.34 mg L^{-1} at the up-stream site to 8.06 ± 1.02 mg L^{-1} at the down-stream site. The riparian groundwater level (2 m from the stream channel) was 50 ± 10 cm below the soil surface (Bernal et al., 2015). At the down-stream site, mean riparian groundwater concentration was 400 ± 200 μg N L^{-1} for NO_3^-, 11.4 ± 4 mg L^{-1} for Cl^-, and 4.2 ± 1.5 mg O_2 L^{-1} for DO (averaged from 7 piezometers) (Poblador, unpublished data).

6.2.2 Field Sampling and Laboratory Analysis

The field sampling was performed during two consecutive water years (2010-2011 and 2011-2012), each of which was devoted to accomplish different complementary objectives of our research. From September 2010 to August 2011 (water-year 2010-2011), we collected stream water samples twice a week at 12 h intervals at the three sampling sites (up-, mid-, and down-stream) in order to explore the temporal pattern of diel variation in stream NO_3^- and Cl^- concentrations along the study elevation gradient. We considered Cl^- as a conservative solute, little affected by biogeochemical processes (Kirchner et al. 2001). Moreover, we collected water samples every day (at noon) to calculate stream solute loads (see below). At each sampling site, water samples were collected with an auto-sampler (Teledyne Isco Model 1612), which was connected to a water pressure sensor (HOBO U20-001-04) that monitored stream water level at 15 min intervals. We measured Q_i at each sampling site fortnightly by using the "slug" chloride addition method technique (Gordon et al. 1992). We inferred Q_i from water level measurements by estimating the linear regression between stream water level and empirically measured Q_i (n = 57, 60 and 61 for up-, mid- and down-stream sites, respectively; in all cases: $R^2 > 0.97$).

From March to July 2012 (spring 2012), we focused on investigating the relationship between the diel variation in stream NO_3^- concentration and daily stream metabolism. The sampling effort was concentrated at the down-stream site, where both stream

metabolism and diel variations in stream NO_3^- concentration were expected to be the highest. A Teledyne Isco auto-sampler was used to collect stream water samples at 6 h intervals: mid-night (0h), dawn (6h), noon (12h) and before sunset (18h). Q_i was measured as in 2010-2011. Daily stream metabolism was calculated from stream DO (in mg O_2 L^{-1}) recorded at 30 min intervals with an YSI ProODO oxymeter. We examined whether diel variations in stream solute concentration were related to riparian groundwater table fluctuations by monitoring riparian groundwater level (every 15 min), NO_3^- and Cl^- concentrations (every 12 h) and DO concentration (every 30 min) at a piezometer placed ~2 m from the stream channel. On average, riparian groundwater level and solute concentrations differed < 9% between this piezometer and the 6 others located nearby, and thus, we considered this piezometer representative of riparian groundwater at the down-stream site (Poblador, unpublished data). In addition, we monitored the temporal pattern of temperature and light inputs to the stream along the study elevation gradient by installing HOBO sensors (HOBO U20-001-04) at the three sampling sites. The HOBOs recorded stream water temperature and photosynthetic active radiation (PAR) at 30 min intervals.

All water samples were filtered (Whatman GF/F) and kept cold (< 4ºC) until laboratory analysis (< 24 h after collection). Water samples were analyzed for Cl^- and for DIN (NO_3^- and NH_4^+). Cl^- was analyzed by ionic chromatography (Compact IC-761, Methrom). NO_3^- was analyzed by the cadmium reduction method (Keeney and Nelson 1982) using a Technicon Autoanalyzer (Technicon 1976). NH_4^+ was manually analyzed by the salicilate-nitropruside method (Baethgen and Alley 1989) using a spectrophotometer (PharmaSpec UV-1700 SHIMADZU). Stream NH_4^+ concentration was low and showed no diel variation for any of the three stream sites, and because of that NH_4^+ was not included in further data analysis.

6.2.3 Data Analysis

Temperature and light conditions

We explored whether environmental conditions favoring in-stream photoautotrophic activity (temperature and PAR) were similar along the study stream continuum. For each sampling site, we calculated mean daily temperature (T, in ºC) and accumulated daily PAR (ΣPAR, in mol m^{-2} d^{-1}), and then we computed the number of days for which T and ΣPAR were optimal for photoautotrophic activity. Moreover, we computed the number of hours per day during which instantaneous PAR (PAR_i, in μmol m^{-2} s^{-1}) was optimal for photosynthetic activity. We considered T = 10ºC as

the threshold upon which photoautotrophs are not temperature-limited (DeNicola 1996). A value of $\Sigma PAR = 4$ mol m^{-2} d^{-1} was considered the minimum daily input of light required to ensure the activity of photoautotrophs (Hill et al. 1995). Finally, we assumed that $PAR_i > 200$ μmol m^{-2} s^{-1} was the optimal irradiance for photosynthetic activity (Hill et al. 1995). Differences in T, ΣPAR and PAR_i between the three sampling sites were established with a Wilcoxon paired rank sum test (Zar 2010).

Temporal pattern of stream solute concentrations

We examined the temporal pattern of day-night variations in Cl^- and NO_3^- concentrations by calculating the relative difference between midnight and noon solute concentrations (Δ_{solute}, in %) with the following equation:

$$\Delta_{solute} = \frac{[solute]_{0h}-[solute]_{12h}}{[solute]_{0h}} \times 100 \quad (6.1)$$

where $[solute]_{0h}$ and $[solute]_{12h}$ are the solute concentration (in mg L^{-1}) at midnight and noon, respectively. Values of $\Delta_{solute} \sim 0$ indicate small or null variation in solute concentration between day and night, as expected for conservative solutes if the contribution of water sources to stream runoff does not vary between day and night time. Values of $\Delta_{solute} > 0$ indicate higher solute concentrations at night than at day time, whereas values of $\Delta_{solute} < 0$ indicate the opposite. Previous studies have shown that peaks of NO_3^- concentration often occur near predawn and minima later in the afternoon (Heffernan and Cohen 2010, Halliday et al. 2013). Therefore, values of Δ_{solute} may underestimate, to some extent, the amplitude of diel variation because we collected the night-time sample at midnight.

To explore whether day-night variations in solute concentration were significant, we compared noon and midnight concentrations of either, Cl^- or NO_3^- by applying a Wilcoxon paired rank sum test. For the water year 2010-2011, we compared midnight and noon solute concentrations for each month and for each sampling site. For spring 2012, we compared midnight and noon solute concentrations at the down-stream site for each week for both stream and riparian groundwater.

To examine the potential influence of day-night variations in NO_3^- concentration on the 2010-2011 stream NO_3^- flux, we calculated the stream NO_3^- flux from the down-stream site with and without including day-night variations of NO_3^- concentration. The annual load of NO_3^- was calculated by multiplying Q_i by stream NO_3^- concentration and integrating instantaneous NO_3^- loads over the water year (from 1 September to

31 August). To account for day-night variations, instantaneous stream NO_3^- concentration was estimated by linearly interpolating NO_3^- concentration measured at noon and midnight, whereas only noon values of NO_3^- concentration were considered when excluding day-night variation. Because midnight samples were collected twice a week, instantaneous midnight stream NO_3^- concentration for each day was estimated by linearly interpolating midnight NO_3^- concentration measured during consecutive sampling dates. Differences between the two approaches (with and without day-night variations) were attributed to the effect of in-stream processes on stream NO_3^- concentration. The same procedure was repeated to calculate stream NO_3^- loads in spring 2012.

Stream metabolism

During spring 2012, we calculated daily rates of GPP and ER at the down-stream site by using the single-station diel DO change method (Bott 2006). This method was appropriate because in-stream conditions were uniform throughout the reach and groundwater inputs were small compared to stream discharge (< 10%) (Bott 2006). DO curves were corrected for the reaeration flux by applying the night-time regression method to estimate the reaeration coefficient (Young and Huryn 1998). Daily ER was estimated by averaging the change in night time reaeration-corrected DO at a 30 min interval and multiplying it by 24 h, assuming that instantaneous ER was constant during the entire day (Bott 2006). Daily GPP was computed by integrating the difference between the change in reaeration-corrected DO and ER at 30 min intervals (both measures in mg O_2 L^{-1} min^{-1}). We multiplied GPP and ER by the mean reach depth (in m) to obtain areal estimates (in g O_2 m^{-2} d^{-1}). Mean reach depth was calculated weekly by averaging the water column depth measured at 20 cm intervals across 5 transects along a 40 m reach.

We examined the relationship between environmental variables (T and ΣPAR), metabolic rates (daily ER and daily GPP) and daily Δ_{NO3} using linear regression models. We further investigated the contribution of GPP to diel variations in stream NO_3^- concentration by comparing measured NO_3^- concentrations with those predicted based only on stoichiometric principles (Hall and Tank 2003). First, we inferred instantaneous NO_3^- uptake rates by the stream photoautotrophic community (U_{GPP}, mg N L^{-1} min^{-1}) from instantaneous GPP (mg O_2 L^{-1} min^{-1}). We assumed that (i) the molar ratio for CO_2:O_2 was 1:1 during photosynthesis (Hall and Tank 2003), and (ii) the C:N ratio of the epilithic photoautotrophic community was 14:1 (C:N = 13.7 ± 1.3 in light exposed epilithic biofilm at the study stream, Pastor et al. 2014). We acknowledged that these are rough estimates because not all GPP is translated into biomass accrual (Hall and Beaulieu 2013), and not all epilithic biofilm is composed of photoautotrophic organisms

(Volkmar et al. 2011). However, this was a useful exercise for our own purpose because we inferred N uptake by photoautotrophs from stoichiometric principles, independently of the diel variations in stream NO_3^- concentration. Then, at each time step (t = 0, 6, 12, and 18 h), we calculated the predicted stream NO_3^- concentration ($[NO_3]'_t$, in μg N L^{-1}) as follows:

$$[NO_3]'_t = [NO_3]'_{t-1} - (\overline{U_{GPP}} \times \Delta t) \quad (6.2)$$

where $[NO_3]'_{t-1}$ is the predicted stream NO_3^- concentration (in μg N L^{-1}) at sampling time t-1, $\overline{U_{GPP}}$ is the average U_{GPP} between sampling time intervals, and Δt is the time interval between sampling times (360 min) (Heffernan and Cohen 2010). The initial condition to run the model was the observed stream NO_3^- concentration at the beginning of spring 2012. We evaluated the goodness of fit between predicted and observed NO_3^- concentration and Δ_{NO3} by ordinary least squares. Moreover, we tested whether the slope of the linear regression between predicted and observed values was similar to 1 with a slope test (Zar 2010). We expected a slope similar to 1 between predicted and observed values when GPP is the main driver of diel variations in stream NO_3^- concentration. Further, the residuals between predicted and observed Δ_{NO3} were examined for evaluating the ability of the model to predict changes in Δ_{NO3} over time.

All the statistical analyses were carried out with the R 2.15.1 statistical software (R-project 2012). We chose non-parametric tests for the statistical analysis because not all data sets had a normal distribution. In all cases, differences were considered statistically significant when $p < 0.05$.

6.3 RESULTS

6.3.1 Temperature and Light Inputs along the Stream

During spring 2012, environmental conditions were more favorable for photosynthetic activity at the mid- and down-stream sites than at the up-stream site. Both T and ΣPAR were higher at the down- than at the up-stream site (Table 6.1). Moreover, T > 10ºC was reached during 50%, 85%, and 90% of the days at the up-, mid-, and down-stream sites, respectively (Table 6.1 and Figure 6.2a). The percentage of days with ΣPAR > 4 mol m^{-2} d^{-1} increased along the stream continuum, being 59%, 74% and 93% at the up-, mid-, and down-stream sites, respectively (Table 6.1 and Figure 6.2b).

At the down-stream site, T remained around 9.6 ± 2.1ºC from mid-March to mid-April, and then it increased to 15ºC until the end of the study period in July (Figure 6.3a). Diel variations in temperature remained small during spring 2012, being 1.5 ± 0.8ºC higher at noon than at night-time (Figure 6.3a). Light inputs to the stream (PAR_i) increased from mid-March until two weeks after the riparian leaf-out in early-April (Figure 6.3b). As the riparian canopy developed (from mid-April to late-May), PAR_i and diel variation in PAR_i sharply decreased, and then remained low until the end of the experiment in July (Figure 6.3b).

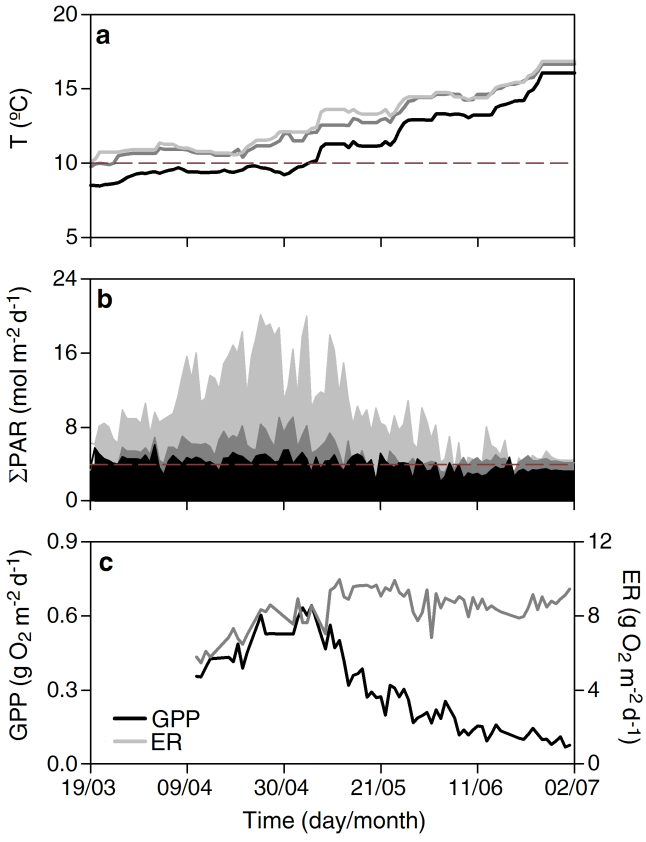

Figure 6.2 Temporal pattern of (a) mean daily stream water temperature (T), (b) daily photosynthetically active radiation (ΣPAR) and (c) stream metabolism during spring 2012 at the down-stream site. In panel (a) and (b), different colors showed data for the up-stream (black), mid-stream (dark grey) and down-stream (grey) sampling site. Dashed lines indicate thresholds upon which photoautotrophs are not limited by temperature (T = 10ºC) or light (ΣPAR = 4 mol m^{-2} d^{-1}). In panel (c), different colors showed data for GPP (black) and ER (grey).

Table 6.1 Mean daily stream water temperature (T), daily photosynthetically active radiation (ΣPAR), hours per day with instantaneous PAR > 200 µmol m^{-2} s^{-1} (PAR_{200}), days with T > 10 ºC (T_{10}), and days with (ΣPAR > 4 mol m^{-2} d^{-1} (ΣPAR) for the up-, mid-, and down-stream sites during spring 2012. Values are medians and the 25th and 75th percentile are shown in brackets. For T, (ΣPAR and PAR_{200}, different letters indicate statistical significant differences between sampling sites (Wilcoxon paired rank sum test, $p < 0.05$, df = 1; for the three variables n = 112).

Site	T (ºC)	ΣPAR (mol $m^{-2}d^{-1}$)	PAR_{200} (hours d^{-1})	T_{10} (days)	$ΣPAR_4$ (days)
Up-stream	10.2 [8.6, 13.2] ^{A}	4.1 [3.6, 4.8] ^{A}	0.5 [0.0, 1.5] ^{A}	57	66
Mid-stream	12.2 [10.4, 14.5] ^{B}	5.2 [4.1, 6.1] ^{B}	1.0 [0.5, 1.5] ^{A}	99	83
Down-stream	12.4 [10.4, 14.5] ^{B}	8.9[6.3, 11.9] ^{C}	2.5 [1.5, 4.0] ^{B}	103	104

6.3.2 Temporal Patterns of Day-Night Variation in Stream and Riparian Groundwater Solute Concentrations

During the water year 2010-2011, Cl^- concentration did not differ between midnight and noon in any month and at any of the three stream sites (for the 12 months and the 3 sites: Wilcoxon paired rank sum test, $Z > Z_{0.05,}$ degrees of freedom [df] = 11, $p > 0.05$) (Figure 6.4, white circles). In contrast, the day-night variation in NO_3^- concentration differed between stream sites. At the up-stream site, there were no differences between midnight and noon stream NO_3^- concentration at any month (for all months: $Z > Z_{0.05,}$ df = 11, $p > 0.05$) (Figure 6.4a, black circles). At the mid- and down-stream sites, stream NO_3^- concentration at midnight was higher than at noon during the spring months (from April to June, and from April to May for the mid- and down-stream sites, respectively; in all cases $Z > Z_{0.05,}$ df = 11, $p < 0.05$). During that period, monthly median Δ_{NO3} ranged from 6.3% to 19.1% (Figures 6.4b and Figure 6.4c, black circles). In November, stream NO_3^- concentration was 12.8% higher at noon than at midnight at the down-stream site ($Z = -1.825$, df = 11, $p < 0.05$) (Figure 6.4c, black circles).

Such day-night variations in stream NO_3^- concentration influenced stream N fluxes mainly during spring, reducing the NO_3^- load at the down-stream site by 11%. The reduction in stream NO_3^- load was similar during spring 2012 (9%). During autumn, winter and summer, diel variations in NO_3^- concentration had a small effect on stream NO_3^- loads (< 5%).

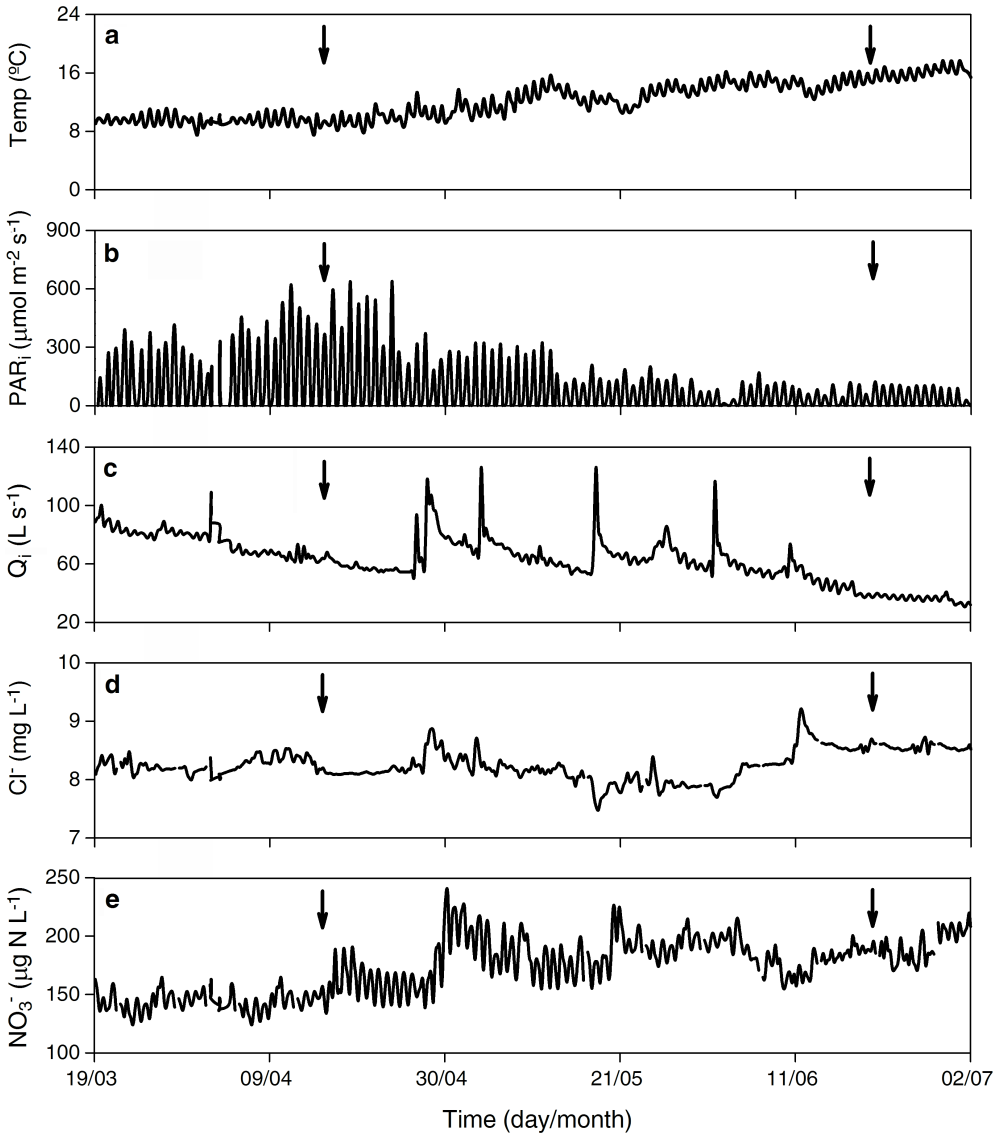

Figure 6.3 Diel variation of (a) stream water temperature (Temp), (b) photosynthetically active radiation (PAR_i), (c) stream discharge (Q_i), (d) stream Cl^- concentration, and (e) stream NO_3^- concentration during spring 2012 at the down-stream site. Black arrows indicate the beginning and the end of the leaf emergence period (Poblador, unpublished data).

During spring 2012, the diel pattern of stream solute concentrations at the down-stream site was similar to spring 2011. Stream Cl^- concentration averaged 8.3 ± 0.3 mg L^{-1} and it slightly increased from March to July, showing the opposite pattern than stream Q_i

(Figures 6.3c and Figure 6.3d). Diel variations for both Q_i and Cl^- concentration remained low (< 5%) and did not differ between midnight and noon during the sampling period (from March to June: $Z > Z_{0.05}$, df = 6, $p > 0.1$) (Figure 6.5a, white circles). Stream NO_3^- concentration ranged from 120 to 230 μg N L^{-1}, and showed higher values at midnight than at noon from mid-March to late-May (for all weeks: $Z < Z_{0.05}$, df = 6, $p < 0.05$) (Figure 6.3e). The Δ_{NO3} increased from mid-March to the beginning of May (three weeks after the riparian leaf-out), and then declined until the riparian canopy was fully closed in June (Figure 6.5a, black circles). No day-night variations in stream NO_3^- concentration were found later on (for all June weeks: $Z > Z_{0.05}$, df = 6, $p > 0.1$).

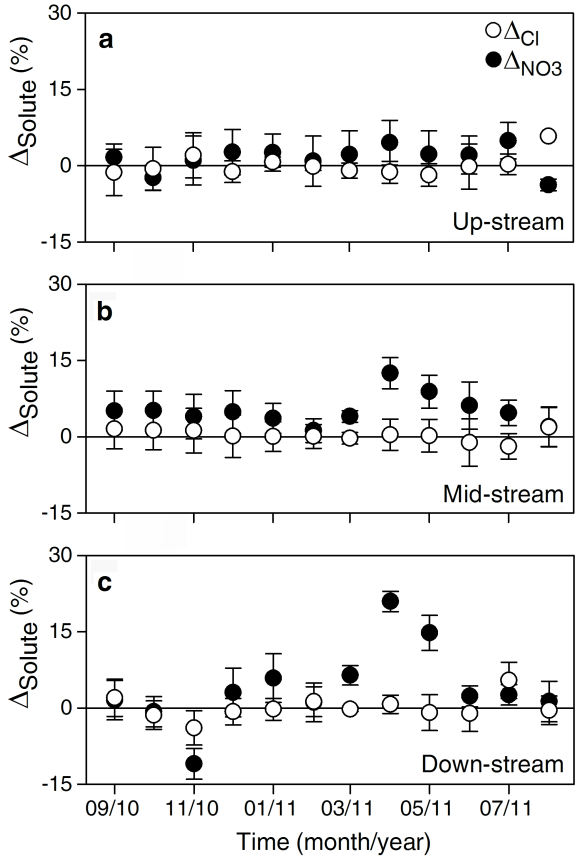

Figure 6.4 Temporal pattern of the relative difference between midnight and noon stream water concentrations (Δ_{solute}) for both chloride (white) and nitrate (black) at the (a) up-stream, (b) mid-stream, and (c) down-stream sites during the water-year 2010-2011. Circles are the median of Δ_{solute} for each month and whiskers denote the 25th and 75th percentile. The black line indicates no differences between midnight and noon solute concentrations.

During spring 2012, riparian groundwater DO concentration was 4.72 ± 1.47 mg O_2 L^{-1} and it slightly decreased from March to June, showing the same pattern than riparian groundwater level. Riparian groundwater concentration averaged 11.3 ± 0.5 mg L^{-1} for Cl^- and 460 ± 80 μg N L^{-1} for NO_3^-. Diel variations in riparian groundwater level, DO, Cl^- and NO_3^- concentration did not differ between midnight and noon during the sampling period (for the four variables and for each of the 15 weeks: $Z > Z_{0.05}$, df = 6, $p > 0.1$) (Figure 6.5b).

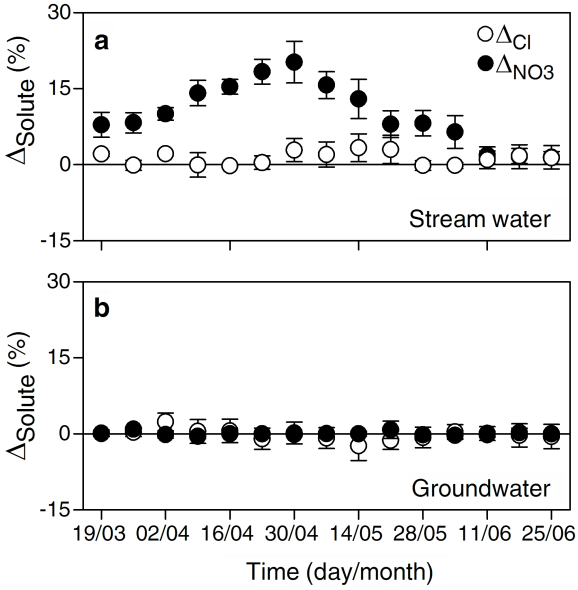

Figure 6.5 Temporal pattern of the relative difference between midnight and noon concentrations (Δ_{solute}) for both chloride (white) and nitrate (black) in (a) stream water, and (b) riparian groundwater during spring 2012 at the down-stream site. Circles are the median of Δ_{solute} for each week and whiskers denote the 25th and 75th percentile. The black line indicates no differences between midnight and noon solute concentrations.

6.3.3 Relationship between Diel Variation in Nitrate Concentration and Stream Metabolism

During spring 2012, daily rates of ER at the down-stream site ranged from 5.5 to 10.0 g O_2 m^{-2} d^{-1}, increasing from April to mid-May and then remaining relatively constant at 8.4 ± 1.0 g O_2 m^{-2} d^{-1} (Figure 6.2c). This temporal pattern was positively related to the temporal pattern of T (linear regression [l.r.], $R^2 = 0.38$, $p < 0.05$, $n = 44$).

Daily rates of GPP were between 10-100 fold lower than daily rates of ER, indicating that stream metabolism was dominated by heterotrophic activity during spring. Daily rates of GPP increased from April (0.35 g O_2 m^{-2} d^{-1}) to mid-May (0.64 g O_2 m^{-2} d^{-1}), and then decreased until June (0.07 g O_2 m^{-2} d^{-1}) (Figure 6.2c). This temporal pattern was positively related to the temporal pattern of ΣPAR (Figure 6.6a). No relationship was found between daily rates of GPP and ER (l.r., $R^2 = 0.02$, $p > 0.1$, $n = 44$).

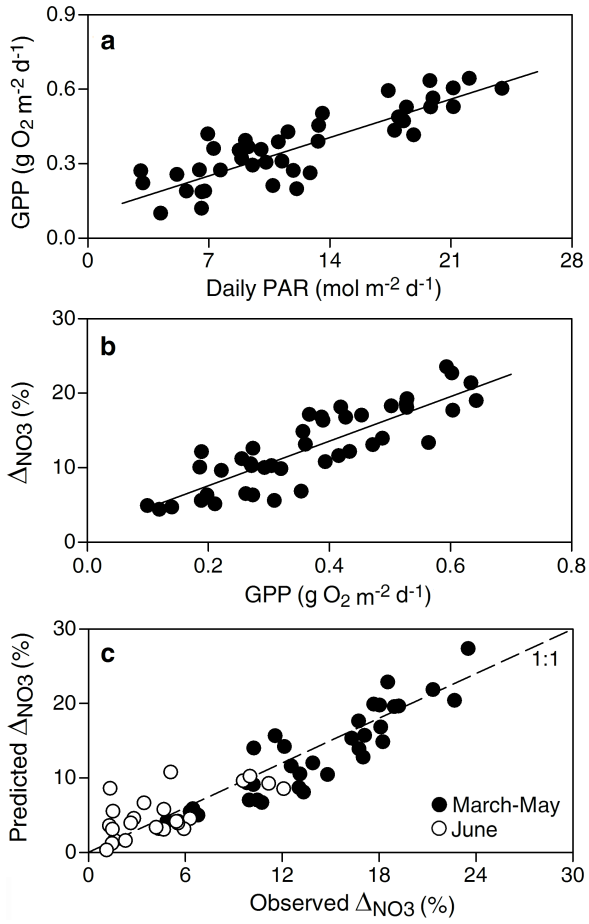

Figure 6.6 Relationship between (a) daily photosynthetically active radiation (ΣPAR) and daily gross primary production (GPP), (b) daily GPP and day-night variations in stream nitrate concentration (Δ_{NO3}), and (c) observed and stoichiometrically predicted day-night variations in stream nitrate concentration during spring 2012 at the down-stream site. The black line in panels (a) and (b) is the linear regression between variables (GPP vs. ΣPAR: l.r., $R^2 = 0.74$, $p < 0.001$; Δ_{NO3} vs. GPP: l.r., $R^2 = 0.74$, $p < 0.001$). The 1:1 line is indicated in panel (c) with a dashed line. White circles in panel (c) indicated day-night variations in stream nitrate concentration in June.

There was no relationship between daily Δ_{NO3} and daily ER (l.r., $R^2 = 0.01$, $p > 0.1$, $n = 44$), while daily Δ_{NO3} was positively related to daily GPP (Figure 6.6b). There was a good fit between observed stream NO_3^- concentrations and those predicted from stoichiometric principles as indicated by both the strong relationship between observed and predicted values (l.r., $R^2 = 0.73$, $p < 0.001$, $n = 201$), and non-significant divergences from the 1:1 line (slope test, $F = 1.01$, $df = 200$, $p > 0.1$). Similarly, there was a good fit between observed and predicted Δ_{NO3} (l.r., $R^2 = 0.85$, $p < 0.001$, $n = 44$; slope test, $F = 0.55$, $df = 43$, $p > 0.1$) (Figure 6.6c). Divergences between observed and predicted Δ_{NO3} were < 4% during March, April and May, while on average predicted values were overestimated by 14% in June.

6.4 DISCUSSION

This study aimed to investigate the importance of terrestrial and in-stream biogeochemical processes on controlling fine-scale temporal N dynamics along a stream continuum, and to assess the influence of such diel NO_3^- fluctuations on stream N fluxes at seasonal scale. Our results indicated that the temporal pattern of diel variation in stream NO_3^- concentration varied substantially along the stream. No diel NO_3^- variations were observed at the up-stream site, while day-night variations in NO_3^- concentration peaked during the onset of riparian leaf emergence at the mid- and down-stream sites as reported in previous studies (Roberts and Mulholland 2007, Rusjan and Mikoš 2009). These contrasting patterns in fine-scale N dynamics were accompanied by longitudinal increases in temperature and light availability, suggesting that these two environmental factors were controlling the extent to which in-stream processes modified fine-scale NO_3^- dynamics along the stream continuum.

The results obtained during spring 2012 convincingly showed that terrestrial processes did not control diel variations in NO_3^- concentration because no simultaneous diel variations in stream discharge, riparian groundwater level or N concentration were observed. Moreover, simple mass balance calculations indicate that hydrological mixing with riparian groundwater inputs could not explain midnight increases in stream NO_3^- concentration because median Δ_{NO3} would then have been 0.6% instead of 13% (Appendix A). Conversely, the strong relationship and synchronicity between daily GPP and Δ_{NO3} supports the hypothesis that in-stream photoautotrophic activity was a major driver of the observed diel variations in stream NO_3^- concentration. These results are in agreement with findings from lowland rivers (Heffernan and Cohen 2010),

headwater forested streams (Roberts and Mulholland 2007) and even coastal ecosystems (Johnson et al. 2006). However, these previous studies were performed during periods of relatively high photoautotrophic activity (GPP = 5-20 g O_2 m^{-2} d^{-1}, GPP:ER ~ 1) compared to the values measured in this study (GPP < 0.7 g O_2 m^{-2} d^{-1}, GPP:ER < 0.01). Therefore, our study is novel in showing the potential of photoautotrophic activity to regulate in-stream NO_3^- dynamics even in extremely low productivity streams dominated by heterotrophic metabolism.

Our results add to the growing body of research demonstrating that GPP is a strong driver of in-stream NO_3^- uptake (Hall and Tank 2003, Mulholland et al. 2008a), though the relationship between stream metabolism and fine-scale N dynamics can vary among streams. For instance, diel NO_3^- variations in April were similar (10-20 μg N L^{-1}) on Walker Branch (TN, USA; Roberts and Mulholland 2007) and Font del Regàs (this study), despite daily rates of GPP that were 10 fold larger at Walker Branch. On the other hand, GPP at Walker Branch was similar to Sycamore Creek (AZ, USA; Grimm 1987) and Ichetucknee river (FL, USA; Heffernan and Cohen 2010) (7-14 g O_2 m^{-2} d^{-1}), though diel NO_3^- variations were 4-6 fold lower at Walker Branch (10-20 vs.75-100 μg N L^{-1}). Midday decline in stream NO_3^- concentrations is likely driven by photoautotrophic N demand relative to N supply (Sterner and Elser 2002, Appling and Heffernan 2014). Thus, divergences between GPP and diel NO_3^- variations among streams could be explained by differences in both N availability (from 120 to 420 μg N L^{-1} at Font del Regàs and Ichetucknee river, respectively) and the C:N ratio of primary uptake compartments (from 14:1 in Font del Regàs epilithic biofilms to 25:1 in Ichetucknee macrophytes). A good assessment of the stream biota stoichiometry is thus crucial to constrain the uncertainty associated with mechanistic models linking stream metabolism and fine-scale nutrient dynamics.

Despite the strong match between day-night variations measured at the down-stream site and those predicted from GPP instantaneous rates during early spring, divergences between measured and predicted Δ_{NO3} were evident in late spring. These biases in model prediction could be explained by changes in the stoichiometry of the algal community (Sterner and Elser 2002, Heffernan and Cohen 2010) or in the respiration rate of photoautotrophs (Hall and Beaulieu 2013), which could be induced by decreased light inputs after riparian leaf-out. Additionally, these mismatches could be explained by shifts in the main processes regulating diel NO_3^- variations after leaf-out such as in-stream nitrification or denitrification (Gammons et al. 2011, Baulch et al. 2012). Diel cycles of these two processes could probably be suited for day-night NO_3^- variations during the peak of leaf litter accumulation in November, which resulted in

midnight decline in stream NO_3^- concentrations (Laursen and Seitzinger 2004). However, it seems unlikely that nitrification could account for the observed diel NO_3^- patterns in spring because no diel variations in stream NH_4^+ concentration occurred to support nitrification, while relatively high DO concentration in the stream (10.7 ± 0.5 mg O_2 L^{-1}) and hyporheic zone (7.8 ± 1.6 mg O_2 L^{-1}; Poblador, unpublished data) suggest low denitrification in stream sediments (Kemp and Dodds 2002, Johnson and Tank 2009). The lack of correlation between Δ_{NO3} and ER, further supports that GPP was a major player regulating fine-scale NO_3^- dynamics. The current understanding of the influence of metabolism on stream N dynamics has been mostly based on correlational analysis (e.g. Hall and Tank 2003). Nonetheless, our study shows that stoichiometric models based on diel nutrient variation are complementary and powerful tools that can contribute to disentangle the mechanisms driving stream nutrient cycling over time and space.

There is still little research available on whether diel variations in nutrient concentration can have any implication at larger spatial and temporal scales, and how the mechanisms underlying such fine-scale patterns can ultimately modify catchment nutrient fluxes. Our study indicated that the contribution of photoautotrophic N uptake to regulate NO_3^- fluxes at the down-stream site was small in annual terms (4%), as expected in a low productivity stream such as Font del Regàs (Battin et al. 2008, Valett et al. 2008). However, during spring, increased photoautotrophic N uptake led to a decrease in catchment NO_3^- export of ~20 g N ha^{-1}, which was equivalent to a ~10% reduction in the stream NO_3^- export. Since maxima NO_3^- and minima DO concentrations usually coincide over a daily cycle (Heffernan and Cohen 2010, Halliday et al. 2013), our estimations may be slightly underestimated because we measured NO_3^- at 0h, while minima DO occurred between 0-3h. Nevertheless, we estimated a similar decrease in spring NO_3^- loads (15 g N ha^{-1}, ~ 12%) for Walker Branch (38.4 ha, 6-14 L s^{-1}) based on mean NO_3^- concentration (200-500 μg N L^{-1}) and Δ_{NO3} (2-15 μg N L^{-1}) as reported by Roberts and Mulholland (2007). These estimations for Font del Regàs and Walker Branch suggest that benthic algae is an important transitory sink of DIN in these headwater forested streams, similarly to the vernal dam described for spring ephemeral plants by Muller and Bormann (1976). Nonetheless, the relevance of photoautotrophic N retention at longer time scales would ultimately depend on the turnover rates of the primary uptake compartments, which can vary widely between epilithic biofilms (few days) to macrophytes (months) (Riis et al. 2012).

The influence of fine-scale N patterns on N fluxes could be even higher in open-canopy and lowland streams for which reported diel NO_3^- variations are larger compared to headwater forested streams (Grimm 1987, Heffernan et al. 2010, Halliday et al. 2013).

For instance, we estimated that spring diel NO_3^- variation may reduce catchment NO_3^- exports by ~70 g N ha^{-1} (~ 16%) at the Ichetucknee river (770 km^2, 8900 L s^{-1}), based on mean daily minima and maxima NO_3^- concentrations (380 and 460 μg N L^{-1}) reported by Heffernan and Cohen (2010). The contribution of fine-scale N dynamics to reduce catchment N export was even larger at the Upper Hafren river in UK (122 ha, 60 L s^{-1}), an open stream where spring diel NO_3^- variations (from 14 to 18 μg N L^{-1}) reduced stream NO_3^- loads by 154 g N ha^{-1} (22 %) (Halliday et al. 2013). These back-of-the-envelope calculations highlight that fine-scale N dynamics can not only indicate the preferential mechanisms of in-stream N uptake, but also provide a relevant evaluation of their contribution on regulating NO_3^- downstream fluxes at the catchment scale.

6.5 CONCLUSIONS

This study adds to the growing evidence demonstrating that in-stream processes can substantially modify stream N concentration and fluxes (Peterson et al. 2001, Bernhardt et al. 2005, Arango et al. 2008, Bernal et al. 2012a). In-stream GPP was the major driver of diel variations in stream NO_3^- concentration in this highly heterotrophic headwater stream, while the contribution of other in-stream, riparian, and upland processes was minimal. From a network perspective, the temporal pattern of such diel NO_3^- variations and, consequently, their influence on stream N fluxes, varied along the stream continuum depending on light and temperature regimes. Finally, and in line with previous work, our study indicates that discrete measurements performed at midday can limit our understanding of in-stream nutrient cycling as well as the assessment of reliable nutrient budgets at long time scales even in low productivity streams (Mulholland et al. 2006). These biases could be even larger (up to 15-20%) for highly productive streams given that the capacity of stream biota to regulate diel and seasonal stream N dynamics could increase along the river continuum, as observed in this study. Overall, monitoring nutrient data at fine-scale temporal resolution can provide mechanistic explanations about the relevance of in-stream and terrestrial processes on regulating stream nutrient concentrations and their implications on long-term fluxes at the catchment scale.

ACKNOWLEDGEMENTS

We are thankful to Miquel Ribot and Sílvia Poblador for their invaluable assistance in the field, and to S. Poblador for providing data on Font del Regàs riparian groundwater and hyporheic zone. Special thanks are extended to Jennifer Drummond, Stuart Findlay and two anonymous reviewers for helpful comments on an earlier version of the manuscript. Financial supported was provided by the Spanish Government through the projects MEDFORESTREAM (CGL2011-30590) and MONTES-Consolider (CSD2008-00040-MONTES). AL was supported by a FPU PhD fellowship from the Spanish Ministry of Education and Science (AP-2009-3711). SB work was funded by the Spanish Research Council (JAE-DOC027), the Spanish CICT (Juan de la Cierva contract JCI-2008-177), European Social Funds (FSE), and the MEDFORESTREAM and NICUS (CGL-2014-55234-JIN) projects. We also thank site cooperators, including Vichy Catalan and the Catalan Water Agency (ACA) for permission to sample at the Font del Regàs catchment.

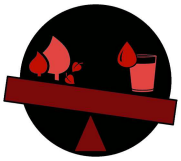

CHAPTER 7

Riparian and In-Stream Controls on Nutrient Concentrations and Fluxes in a Headwater Forested Stream

Headwater streams are recipients of water sources draining through terrestrial ecosystems. Moreover, stream biota can transform nutrients dissolved in stream water. However, studies considering these two sources of variation in stream nutrient chemistry are rare. We analyzed stream and riparian groundwater concentrations as well as in-stream net uptake rates for nitrate (NO_3^-), ammonium (NH_4^+), and soluble reactive phosphorus (SRP) along a 3.7 km reach. Chloride concentrations (used as conservative tracer) indicated a strong hydrological connection at the riparian-stream interface. However, stream and riparian groundwater nutrient concentrations showed a moderate to null correlation, suggesting high in-stream biogeochemical processing. In-stream net nutrient uptake (F_{sw}) was highly variable over time and space. For NH_4^+, the occurrence of $F_{sw} > 0$ (gross uptake > release) was high, while for NO_3^-, the occurrence of $F_{sw} < 0$ (gross uptake < release) increased along the reach. Within segments and dates, F_{sw} accounted for a median 6%, 18%, and 20% of the inputs of NO_3^-, NH_4^+, and SRP, respectively. Whole-reach mass balance calculations indicated that in-stream net uptake reduced stream NH_4^+ flux up to 90%, while the stream acted mostly as a source of NO_3^- and SRP. During the dormant period, concentrations decreased along the reach for NO_3, but increased for NH_4^+ and SRP. During the vegetative period, NH_4^+ decreased, SRP increased, and NO_3^- showed a U-shaped pattern along the reach. These longitudinal trends resulted from the combination of hydrological mixing with terrestrial inputs and in-stream nutrient processing. Thus, the assessment of these two sources of variation of stream water chemistry is crucial to understand the contribution of in-stream processes to stream nutrient dynamics at relevant ecological scales.

Original Work: Bernal, S., A. Lupon, M. Ribot, F. Sabater and E. Martí. 2015. Riparian and in-stream controls on nutrient concentrations and fluxes in a headwater forested stream. Biogeosciences 12:1941–1954.

7.1 INTRODUCTION

Stream water chemistry integrates hydrological and biogeochemical processes occurring within its drainage area, and thus, the temporal variation of stream solute concentrations at the catchment outlet is considered a good indicator of the response of terrestrial and aquatic ecosystems to environmental drivers (Bormann and Likens 1967, Bernhardt et al. 2003, Houlton et al. 2003). Less attention has been paid to the spatial variation of water chemistry along the stream, though it can be considerably important because stream nutrient concentrations are influenced by changes in hydrological flow paths, vegetation cover, and soil characteristics (Dent and Grimm 1999, Likens and Buso 2006). For instance, spatial variation in nutrient concentration along the stream has been attributed to changes in soil nitrification rates (Bohlen et al. 2001), soil organic carbon availability (Johnson et al. 2000), and organic soil depth across altitudinal gradients (Lawrence et al. 2000). Moreover, nutrient cycling within the riparian zone can strongly influence stream nutrient concentrations along the stream because these ecosystems are hot spots of biogeochemical processing (McClain et al. 2003, Vidon et al. 2010). In addition, processes occurring at the riparian-stream interface have a major influence on stream water chemistry than those occurring at catchment locations further from the stream (Ross et al. 2012). Finally, stream ecosystems have a strong capacity to transform and retain nutrients; thus, in-stream biogeochemical processes can further influence nutrient chemistry along the stream (Peterson et al. 2001, Dent et al. 2007). Therefore, consideration of these multiple sources of variation of stream water chemistry is important to understand drivers of stream nutrient dynamics.

Our understanding of nutrient biogeochemistry within riparian zones and streams is mainly based on field studies performed at the plot scale or in small stream reaches (few hundred meters) (Lowrance et al. 1997, Peterson et al. 2001, Mayer et al. 2007, von Schiller et al. 2015). These empirical studies have widely demonstrated the potential of riparian and stream ecosystems as either sinks or sources of nutrients, which ultimately influence the transport of nutrients to downstream ecosystems. Riparian and stream biota are capable to decrease the concentration of essential nutrients, such as dissolved inorganic nitrogen (DIN) and phosphate, especially when increasing water storage and residence time (Valett et al. 1996, Hedin et al. 1998, Peterson et al. 2001, Vidon and Hill 2004a). Conversely, riparian forests can become sources rather than sinks of nutrients when N_2-fixing species predominate (Helfield and Naiman 2002, Compton et al. 2003). Moreover, in-stream nutrient release can be important during some periods (Bernhardt et al. 2002, von Schiller et al. 2015). Finally, there is an intimate hydrological linkage between riparian and stream ecosystems that can result in strong biogeochemical

feedbacks between these two compartments (Morrice et al. 1997, Martí et al. 2000, Bernal and Sabater 2012). However, studies integrating biogeochemical processes at these two nearby ecosystems are rare (but see Dent et al. 2007), and the exchange of water and nutrients between stream and groundwater is unknown in most studies assessing in-stream gross and net nutrient uptake (Roberts and Mulholland 2007, Covino et al. 2010, von Schiller et al. 2011). There is a wide body of knowledge showing the potential of riparian and stream ecosystems to modify either groundwater or stream nutrient concentrations. However, a comprehensive view of the influence of riparian and in-stream processes on stream water chemistry at the catchment scale is still lacking (but see Meyer and Likens 1979). This gap of knowledge mostly exists because hydrological and biogeochemical processes can vary substantially along the stream (Covino and McGlynn 2007, Jencso et al. 2009), which limits our ability to extrapolate small plot- and reach- scale measurements to larger spatial scales. Some authors have proposed that nutrient concentrations should decline along the stream if in-stream net uptake is high enough and riparian groundwater inputs are relatively small (Brookshire et al. 2009). This declining pattern is not systematically observed in reach-scale studies, which could bring us to the conclusion that terrestrial inputs are the major driver of stream water chemistry because in-stream gross uptake and release counterbalance each other most of the time (Brookshire et al. 2009). However, synoptic studies have revealed that nutrient concentrations are patchy and highly variable along the stream as a result of spatial patterns in upwelling and in-stream nutrient processing (Dent and Grimm 1999). Thus, in-stream nutrient cycling could be substantial, but it might not necessarily lead to longitudinal increases or declines in nutrient concentration, a question that probably needs to be addressed at spatial scales larger than few hundred meters.

The goal of this study was to gain a better understanding of the influence of riparian groundwater inputs and in-stream biogeochemical processing on stream nutrient chemistry and fluxes in a headwater forested catchment. To approach this question, we explored the longitudinal pattern of stream nutrient (nitrate, ammonium, and phosphate) concentration along a 3.7 km reach during 1.5 years. We chose a headwater catchment as a model system to investigate drivers of spatial patterns in stream water chemistry because they typically show pronounce changes in riparian and stream features across relatively short distances (Uehlinger 2000). First, we evaluated riparian groundwater inputs and in-stream nutrient processing as sources of variation of stream nutrient concentration along the reach. We expected stream and riparian groundwater nutrient concentrations to be similar and strongly correlated if riparian groundwater is a major source of nutrients to the stream. In addition, we estimated the in-stream

nutrient processing capacity for 14 contiguous segments along the reach with a mass balance approach. Second, we evaluated the relative contribution of riparian groundwater inputs and in-stream biogeochemical processing to stream nutrient fluxes at the whole-reach scale by applying a mass balance approach that included all hydrological input and output fluxes along the reach.

7.2 MATERIALS AND METHODS

7.2.1 Study Site

The research was conducted in the Font del Regàs catchment (14.2 km^2) (Figure 7.1), located in the Montseny Natural Park, NE Spain (41°50'N, 2°30'E, 500-1500 m above the sea level (a.s.l.)) during the period 2010-2011. Total inorganic N deposition in this area oscillates between 15 and 30 kg N ha^{-1} yr^{-1} (Àvila and Rodà 2012). The climate at the Montseny Mountain Range is subhumid Mediterranean. The long-term mean annual precipitation is 925 ± 151 mm and the long-term mean annual air temperature is 12.1 ± 2.5 ºC (mean ± SD, period: 1940-2000, Catalan Metereologic Service). During the study period, mean annual precipitation (975 mm) and temperature (12.9ºC) fell within the long-term average (data from a meteorological station within the study catchment). In this period, summer was the driest season (140 mm) while most of the precipitation occurred in winter 2010 (370 mm) and autumn 2011 (555 mm) (Figure 7.2a).

The catchment is dominated by biotitic granite and it has steep slopes (28%) (Cartographic and Geological Institute of Catalonia). Evergreen oak (*Quercus ilex*) and European beech (*Fagus sylvatica*) forests cover 54% and 38% of the catchment area, respectively (Figure 7.1). The upper part of the catchment (2%) is covered by heathlands and grasslands. The catchment has a low population density (< 1 person km^{-2}) which is concentrated in the valley bottom. Hillslope soils (pH ~ 6) are sandy, with high content of rocks (33-36%). Soils at the hillslopes have a 4 cm deep O horizon and a 5 to 23 cm deep A horizon (averaged from 10 soil profiles).

The riparian zone is relatively flat (slope < 10%), and it covers 6% of the catchment area. Riparian soils (pH ~ 7) are sandy loam with low rock content (13%) and a 5 cm deep O horizon followed by a 30 cm deep A horizon (averaged from five soil profiles). Along the 3.7 km reach, the width of the riparian zone increases from 6 to 32 m, whereas the total basal area of riparian trees increases by 12 fold (based on forest

inventories of 30 m plots every ca. 150 m). *Alnus glutinosa*, *Robinia pseudoacacia*, *Platanus hybrida*, and *Fraxinus excelsior* are the most abundant riparian tree species followed by *Corylus avellana*, *Populus tremula*, *Populus nigra*, and *Sambucus nigra*. The abundance of N_2-fixing species (*A. glutinosa* and *R. pseudoacacia*) increases from 0% to > 60% along the longitudinal profile. During base flow conditions, riparian groundwater (< 1.5 m from the stream channel) flows well below the soil surface (0.5 ± 0.1 m), and thus, the interaction with the riparian organic soil is minimal (averaged from 15 piezometers, n = 165). During the period of study, riparian groundwater temperature ranged from 5 to 19.5ºC.

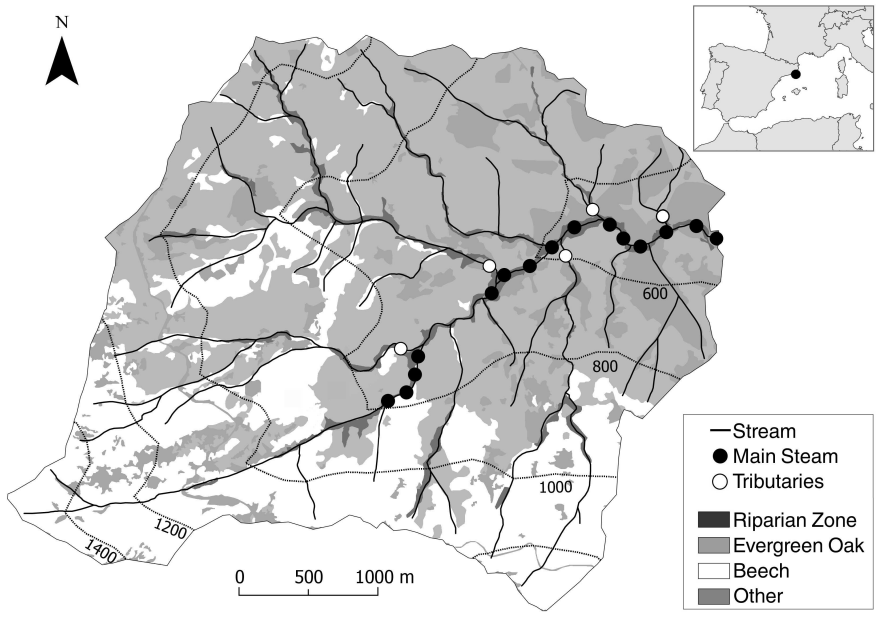

Figure 7.1 Map of the Font del Regàs catchment (Montseny Natural Park, NE Spain). The vegetation cover and the main stem sampling stations along the 3.7 km reach are indicated. There were 5 and 10 sampling stations along the 2nd and 3rd order sections, respectively. Four permanent tributaries discharged to the main stem from the upstream- to the downstream-most site (white circles). Additional water samples were collected from a small tributary draining through the inhabited area at the lowest part of the reach. The remaining tributaries were dry during the study period.

The 3.7 km study reach is a second-order stream along the first 1.5 km and a third-order stream for the remaining 63% of its length. The geomorphology of the stream bed changes substantially with stream order. The stream bed along the second-order section is mainly composed of rocks and cobbles (70%) with a small contribution of

sand (~ 10%). At the valley bottom, sands and gravels represent 44% of the stream substrate and the presence of rocks is minor (14%). Mean wetted width and water velocity increase between the second- and third-order section (from 1.6 to 2.7 m and from 0.24 to 0.35 m s^{-1}, respectively). During the study period, stream water temperature ranged from 5 to 18ºC. Stream discharge was low in summer (0.33 mm) and peaked in spring (0.79 mm).

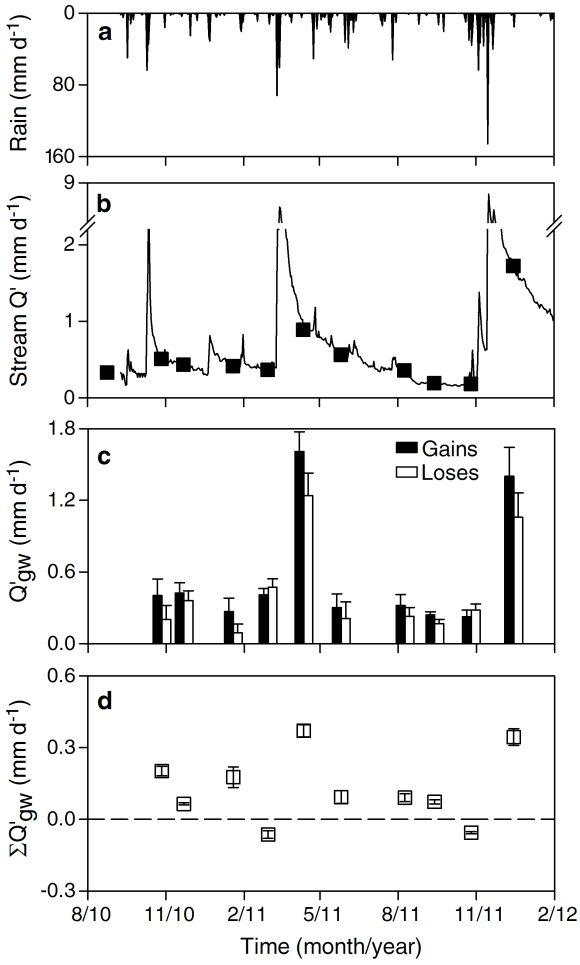

Figure 7.2 Temporal pattern of area-specific (a) rainfall, (b) stream discharge, (c) whole-reach gross hydrological gains and losses, and (d) cumulative net groundwater inputs at the downstream-most site. Black squares in (b) are dates of field campaigns. Error bars in (c) and (d) show the uncertainty associated with the empirical estimation of *Q* from tracer slug additions. Error bars in (b) are smaller than the symbol size.

7.2.2 Field Sampling and Laboratory Analysis

We selected 15 sampling sites along the 3.7 km study reach. The distance between consecutive sampling sites ranged from 110 to 600 m (Figure 7.1). At each sampling site, we installed a 1 m long PVC piezometer (3 cm Ø) in the riparian zone at ~ 1.5 m from the stream channel.

For each sampling site, we sampled stream water (from the thalweg) and riparian groundwater every 2 months from August 2010 to December 2011. We used pre-acid-washed polyethylene bottles to collect water samples after triple-rinsing them with either stream or groundwater. On each sampling date, we also measured dissolved oxygen concentration (DO, in mg L^{-1}) and water temperature (in ºC) with an YSI ProODO device in both stream water and in riparian groundwater. We avoid sampling soon after storms to ensure that our measurements were representative of low-flow conditions, when the influence of in-stream biogeochemical processes on stream nutrient concentrations and fluxes is expected to be the highest. All field campaigns were performed at least 9 days after storm events, except in October 2011 (Figure 7.2b, black squares). On each sampling date and at each sampling site, we measured groundwater table elevation (in cm below soil surface (b.s.s.)) with a water level sensor (Eijkelkamp 11.03.30) as well as wetted width (in m), instantaneous stream discharge (Q_i, in L s^{-1}), and water velocity (m s^{-1}). Q_i and water velocity were estimated with the slug-addition technique by adding 1 L of NaCl-enriched solution to the stream (electrical conductivity = 75-90 mS cm^{-1}, n = 11) (Gordon et al. 1992). The uncertainty associated with Q_i measurements was calculated as the relative difference in Q_i between pairs of tracer additions under equal water depth conditions (difference < 1 mm). The pairs of data were selected from a set of 126 slug additions and water level measurements obtained from the permanent field stations at Font del Regàs (Chapter 5). The measured uncertainty was relatively small (1.9%, n = 11). On each sampling date, we also collected stream water and measured Q_i at the four permanent tributaries discharging to Font del Regàs stream, which drained 1.9, 3.2, 1.8, and 1.1 km^2, respectively (Figure 7.1). These data were used for mass balance calculations (see below). Additional stream water samples were collected from a small permanent tributary that drained through an area (< 0.4 km^2) with few residences and crop fields for personal consumption.

Water samples were filtered (Whatman GF/F) and kept cold (< 4ºC) until laboratory analysis (< 24 h after collection). Chloride (Cl^-) was used as a conservative hydrological tracer and analyzed by ionic chromatography (Compact IC-761, Methrom). Nitrate (NO_3^-) was analyzed by the cadmium reduction method (Keeney and Nelson 1982)

using a Technicon autoanalyzer (Technicon 1976). Ammonium (NH_4^+) was manually analyzed by the salicilate-nitropruside method (Baethgen and Alley 1989) using a spectrophotometer (PharmaSpec UV-1700 SHIMADZU). Soluble reactive phosphorus (SRP) was manually analyzed by the acidic molybdate method (Murphy and Riley 1962) using a spectrophotometer (PharmaSpec UV-1700 SHIMADZU).

7.2.3 Data Analysis

The seasonality of biological activity can strongly affect both riparian groundwater chemistry and in-stream biogeochemical processes (Groffman et al. 1992, Hill et al. 2001). Therefore, the data set was separated in two groups based on sampling dates during the vegetative and dormant period (seven and four sampling dates, respectively). As a reference, we considered the vegetative period starting at the beginning of riparian leaf out (April) and ending at the peak of leaf litterfall (October), coinciding with the onset and offset of riparian tree evapotranspiration, respectively (Nadal-Sala et al. 2013). During the study period, rainfall was similar between the vegetative and dormant period (775 and 876 mm, respectively).

Patterns of stream discharge, riparian groundwater inputs, and stream solute concentrations

For each period, we examined the longitudinal pattern of stream discharge, riparian groundwater inputs, and stream solute concentrations along the reach. On each sampling date, we calculated area-specific stream discharge by dividing instantaneous discharge by catchment area (Q', in mm d^{-1}) at each sampling site. We used Q' rather than Q_i to be able to compare water fluxes from the 15 nested catchments along the reach. We examined the longitudinal patterns of Q' and stream solute concentration (C_{sw}) by applying regression models (linear, exponential, potential, and logarithmic). Model selection was performed by ordinary least square (Zar 2010). We referred only to the best fit model in each case.

The contribution of net riparian groundwater inputs to surface water along each stream segment (Q_{gw}) was estimated as the difference in Q_i between consecutive sampling sites (Covino et al. 2010). The empirical uncertainty associated with Q_i was used to calculate a lower and upper limit of Q_{gw}. We considered that Q_{gw} was representative of the net riparian groundwater flux draining to the stream within each stream segment. We acknowledge that this approach oversimplifies the complex hydrological interactions at the riparian-stream interface because it does not consider concurrent hydrological gains

and losses within each segment (Payn et al. 2009), but we consider that it provides a representative estimate at the scale of this study. To investigate the longitudinal pattern of riparian groundwater inputs, we calculated the cumulative area-specific net riparian groundwater input ($\Sigma Q'_{gw}$, in mm d^{-1}) by summing up Q_{gw} from the upstream-most site to each of the downstream segments and dividing it by the cumulative catchment area.

For each sampling date, we examined whether the 3.7 km reach was either net gaining or net losing water by comparing concurrent gross hydrological gains and losses over the entire reach (Payn et al. 2009). For this spatial scale, we considered that stream segments exhibiting $Q_{gw} > 0$ contributed to gross hydrological gains ($\Sigma Q_{gw} > 0$), while segments with $Q_{gw} < 0$ contributed to gross hydrological losses ($\Sigma Q_{gw} < 0$). Note that gross riparian groundwater fluxes divided by the total catchment area are equal to $\Sigma Q'_{gw}$ at the downstream-most site. For each sampling date, we calculated the relative contribution of different water sources to stream discharge at the downstream-most site (Q_{bot}), with Q_{top}/Q_{bot}, $\Sigma Q_{ef}/Q_{bot}$, and $\Sigma Q_{gw}/Q_{bot}$ for upstream, tributaries and riparian groundwater, respectively.

Sources of variation of stream nutrient concentration along the reach

Riparian groundwater inputs. We investigated whether longitudinal patterns in stream solute concentration were driven by riparian groundwater inputs by comparing solute concentrations between stream water and riparian groundwater with a Wilcoxon paired rank sum test. A non-parametric test was used because solute concentrations were not normally distributed (Shapiro-Wilk test, $p < 0.01$ for all study solutes) (Zar 2010).

Moreover, we examined the degree of hydrological interaction at the riparian-stream interface by exploring the relationship between stream and riparian groundwater Cl^- concentrations with a Spearman correlation. For each period, we quantified the difference between Cl^- concentrations in the two water bodies by calculating divergences from the 1:1 line with the relative root mean square error (RRMSE, in %) as:

$$\mathrm{RRMSE} = \frac{\sqrt{\sum_{i=1}^{n}(C_{sw} - C_{gw})^2}}{n \times \overline{C_{gw}}} \times 100 \qquad (7.1)$$

where C_{sw} and C_{gw} are stream and riparian groundwater solute concentrations, respectively, n is the total number of observations, and $\overline{C_{gw}}$ is the average of C_{gw}. A strong correlation and a low RRMSE between stream and riparian groundwater Cl^- concentrations indicate a strong hydrological connection between the two water bodies. Similarly, we examined the correlation between stream and riparian groundwater nutrient

concentrations. We expected a weak correlation and a high RRMSE value between nutrient concentrations measured at the two water bodies if the stream has a high nutrient processing capacity and in-stream gross uptake and release do not outweigh each other.

In-stream nutrient processing. We investigated the influence of in-stream biogeochemical processes on the longitudinal pattern of stream nutrient concentrations by applying a mass balance approach for each individual segment (Roberts and Mulholland 2007). For each nutrient, we calculated changes in stream flux between contiguous sampling sites (F_{sw}, in μg m^{-1} s^{-1}), being F_{sw} the net flux resulting from in-stream gross uptake and release along a particular stream segment (von Schiller et al. 2011). We expressed F_{sw} by unit of stream length in order to compare net changes in stream flux between segments differing in length. For each sampling date and for each nutrient, F_{sw} was approximated with:

$$F_{sw} = (F_{top} + F_{ef} + F_{gw} - F_{bot}) / x \quad (7.2)$$

where F_{top} and F_{bot}, are the nutrient flux at the top and at the bottom of each stream segment, F_{gw} is the nutrient flux from net riparian groundwater inputs, and F_{ef} is the nutrient flux from effluent inputs for those reaches including a tributary (all in μg s^{-1}) (Figure 7.3). F_{top} and F_{bot} were calculated by multiplying Q_i by C_{sw} at the top and at the bottom of the segment, respectively. F_{gw} was estimated by multiplying net groundwater inputs (Q_{gw}) by nutrient concentration in either riparian groundwater or stream water. For net gaining segments ($Q_{gw} > 0$), we assumed that the chemistry of net water inputs was similar to that measured in riparian groundwater, and thus, C_{gw} was the average between riparian groundwater nutrient concentration at the top and bottom of the reach. For net losing segments ($Q_{gw} < 0$), we assumed that the chemistry of net water losses was similar to that measured in stream water, and thus, C_{gw} averaged stream water concentration at the top and at the bottom of each reach segment (C_{top} and C_{bot}, respectively). For those cases in which stream segments received water from a tributary, F_{ef} was calculated by multiplying Q_i and C at the outlet of the tributary. We calculated an upper and lower limit of F_{sw} based on the empirical uncertainty associated with water fluxes (Q_i and Q_{gw}). Finally, x (in m) is the length of the segment between two consecutive sampling sites. The same approach was applied for Cl^-, a conservative tracer that was used as a hydrological reference. For Cl^-, we expected $F_{sw} \sim 0$ if inputs from upstream, tributaries, and riparian groundwater account for most of the stream

Cl^- flux. For nutrients, F_{sw} can be positive (gross uptake > release), negative (gross uptake < release) or zero (gross uptake ~ release). Therefore, we expected $F_{sw} \neq 0$ if in-stream gross uptake and release processes do not fully counterbalance each other (von Schiller et al. 2011). To investigate whether stream segments were consistently acting as net sinks or net sources of nutrients along the stream during the study period, we calculated the frequency of $F_{sw} > 0$, $F_{sw} < 0$, and $F_{sw} = 0$ for each nutrient and for each segment. We assumed that F_{sw} was undistinguishable from 0 when its upper and lower limit contained zero.

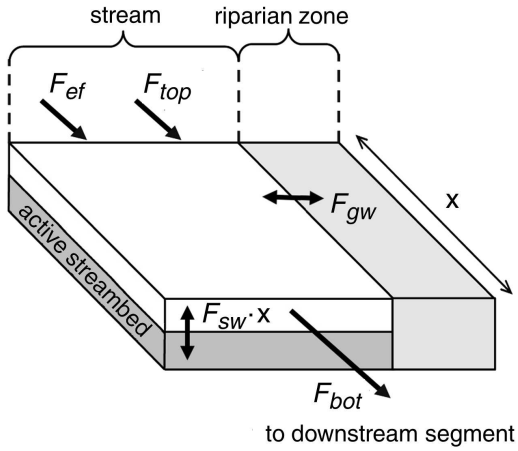

Figure 7.3 Conceptual representation of nutrient fluxes considered to estimate in-stream net nutrient uptake for each stream segment ($F_{sw} \cdot x$, Equation 7.2). For each segment of length x, the considered nutrient input fluxes were upstream (F_{top}) and tributaries (F_{ef}). Nutrient fluxes exiting the stream segment (F_{bot}) were F_{top} for the contiguous downstream segment. Riparian groundwater nutrient fluxes could either enter ($F_{gw} > 0$) or exit ($F_{gw} > 0$) the stream. Nutrient fluxes for each component were estimated by multiplying its water flux (Q) by its nutrient concentration (C). In-stream net nutrient uptake ($F_{sw} \cdot x$) is the result of gross nutrient uptake and release by the active streambed. $F_{sw} \cdot x$ can be positive (gross uptake > release), negative (gross uptake < release), or nil (gross uptake ~ release). See text for details.

Since in-stream nutrient cycling can substantially vary with reach length (Meyer and Likens 1979, Ensign and Doyle 2006), we also calculated F_{sw} for the whole 3.7 km reach by including all hydrological input and output fluxes (solute fluxes from the upstream-most site, tributaries, and riparian groundwater gross gains and losses) in a mass balance at the whole-reach scale. For the two spatial scales (segment and whole reach), we examined whether F_{sw} differed among nutrients with a Mann-Whitney test.

Relative contribution of riparian groundwater and in-stream nutrient processing to stream nutrient fluxes

To assess the relevance of F_{sw} compared to input solute fluxes, we calculated the ratio between $F_{sw} \cdot x$ (absolute value) and the total input flux (F_{in}) for each solute and sampling date. For the two spatial scales (segment and whole reach), F_{in} was the sum of upstream (F_{top}), tributaries (F_{ef}), and net riparian groundwater inputs (F_{gw}). The latter was included when $Q_{gw} > 0$. We interpreted a high $|F_{sw} \cdot x / F_{in}|$ ratio as a strong potential of in-stream processes to modify input fluxes (either as a consequence of gross uptake or release). For each spatial scale, we explored whether $|F_{sw} \cdot x / F_{in}|$ differed among nutrients with a Mann-Whitney test.

We used a whole-reach mass balance approach to assess the relative contribution of net riparian groundwater inputs ($F_{gw} > 0 / F_{in}$) to stream solute fluxes. In addition, we calculated the contribution of upstream (F_{top}/F_{in}) and tributary inputs (F_{ef}/F_{in}) to stream solute fluxes. For each solute, we analyzed differences in the relative contribution of different sources to stream input fluxes with a Mann-Whitney test. Finally, when the whole reach was acting as a net sink for a particular nutrient ($F_{sw} > 0$), we calculated the relative contribution of in-stream net uptake to reduce stream nutrient fluxes along the 3.7 km reach with $F_{sw} \cdot x / F_{in}$.

7.3 RESULTS

7.3.1 Hydrological Characterization of the Stream Reach

During the study period, mean Q' decreased from 0.82 ± 0.13 to 0.54 ± 0.11 mm d^{-1} (mean ± SE) along the reach (linear regression [l.reg], $R^2 = 0.79$, degrees of freedom [df] = 14, $F = 51.4$, $p < 0.0001$) (Figure 7.4a). This pattern hold for the two seasonal periods considered (dormant and vegetative; Wilcoxon rank sum test, $p > 0.05$).

On average, the stream was net gaining water along the 3.7 km reach, though the hydrological interaction between the riparian zone and the stream was highly variable across contiguous segments (Figure 7.4b). The stream was consistently gaining water along the first 1.5 km and the last 0.5 km, while hydrological losses were evident along the intermediate 2 km (Figure 7.4b). At the whole-reach scale, gross hydrological gains exceed gross losses in 8 out of 10 field dates (Figure 7.2c and Figure 7.2d). This was especially noticeable in April and December 2011, the two sampling dates that were most

influenced by storm events. In contrast, the whole reach was acting as net hydrological losing in March and October 2011.

Stream Cl^- concentrations showed a 40% increase along the reach (l.reg, $R^2 = 0.88$, df = 14, F = 44.6, $p < 0.001$), which contrasted with the longitudinal pattern exhibited by stream discharge (Figure 7.4c). The two periods showed a similar longitudinal pattern, though stream Cl^- concentration was lower during the dormant than during the vegetative period (Wilcoxon rank sum test, Z = -6.4, $p < 0.001$) (Table 7.1). The same seasonal pattern was exhibited by the five permanent tributaries (Figure 7.4c). There was a strong correlation between stream and riparian groundwater Cl- concentrations, which fitted well to the 1:1 line (low RRMSE for the two periods) (Table 7.2).

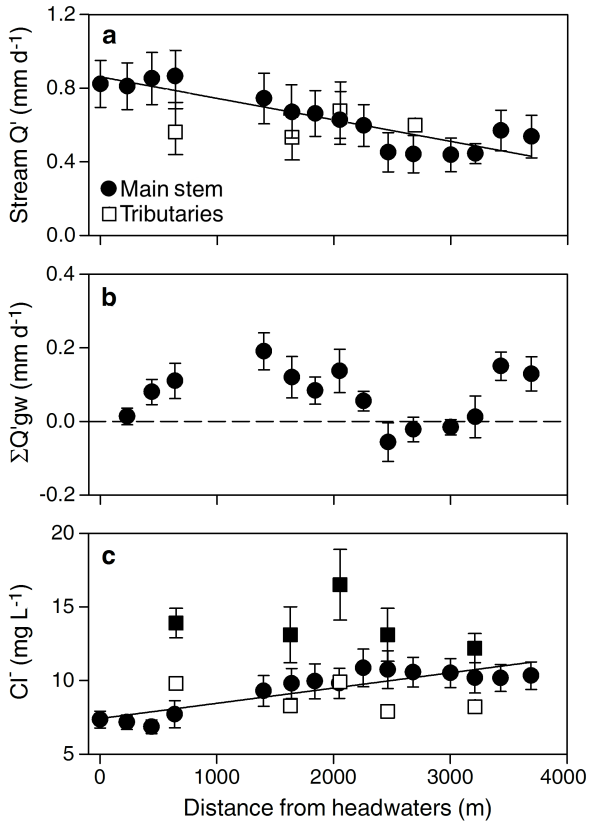

Figure 7.4 Longitudinal pattern of (a) area-specific stream discharge, (b) cumulative area-specific net groundwater inputs along the reach, and (c) stream chloride concentration. Symbols are average and standard error (whiskers) for the study period. Squares are values for tributaries. Stream chloride concentration in tributaries is shown separately for the dormant (white) and vegetative (black) period. Tributaries showed no differences in discharge between the two periods. Model regressions are indicated with a solid line only when significant (tributaries not included in the model).

The median net change in Cl^- flux within individual segments was 6 µg m^{-1} s^{-1}, which represented a small fraction of the Cl^- input flux ($F_{sw} \cdot x / F_{in}$ = 3%). Similar results were obtained when calculating Cl^- budgets for the whole-reach approach (Table 7.3). The stream Cl^- flux was mainly explained by inputs from tributaries followed by riparian groundwater and upstream. Similar results were obtained when calculating the relative contribution of different water sources to stream discharge at the whole-reach scale (Table 7.4).

7.3.2 Longitudinal Pattern of Stream Nutrient Concentration

The longitudinal pattern of stream concentration differed between nutrients and periods. During the dormant period, stream NO_3^- concentration decreased along the reach especially within the first 1.5 km (l.reg, $R^2 = 0.47$, df = 15, F = 11.4, $p < 0.005$) (Figure 7.5a). During the vegetative period, stream NO_3^- concentration showed a U-shaped pattern: it decreased along the first 1.5 km, remained constant along the following 1 km, and increased by 60% along the last kilometer of the reach (Figure 7.5a). Despite these differences, stream NO_3^- concentration was similar between the dormant and vegetative period for both the main stem and tributaries (in all cases: Wilcoxon rank sum test, $p > 0.05$) (Table 7.1).

Stream NH_4^+ concentration showed an increasing longitudinal pattern during the dormant period (exponential regression [e.reg], $R^2 = 0.45$, df = 15, F = 10.5, $p < 0.01$), while concentration decreased during the vegetative period (logarithmic regression [lg.reg], $R^2 = 0.42$, df = 15, F = 9.6, $p < 0.01$) (Figure 7.5b). The main stem showed higher NH_4^+ concentration during the vegetative than during the dormant period (Wilcoxon rank sum test, Z = -3.5, $p < 0.001$) (Table 7.1). For the tributaries, NH_4^+ concentration was similar between the two periods (in all cases: Wilcoxon rank sum test, $p > 0.01$).

Stream SRP concentration showed an increased along the reach during both the dormant (e.reg, $R^2 = 0.59$, F = 18.5, df = 14, $p < 0.01$) and vegetative period (l.reg, $R^2 = 0.49$, F = 12.4, df = 14, $p < 0.01$) (Figure 7.5c). Similar to NH_4^+, the main stem showed higher SRP concentration during the vegetative than during the dormant period (Wilcoxon rank sum test, Z = -6.6, $p < 0.001$) (Table 7.1). For the tributaries, SRP concentration was similar between the two periods (in all cases: Wilcoxon rank sum test, $p > 0.01$).

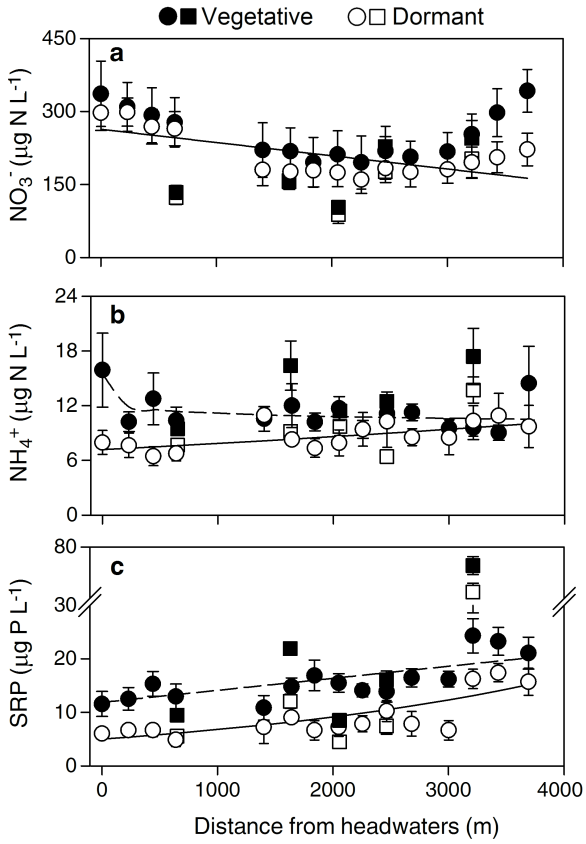

Figure 7.5 Longitudinal patterns of stream nutrient concentrations for (a) nitrate, (b) ammonium, and (c) solute reactive phosphorus at Font del Regàs. Symbols are average and standard error (whiskers) for the main stem (circles) and tributaries (squares). Lines indicate significant longitudinal trends for the dormant (solid) and vegetative (dashed) period (tributaries not included in the model).

7.3.3 Sources of Variation in Stream Nutrient Concentration

Riparian groundwater inputs

The relationship between stream and riparian groundwater concentrations differed between nutrients and periods. During the dormant period, stream and riparian groundwater NO_3^- concentrations were similar, while the stream showed higher concentrations during the vegetative period (Table 7.1). During the two periods, stream and riparian groundwater NO_3^- concentrations were positively correlated and showed relatively small RRMSE (Table 7.2). NH_4^+ concentration in stream water was 2-3 fold lower than in riparian groundwater (Table 7.1), and further, stream and

groundwater concentrations were no correlated either during the dormant or vegetative periods (Table 7.2). Stream and riparian groundwater SRP concentrations were similar in the two periods (Table 7.1). During the dormant period, SRP concentration showed a significant correlation between the two water bodies, while no correlation and relatively high RRMSE occurred during the vegetative period (Table 7.2). The differences in nutrient concentrations between stream and riparian groundwater in the two study periods were accompanied by consistently higher DO concentrations in the stream than in riparian groundwater (Table 7.1).

Table 7.1 Median and interquartile range [25th, 75th percentiles] of stream and riparian groundwater solute concentrations for the dormant and vegetative period. The number of cases is shown in parenthesis for each group. For each variable, the asterisk indicates statistically significant differences between the two water bodies (Wilcoxon paired rank sum test, $p < 0.01$).

		Stream	Riparian groundwater
Dormant	**Cl^- (mg L^{-1})**	7.6 [6.5, 8] (60)	7.7 [7.2, 8.8] (57)*
	NO_3^- (µg N L^{-1})	192 [159, 262] (60)	194 [109, 298] (56)
	NH_4^+ (µg N L^{-1})	8.9 [6.5, 10.3] (60)	19 [13.8, 34.2] (56)*
	SRP (µg P L^{-1})	7.6 [4.5, 11.7] (60)	8 [6, 20] (51)
	DO (mg L^{-1})	12.9 [11.5, 16] (60)	3.5 [1.5, 4.6] (54)*
Vegetative	**Cl^- (mg L^{-1})**	8.8 [7.9, 13.5] (100)	10.1 [8.6, 15] (98)*
	NO_3^- (µg N L^{-1})	223 [155, 282] (102)	168 [77, 264] (98)*
	NH_4^+ (µg N L^{-1})	10 [8.7, 12.8] (103)	27 [18.2, 37.1] (101)*
	SRP (µg P L^{-1})	16.5 [11.7, 21.3] (103)	14.1 [9.3, 23.3] (97)
	DO (mg L^{-1})	9.9 [9.1, 11.1] (84)	1.7 [0.8, 2.5] (98)*

In-stream nutrient processing

The influence of in-stream nutrient processing on stream water chemistry differed among nutrients. During the study period, median F_{sw} was negative for NO_3^-, positive for NH_4^+, and close to 0 for SRP (Table 7.3). However, between-nutrient differences in F_{sw} were not statistically significant among nutrients for either the vegetative or dormant period (for both periods: Mann-Whitney test with post hoc Tukey test, $p > 0.05$). Similar F_{sw} values were obtained when calculating nutrient budgets either by segment or whole reach (Table 7.3).

Table 7.2 Spearman ρ coefficient between stream water and riparian groundwater solute concentrations for each period and for the whole data set collected at the Font del Regàs during the study period. The relative root mean square error (RRMSE) indicates divergences from the 1:1 line. The number of cases is shown in parenthesis for each variable. ns, no significant; *p < 0.001.

	Dormant			Vegetative			All data		
	ρ	RRMSE (%)	n	ρ	RRMSE (%)	n	ρ	RRMSE (%)	n
Cl^- (mg L^{-1})	0.78*	2.1	53	0.8*	2.9	98	0.84*	2.8	151
NO_3^- (µg N L^{-1})	0.48*	8.1	57	0.34*	8.3	101	0.37*	6	158
NH_4^+ (µg N L^{-1})	ns	11.7	57	ns	9.1	101	ns	7.3	158
SRP (µg P L^{-1})	ns	17.9	57	0.43*	5.5	101	0.41*	7.3	158

Table 7.3 Median and interquartile range [25th, 75th percentile] of in-stream net nutrient uptake flux (F_{sw}) and the potential of F_{sw} to modify solute input fluxes ($|F_{sw} \cdot x/F_{in}|$) for both the stream segment and whole reach during the study period. n = 150 and 10 for segments and whole-reach data sets, respectively.

		By segment	By whole reach
F_{sw} (µg m^{-1} s^{-1})	Cl^-	6 [-37, 80]	12 [2, 33]
	NO_3^-	-0.4 [-4.4, 1.3]	-1.0 [-3.4, 1.6]
	NH_4^+	0.2 [-0.1, 0.6]	0.2 [-0.0, 1.1]
	SRP	0.0 [-0.6, 0.2]	-0.06 [-0.21, 0.01]
$\lvert F_{sw} \cdot x / F_{in} \rvert$ (%)	Cl^-	3 [1, 10]	4 [2, 9]
	NO_3^-	6 [2, 14]	24 [8, 67]
	NH_4^+	18 [10, 35]	48 [25, 71]
	SRP	21 [3, 41]	16 [6, 66]

The frequency of an individual segment to act either as a nutrient sinks or source differed among nutrients and along the reach. For NO_3^-, the frequency of $F_{sw} < 0$ (gross uptake < release) increased from 9% to > 50% along the reach (l.reg, $R^2 = 0.55$, df = 13, F = 14.67, p < 0.01) (Figure 7.6a). For NH_4^+, the frequency of $F_{sw} > 0$ (gross uptake > release) was high across individual segments, ranging from 20% to 90% (Figure 7.6b). For SRP, the frequency of $F_{sw} < 0$, > 0, or ~ 0 did not show any consistent longitudinal pattern (Figure 7.6c). Overall, the frequency of sampling dates for which in-stream biogeochemical processes were imbalanced ($F_{sw} \neq 0$) was lower for NO_3^- (36%) than for NH_4^+ (80%) and SRP (68%) (Figure 7.6).

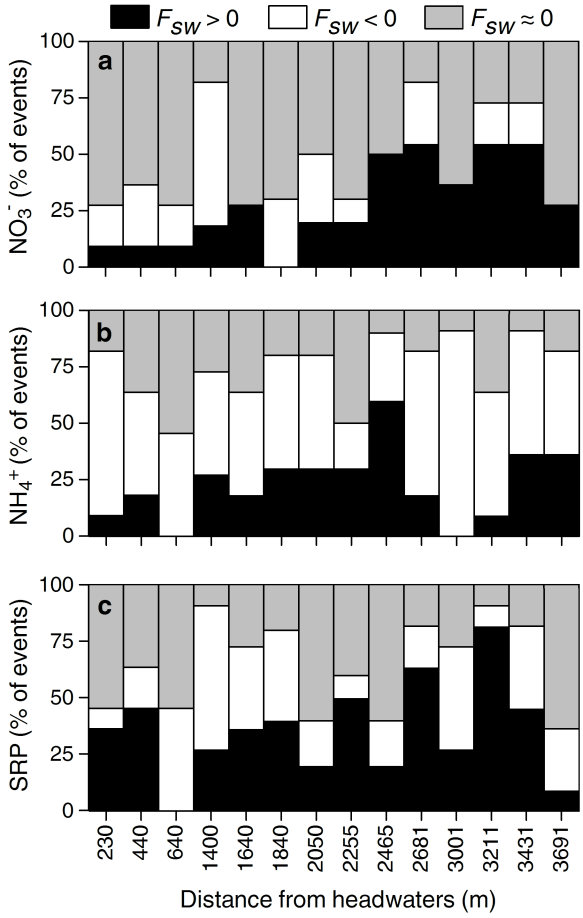

Figure 7.6 Frequency of dates for which $F_{sw} < 0$ (gross uptake < release), $F_{sw} > 0$ (gross uptake > release), and $F_{sw} \sim 0$ (gross uptake ~ release) for (a) nitrate, (b) ammonium, and (c) soluble reactive phosphorus for the 14 contiguous segments along the study reach from August 2010 to December 2011 (n = 11). The frequency is expressed as number of events in relative terms.

7.3.4 Relative Contribution of Riparian Groundwater and In-stream Processing to Stream Nutrient Fluxes at the Segment and Whole-reach Scale

The capacity of in-stream processes to modify stream input fluxes differed between nutrients and spatial scales. For individual segments, $|F_{sw} \cdot x/F_{in}|$ was smaller for NO_3^- (6%) than for NH_4^+ and SRP (~20%) (Mann-Whitney test with post hoc Tukey test, $p < 0.01$, Table 7.3). However, $|F_{sw} \cdot x/F_{in}|$ increased substantially for NO_3^- and NH_4^+ when nutrient budgets were calculated at the whole-reach scale (Table 7.3).

According to whole-reach mass balance calculations, the stream acted as a net source of NO_3^- on 7 out of the 10 sampling dates for which whole-reach budgets were calculated. The contribution of in-stream release to stream NO_3^- fluxes was as important as that of riparian groundwater and upstream fluxes (Table 7.4). In-stream net NO_3^- retention at the whole-reach scale was observed only in spring (March and April 2011) and December 2011 (Figure 7.7a).

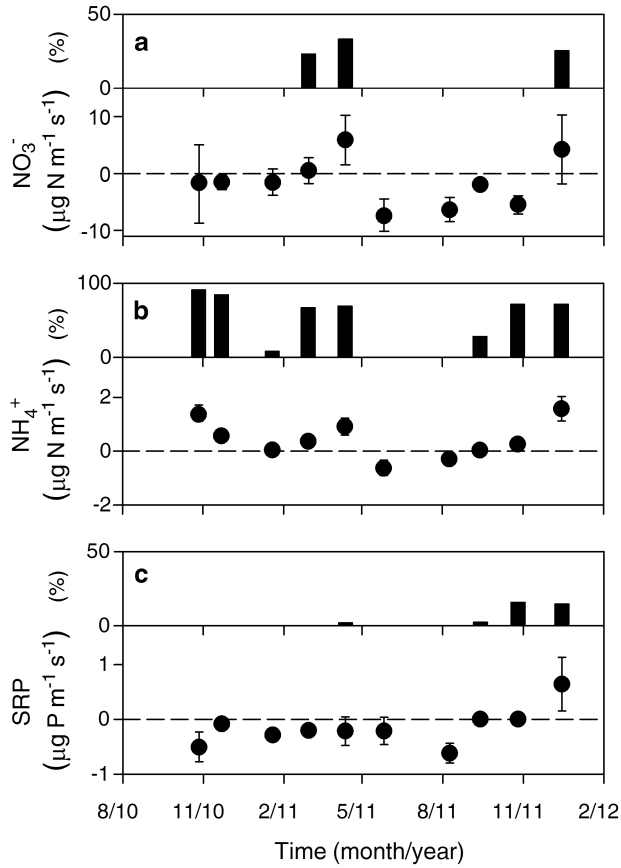

Figure 7.7 Temporal pattern of in-stream net nutrient uptake (F_{sw}, in µg m^{-1} s^{-1}) for (a) nitrate, (b) ammonium, and (c) soluble reactive phosphorus at the whole-reach scale. Whiskers are the uncertainty associated with the estimation of stream discharge from slug tracer additions. $F_{sw} > 0$ indicates that gross uptake prevailed over release, while $F_{sw} < 0$ indicates the opposite. For those cases for which $F_{sw} > 0$, the contribution of in-stream net nutrient uptake to reduce stream nutrient fluxes ($F_{sw} \cdot x/F_{in}$, in %) is shown (black bars).

The stream acted as a net source of SRP in 6 out of the 10 sampling dates. The contribution of in-stream release to stream SRP fluxes was as important as that of riparian groundwater (Table 7.4). In-stream net SRP retention was minimal, except in autumn 2011 (October and December 2011) (Figure 7.7c).

Table 7.4 Median and interquartile range [25th, 75th percentile] of the relative contribution of inputs from upstream (F_{top} / F_{in}), net riparian groundwater ($F_{gw} > 0 / F_{in}$), tributaries (F_{ef} / F_{in}), and in-stream release ($F_{sw} < 0 / F_{in}$|) to stream solute fluxes. For each solute, different capital letters indicate statistically significant differences between solute sources (Mann Whitney test with post-hoc Tukey test, $p > 0.01$). n = 10 for all four solutes.

Relative contribution (%)	Cl^-	NO_3^-	NH_4^+	SRP
Upstream	15 [12, 17]^{B}	22 [20, 35]^{A}	8 [6, 13]^{BC}	11 [6, 17]^{B}
Riparian groundwater	28 [14, 38]^{B}	17 [5, 47]^{A}	63 [43, 75]^{A}	21 [7, 38]^{AB}
Tributaries	59 [46, 69]^{A}	22 [19, 24]^{A}	21 [17, 30]^{B}	34 [26, 50]^{A}
In-stream release	0 [0, 0.3]^{C}	22 [0, 50]^{A}	0 [0, 6]^{C}	19 [0, 55]^{B}

7.4 DISCUSSION

In terms of hydrology, the study headwater stream was a net gaining reach, though the hydrological interaction between the riparian zone and the stream was complex as indicated by the longitudinal variation in net riparian groundwater inputs. Moreover, the longitudinal decrease in area-specific discharge suggests that hydrological retention increased at the valley bottom compared to upstream segments as reported in previous studies (Covino et al. 2010). Despite the complex hydrological processes along the reach, the strong positive correlation between stream and riparian groundwater Cl^- concentration suggests high hydrological connectivity at the riparian-stream interface (Bernal et al. 2003). In addition, we found that the permanent tributaries, which comprised ~ 50% of the catchment area, contributed 56% of stream discharge; and thus, were an essential component for understanding stream nutrient chemistry and loads. Hydrological mixing of stream water with water from tributaries could partially explain the longitudinal increase in Cl^- because its concentration was higher at the tributaries than at the main stem, especially during the vegetative period. In addition, riparian groundwater inputs to the stream could further contribute to the longitudinal

increase in stream Cl^- concentration because they contributed 26% of stream discharge and also exhibited higher Cl^- concentration than stream water.

Based on the strong hydrological connectivity between the stream and the riparian groundwater and the large contribution of tributaries to stream discharge, one would expect a strong influence of these water sources on the longitudinal variation in stream nutrient chemistry. However, the relationship between stream and riparian groundwater nutrient concentration was from moderate to weak for NO_3^- and SRP, and zero for NH_4^+. Further, the contribution of tributaries to stream nutrient fluxes was relatively small (from 21% to 34%) compared to their contribution to stream Cl^- and water fluxes (> 50%). Together these data suggest that longitudinal patterns of stream nutrient concentration could not be explained by hydrological mixing alone, thus pointing to in-stream biogeochemical processing as a likely mechanism to modify nutrient concentrations along the study reach. In fact, the estimates of in-stream net nutrient uptake (F_{sw}) at the different stream segments supported this idea and agreed with previous studies showing that in-stream processes can mediate stream nutrient chemistry and downstream nutrient export (McClain et al. 2003, Harms and Grimm 2008).

Our results revealed an extremely high variability in F_{sw}, which could range by up to one order of magnitude, across individual segments and over time, which agrees with findings from other headwater streams (von Schiller et al. 2011). However, some general trends appeared when comparing patterns for the different studied nutrients. For instance, the frequency of dates for which in-stream gross uptake and release were imbalanced ($F_{sw} \neq 0$) was higher for NH_4^+ (80%) and SRP (68%) than for NO_3^- (37%). Further, the potential of in-stream processes to modify stream fluxes within stream segments ($|F_{sw} \cdot x/F_{in}|$) was 3 fold higher for NH_4^+ and SRP than for NO_3^-. Our findings are concordant with studies performed at short stream reaches (< 300 m) worldwide, which show that in-stream gross uptake velocity (as a proxy of nutrient demand) is typically higher for NH_4^+ and SRP than for NO_3^- (Ensign and Doyle 2006). This difference among nutrients is commonly attributed to the higher biological demand for NH_4^+ and SRP than for NO_3^-. However, we found that F_{sw} was similar among nutrients; thus, differences in $|F_{sw} \cdot x/F_{in}|$ were mainly associated with differences in the concentration of the inputs, which tend to be 20 fold lower for NH_4^+ and SRP than for NO_3^-. Divergences between F_{sw} and $|F_{sw} \cdot x/F_{in}|$ were even more remarkable when nutrient budgets were considered at the whole-reach scale, especially for DIN forms. NO_3^- and NH_4^+ showed no differences in F_{sw} between the two scales of observation; however, they showed a substantial increase in $|F_{sw} \cdot x/F_{in}|$ at the whole-reach scale (length of kilometers) compared to the segment scale (length

of hundreds of meters). Similarly, previous nutrient spiraling studies have reported an increase in the proportion of nutrient removal with stream order despite no changes in gross uptake rates among stream reaches (Wollheim et al. 2006, Ensign and Doyle 2006). This pattern has been attributed to variation in intrinsic stream characteristics, such as stream nutrient concentration, discharge, stream width, and the size of the hyporheic zone (Wollheim et al. 2006, Alexander et al. 2009), which may also hold for our study since these characteristics varied along the 3.7 km reach. However, our results also indicate that the assessment of riparian groundwater inputs is crucial to understand the contribution of in-stream processes to stream nutrient fluxes. Overall, our findings add to the growing evidence that streams are hot spots of nutrient processing (Peterson et al. 2001, Dent et al. 2007), and that in-stream processes can substantially modify stream nutrient fluxes at the catchment scale (Ensign and Doyle 2006, Bernal et al. 2012b).

The potential of in-stream processes to regulate stream nutrient fluxes was especially remarkable for NH_4^+. There was no relationship between stream and riparian groundwater NH_4^+ concentrations; further, whole-reach budgets indicated that in-stream net uptake could reduce the flux of NH_4^+ up to 90% along the reach. This high in-stream bioreactive capacity could be favored by the sharp increase in redox conditions from riparian groundwater to stream water (Hill et al. 1998, Dent et al. 2007). Concordantly, NH_4^+ concentrations were higher in riparian groundwater than in the stream, while the opposite occurred for NO_3^- (although only during the vegetative period). These results suggest fast nitrification of groundwater inputs within the stream as environmental conditions become well oxygenated (Jones et al. 1995). However, the marked increase in stream NO_3^- concentration observed along the last 700 m of the reach during the vegetative period could not be explained entirely by nitrification of riparian groundwater NH_4^+ because this flux ($F_{sw} \sim 2$ μg N m^{-1} s^{-1}) was not large enough to sustain in-stream NO_3^- release ($F_{sw} < 0$) (~ 10 μg N m^{-1} s^{-1}). This finding suggests an additional source of N at the valley bottom. Previous studies have shown that leaf litter from riparian trees, and especially from N_2-fixing species, can enhance in-stream nutrient cycling because of its high quality and degradability (Starry et al. 2005, Mineau et al. 2011). Thus, the increase in NO_3^- and SRP concentrations and in-stream NO_3^- release observed at the lowest part of the catchment during the vegetative period could result from the combination of warmer temperatures and the mineralization of large stocks of alder and black locust leaf litter stored in the stream bed (Strauss and Lamberti 2000, Bernhardt et al. 2002b, Starry et al. 2005).

Alternatively, increases in stream NO_3^- and SRP concentration could result from human activities, which were concentrated at the lowest part of the catchment. However,

regarding NO_3^-, anthropogenic sources seem unlikely because DIN concentrations at the tributary draining through the inhabited area were low. In contrast, this tributary showed high SRP concentrations (from 2 to 6 fold higher than in the main stem), though its discharge should have had to be ca. 4 fold higher than expected for its drainage area (< 0.4 km^2) to explain the observed changes in concentration. Another possible explanation for the increase in stream N concentration at the valley bottom could be increased N fixation by stream algae (Finlay et al. 2011). However, in-stream DIN release (NO_3^- and NH_4^+) peaked in late spring and summer (May and August 2011), when light penetration was limited by riparian canopy and in-stream photoautotrophic activity was low (see Chapter 6). Altogether, these data suggest that the sharp increase in nutrient availability along the last 700 m of the reach was likely related to the massive presence of the invasive black locust at the valley bottom. Black locust is becoming widespread throughout riparian floodplains in the Iberian Peninsula (Castro-Díez et al. 2014) and its potential to subsidize N to stream ecosystems via root exudates and leaf litter could dramatically alter in-stream nutrient processing and downstream nutrient export (Stock et al. 1995, Mineau et al. 2011). However, further research is needed to test the hypothesis that this invasive species can alter stream nutrient dynamics in riparian floodplains.

It is worth noting that longitudinal trends in stream nutrient concentration showed no simple relationship to in-stream processes. This finding evidenced that other sources of variation of stream water chemistry were counterbalancing the influence of in-stream processes on stream nutrient fluxes. In this sense, results from NH_4^+ were paradigmatic. The mass balance approach clearly showed that in-stream gross uptake of NH_4^+ exceeded release; concordantly, NH_4^+ concentration was consistently lower in the stream than in riparian groundwater. However, stream NH_4^+ concentration showed small longitudinal variation likely because in-stream net uptake balanced the elevated inputs from riparian groundwater. Therefore, our results challenge the idea that stream nutrient concentration should decrease in the downstream direction when in-stream processes are efficient in taking up nutrients from receiving waters (Brookshire et al. 2009). Conversely, our findings convincingly show that in-stream processes can strongly affect stream nutrient chemistry and downstream nutrient export despite this may not result in consistent longitudinal gradients in nutrient concentration. For NO_3^-, our data suggest that the marked increase in concentration along the last 700 m could be a consequence of in-stream mineralization of N-rich leaf-litter stocks. However, the observed decrease in NO_3^- concentration along the first 1.5 km of the reach could barely be explained by in-stream processing alone because its contribution to reduce stream NO_3^- fluxes was too low, even when the whole-reach budget was recalculated

excluding the last 700 m of the reach (F_{sw} = 0.61 μg N m^{-1} s^{-1} and F_{sw} /F_{in} = 10%). Therefore, the declining pattern was likely a combination of both in-stream nutrient processing and hydrological mixing with riparian groundwater and tributary inputs. For SRP, the longitudinal increase in concentration could neither be fully explained by in-stream release because $F_{sw} < 0$ was not widespread along the reach and the stream only contributed to input fluxes by 19% (6% when excluding the last 700 m). Again, stream nutrient chemistry along the reach was the combination of both in-stream nutrient processing and hydrological mixing as indicated by our whole-reach mass balance. Recent studies have concluded that riparian groundwater is a major driver of longitudinal patterns in stream nutrient concentration in headwater streams (Bernhardt et al. 2002, Asano et al. 2009, Scanlon et al. 2010). Our study adds to our knowledge of catchment biogeochemistry by showing that stream nutrient chemistry results from the combination of both hydrological mixing from the riparian zone and in-stream nutrient processing, which can play a pivotal role in shaping stream nutrient concentrations and fluxes at the catchment scale.

7.5 CONCLUSIONS

The synoptic approach adopted in this study highlighted that the Font del Regàs stream had a strong potential to transform nutrients. Longitudinal pattern in stream nutrient concentrations could not be explained solely by hydrological mixing with riparian groundwater and tributary sources because dissolved nutrients underwent biogeochemical transformation while travelling along the stream channel. Our results revealed that in-stream processes were highly variable over time and space, though in most cases this variability could not be associated with either physical longitudinal gradients or shifts in environmental conditions between the dormant and vegetative period. Nevertheless, results from a mass balance approach showed that in-stream processes contributed substantially to modify stream nutrient fluxes and that the stream could act either as a net nutrient sink (for NH_4^+) or as a net nutrient source (for SRP and NO_3^-) at the catchment scale. These results add to the growing evidence that in-stream biogeochemical processes need to be taken into consideration in either empirical or modeling approaches if we are to understand drivers of stream nutrient chemistry within catchments.

Recent studies have proposed that riparian groundwater is a major control of longitudinal patterns of nutrient concentration because in-stream gross nutrient uptake and release tend to counterbalance each other most of the time (Brookshire et al. 2009, Scanlon et

al. 2010). Conversely, our study showed that in-stream processes can influence stream nutrient chemistry and downstream exports without generating longitudinal gradients in concentration and flux because changes in stream nutrient chemistry are the combination of both in-stream processing and nutrient inputs from terrestrial sources. Our results imply that the assessment of these two sources of variation of stream nutrient chemistry is crucial to understand the contribution of in-stream processes to stream nutrient dynamics at relevant ecological scales.

Reliable measurements of riparian groundwater inputs are difficult to obtain because spatial variability can be high (Lewis et al. 2006) and to determine the chemical signature of the groundwater that really enters the stream is still a great challenge (Brookshire et al. 2009). In this study, we installed 15 piezometers along the reach (one per sampling site), which may not be representative enough of the variation of riparian groundwater chemistry. However, and despite its limitations, riparian groundwater sampling near the stream can help to constrain the uncertainty associated with this water source and provide more reliable estimations of in-stream net nutrient uptake for both nutrient mass balance and spiraling empirical approaches (von Schiller et al. 2011).

AKNOWLEDGEMENTS

We thank Aitana Oltra for assisting with GIS, and Sílvia Poblador, Eduardo Martín, and Clara Romero for field assistance. SB was funded by the Spanish Ministry of Economy and Competitiveness (MINECO) with a Juan de la Cierva contract (JCI-2010-06397), the Spanish Research Council (CSIC) (JAEDOC027) and the MICECO-funded project MED_FORESTREAM (CGL2011-30590). AL was supported by a FPU PhD fellowship from the Spanish Ministry of Education and Science (AP-2009-3711). MR was funded by a technical training contract from the MINECO-funded project ISONEF (CGL2008-05504-C02-02) and MED_FORESTREAM. Additional financial support was provided by the European Union-funded project REFRESH (FP7-ENV-2009-1-244121) and the MINECO-funded project MONTES-Consolider (CSD 2008-00040). The Vichy Catalan Company, the Regàs family and the Catalan Water Agency (ACA) graciously gave us permission for at the Font del Regàs catchment.

PART IV

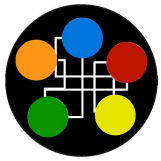

CHAPTER 8

General Discussion: Learning about the Role of Mediterranean Riparian Zones as Regulators of Stream Hydrology and Nitrogen Biogeochemistry within Catchments

Riparian zones are hot spots of water and nutrient cycling within landscapes, and thus, integrating these ecosystems within catchment hydrological, biogeochemical, and ecological perspectives is an important challenge that landscape ecologists need to face at the present time. Which is the quantitative influence of riparian zones on stream hydrology and N biogeochemistry across biomes? Does it vary over time and along the fluvial network? This chapter synthesizes the most relevant results obtained in this dissertation, and puts them in a broader context in order to answer, to some extent, these questions. Furthermore, it discusses the implication of our research in the catchment ecology domain and the potential role of Mediterranean riparian zones as catchment nitrogen buffers.

8.1 INTRODUCTION

Despite riparian zones have been studied since the 40s (Dunford and Fletcher 1947), quantifying the ecological role of these systems within catchments has been challenging for ecologists, likely because of its diverse and dynamic character (Naiman et al. 2005, Pinay et al. 2015). In this dissertation, we have combined different empirical and modelling approaches in order to examine in detail some of the processes and mechanisms by which Mediterranean riparian zones can regulate stream hydrology and nitrogen (N) dynamics. In addition, the inclusion of different catchment pools in our monitoring strategies (i.e., upland and riparian soils, stream water, riparian groundwater, upland springs, and lixiviates), as well as the consideration of different temporal scales (ranging from sub-daily to annual), have enabled the analysis of the riparian system within the upland-riparian-stream context.

The results obtained from this dissertation highlight the close and inseparable hydrological and biogeochemical links between landscape units and, most importantly, provide valuable insights on the potential role of Mediterranean riparian zones as N buffers within catchments. This sort of knowledge, until the date mostly available at plot or reach scale, is crucial for dissecting and understanding the overall structure and function of Mediterranean landscapes. Moreover, understanding the functioning of riparian zones at the catchment scale can be especially relevant in the current context of climate change because future warming and drying may change their role within the catchment, which may have important implications for the water quality (and quantity) of Mediterranean stream and rivers (Martí et al. 2010).

This general discussion focuses on four of the main contributions from the present dissertation: (i) the role of riparian zones as hot spots of soil N cycling within catchments, (ii) the contribution of hot moment of soil N cycling on annual basis, (iii) the relevance of riparian evapotranspiration on stream hydrology, and (iv) the potential role of Mediterranean riparian zones as catchment N buffers.

8.2 RIPARIAN ZONES AS HOT SPOTS OF SOIL N CYCLING

Riparian zones are recognized for being highly bioreactive ecosystems compared to the surrounding areas (McClain et al. 2003, Vidon et al. 2010). The Font del Regàs was no exception, because the riparian zone exhibited much higher rates of net N mineralization (NNM), and especially net nitrification (NN), compared to upland soils (Chapter 3). As

expected, these disproportional high rates of microbial N supply increased riparian soil NO_3^- availability compared to upland forest soils (6-12 vs. 1 mg N kg^{-1}), though values were similar to those found in other Mediterranean riparian zones (5-20 mg N kg^{-1}) (Bernal et al. 2007, Evans and Schoenholtz 2011, Smith et al. 2012).

Increased microbial N activity in riparian soils has been previously attributed to surplus of organic N (Booth et al. 2005), an explanation that holds for this Mediterranean riparian site because N_2-fixing tree species were abundant at the valley bottom (> 80% of total tree riparian basal area) and soils exhibited relatively low C:N ratios (< 20) (Chapter 3). Moreover, the characteristic wet conditions of these riparian soils relatively to upland areas may also contribute to sustain the observed high NNM and NN rates. According to our model simulations (Chapter 4), riparian NNM and NN rates were not water-limited, which contrasted with the oak and beech upland systems, where soil dryness severely reduced soil microbial activity and soil N availability.

To explore whether the observed differences in microbial N supply between upland and riparian soils are found in other catchments elsewhere, we compiled mean daily NN rates for a set of 66 studies encompassing Mediterranean, arid, and temperate biomes (Appendix B). For this data analysis, the study sites were classified by their mean annual precipitation (MAP), which ranged from < 500 mm for arid systems to > 1000 mm for temperate systems. Mediterranean systems held an intermediate position (MAP between 500-1000 mm), and exhibited severe summer droughts.

For Mediterranean systems, mean daily NN rates in riparian zones were, on average, 5 fold higher than those reported on upland systems, including oak, beech, and pine woodlands (Figure 8.1). This pattern is coincident with that found at Font del Regàs, supporting the idea that Mediterranean riparian soils tend to act as hot spots of microbial N supply within catchments, likely because they keep relatively wet throughout the year (WFPS for the studies included in this data analysis ranged from 40-80%). Importantly, our model simulations (Chapter 4) suggested that the potential for nitrification of Mediterranean riparian soils could increase in the future because riparian soils appeared to be highly sensitive to warming, while upland forests showed insensitivity to increments in temperature due to water limitation. Therefore, the storage of inorganic N in Mediterranean riparian soils could increase in the next decades, as well as their potential as hot spots of N supply within catchments.

Interestingly, the spatial pattern exhibited by Mediterranean sites does not apparently hold for arid and temperate biomes. Arid and semiarid systems (MAP < 500 mm) exhibited extremely low mean daily NN rates for both riparian and upland soils (Figure 8.1), likely because soils remained dry during most of the time in the two

landscape units (WFPS ranging from 2-30%). Supporting this idea, our model simulations (Chapter 4) suggested strong decrements of NNM and NN during severe dry conditions (WFPS < 20%), as well as a slow turnover of inorganic N in soils experiencing extended drought. Therefore, soil NO_3^- availability in arid riparian zones (0.01-2 mg N kg^{-1}) appears to contribute minimally to the overall catchment N budgets (Booth et al. 2003, Adair et al. 2004, Dijkstra et al. 2012).

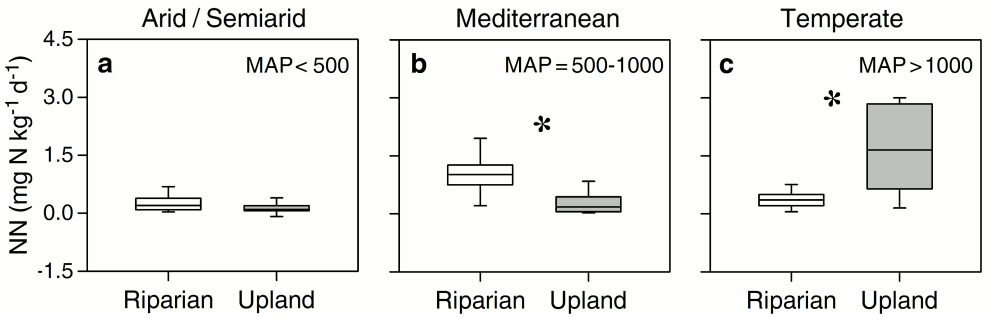

Figure 8.1 Comparison of mean daily net nitrification rates (NN) between riparian and upland systems in (a) arid/semiarid, (b) Mediterranean, and (c) temperate regions. Asterisks indicate significant differences between riparian and upland NN rates (Wilcoxon rank sum test, $p < 0.01$). The number of cases (n) for riparian and upland systems was: 10 and 10, 10 and 12, and 11 and 13 for arid/semiarid, Mediterranean, and temperate regions, respectively. Studies were classified according to its mean annual precipitation (MAP). References and characterization of the study sites are in Appendix B.

Finally, temperate regions (MAP > 1000 mm) exhibited the opposite pattern than Mediterranean systems, with mean daily NN rates being 3.5 fold lower in riparian soils than in upland soils (Figure 8.1). In this case, low riparian NN rates can be likely attributed to soil waterlogged conditions (WFPS for the studies included in this data analysis > 70%), which would limit aerobic nitrification while fostering denitrification. Accordingly, high denitrification rates (0.2-0.8 mg N kg^{-1} d^{-1}) and low soil NO_3^- concentrations (< 4 mg N kg^{-1}) have been reported in temperate riparian soils (Clément et al. 2003, Vidon and Hill 2004b). In contrast, soil moisture conditions for the temperate upland forests (WFPS 40-50%) were generally within the optimal range for NNM and NN (according to the model simulations in Chapter 4). Therefore, the combination of high denitrification in riparian soils and high nitrification in upland soils may explain the spatial pattern found for the temperate systems.

Despite the relatively small number of studies included in this data analysis, our exercise points out that the soil N cycle strongly relies on microclimatic conditions; and that the role of riparian zones on whole catchment N budgets can vary widely among biomes. As

conceptualized in Figure 8.2, this data compilation supports the idea that water scarcity limits microbial N supply in arid and semiarid systems compared to more humid systems in both riparian and upland forests (Harms and Grimm 2008, Dijkstra et al. 2012). In Mediterranean systems, which hold an intermediate position across the climatic gradient, riparian zones appear to be hot spots of soil microbial N supply compared to the more water-limited upland forests. As such, riparian soils may have a disproportionally large impact on the overall catchment N cycling despite that they occupy a small area. Finally, in temperate systems, microbial activity in upland forests may be the major contributor to soil N supply within catchments (Kendall et al. 2007, Goodale et al. 2009), while riparian soils tend to be hot spots of denitrification, thus contributing substantially to N removal at the catchment scale (McClain et al. 2003).

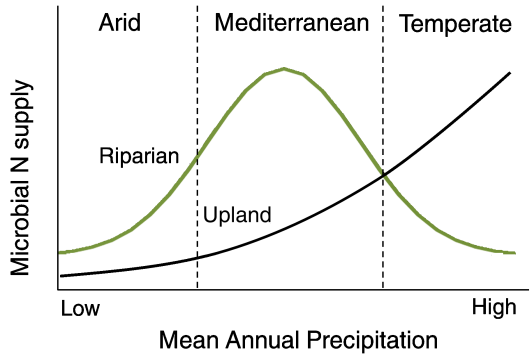

Figure 8.2 Conceptualization of the contribution of soil microbial N supply to catchment N budgets across biomes based on the data compilation shown in Figure 8.1. The relative contribution of upland soils to catchment N export increases with increasing mean annual precipitation (black line). Conversely, riparian soils exhibit a bell-shaped curve, being their contribution maxima in Mediterranean systems (green line).

8.3 ON THE UNDERSTANDING THE HOT MOMENT BEHAVIOR

Although constrained in time, biogeochemical pulses (or *hot moments*) have the ability to alter nutrient budgets at both plot and catchment scales. Hence, there is a growing consensus that the consideration of pulse dynamics within terrestrial and water quality models is of great importance for conceptual and mathematical modelling exercises (e.g., *present study,* Borken and Matzner 2009, Vidon et al. 2010). However, our understanding of the implications of hot moments on the N cycle at relevant spatial and temporal scales is far from complete because most of the available studies have

been performed in systems with strong water limitation (i.e., arid scrublands) and for short time periods (from days to few months).

Perhaps one of the major contributions of the present dissertation is the finding that short-time pulses of soil N cycling (at the scale of days and weeks) contribute substantially to the soil N cycling at seasonal and annual scales, at least in the studied Mediterranean forests. Our results revealed, first, that microbial pulses could contribute at least 25-40% to annual mineralization and nitrification rates (Chapter 3); and second, that rewetting events were essential to understand the temporal pattern of soil N mineralization and nitrification in the three studied forest types (Chapter 4). Interestingly, not all precipitation events led to soil microbial pulses (Chapter 3), highlighting that the occurrence of hot moments depends on a myriad of climatic and ecosystem internal factors, which would be likely identified and disentangled in future studies.

In addition, our research shed new light on the soil N biogeochemistry of Mediterranean riparian ecosystems by showing peaks of soil mineralization and nitrification in summer. This pattern has been described on more temperate systems (Goodale et al. 2009, Brookshire et al. 2011), but it was an unexpected results for this study site. Moreover, this finding reveals that warming can have a similar, or even a higher, triggering effect than rewetting in these Mediterranean riparian soils (Chapter 3). Overall, these findings underscore the complexity of the microbial pulse behavior, and clearly stress that more intensive monitoring is needed to get a real understanding on how such pulses could affect ecosystem productivity and nutrient budgets at the catchment scale.

8.4 RIPARIAN EVAPOTRANSPIRATION: INSIGNIFICANT BUT CRUCIAL

Riparian trees can obtain water directly from the stream channel, the riparian groundwater, and/or the soil unsaturated zone (Snyder and Williams 2000, Brooks et al. 2009). In either case, the ET requirements of riparian trees are generally high (from 400 to 1300 mm yr^{-1}; Goodrich et al. 2000, Scott et al. 2008), especially when compared to mean annual ET rates of other tree species across the globe (503 ± 338 mm, Baldocchi and Ryu 2011).

However, the contribution of riparian ET to catchment water budgets ultimately depends on the climatic regime, which dictates the balance between water demand and water availability. Accordingly, a compilation of published data for different biomes around the world shows that the relative importance of annual riparian ET for

catchment water fluxes decreases with increasing water availability (here represented by the aridity index (AI), UNEP 1992). Therefore, water demand by riparian tress can account for 0% to > 30% of annual catchment water depletion as one moves from tropical (AI > 2) to arid regions (AI < 0.5) (Figure 8.3). Riparian ET at the Font del Regàs catchment (450 mm yr^{-1}) holds an intermediate position, contributing 4.5% of the total annual catchment water depletion (Chapter 5). Noteworthy, relatively small decrements in AI below a threshold of 0.8 tend to markedly increase the relative contribution of riparian ET to annual catchment water budgets (Figure 8.3). Therefore, future alterations in precipitation and temperature induced by climate change could exacerbate the impact of riparian zones on catchment water resources, especially in regions experiencing some degree of water limitation (AI ~ 0.8).

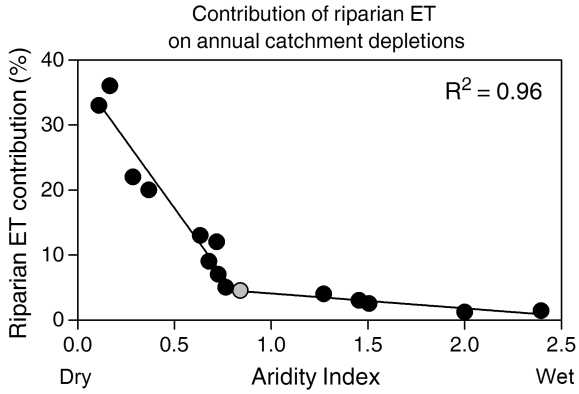

Figure 8.3 Relationship between the relative contribution of riparian evapotranspiration (ET) to annual catchment water depletion and the Aridity Index for a set of catchments worldwide (n = 15). Aridity Index is the ratio between annual precipitation and annual potential evapotranspiration; higher values indicate higher water availability. Total water output fluxes from the catchment are stream discharge, catchment evapotranspiration, riparian evapotranspiration, and anthropogenic extraction (if applies). The Font del Regàs catchment (present study) is indicated with a gray circle. References and characterization of the study sites are in Appendix B.

Riparian ET can influence stream hydrology at different time scales, ranging from hours to decades (Salemi et al. 2012). Concordantly, we showed that sub-daily fluctuations in stream discharge, as well as seasonal patterns of both riparian groundwater elevation and stream hydrological retention, were strongly linked to the sap flow measurements of riparian trees (Chapter 5). To the best of our knowledge, this is the first time that a clear link between riparian ET and stream hydrological retention is established, although there were previous indications that a high riparian water demand could induce strong hydrological retention in other Mediterranean systems (Bernal and Sabater 2012).

At the end, our results highlight the close hydrological link between riparian and stream ecosystems, and suggest that riparian ET could be essential to predict stream discharge, especially in regions experiencing some water limitation. As an example to illustrate this idea, here we present some preliminary results obtained with the PERSiST[1] semi-distributed model, one of the few up-to-date hydrological models including the riparian compartment (Futter et al. 2013) (Figure 8.4).

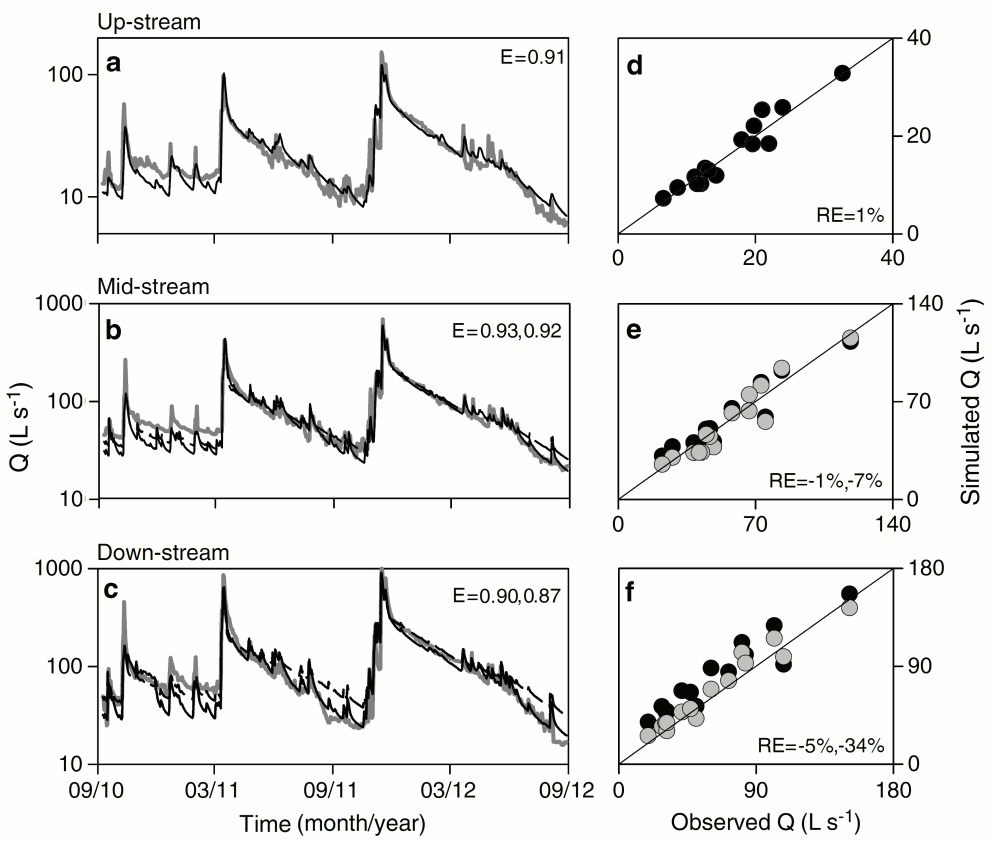

Figure 8.4 Temporal pattern of stream discharge at Font del Regàs for the (a) up-stream, (b) mid-stream, and (c) down-stream sites. The gray line represents observed values. Simulated values obtained with (solid black) and without (dashed black) including the riparian zone are shown. Panels (d), (e) and (f) show the relationship between observed and simulated monthly mean values for the scenarios with (gray circles) and without (black circles) riparian zone only for the vegetative period. The 1:1 line is indicated in black. The Nash-Sutcliffe model efficiency coefficient (E) and relative error (RE) between observed and simulated stream discharge are also shown for the scenarios with and without riparian zone (first and second value, respectively). Note that the up-stream site had no riparian forest.

[1] Precipitation, Evapotranspiration and Runoff Simulator for Solute Transport

The calibration of stream discharge for the up-, mid- and down-stream sites sampled at Font del Regàs (as described in Appendix C) reveals that the riparian compartment was required for successfully simulating the temporal pattern of stream hydrology at the down-stream site, and to a lower extent, at the mid-stream site (Figure 8.4). This initial exploration with the PERSiST model concurs with previous work performed by Medici et al. (2008), showing that the riparian pool was a key element to simulate the non-linear hydrological behavior of a Mediterranean intermittent stream.

Overall, this dissertation adds a novel piece of knowledge on catchment hydrology by showing that riparian ET are able to play a pivotal role on regulating catchment water fluxes and temporal patterns of stream discharge not only in arid systems, but also in relatively wet catchments ($0.5 < AI < 1$). Therefore, we propose that this catchment pool should be considered to a further extent when modeling stream hydrology, as well as for a sound and integrated management of catchment water resources.

8.5 DO MEDITERRAEAN RIPARIAN ZONES BUFFER STREAM NITROGEN CONCENTRATION?

Over the last decades, a growing body of knowledge has recognized the N buffer capacity of riparian zones (McClain et al. 2003, Pinay et al. 2007). The main part of these studies has been conducted at plot scale and in temperate regions. However, the findings obtained in the present dissertation question this well-established idea, at least for Mediterranean catchments such as Font del Regàs, by showing that Mediterranean riparian soils can act as N sources (*Part II*), and that these riparian zones may have a limited capacity to reduce stream N concentrations at the catchment scale (*Part III*).

In *Part II* of this dissertation, we showed that the studied Mediterranean riparian soils can act as a source of N on the adjacent stream because stream N loads increased exponentially soon after riparian nitrification pulses (Chapter 3). Conversely, and as expected on N-limited ecosystems (Dijkstra et al. 2012, Jongen et al. 2013), most of the NO_3^- produced in upland soils tended to be retained within the catchment. These results suggest that Mediterranean riparian soils are not only hot spots of microbial N supply, but also that they can enhance catchment N losses (i.e., they are hot spots of N transport) due to their proximity and strong hydrological connection with adjacent aquatic ecosystems. The NO_3^- stored in riparian soils can arrive to the stream via a quick surface flow path (during storms), or either via groundwater after infiltration. The two flow paths may occur at Font del Regàs, because riparian soils had higher

DIN concentration (12-24 mg N kg^{-1}) than upland soils (2-8 mg N kg^{-1}), whereas riparian groundwater often exhibited higher DIN concentrations (80-350 μg N L^{-1}, n = 154) than upland groundwater and springs (40-190 μg N L^{-1}, n = 64, unpublished data). Consequently, one would expect increments in stream NO_3^- concentrations along stream reaches flanked by well-developed Mediterranean riparian zones, as observed at Font del Regàs.

In *Part III* of this dissertation, the results obtained do not support the idea that this Mediterranean riparian zone was acting as a natural buffer of N at catchment scale. During the dormant season, we did not find any evidence of N removal in the riparian zone based on the small differences in N concentration between headwater and valley groundwater (Chapter 5*)*. Furthermore, during the vegetative period, diel fluctuations in stream N concentration were not associated with diel variations in riparian ET, suggesting little influence of plant N uptake on diel stream N dynamics (Chapter 6). Finally, during periods of stream hydrological retention, the hypothetical N removal attributed to biogeochemical processes at the stream-riparian interface was not enough to decrease stream N concentrations and fluxes (Chapter 5). Nonetheless, we cannot discard the idea that the studied riparian zones may be actually removing N from the groundwater arriving from the adjacent upland ecosystems because we did not measure changes in DIN concentration across riparian groundwater sections. Moreover, there could be the possibility that pulses of soil and/or groundwater denitrification could contribute to N removal during some periods. The influence of these processes at the catchment scale should be carefully considered in future studies.

Perhaps, one of the major findings unveiled in this dissertation is the extraordinary potential of in-stream processes to regulate stream N fluxes in this Mediterranean catchment, which could even screen the influence of terrestrial (and riparian) processes on stream nutrient dynamics. Indeed, whole-reach mass balance calculations based on monthly samplings revealed that in-stream N processing was at least as important as net riparian groundwater inputs for understanding the longitudinal pattern of stream DIN concentrations (Chapter 7). The contribution of in-stream processes to regulate stream N dynamics was especially noticeable at the valley bottom where the stream was wide, flat, and unconstrained.

At finer temporal scales (Chapter 6), we found that increments in light availability and stream temperature in spring favored in-stream gross primary production at the valley bottom, which caused marked variations in stream N concentrations at sub-daily time scales comparable to those reported for high productivity rivers (Roberts and Mulholland 2007, Heffernan and Cohen 2010) (Chapter 6). Such diel fluctuations

decreased spring N loads by 10%, highlighting that photoautotrophs can substantially contribute to transitorily reduce catchment N losses even in highly heterotrophic forested streams (Chapters 6).

Contrarily to the spring season, in-stream NO_3^- release (i.e., nitrification) dominated over uptake during summer and early-autumn, leading to increments in stream NO_3^- concentration (Chapter 5). We showed that groundwater NH_4^+ inputs did not suffice to sustain the observed increments in stream NO_3^- concentration (Chapter 7), suggesting that stream nitrifiers were feeding on an additional N source. We proposed that large stocks of riparian leaf litter were promoting these high rates of in-stream nitrification at the valley bottom of Font del Regàs, an explanation that suits if (as it was the case) discharges are low and hyporheic zones are well oxygenated (Starry et al. 2005, Mineau et al. 2011). In addition, warm temperatures could also stimulate in-stream mineralization and nitrification as reported for soil microbial processes (Chapter 4) because high rates of in stream NO_3^- release concurred with summer pulses of microbial N supply in riparian soils (Chapter 3 and Chapter 5). Therefore, Mediterranean riparian zones may not only deliver DIN to streams via surface and groundwater flow paths, but also may be important sources of organic N via litterfall, which can be transformed to NO_3^- by in-stream biota when environmental conditions are suitable. The presence of N_2-fixing species such as the invasive *Robinea pseudoacacia* could enhance stream N cycling by providing N-rich leaf litter, and thus, natural or human induced changes in riparian species composition could have a strong impact on stream nutrient dynamics.

Overall, results from this dissertation stress the importance of understanding the relevance of particular biogeochemical processes or systems within a broader context in order to get a more complete picture of their ecological role at relevant spatial and temporal scales. Based on what we have learned, we suggest that future catchment research should take into account, as much as possible, the links between upland, riparian, and in-stream biogeochemical cycles to be able to quantify their potential role as regulators of water, nutrients, sediments, and pollutants within landscapes.

8.6 FINAL CONSIDERATIONS

8.6.1 Time matters: The Revolution of Fine-Temporal Resolution Monitoring

Over the last years, technological advances in analytical field equipment have facilitated the monitoring of soil and water physicochemical properties at fine-scale temporal resolution (minutes or hours), something that was only possible for discharge and climate

data until recently. This high-resolution temporal data is enabling a revolution in environmental sciences by providing a refined holistic method to study already known processes, revealing unknown processes, and improving our understanding of sources, residence times, and flow path dynamics (Kirchner et al. 2004, Heffernan and Cohen 2010). Although we had no access to sensors for recording at such high frequencies, we have shown the usefulness of fine-scale temporal measurements in several chapters of this dissertation. Here, we briefly highlight some of the new opportunities that high-temporal resolution data can provide in the forthcoming years for improving our understanding of the N cycle in both terrestrial and aquatic ecosystems.

In terrestrial systems, high-frequency data on soil nutrient concentrations may be essential for integrating hot moments of soil microbial activity at longer time scales, as well as for improving our understanding of the factors governing such microbial pulse behavior (Xu et al. 2004, Borken and Matzner 2009, Vidon et al. 2010). We have learned about the importance of hot moments of soil N cycling in the studied Mediterranean soils by performing soil incubations and monitoring soil N fluxes fortnightly using standard methods (Chapter 3). Undoubtedly, this methodology could have been improved by increasing the sampling frequency with the help of optic sensors and portable gas chromatographs. This sort of information would allow the incorporation of microbial biogeochemical pulses into reactive transport models, which still remain a challenge in terrestrial ecology. Moreover, we showed that fusing a simple process-based model with detailed soil data (despite being relatively short data sets) can provide insightful simulations of the soil N cycle (Chapter 4). Therefore, new technologies would allow the development of more realistic models, as we would be able to perform direct model-data comparisons for several biogeochemical processes.

In stream ecosystems, fine-scale temporal monitoring has been proved to be useful for understanding the contribution of terrestrial processes on stream nutrient dynamics and for performing reliable estimations of catchment water and nutrient exports (Wade et al. 2002, Medici et al. 2010, Seibert and Vis 2012). Diel discharge fluctuations can reveal information about riparian evapotranspiration, hydrologic upland-stream connectivity, temporal changes in freezing–thawing processes, and, in human–treated reaches, the groundwater extracted by anthropogenic activities (Lundquist and Cayan 2002, Gribovszki et al. 2010). As already done in previous studies (Gribovszki et al. 2008, Cadol et al. 2012), we used high-frequency temporal data for quantifying riparian evapotranspiration at Font del Regàs (Chapter 5). Sub-daily variations have been used to infer riparian evapotranspiration for years (White 1932), though new sensors are more reliable and have higher accuracy, unveiling uncovered information residing in

diurnal cycles of hydrological variables, such as the source of these signals or the manner in which they propagated (Gribovszki et al. 2010, Graham et al. 2013).

Finally, fine-scale temporal monitoring of stream nutrient concentrations have the potential of amplifying our understanding of in-stream biogeochemical processes and revealing complex in-stream nutrient dynamics never before seen (Heffernan and Cohen 2010, Nimick et al. 2011). In this dissertation, the fine-scale temporal monitoring of both stream and riparian groundwater chemistry allowed us to provide a mechanistic explanation of the influence of photoautotrophic activity on regulating Mediterranean catchment N exports (Chapter 6). Moreover, our results supported the growing body of knowledge showing that discrete measurements taken monthly, weekly, or even daily (in some instances) can limit our ability to identify the driving forces of stream nutrient patterns, as well as the assessment of reliable nutrient budgets at long time scales.

In the forthcoming years, the combination of already widespread water level probes and novel optical sensors may help us to move one step forward in catchment biogeochemistry by integrating short-time scale variations in stream discharge and stream chemistry. Furthermore, high-temporal resolution data would allow better predictions of how terrestrial and aquatic ecosystems respond to changing conditions of contaminant loading, eutrophication, climate change, drought, industrialization, or urban development, as well as for developing earlier system alerts.

8.6.2 Space Matters: The Riparian Continuum Concept

Longitudinal changes in stream physical (light availability and water temperature), biogeochemical (sources of nutrients and organic matter), and biological (invertebrates and fishes communities) variables have been widely reported in the literature since the formulation of the River Continuum Concept presented by Vannote et al. (1980). However, the links between these longitudinal patterns and changes in the structural and functional traits of riparian ecosystems along the longitudinal axis have not been always considered, and often remain poorly understood. In several chapters of this dissertation we have shown that the capacity of riparian zones to regulate stream discharge and N dynamics can increase markedly from headwaters (order 1 and 2) to the valley bottom (order 3). For instance, we have demonstrated that the influence of riparian ET on stream hydrology, as well as the capacity of riparian trees to regulate stream light availability increased along the stream continuum (Chapter 5 and Chapter 6), which ultimately influenced in-stream N cycling and N fluxes. We suggest that, similarly

to the classical theoretical framework proposed by Vannote et al. (1980), the influence of riparian ecosystems on stream water and nutrient dynamics along the fluvial network can also be understood as a Riparian Continuum Concept (Figure 8.5).

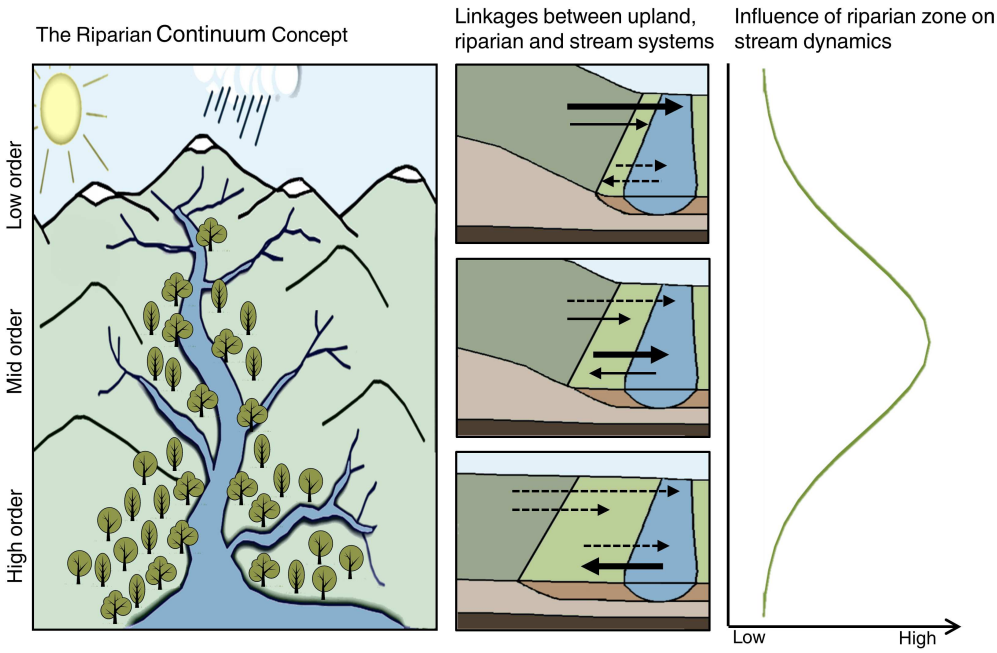

Figure 8.5 Schematic representation of the Riparian Continuum Concept for mountainous forested catchments. The illustration describes the relative importance of riparian ecosystems on regulating the flux of matter and energy between uplands and stream ecosystems along the river continuum. The influence of riparian zone on stream dynamics is minimal in headwater streams (orders 1-2), increases at mid-order stream (order 3-5) and diminishes in lowland rivers (order >5). In the center panels, upland, riparian, and stream ecosystems are represented in dark green, light green, and blue, respectively. Physical, hydrological, and biogeochemical links between the considered systems are indicated with arrows. Dashed, thin, and bold arrows represent minimal, small, and large influence of a particular system on the dynamics of another system, respectively.

In small mountainous forested streams (orders 1-2), steep slopes generally promote a strong hydrological flux from upland to streams ecosystems and short residence time of water within the riparian aquifer (McGlynn and McDonnell 2003, Jencso et al. 2009). Thus, one would expect a minimal effect of riparian ET on stream hydrology and biogeochemistry, even though streams are generally net gaining reaches (present dissertation, Covino et al. 2010). Moreover, the potential of the riparian canopy to regulate stream water temperature and light inputs may be small because these headwater

catchments are typically confined in V-shaped valleys (present dissertation, Vannote et al. 1980, Naiman et al. 1987). Finally, narrow riparian strips may be relatively small sources of organic matter and nutrients to streams compared to upland sources (Valett et al. 2008), and thus, their overall influence on in-stream biogeochemical cycles may be limited.

In mid-stream reaches (orders 3-5), upland-riparian hydrological connectivity tends to decrease (Jencso et al. 2009) while water demanded by riparian trees increases. Therefore, one would expect a higher potential of riparian ecosystems for regulating the temporal pattern of stream discharge and stream hydrological retention than in headwater reaches (present dissertation, Covino et al. 2010, Bernal and Sabater 2012). Moreover, at these intermediate positions, riparian zones tend to be larger in size than stream channels, and thus, one would expect a higher influence of these ecosystems on regulating light, organic matter, and nutrients inputs to streams (present dissertation, Hill and Dimick 2002, Mineau et al. 2011).

Finally, in the lower down of the river network (orders > 5), stream biota often relies on autochthonous sources of nutrients and organic matter (Vannote et al. 1980, Valett et al. 2008, Finlay et al. 2011b). Furthermore, wide stream channels reduce the shading capacity of riparian trees (Naiman et al. 1987, Allan 1995). Hence, one would expect that the potential of riparian zones on regulating nutrient biogeochemistry would decrease in these large rivers, despite riparian ecosystems occupying large areas. Conversely, streams can supply large amount of water and nutrients to riparian floodplain ecosystems, which can reach high levels of water demand and productivity (Dahm et al. 2002, Scott et al. 2008).

Nowadays, riparian areas are one of the most threatened ecosystems in the world, especially at mid-order and low-order stream reaches. Human activities, such as changes in the hydrological regime (i.e., stream and groundwater extractions), riparian topography (i.e., urbanization of floodplains), and riparian biota (i.e., introduction of invasive species) can seriously compromise the role of riparian zones as regulators of water, nutrients, and pollutants along the stream network. The proposed Riparian Continuum Concept is a simple theoretical framework that could be tested and refined in future synoptic studies aiming to understand how natural and human-induced changes in riparian ecosystems ultimately impact on stream and catchment biogeochemistry. Therefore, an integrated view of the different catchment units along the stream continuum is essential for identifying key ecological processes, making feasible predictions of catchment nutrient losses, and developing meaningful catchment management schemes.

CHAPTER 9

General Conclusions

The studies included in this dissertation guided us to the following outcomes:

CHAPTER THREE

- On annual terms, median net nitrogen mineralization and net nitrification varied widely among the three forest sites. Soil microbial rates were higher at the riparian than at the upland sites, while extremely low net nitrification rates were recorded in the beech site.

- Pulses of net nitrogen mineralization and net nitrification occurred following spring rewetting events at the three studied forest soils, while warm temperatures promoted pulses of microbial activity only at the riparian site. No microbial pulses were observed in autumn or winter likely due to high microbial nitrogen demand and/or cold temperatures.

- Pulse events of microbial activity were constrained in time (0-20%), yet they contributed substantially (25-40%) to annual rates of net nitrogen mineralization and net nitrification at the three studied forest soils. Hence, pulse events are important for understanding soil nitrogen cycling in Mediterranean systems.

- Soil nitrate availability and stream nitrate loads increased disproportionally after pulses of riparian net nitrification, and thus, these riparian soils could be acting as nitrogen sources to streams within the catchment.

CHAPTER FOUR

- Soil moisture, temperature, and precipitation were important drivers of temporal dynamics of the nitrogen cycle in these Mediterranean systems, and the three climatic variables generally had a positive effect on soil microbial processing rates.

- The sensitivity of the soil N cycle to climatic factors differed among processes and forests. Soil moisture was the major driver of soil nitrogen mineralization and nitrification at the oak and beech forests, while these two processes were mainly driven by temperature and precipitation at the riparian forest. In addition,

net nitrification was generally more sensitive to climatic variables than net nitrogen mineralization.

- According to our model simulation of future climate scenarios, the antagonistic effect of warming and drying on the soil N cycle could lead to small changes on mean daily soil N processing rates, and thus, to minimal changes of soil nitrate pools in these forest ecosystems.

CHAPTER FIVE

- Despite its modest contribution to water budgets at annual scale, riparian evapotranspiration exerted a strong control on the temporal pattern of riparian groundwater and stream hydrology across daily and seasonal scales.

- From a network perspective, the influence of riparian evapotranspiration on stream hydrology increased along the stream continuum and promoted stream hydrological retention at the valley reach.

- The combined effect of stream hydrological retention, large stocks of nitrogen rich leaf litter, and well oxygenated hyporheic zones likely enhanced in-stream nitrification during most of the vegetative period at the valley reach.

- There was no evidence of the riparian zone acting as a catchment nitrogen buffer during neither the vegetative nor the dormant period, questioning the efficiency of this Mediterranean riparian zone as a natural filter of nitrogen.

CHAPTER SIX

- In-stream gross primary production drove diel variations in stream nitrate concentration in spring, while the contribution of other in-stream, riparian, and upland processes was minimal.

- From a network perspective, the temporal pattern of such diel nitrate variations, and thus, their influence on stream nitrogen fluxes, increased along the stream continuum following light and temperature regimes.

- Diel variations in stream nitrate concentration at the down-stream site decrease catchment nitrate exports by a 10% during the spring season, suggesting that the stream photoautotrophic community can be a transitory sink of nitrogen even in low productivity streams.

CHAPTER SEVEN

- Longitudinal changes in stream nutrient concentration were weakly correlated to riparian groundwater inputs for nitrate and soluble reactive phosphorous, and no correlation was found between riparian groundwater and stream ammonium concentrations.

- At the whole-reach scale, the Font del Regàs stream tend to act as a net sink of ammonium, and as a net source of nitrate and soluble reactive phosphorous. However, in-stream processes were highly variable over time and space, and this variability could not be associated with neither physical longitudinal gradients nor shifts in environmental conditions between the dormant and the vegetative period.

- Changes in stream nutrient chemistry along the stream resulted from the combination of both in-stream cycling and nutrient inputs from terrestrial (and riparian) sources. This result implies that the assessment of these two sources of variation of the stream nutrient chemistry is crucial to understand the contribution of riparian and in-stream processes to stream nutrient dynamics at the whole-reach scale.

REFERENCES

Adair, E. C., D. Binkley, and D. C. Andersen. 2004. Patterns of nitrogen accumulation and cycling in riparian floodplain ecosystems along the Green and Yampa rivers. Oecologia 139:108–116.

Akaike, H. 1974. A new look at the statistical model identification. IEEE Transactions on Automatic Control 19:716–723.

Alexander, R. B., J. K. Böhlke, E. W. Boyer, M. B. David, J. W. Harvey, P. J. Mulholland, S. P. Seitzinger, C. R. Tobias, C. Tonitto, and W. M. Wollheim. 2009. Dynamic modeling of nitrogen losses in river networks unravels the coupled effects of hydrological and biogeochemical processes. Biogeochemistry 93:91–116.

Alexander, R. B., E. W. Boyer, R. A. Smith, G. E. Schwarz, and R. B. Moore. 2007. The role of headwater streams in downstream water quality. Journal of the American Water Resources Association 43:41–59.

Allan, J. D. 1995. Running Waters. In J. D. Allan, and M. M Castillo, editors. Stream ecology: structure and function of running waters. Chapman and Hall, London, UK.

Andrianarisoa, K. S., B. Zeller, J. L. Dupouey, and E. Dambrine. 2009. Comparing indicators of N status of 50 beech stands (Fagus sylvatica L.) in northeastern France. Forest Ecology and Management 257:2241–2253.

Appling, A. P., and J. B. Heffernan. 2014. Nutrient limitation and physiology mediate the fine-scale (de)coupling of biogeochemical cycles. The American Naturalist 184:384–406.

Arango, C. P., J. L. Tank, S. L. Johnson, and S. K. Hamilton. 2008. Assimilatory uptake rather than nitrification and denitrification determines nitrogen removal patterns in streams of varying land use. Limnology and Oceanography 53:2558–2572.

Asano, Y., T. Uchida, Y. Mimasu, and N. Ohte. 2009. Spatial patterns of stream solute concentrations in a steep mountainous catchment with a homogeneous landscape. Water Resources Research 45:1–9.

Austin, A. T. 2011. Has water limited our imagination for aridland biogeochemistry? Trends in Ecology & Evolution 26:229–35.

Àvila, A., D. Bonilla, F. Rodà, J. Piñol, and C. Neal. 1995. Soil water chemistry in a holm oak (*Quercus ilex*) forest: inferences on biogeochemical processes for a montane-Mediterranean area. Journal of Hydrology 166:15–35.

Àvila, A., C. Neal, and J. Terradas. 1996. Climate change implications for streamflow and streamwater. Journal of Hydrology 177:99–116.

Àvila, A., A. Rodrigo, and F. Rodà. 2002. Nitrogen circulation in a Mediterranean holm oak forest. Hydrology and Earth System Sciences 6:551–557.

Àvila, A., and F. Rodà. 2012. Changes in atmospheric deposition and streamwater chemistry over 25 years in undisturbed catchments in a Mediterranean mountain environment. The Science of the Total Environment 434:18–27.

Baethgen, W., and M. Alley. 1989. A manual colorimetric procedure for ammonium nitrogen in soil and plant Kjeldahl digests. Communications in Soil Sicence and Plant Analysis 20:961–969.

Bai, E., S. Li, W. Xu, W. Li, W. Dai, and P. Jiang. 2013. A meta-analysis of experimental warming effects on terrestrial nitrogen pools and dynamics. The New Phytologist 199:431–40.

Baldocchi, D. D., and Y. Ryu. 2011. A synthesis of forest evaporation fluxes - from days to years- as measured with Eddy covariance. Pages 101–116 in D. F. Levia, D. Carlyle-Moses, and T. Tanaka, editors. Forest hydrology and biogeochemistry. Springer, Dordrecht, Netherlands.

Battin, T. J., L. A. Kaplan, S. Findlay, C. S. Hopkinson, E. Martí, A. I. Packman, J. D. Newbold, and F. Sabater. 2008. Biophysical controls on organic carbon fluxes in fluvial networks. Nature Geoscience 1:95–100.

Baulch, H. M., P. J. Dillon, R. Maranger, J. J. Venkiteswaran, H. F. Wilson, and S. L. Schiff. 2012. Night and day: short-term variation in nitrogen chemistry and nitrous oxide emissions from streams. Freshwater Biology 57:509–525.

Bechtold, J. S., and R. J. Naiman. 2006. Soil texture and nitrogen mineralization potential across a riparian toposequence in a semi-arid savanna. Soil Biology and Biochemistry 38:1325–1333.

Bell, C., N. McIntyre, S. Cox, D. Tissue, and J. Zak. 2008. Soil microbial responses to temporal variatons of moisture and temperature in a Chihuahuan desert grassland. Microbilological Ecology 56:153–167.

Berger, T. W., E. Inselsbacher, F. Mutsch, and M. Pfeffer. 2009. Nutrient cycling and soil leaching in eighteen pure and mixed stands of beech (Fagus sylvatica) and spruce (Picea abies). Forest Ecology and Management 258:2578–2592.

Bernal, S., A. Butturini, E. Nin, F. Sabater, and S. Sabater. 2003. Leaf litter dynamics and nitrous oxide emission in a Mediterranean riparian forest: implications for soil nitrogen dynamics. Journal of Environmental Quality 32:191–7.

Bernal, S., A. Butturini, J. L. Riera, E. Vázquez, and F. Sabater. 2004. Calibration of the INCA model in a Mediterranean forested catchment: the effect of hydrological inter-annual variability in an intermittent stream. Hydrology and Earth System Sciences 8:729–741.

Bernal, S., F. Sabater, A. Butturini, E. Nin, and S. Sabater. 2007. Factors limiting denitrification in a Mediterranean riparian forest. Soil Biology and Biochemistry 39:2685–2688.

Bernal, S., and F. Sabater. 2012. Changes in discharge and solute dynamics between hillslope and valley-bottom intermittent streams. Hydrology and Earth System Sciences 16:1595–1605.

Bernal, S., L. O. Hedin, G. E. Likens, S. Gerber, and D. C. Buso. 2012a. Complex response of the forest nitrogen cycle to climate change. Proceedings of the National Academy of Sciences of the United States of America 109:3406–3411.

Bernal, S., D. von Schiller, E. Martí, and F. Sabater. 2012b. In-stream net uptake regulates inorganic nitrogen export from catchments under base flow conditions. Journal of Geophysical Research: Biogeosciences 117:1–10.

Bernal, S., C. Belillas, J. J. Ibáñez, and A. Àvila. 2013. Exploring the long-term response of undisturbed Mediterranean catchments to changes in atmospheric inputs through time series analysis. The Science of the Total Environment 458-460:535–45.

Bernal, S., A. Lupon, M. Ribot, F. Sabater, and E. Martí. 2015. Riparian and in-stream controls on nutrient concentrations and fluxes in a headwater forested stream. Biogeosciences 12:1941–1954.

Bernhardt, E. S., R. O. Hall, Jr., and G. E. Likens. 2002. Whole-system estimates of nitrification and nitrate uptake in streams of the Hubbard Brook experimental forest. Ecosystems 5:419–430.

Bernhardt, E. S., G. E. Likens, D. C. Buso, and C. T. Driscoll. 2003. In-stream uptake dampens effects of major forest disturbance on watershed nitrogen export. Proceedings of the National Academy of Sciences of the United States of America 100:10304–10308.

Bernhardt, E. S., G. E. Likens, R. O. Hall, Jr., D. C. Buso, S. G. Fisher, T. M. Burton, J. L. Meyer, W. H. Mcdowell, M. S. Mayer, W. B. Bowden, S. E. G. Findlay, K. H. Macneale, R. S. Stelzer, and W. H. Lowe. 2005. Can't see the forest for the stream? In-stream processing and terrestrial nitrogen exports. BioScience 55:219–230.

Binkley, D., and S. C. Hart. 1989. The Components of Nitrogen Availability Assessments in Forest Soils. Advances in Soil Science 10:57–112.

Binkley, D., P. Sollins, R. Bell, D. Sachs, and D. Myrold. 1992. Biogeochemistry of adjacent conifer and alder-conifer stands. Ecology 73:2022–2033.

Björsne, A. K., T. Rütting, and P. Ambus. 2014. Combined climate factors alleviate changes in gross soil nitrogen dynamics in heathlands. Biogeochemistry 120:191–201.

Bohlen, P. J., P. M. Groffman, C. T. Driscoll, T. J. Fahey, and T. G. Siccama. 2001. Plant-soil-microbial interactions in a northern hardwood forest. Ecology 82:965–978.

Bolós, O. 1983. La vegetació del Montseny. Diputació de Barcelona, Barcelona, Spain.

Bond, B. J., J. A. Jones, G. Moore, N. Phillips, D. Post, and J. J. McDonnell. 2002. The zone of vegetation influence on baseflow revealed by diel patterns of streamflow and vegetation water use in a headwater basin. Hydrological Processes 16:1671–1677.

Bonilla, D., and F. Rodà. 1992. Soil nitrogen dynamics in a holm oak forest. Vegetatio 99-100:247–257.

Booth, M. S., J. M. Stark, and M. M. Caldwell. 2003. Inorganic N turnover and availability in annual- and perennial-dominated soils in a northern Utah shrub-steppe ecosystem. Biogeochemistry 66:311–330.

Booth, M. S., J. M. Stark, and E. Rastertter. 2005. Controls on nitrogen cycling in terrestrial ecosystems: a synthetic analysis of literature data. Ecological Monographs 75:139–157.

Borken, W., and E. Matzner. 2009. Reappraisal of drying and wetting effects on C and N mineralization and fluxes in soils. Global Change Biology 15:808–824.

Bormann, F. H., and G. E. Likens. 1967. Nutrient cycling. Science 155:424–429.

Bott, T. L. 2006. Primary productivity and community respiration. Pages 663–690 in F. R. Hauer and G. A. Lamberti, editors. Methods in stream ecology. Academic Press, San Diego, CA, USA.

Brooks, R. J., H. R. Barnard, R. Coulombe, and J. J. McDonnell. 2009. Ecohydrologic separation of water between trees and streams in a Mediterranean climate. Nature Geoscience 3:100–104.

Brookshire, J. E. N., H. M. Valett, and S. Gerber. 2009. Maintenance of terrestrial nutrient loss signatures during in-stream transport. Ecology 90:293–299.

Brookshire, J. E. N., S. Gerber, J. R. Webster, J. M. Vose, and W. T. Swank. 2011. Direct effects of temperature on forest nitrogen cycling revealed through analysis of long-term watershed records. Global Change Biology 17:297–308.

Burnham, K. P., and D. R. Anderson. 2002. Information and Likelihood theory: A basis for model selection and inference. Pages 49-97 in K. P. Burnham, and D. R. Anderson, editors. Model selection and multimodel inference: a practical information-theoretic approach. Springer-Verlag, New York, NJ, USA.

Burt, T. P., G. Pinay, F. E. Matheson, N. E. Haycock, A. Butturini, J. C. Clément, S. Danielescu, D. J. Dowrick, M. M. Hefting, A. Hillbright-Ilkowska, and V. Maître. 2002.

Water table fluctuations in the riparian zone: Comparative results from a pan-European experiment. Journal of Hydrology 265:129–148.

Burt, T., G. Pinay, and S. Sabater. 2010. What do we still need to know about the ecohydrology of riparian zones? Ecohydrology 377:373–377.

Butler, S. M., J. M. Melillo, J. E. Johnson, J. Mohan, P. A. Steudler, H. Lux, E. Burrows, R. M. Smith, C. L. Vario, L. Scott, T. D. Hill, N. Aponte, and F. Bowles. 2012. Soil warming alters nitrogen cycling in a New England forest: implications for ecosystem function and structure. Oecologia 168:819–28.

Butturini, A., S. Bernal, E. Nin, C. Hellin, L. Rivero, S. Sabater, and F. Sabater. 2003. Influences of the stream groundwater hydrology on nitrate concentration in unsaturated riparian area bounded by an intermittent Mediterranean stream. Water Resources Research 39:1–13.

Cadol, D., S. Kampf, and E. Wohl. 2012. Effects of evapotranspiration on baseflow in a tropical headwater catchment. Journal of Hydrology 462-463:4–14.

Cameron, D. R., M. Van Oijen, C. Werner, K. Butterbach-Bahl, R. Grote, E. Haas, G. B. M. Heuvelink, R. Kiese, J. Kros, M. Kuhnert, A. Leip, G. J. Reinds, H. I. Reuter, M. J. Schelhaas, W. De Vries, and J. Yeluripati. 2013. Environmental change impacts on the C- and N-cycle of European forests: a model comparison study. Biogeosciences 10:1751–1773.

Castro-Díez, P., N. Fierro-Brunnenmeister, N. González-Muñoz, and A. Gallardo. 2012. Effects of exotic and native tree leaf litter on soil properties of two contrasting sites in the Iberian Peninsula. Plant and Soil 350:179–191.

Castro-Díez, P., G. Valle, N. González-Muñoz, and Á. Alonso. 2014. Can the life-history strategy explain the success of the exotic trees Ailanthus altissima and Robinia pseudoacacia in Iberian floodplain forests? PLoS ONE 9:30–32.

Chang, C. T., S. Sabaté, D. Sperlich, S. Poblador, F. Sabater, and C. Gracia. 2014. Does soil moisture overrule temperature dependence of soil respiration in Mediterranean riparian forests? Biogeosciences 11:6173–6185.

Chen, I. C., J. K. Hill, R. Ohlemüller, D. B. Roy, and C. D. Thomas. 2011. Rapid range shifts of species associated with high levels of climate warming. Science 333:1024–1026.

Clément, J.C., G. Pinay, and P. Marmonier. 2002. Seasonal dynamics of denitrification along topohydrosequences in three different riparian wetlands. Journal of Environment Quality 31:1025–1037.

Clément, J.C., L. Aquilina, O. Bour, K. Plaine, T. P. Burt, and G. Pinay. 2003. Hydrological flowpaths and nitrate removal rates within a riparian floodplain along a fourth-order stream in Brittany (France). Hydrological Processes 17:1177–1195.

Collins, S. L., R. L. Sinsabaugh, C. Crenshaw, L. Green, A. Porras-Alfaro, M. Stursova, and L. H. Zeglin. 2008. Pulse dynamics and microbial processes in aridland ecosystems. Journal of Ecology 96:413–420.

Colwell, R. K., G. Brehm, C. L. Cardelús, A. C. Gilman, and J. T. Longino. 2008. Global warming, elevational range, shifts, and lowland biotic attrition in the wet tropics. Science 322:258–261.

Compton, J. E., M. R. Church, S. T. Larned, and W. E. Hogsett. 2003. Nitrogen export from forested watersheds in the Oregon coast range: The role of N_2 fixing red alder. Ecosystems 6:773–785.

Contreras, S., E. G. Jobbágy, P. E. Villagra, M. D. Nosetto, and J. Puigdefábregas. 2011. Remote sensing estimates of supplementary water consumption by arid ecosystems of central Argentina. Journal of Hydrology 397:10–22.

Cooper, S. D., P. S. Lake, S. Sabater, J. M. Melack, and J. L. Sabo. 2013. The effects of land use changes on streams and rivers in Mediterranean climates. Hydrobiologia 719:383–425.

Covino, T. P., and B. L. McGlynn. 2007. Stream gains and losses across a mountain-to-valley transition: Impacts on watershed hydrology and stream water chemistry. Water Resources Research 43:W10431.

Covino, T. P., B. McGlynn, and M. A. Baker. 2010. Separating physical and biological nutrient retention and quantifying uptake kinetics from ambient to saturation in successive mountain stream reaches. Journal of Geophysical Research 115:G04010.

Dahm, C. N., J. R. Cleverly, J. Coonrod, E. Allred, J. R. Thibault, D. E. McDonnell, and D. J. Gilroy. 2002. Evapotranspiration at the land/ water interface in a semi-arid drainage basin. Freshwater Biology 47:831–844.

Darrouzet-Nardi, A., and W. D. Bowman. 2011. Hot spots of inorganic nitrogen availability in an alpine-subalpine ecosystem, Colorado Front Range. Ecosystems 14:848–863.

DeNicola, D. M. 1996. Periphyton responses to temperature at different ecological levels. Pages 149–181 in R. J. Stevenson, M. L. Bothwell, and R. L. Lowe, editors. Algal ecology. Elsevier, San Diego, CA, USA.

Dent, C. L., and N. B. Grimm. 1999. Spatial heterogeneity of stream water nutrient concentrations over successional time. Ecology 80:2283–2298.

Dent, C. L., N. B. Grimm, E. Martí, J. W. Edmonds, J. C. Henry, and J. R. Welter. 2007. Variability in surface-subsurface hydrologic interactions and implications for nutrient retention in an arid-land stream. Journal of Geophysical Research 112:G04004.

Dessureault-Rompré, J., B. J. Zebarth, A. Georgallas, D. L. Burton, C. A. Grant, and C. F. Drury. 2010. Temperature dependence of soil nitrogen mineralization rate: Comparison of mathematical models, reference temperatures and origin of the soils. Geoderma 157:97–108.

Detty, J. M., and K. J. McGuire. 2010. Topographic controls on shallow groundwater dynamics: implications of hydrologic connectivity between hillslopes and riparian zones in a till mantled catchment. Hydrological Processes 24:2222–2236.

Dijkstra, F. A., D. J. Augustine, P. Brewer, and J. C. von Fischer. 2012. Nitrogen cycling and water pulses in semiarid grasslands: are microbial and plant processes temporally asynchronous? Oecologia 170:799–808.

Dimopoulos, P., and S. Zogaris. 2008. Flora y vegetación de ribera. Pages 66–83 in D. Arizpe, A. Mendes, and J. E. Rabaça, editors. Areas de Ribera Sostenibles: Una guía para su gestión. Generalitat Valenciana, Valencia, Spain.

Dise, N. B. 2009. Environmental science. Peatland response to global change. Science 326:810–811.

Doble, R., C. Simmons, I. Jolly, and G. Walker. 2006. Spatial relationships between vegetation cover and irrigation-induced groundwater discharge on a semi-arid floodplain, Australia. Journal of Hydrology 329:75–97.

Dobson, M., J. M. Mathooko, F. K. Ndegwa, and C. M'Erimba. 2004. Leaf litter processing rates in a Kenyan highland stream, the Njoro River. Hydrobiologia 519:207–210.

Dosskey, M. G., P. Vidon, N. P. Gurwick, C. J. Allan, T. P. Duval, and R. Lowrance. 2010. The role of riparian vegetation in protecting and improving chemical water quality in streams. Journal of the American Water Resources Association 1-18:1–19.

Dunford, E. G., and P. W. Fletcher. 1947. Effect of removal of stream-bank vegetation upon water yield. American Geophysics Union 28:105–110.

Duncan, J. M., L. E. Band, P. M. Groffman, and E. S. Bernhardt. 2015. Mechanisms driving the seasonality of catchment scale nitrate export: evidence for riparian ecohydrologic controls. Water Resources Research 51:3982–3997.

Duval, T. P., and A. R. Hill. 2006. Influence of stream bank seepage during low-flow conditions on riparian zone hydrology. Water Resources Research 42:W10425.

Duval, T. P., and A. R. Hill. 2007. Influence of base flow stream bank seepage on riparian zone nitrogen biogeochemistry. Biogeochemistry 85:185–199.

Edwards, A. W. F. 1992. Likelihood. John Hopkins University Press, Baltimore, MD, USA.

Ellenberg, H. 1977. Nitrogen as soil factor, especially for central European plant populations. Oecologia Plantarum 12:1–22.

Emmett, B. A., C. Beier, M. Estiarte, A. Tietema, H. L. Kristensen, D. Williams, J. Peñuelas, I. Schmidt, and A. Sowerby. 2004. The response of soil processes to climate change: results from manipulation studies of shrublands across an environmental gradient. Ecosystems 7:625–637.

Eno, C. F. 1960. Nitrate production in the field by incubating the soil in polyethylene bags. Soil Sicence Society of American 24:277–279.

Ensign, S. H., and M. W. Doyle. 2006. Nutrient spiraling in streams and river networks. Journal of Geophysical Research: Biogeosciences 111:G04009.

Evans, D. M., and S. H. Schoenholtz. 2011. Nitrogen mineralization in riparian soils along a river continuum within a Multi-Land-Use basin. Soil Science Society of America Journal 75:719–728.

Finlay, J. C., J. M. H. Hood, M. P. Limm, M. E. Power, J. D. Schade, and J. R. Welter. 2011a. Light-mediated thresholds in stream-water nutrient composition in a river network. Ecology 92:140–150.

Flewelling, S. A., G. M. Hornberger, J. S. Herman, A. L. Mills, and W. M. Robertson. 2013. Diel patterns in coastal-stream nitrate concentrations linked to evapotranspiration in the riparian zone of a low-relief, agricultural catchment. Hydrological Processes 28:2150–2158.

Folch, A., and N. Ferrer. 2015. The impact of poplar tree plantations for biomass production on the aquifer water budget and base flow in a Mediterranean basin. The Science of the Total Environment 524-525:213–24.

Follstad Shah, J, J., and C. N. Dahm. 2008. Flood regime and leaf fall determine soil inorganic nitrogen dynamics in semiarid riparian forests. Ecological Applications 18:771–788.

Frank, D. A., and P. M. Groffman. 1998. Ungulate vs. landscape control of soil C and N processes in grasslands of Yellowstone National Park. Ecology 79:2229–2241.

Futter, M. N., M. A. Erlandsson, D. Butterfield, P. G. Whitehead, S. K. Oni, and A. J. Wade. 2013. PERSiST: the precipitation, evapotranspiration and runoff simulator for solute transport. Hydrology and Earth System Sciences Discussions 10:8635–8681.

Galloway, J., F. Dentener, and D. Capone. 2004. Nitrogen cycles: past, present, and future. Biogeochemistry 70(2):153-226.

Gammons, C. H., J. N. Babcock, S. R. Parker, and S. R. Poulson. 2011. Diel cycling and stable isotopes of dissolved oxygen, dissolved inorganic carbon, and nitrogenous species in a stream receiving treated municipal sewage. Chemical Geology 283:44–55.

Gerber, S., and E. N. J. Brookshire. 2014. Scaling of physical constraints at the root-soil interface to macroscopic patterns of nutrient retention in ecosystems. The American Naturalist 183:418–30.

Gilliam, F. S., B. M. Yurish, and M. B. Adams. 2001. Temporal and spatial variation of nitrogen transformations in nitrogen-saturated soils of a central Appalachian hardwood forest. Canadian Journal of Forest Research 31:1768–1785.

Gold, A. J., P. M. Groffman, K. Addy, D. Q. Kellogg, M. Stolt, and A. E. Rosenblatt. 2001. Landscape attributes as controls on ground water nitrate removal capacity of riparian zones. Journal of the American Water Resources Association 37:1457–1464.

Goodale, C. L., and J. D. Aber. 2001. The long-term effects of land-use history on nitrogen cycling in northern hardwood forests. Ecological Applications 11:253–267.

Goodale, C. L., K. Lajtha, K. J. Nadelhoffer, E. W. Boyer, and N. A. Jaworski. 2004. Forest nitrogen sinks in large eastern U. S. watersheds: estimates from forest inventory and an ecosystem. Biogeochemistry 57/58:239–266.

Goodale, C. L., S. A. Thomas, G. Fredriksen, E. M. Elliott, K. M. Flinn, T. J. Butler, and M. T. Walter. 2009. Unusual seasonal patterns and inferred processes of nitrogen retention in forested headwaters of the Upper Susquehanna River. Biogeochemistry 93:197–218.

Goodrich, D. C., R. Scott, J. Qi, B. Goff, C. L. Unkrich, M. S. Moran, D. Williams, S. Schaeffer, K. Snyder, R. MacNish, T. Maddock, D. Pool, A. Chehbouni, D. I. Cooper, W. E. Eichinger, W. J. Shuttleworth, Y. Kerr, R. Marsett, and W. Ni. 2000. Seasonal estimates of riparian evapotranspiration using remote and in situ measurements. Agricultural and Forest Meteorology 105:281–309.

Gordon, N. D., T. A. McMahon, and B. L. Finlayson. 1992. How to have a field day and still collect some useful information. Pages 75-125 in Gordon, N. D., T. A. McMahon, B. L. Finlayson, C. J. Gippel, and R. J. Nathan, editors. Stream hydrology: an introduction for ecologists. John Willey and Sons, New Jersey, NJ, USA.

Graham, C. B., H. R. Barnard, K. L. Kavanagh, and J. P. McNamara. 2013. Catchment scale controls the temporal connection of transpiration and diel fluctuations in streamflow. Hydrological Processes 27:2541–2556.

Gribovszki, Z., P. Kalicz, J. Szilágyi, and M. Kucsara. 2008. Riparian zones evapotranspiration estimation from diurnal groundwater level fluctuations. Journal of Hydrology 349:6–17.

Gribovszki, Z., J. Szilágyi, and P. Kalicz. 2010. Diurnal fluctuations in shallow groundwater levels and streamflow rates and their interpretation – A review. Journal of Hydrology 385:371–383.

Grimm, N. B. 1987. Nitrogen dynamics during succession in a desert stream. Ecology 68:1157–1170.

Groffman, P. M., A. J. Gold, and R. C. Simmons. 1992. Nitrate dynamics in riparian forests: Microbial studies. Journal of Environment Quality 21:666.

Groffman, P. M., K. Butterbach-Bahl, R. W. Fulweiler, A. J. Gold, J. L. Morse, E. K. Stander, C. Tague, C. Tonitto, and P. Vidon. 2009. Challenges to incorporating spatially and temporally explicit phenomena (hotspots and hot moments) in denitrification models. Biogeochemistry 93:49–77.

Guckland, A., M. D. Corre, and H. Flessa. 2010. Variability of soil N cycling and N_2O emission in a mixed deciduous forest with different abundance of beech. Plant Soil 336:25–38.

Hall Jr., R. O., and J. L. Tank. 2003. Ecosystem metabolism controls nitrogen uptake in streams in Grand Teton National Park, Wyoming. Limnology and Oceanography 48:1120–1128.

Hall Jr., R. O., and J. J. Beaulieu. 2013. Estimating autotrophic respiration in streams using daily metabolism data. Freshwater Science 32:507–516.

Halliday, S. J., R. A. Skeffington, A. J. Wade, C. Neal, B. Reynolds, D. Norris, and J. W. Kirchner. 2013. Upland streamwater nitrate dynamics across decadal to sub-daily timescales: a case study of Plynlimon, Wales. Biogeosciences 10:8013–8038.

Hanson, G. C., P. M. Groffman, and A. J. Gold. 1994. Symtoms of nitrogen saturation in a riparian wetland. Ecological Applications 4:750–756.

Harms, T. K., and N. B. Grimm. 2008. Hot spots and hot moments of carbon and nitrogen dynamics in a semiarid riparian zone. Journal of Geophysical Research: Biogeoscience 113:1–14.

Harms, T. K., E. A. Wentz, and N. B. Grimm. 2009. Spatial heterogeneity of denitrification in semi-arid floodplains. Ecosystems 12:129–143.

Harms, T. K., and N. B. Grimm. 2010. Influence of the hydrologic regime on resource availability in a semi-arid stream-riparian corridor. Ecohydrology 3:349–359.

Harris, M. M., and S. J. Riha. 1991. Carbon and nitrigen dynamics in forest floor during short-term. Soil Biology and Biochemistry 23:1035–1041.

Hedin, L. O., J. J. Armesto, and A. H. Johnson. 1995. Patterns of nutrient loss from unpolluted, old-growth temperate forests: Evaluation of biogeochemical theory. Ecology 76:493–509.

Hedin, L. O., J. C. von Fischer, N. E. Ostrom, B. P. Kennedy, M. G. Brown, and G. P. Robertson. 1998. Thermodynamic constraints on nitrogen transformations and other biogeochemical processes at soil-stream interfaces. Ecology 79:684–703.

Heffernan, J. B., and R. A. Sponseller. 2004. Nutrient mobilization and processing in Sonoran desert riparian soils following artificial re-wetting. Biogeochemistry 70:117–134.

Heffernan, J. B., and M. J. Cohen. 2010. Direct and indirect coupling of primary production and diel nitrate dynamics in a subtropical spring-fed river. Limnology and Oceanography 55:677–688.

Heffernan, J. B., M. J. Cohen, T. K. Frazer, R. G. Thomas, T. J. Rayfield, J. Gulley, J. B. Martin, J. J. Delfino, and W. D. Graham. 2010. Hydrologic and biotic influences on nitrate removal in a subtropical spring-fed river. Limnology and Oceanography 55:249–263.

Hefting, M. M., J.C. Clément, D. J. Dowrick, A. C. Cosandey, S. Bernal, C. Cimpian, A. Tatur, T. P. Burt, and G. Pinay. 2004. Water table elevation controls on soil nitrogen cycling in riparian wetlands along a European climatic gradient. Biogeochemistry 67:113–134.

Helfield, J. M., and R. J. Naiman. 2002. Salmon and alter as nitrogen sources to riparian forests in a boreal Alaskan watershed. Oecologia 133:573–582.

Hill, W. R., M. G. Ryon, and E. M. Schilling. 1995. Light limitation in a stream ecosystem: responses by primary producers and consumers. Ecology 76:1297–1309.

Hill, A. R. 1996. Nitrate removal in stream riparian zones. Journal of Environmental Quality 25:743–755.

Hill, A. R., C. F. Labadia, and K. Sanmugadas. 1998. Hyporheic zone hydrology and nitrogen dynamics in relation to the streambed topography of a N-rich stream. Biogeochemistry 42:285–310.

Hill, W. R., P. J. Mulholland, and Marzolf. 2001. Stream ecosystem responses to forest leaf emergence in spring. Ecology 82:2306–2319.

Hill, W. R., and S. M. Dimick. 2002. Effects of riparian leaf dynamics on periphyton photosynthesis and light utilisation efficiency. Freshwater Biology 47:1245–1256.

Hill, A. R. 2011. Buried organic-rich horizons: their role as nitrogen sources in stream riparian zones. Biogeochemistry 104:347–363.

Hoffmann, C. C., C. Kjaergaard, J. Uusi-Kämppä, H. C. B. Hansen, and B. Kronvang. 2007. Phosphorus retention in riparian buffers: review of their efficiency. Journal of Environmental Quality 38:1942–1955.

Houlton, B. Z., C. T. Driscoll, T. J. Fahey, G. E. Likens, P. M. Groffman, E. S. Bernhardt, and D. C. Buso. 2003. Nitrogen dynamics in ice storm-damaged forest ecosystems: implications for nitrogen limitation theory. Ecosystems 6:431–443.

Huppe, H. C., and D. H. Turpin. 1994. Integration of carbon and nitrogen-metabolism in plant and algal cells. Annual Review of Plant Physiology and Plant Molecular Biology 45:577–607.

Institut Cartografic de Catalunya, I. 2010. Orthophotomap of Catalunya 1:25 000. Generalitat de Catalunya. Departament de Política Territorial i Obres. Departament de Política Territorial i Obres Públiques.

Intergovernmental Panel on Climate Change (IPCC). 2013. Summary for policymakers. in T. F. Stocker, D. Qin, G. K. Plattner, M. M. B. Tignor, S. K. Allen, J. Boschung, A. Nauels, Y. Xia, V. Bex, and P. M. Midgley, editors. Climate Change 2013: The Physical Science Basis. Cambridge University Press, Cambridge, UK.

Ise, T., and P. R. Moorcroft. 2006. The global-scale temperature and moisture dependencies of soil organic carbon decomposition: an analysis using a mechanistic decomposition model. Biogeochemistry 80:217–231.

Jacobs, S. M., J. S. Bechtold, H. C. Biggs, N. B. Grimm, S. Lorentz, M. E. McClain, R. J. Naiman, S. S. Perakis, G. Pinay, and M. C. Scholes. 2007. Nutrient vectors and riparian processing: A review with special reference to African semiarid savanna ecosystems. Ecosystems 10:1231–1249.

Jencso, K. G., B. L. McGlynn, M. N. Gooseff, S. M. Wondzell, K. E. Bencala, and L. A. Marshall. 2009. Hydrologic connectivity between landscapes and streams: Transferring reach- and plot-scale understanding to the catchment scale. Water Resources Research 45:W04428.

Johnson, C. E., C. T. Driscoll, T. G. Siccama, and G. E. Likens. 2000. Element fluxes and landscape position in a northern hardwood forest watershed ecosystem. Ecosystems 3:159–184.

Johnson, K. S., L. J. Coletti, and F. P. Chavez. 2006. Diel nitrate cycles observed with in situ sensors predict monthly and annual new production. Deep Sea Research Part I: Oceanographic Research Papers 53:561–573.

Johnson, L. T., and J. L. Tank. 2009. Diurnal variations in dissolved organic matter and ammonium uptake in six open-canopy streams. Journal of the North American Benthological Society 28:694–708.

Jones, J. B., S. G. Fisher, and N. B. Grimm. 1995. Nitrification in the hyporheic zone of a desert stream ecosystem. Journal of the North American Benthological Society 14:249–258.

Jongen, M., X. Lecomte, S. Unger, D. Fangueiro, and J. S. Pereira. 2013. Precipitation variability does not affect soil respiration and nitrogen dynamics in the understorey of a Mediterranean oak woodland. Plant and Soil 372:235–251.

Kaiser, C., L. Fuchslueger, M. Koranda, M. Gorfer, C. F. Stange, B. Kitzler, F. Rasche, J. Strauss, A. Sessitsch, S. Zechmeister-Boltenstern, and A. Richter. 2011. Plants control the seasonal dynamics of microbial N cycling in a beech forest soil by belowground C allocation. Ecology 92:1036–51.

Kauffman, J. B., A. S. Thorpe, and E. N. J. Brookshire. 2004. Livestock exclusion and belowground ecosystem responses in riparian meadows of eastern Oregon. Ecological Applications 14:1671–1679.

Keeney, D. R., and D. W. Nelson. 1982. Nitrogen-inorganic forms. Pages 643–698 in A. L. Page, editor. Methods of Soil Analysis. Agronomy Monography 9. ASA and SSSA, Madison, WI, USA.

Kelly, C. N., S. H. Schoenholtz, and M. B. Adams. 2011. Soil properties associated with net nitrification following watershed conversion from Appalachian hardwoods to Norway spruce. Plant and Soil 344:361–376.

Kellogg, D. Q., A. J. Gold, P. M. Groffman, M. H. Stolt, and K. Addy. 2008. Riparian groundwater flow patterns using flownet analysis: evapotranspiration-induced upwelling and implications for N removal. Journal of the American Water Resources Association 44:1024–1034.

Kemp, M. J., and W. K. Dodds. 2002. The influence of ammonium, nitrate, and dissolved oxygen concentrations on uptake, nitrification, and denitrification rates associated with prairie stream substrata. Limnology and Oceanography 47:1380–1393.

Kendall, C., E. M. Elliott, and S. D. Wankel. 2007. Tracing anthropogenic inputs of nitrogen to ecosystems. Pages 375–449 in R. H. Michener, and K. Lajtha, editors. Stable isotopes in ecology and environmental science. Blackwell Publishing, Oxford, UK.

Kirchner, J. W., X. H. Feng, and C. Neal. 2001. Catchment-scale advection and dispersion as a mechanism for fractal scaling in stream tracer concentrations. Journal of Hydrology 254:82–101.

Kirchner, J. W., C. Neal, and A. J. Robson. 2004. The fine structure of water-quality dynamics: the (high-frequency) wave of the future. Hydrological Processes:1353–1359.

Klute, A. 1986. Methods of soil analysis. Part 1: Physical and mineralogical methods. Agronomy Monography 9. SSSA and ASA, Madison, WI, USA.

Krutz, L. J., T. J. Gentry, S. A. Senseman, I. L. Pepper, and D. P. Tierney. 2006. Mineralization of atrazine, metolachlor and their respective metabolites in vegetated filter strips and cultivated soil. Pest Management Science 62:505–514.

Lamarque, J.-F., F. Dentener, J. McConnell, C.-U. Ro, M. Shaw, R. Vet, D. Bergmann, P. Cameron-Smith, R. Doherty, G. Faluvegi, S. J. Ghan, B. Josse, Y. H. Lee, I. A. MacKenzie, D. Plummer, D. T. Shindell, D. S. Stevenson, S. Strode, and G. Zeng. 2013. Multi-model mean nitrogen and sulfur deposition from the Atmospheric Chemistry and Climate Model Intercomparison Project (ACCMIP): evaluation historical and projected changes. Atmospheric Chemistry and Physics Discussions 13:6247–6294.

Larsen, K. S., L. C. Andresen, C. Beier, S. Jonasson, K. R. Albert, P. Ambus, M. F. Arndal, M. S. Carter, S. Christensen, M. Holmstrup, A. Ibrom, J. Kongstad, L. van der Linden, K. Maraldo, A. Michelsen, T. N. Mikkelsen, K. Pilegaard, A. Priemé, H. Ro-Poulsen, I. K. Schmidt, M. B. Selsted, and K. Stevnbak. 2011. Reduced N cycling in response to elevated CO_2, warming, and drought in a Danish heathland: Synthesizing results of the CLIMAITE project after two years of treatments. Global Change Biology 17:1884–1899.

Laursen, A. E., and S. P. Seitzinger. 2004. Diurnal patterns of denitrification, oxygen consumption and nitrous oxide production in rivers measured at the whole-reach scale. Freshwater Biology 49:1448–1458.

Lawrence, G. B., G. M. Lovett, and Y. H. Baevsky. 2000. Atmospheric deposition and watershed nitrogen export along an elevational gradient in the Catskill Mountains, New York. Biogeochemistry 50:21–43.

Lewis, D. B., J. D. Schade, A. K. Huth, and N. B. Grimm. 2006. The spatial structure of variability in a semi-arid, fluvial ecosystem. Ecosystems 9:386–397.

Likens, G., C. T. Driscoll, D. Buso, and T. Siccama. 1994. The biogeochemistry of potassium at Hubbard Brook. Biogeochemistry 25:61–125.

Likens, G. E., and D. C. Buso. 2006. Variation in streamwater chemistry throughout the Hubbard Brook Valley. Biogeochemistry 78:1–30.

Linn, D. M., and J. W. Doran. 1984. Effect of water-filled pore space on carbon dioxide and nitrous oxide production in tilled and nontilled soils. Soil Science Society of America Journal 48:1267–1272.

Liu, W., Z. Zhang, and S. Wan. 2009. Predominant role of water in regulating soil and microbial respiration and their responses to climate change in a semiarid grassland. Global Change Biology 15:184–195.

Llorens, P., and F. Domingo. 2007. Rainfall partitioning by vegetation under Mediterranean conditions. A review of studies in Europe. Journal of Hydrology 335:37–54.

Lohse, K. A., J. Sanderman, and R. Amundson. 2013. Identifying sources and processes influencing nitrogen export to a small stream using dual isotopes of nitrate. Water Resources Research 49:5715–5731.

Lovett, G. M., K. C. Weathers, M. A. Arthur, and J. C. Schultz. 2004. Nitrogen cycling in a northern hardwood forest: Do species matter? Biogeochemistry 67:289–308.

Lowrance, R., L. S. Altier, J. D. Newbold, R. R. Schnabel, P. M. Groffman, J. M. Denver, D. L. Correll, J. W. Gilliam, J. L. Robinson, R. B. Brinsfield, K. W. Staver, W. Lucas, and A. H. Todd. 1997. Water quality functions of riparian forest buffers in Chesapeake bay watersheds. Environmental Management 21:687–712.

Lucas-Borja, M. E., D. Candel Pérez, F. R. López Serrano, M. Andrés, and F. Bastida. 2012. Altitude-related factors but not Pinus community exert a dominant role over chemical and microbiological properties of a Mediterranean humid soil. European Journal of Soil Science 63:541–549.

Lundquist, J. D., and D. R. Cayan. 2002. Seasonal and spatial patterns in diurnal cycles in streamflow in the western United States. Journal of Hydrometeorology 3:591–603.

Luo, Y., J. Melillo, S. Niu, C. Beier, J. S. Clark, A. T. Classen, E. Davidson, J. S. Dukes, R. D. Evans, C. B. Field, C. I. Czimczik, M. Keller, B. a. Kimball, L. M. Kueppers, R. J. Norby, S. L. Pelini, E. Pendall, E. Rastetter, J. Six, M. Smith, M. G. Tjoelker, and M. S. Torn. 2011. Coordinated approaches to quantify long-term ecosystem dynamics in response to global change. Global Change Biology 17:843–854.

Lupon, A., S. Gerber, F. Sabater, and S. Bernal. 2015. Climate response of the soil nitrogen cycle in three forest types of a headwater Mediterranean catchment. Journal of Geophysical Research: Biogeosciences 120:859–875.

von Lützow, M., and I. Kögel-Knabner. 2009. Temperature sensitivity of soil organic matter decomposition—what do we know? Biology and Fertility of Soils 46:1–15.

Maître, V., A. C. Cosandey, E. Desagher, and A. Parriaux. 2003. Effectiveness of groundwater nitrate removal in a river riparian area: the importance of hydrogeological conditions. Journal of Hydrology 278:76–93.

Malchair, S., and M. Carnol. 2009. Microbial biomass and C and N transformations in forest floors under European beech, sessile oak, Norway spruce and Douglas-fir at four temperate forest sites. Soil Biology and Biochemistry 41:831–839.

Manzoni, S., J. P. Schimel, and A. Porporato. 2012. Responses of soil microbial communities to water stress: results from a meta-analysis. Ecology 93:930–8.

Martí, E., N. B. Grimm, and S. G. Fisher. 1997. Pre- and post-flood retention efficiency of nitrogen in a Sonoran Desert stream. Journal of the North American Benthological Society 16:805–819.

Martí, E., J. D. Schade, and N. B. Grimm. 2000. Flood-frequency and stream-riparian linkages in arid lands. Pages 111–135 in J. B. Jones and P. J. Mulholland, editors. Streams and Ground Waters. Academic Press, London, UK.

Martí, E., J. L. Riera, and F. Sabater. 2010. Effects of wastewater treatment plants on stream nutrient dynamics under water scarcity conditions. Pages 73–195 in S. Sabater, and D. Barceló, editors. Water Scarcity in the Mediterranean: Perspectives under global change. The handbook of environmental chemistry, Springer, London, UK.

Mathers, N. J., B. Harms, and R. C. Dalal. 2006. Impacts of land-use change on nitrogen status and mineralization in the Mulga Lands of Southern Queensland. Austral Ecology 31:708–718.

Matschonat, G., and E. Matzner. 1995. Quantification of ammonium sorption in acid forest soils by sorption isotherms. Plant and Soil 168-169:95–101.

Mayer, P. M., S. K. Reynolds, M. D. McCutchen, and T. J. Canfield. 2007. Meta-analysis of nitrogen removal in riparian buffers. Journal of Environmental Quality 36:1172–80.

McClain, M. E., E. W. Boyer, C. L. Dent, S. E. Gergel, N. B. Grimm, P. M. Groffman, S. C. Hart, J. W. Harvey, C. A. Johnston, E. Mayorga, W. H. McDowell, and G. Pinay. 2003. Biogeochemical hot spots and hot moments at the interface of terrestrial and aquatic ecosystems. Ecosystems 6:301–312.

McGlynn, B. L., and J. J. McDonnell. 2003. Quantifying the relative contributions of riparian and hillslope zones to catchment runoff. Water Resources Research 39: 1310.

McGlynn, B. L., and J. Seibert. 2003. Distributed assessment of contributing area and riparian buffering along stream networks. Water Resources Research 39:1–7.

McIntyre, R. E. S., M. A. Adams, D. J. Ford, and P. F. Grierson. 2009. Rewetting and litter addition influence mineralisation and microbial communities in soils from a semi-arid intermittent stream. Soil Biology and Biochemistry 41:92–101.

Medici, C., A. Butturini, S. Bernal, F. Sabater, and F. Franc. 2008. Modelling the non-linear hydrological behaviour of a small Mediterranean forested catchment. Hydrological Processes 3828:3814–3828.

Medici, C., S. Bernal, A. Butturini, F. Sabater, M. Martin, A. J. Wade, and F. Frances. 2010. Modelling the inorganic nitrogen behaviour in a small Mediterranean forested catchment, Fuirosos (Catalonia). Hydrology and Earth System Sciences 14:223–237.

Meixner, T., and M. Fenn. 2004. Biogeochemical budgets in a Mediterranean catchment with high rates of atmospheric N deposition – Importance of scale and temporal asynchrony. Biogeochemistry 70:331–356.

Merrill, A. G., and T. L. Benning. 2006. Ecosystem type differences in nitrogen process rates and controls in the riparian zone of a montane landscape. Forest Ecology and Management 222:145–161.

Meyer, J. L., and G. E. Likens. 1979. Transport and transformation of phosphorus in a forest stream ecosystem. Ecology 60:1255–1269.

Miller, A. E., J. P. Schimel, T. Meixner, J. O. Sickman, and J. M. Melack. 2005. Episodic rewetting enhances carbon and nitrogen release from chaparral soils. Soil Biology and Biochemistry 37:2195–2204.

Miller, A. E., J. P. Schimel, J. O. Sickman, T. Meixner, A. P. Doyle, and J. M. Melack. 2007. Mineralization responses at near-zero temperatures in three alpine soils. Biogeochemistry 84:233–245.

Mineau, M. M., C. V. Baxter, and A. M. Marcarelli. 2011. A non-native riparian tree (Elaeagnus angustifolia) changes nutrient dynamics in streams. Ecosystems 14:353–365.

Montreuil, O., P. Merot, and P. Marmonier. 2010. Estimation of nitrate removal by riparian wetlands and streams in agricultural catchments: effect of discharge and stream order. Freshwater Biology 55:2305–2318.

Montreuil, O., C. Cudennec, and P. Merot. 2011. Contrasting behaviour of two riparian wetlands in relation to their location in the hydrographic network. Journal of Hydrology 406:39–53.

Moriasi, D. N., J. G. Arnold, M. W. Van Liew, R. L. Bingner, R. D. Harmel, and T. L. Veith. 2007. Model evaluation guidelines for systematic quantification of accuracy in watershed simulations. American Society of Agricultural and Biological Engineers 50:885–900.

Morillas, L., M. Portillo-Estrada, and A. Gallardo. 2013. Wetting and drying events determine soil N pools in two Mediterranean ecosystems. Applied Soil Ecology 72:161–170.

Morrice, J. A., H. M. Valett, C. N. Dahm, and M. E. Campana. 1997. Alluvial characteristics, groundwater–surface water exchange and hydrological retention in headwater streams. Hydrological Processes 11:253–267.

Mulholland, P. J., S. A. Thomas, H. M. Valett, J. R. Webster, and J. J. Beaulieu. 2006. Effects of light on NO_3^- uptake in small forested streams: diurnal and day-to-day variations. Journal of the North American Benthological Society 25:583–595.

Mulholland, P. J., A. M. Helton, G. C. Poole, R. O. Hall, S. K. Hamilton, B. J. Peterson, J. L. Tank, L. R. Ashkenas, L. W. Cooper, C. N. Dahm, W. K. Dodds, S. E. G. Findlay, S. V Gregory, N. B. Grimm, S. L. Johnson, W. H. McDowell, J. L. Meyer, H. M. Valett, J. R. Webster, C. P. Arango, J. J. Beaulieu, M. J. Bernot, A. J. Burgin, C. L. Crenshaw, L. T. Johnson, B. R. Niederlehner, J. M. O'Brien, J. D. Potter, R. W. Sheibley, D. J. Sobota, and S. M. Thomas. 2008a. Stream denitrification across biomes and its response to anthropogenic nitrate loading. Nature 452:202–205.

Mulholland, P. J., J. L. Tank, D. M. Sanzone, W. M. Wollheim, B. J. Peterson, J. R. Webster, and J. L. Meyer. 2008b. Nitrogen cycling in a forest stream determined by a ^{15}N tracer addition. Ecologycal Monographs 70:471–493.

Muller, R. N., and F. H. Bormann. 1976. Role of Erythronium americanum Ker. on energy-flow and nutrient dynamics of a northern hardwood forest ecosystem. Science 193:1126–1128.

Murphy, J., and J. P. Riley. 1962. A modified single solution method for the fetermination of phosphate in natural waters. Analytica Chimica Acta 27:31–36.

Nadal-Sala, D., S. Sabaté, E. Sánchez-Costa, A. Boumghar, and C. A. Gracia. 2013. Different responses to water availability and evaporative demand of four co-occurring riparian tree species in NE Iberian Peninsula. Temporal and spatial sap flow patterns. Acta Horticulturae 991:215–222.

Naiman, R. J., J. M. Melillo, M. A. Lock, T. E. Ford, and R. Seth. 1987. Longitudinal patterns of ecosystem processes and community structure in a subarctic river continuum. Ecology 68:1139–1156.

Naiman, R. J., and H. Décamps. 1997. The ecology of interfaces: riparian zones. Annual Review of Ecology and Systematics 28:621–658.

Naiman, R. J., H. Décamps, and M. E. McClain. 2005. Riparia. Elsevier Academic Press, San Diego, CA, USA.

Niboyet, A., X. Le Roux, P. Dijkstra, B. A. Hungate, L. Barthes, J. C. Blankinship, J. R. Brown, C. B. Field, and P. W. Leadley. 2011. Testing interactive effects of global environmental changes on soil nitrogen cycling. Ecosphere 2: art56.

Nimick, D. A., C. H. Gammons, and S. R. Parker. 2011. Diel biogeochemical processes and their effect on the aqueous chemistry of streams: A review. Chemical Geology 283:3–17.

Novem Auyeung, D. S., V. Suseela, and J. S. Dukes. 2013. Warming and drought reduce temperature sensitivity of nitrogen transformations. Global Change Biology 19:662–76.

Ocampo, C. J., M. Sivapalan, and C. Oldham. 2006. Hydrological connectivity of upland-riparian zones in agricultural catchments: Implications for runoff generation and nitrate transport. Journal of Hydrology 331:643–658.

Pacific, V. J., K. G. Jencso, and B. L. McGlynn. 2010. Variable flushing mechanisms and landscape structure control stream DOC export during snowmelt in a set of nested catchments. Biogeochemistry 99:193–211.

Page, A. L., R. H. Miller, and D. R. Keeney. 1982. Methods of soil analysis. Part 2: Chemical and microbiological properties. Agronomy Monography 9. SSSA and ASA, Madison, WI, USA.

Pärn, J., G. Pinay, and Ü. Mander. 2012. Indicators of nutrients transport from agricultural catchments under temperate climate: A review. Ecological Indicators 22:4–15.

Pastor, A., J. L. Riera, M. Peipoch, L. Cañas, M. Ribot, E. Gacia, E. Martí, and F. Sabater. 2014. Temporal variability of nitrogen stable isotopes in primary uptake compartments in four streams differing in human impacts. Environmental Science and Technology 48:6612−6619.

Pattison, S. N., R. García-Ruiz, and B. A. Whitton. 1998. Spatial and seasonal variation in denitrification in the Swale-Ouse system, a river continuum. The Science of the Total Environment 210/211:289–305.

Payn, R. A., M. N. Gooseff, B. L. McGlynn, K. E. Bencala, and S. M. Wondzell. 2009. Channel water balance and exchange with subsurface flow along a mountain headwater stream in Montana, United States. Water Resources Research 45:W11427.

Pellerin, B. A., B. D. Downing, C. Kendall, R. A. Dahlgren, T. E. C. Kraus, J. Saraceno, R. G. M. Spencer, and B. A. Bergamaschi. 2009. Assessing the sources and magnitude of diurnal nitrate variability in the San Joaquin River (California) with an in situ optical nitrate sensor and dual nitrate isotopes. Freshwater Biology 54:376–387.

Pendall, E., L. Rustad, and J. Schimel. 2008. Towards a predictive understanding of belowground process responses to climate change: have we moved any closer? Functional Ecology 22:937–940.

Peñuelas, J., and M. Boada. 2003. A global change-induced biome shift in the Montseny mountains (NE Spain). Global Change Biology 9:131–140.

Perakis, S. S., and C. H. Kellogg. 2007. Imprint of oaks on nitrogen availability and δ15N in California grassland-savanna: a case of enhanced N inputs? Plant Ecology 191:209–220.

Pert, P. L., J. R. A. Butler, J. E. Brodie, C. Bruce, M. Honzák, D. Metcalfe, D. Mitchell, and G. Wong. 2010. A catchment-based approach to mapping hydrological ecosystem services using riparian habitat: A case study from the Wet Tropics, Australia. Ecological Complexity 7:378–388.

Peterson, B. J., W. M. Wollheim, P. J. Mulholland, J. R. Webster, J. L. Meyer, J. L. Tank, E. Martí, W. B. Bowden, H. M. Valett, A. E. Hershey, W. H. McDowell, W. K. Dodds, S. K. Hamilton, S. Gregory, and D. D. Morrall. 2001. Control of nitrogen export from watersheds by headwater streams. Science 292:86–90.

Petrone, K., I. Buffam, and H. Laudon. 2007. Hydrologic and biotic control of nitrogen export during snowmelt: A combined conservative and reactive tracer approach. Water Resources Research 43: W06420.

Pinay, G., Ruffinoni C., S. M. Wondzell, and F. Gazelle. 1998. Change in groundwater nitrate concentration in a large river floodplain: denitrification, uptake, or mixing? Journal of North American Benthological Society 17:179– 189.

Pinay, G., V. J. Black, A. M. Planty-Tabacchi, B. Gumiero, and H. Décamps. 2000. Geomorphic control of denitrification in large river floodplain soils. Biogeochemistry 50:163–182.

Pinay, G., B. Gumiero, E. Tabacchi, O. Gimenez, A. M. Tabacchi-Planty, M. M. Hefting, T. P. Burt, V. A. Black, C. Nilsson, V. Iordache, F. Bureau, L. Vought, G. E. Petts, and H. Décamps. 2007. Patterns of denitrification rates in European alluvial soils under various hydrological regimes. Freshwater Biology 52:252–266.

Pinay, G., S. Peiffer, J. R. de Dreuzy, S. Krause, D. M. Hannah, J. H. Fleckenstein and L. Hubert-Moy. 2015. Upscaling nitrogen removal capacity from local hotspots to low stream orders' drainage basins. Ecosystems 18:1101–1120.

R Core Team. 2012. R: A language and environment for statistical computing. R Foundation for Statistical Computing, Vienna, Austria.

Raich, J. W., E. B. Rastetter, J. M. Melillo, D. W. Kicklighter, P. A. Steudler, A. L. Grace, B. M. Iii, and C. J. Vörösmarty. 1991. Potential net primary productivity in South America: Application of a global model. Ecological Applications 1:399–429.

Ranalli, A. J., and D. L. Macalady. 2010. The importance of the riparian zone and in-stream processes in nitrate attenuation in undisturbed and agricultural watersheds–A review of the scientific literature. Journal of Hydrology 389:406–415.

Rassam, D. W., C. S. Fellows, R. de Hayr, H. Hunter, and P. Bloesch. 2006. The hydrology of riparian buffer zones; two case studies in an ephemeral and a perennial stream. Journal of Hydrology 325:308–324.

Rastetter, E. B., G. I. Ågren, and G. R. Shaver. 1997. Responses of N-limited ecosystems to increased CO_2: A balanced-nutrition, coupled-element-cycles model. Ecological Applications 7:444–460.

Rennenberg, H., M. Dannenmann, A. Gessler, J. Kreuzwieser, J. Simon, and H. Papen. 2009. Nitrogen balance in forest soils: nutritional limitation of plants under climate change stresses. Plant Biology 11(S1):4–23.

Rey, A., E. Pegoraro, V. Tedeschi, I. de Parri, P. Jarvis, and R. Valentini. 2002. Annual variation in soil respiration and its components in a coppice oak forest in Central Italy. Global Change Biology 8:851–866.

Riis, T., W. K. Dodds, P. B. Kristensen, and A. J. Baisner. 2012. Nitrogen cycling and dynamics in a macrophyte-rich stream as determined by a release. Freshwater Biology 57:1579–1591.

Roberts, B. J., and P. J. Mulholland. 2007. In-stream biotic control on nutrient biogeochemistry in a forested stream, West Fork of Walker Branch. Journal of Geophysical Research 112:G04002.

Rogora, M. 2007. Synchronous trends in $N–NO_3$ export from N-saturated river catchments in relation to climate. Biogeochemistry 86:251–268.

Rosenkranz, P., N. Brüggemann, H. Papen, Z. Xu, G. Seufert, and K. Butterbach-Bahl. 2006. N_2O, NO and CH_4 exchange, and microbial N turnover over a Mediterranean pine forest soil. Biogeosciences 3:121–133.

Ross, D. S., B. C. Wemple, A. E. Jamison, G. Fredriksen, J. B. Shanley, G. B. Lawrence, S. W. Bailey, and J. L. Campbell. 2009. A cross-site comparison of factors influencing soil nitrification rates in northeastern USA forested watersheds. Ecosystems 12:158–178.

Ross, D. S., J. B. Shanley, J. L. Campbell, G. B. Lawrence, S. W. Bailey, G. E. Likens, B. C. Wemple, G. Fredriksen, and A. E. Jamison. 2012. Spatial patterns of soil nitrification and nitrate export from forested headwaters in the northeastern United States. Journal of Geophysical Research 117:1–14.

Rusjan, S., and M. Mikoš. 2009. Seasonal variability of diurnal in-stream nitrate concentration oscillations under hydrologically stable conditions. Biogeochemistry 97:123–140.

Rustad, L., J. L. Campbell, G. Marion, R. J. Norby, M. J. Mitchell, A. Hartley, J. Cornelissen, and J. Gurevitch. 2001. A meta-analysis of the response of soil respiration, net nitrogen mineralization, and aboveground plant growth to experimental ecosystem warming. Oecologia 126:543–562.

Sabater, F., and S. Bernal. 2011. Keeping healthy riparian and aquatic ecosystems in the Mediterranean: challenges and solutions through riparian forest management. Pages 151–155 in Y. Boirot, C. Gracia, and M. Palahí, editors. Water for Forests and People in the Mediterranean Region: A challenging Balanc. European Forest Institute, Joensuu, Finland.

Sabater, F., S. Bernal, A. Lupon, S. Poblador, and E. Martí. 2013. Els boscos de ribera. Pages 178-179 in D. Bueno, editor. Atles Ecosistemes dels Països Catalans. Enciclopèdia Catalana Press, Barcelona, Spain.

Sabater, S., A. Butturini, J. C. Clément, T. Burt, D. Dowrick, M. Hefting, V. Maître, G. Pinay, C. Postolache, M. Rzepecki, and F. Sabater. 2003. Nitrogen removal by riparian buffers along a European climatic gradient: Patterns and factors of variation. Ecosystems 6:20–30.

Salemi, L. F., J. D. Groppo, R. Trevisan, J. Marcos de Moraes, W. de Paula Lima, and L. A. Martinelli. 2012. Riparian vegetation and water yield: A synthesis. Journal of Hydrology 454-455:195–202.

Sánchez-Pérez, J. M., E. Lucot, T. Bariac, and M. Trémolières. 2008. Water uptake by trees in a riparian hardwood forest (Rhine floodplain, France). Hydrological Processes 22:366–375.

Scanlon, T. M., S. M. Ingram, and A. L. Riscassi. 2010. Terrestrial and in-stream influences on the spatial variability of nitrate in a forested headwater catchment. Journal of Geophysical Research 115:1–12.

Scott, D. F. 1999. Managing riparian zone vegetation to sustain streamflow: results of paired catchment experiments in South Africa. Canadian Journal of Forest Research 29:1149– 1157.

Scott, R. L., W. L. Cable, T. E. Huxman, P. L. Nagler, M. Hernandez, and D. Goodrich. 2008. Multiyear riparian evapotranspiration and groundwater use for a semiarid watershed. Journal of Arid Environments 72:1232–1246.

Schade, J. D., E. Martí, J. R. Welter, S. G. Fisher, and N. B. Grimm. 2002. Sources of nitrogen to the riparian zone of a desert stream: Implications for riparian vegetation and nitrogen retention. Ecosystems 5:68–79.

Schade, J. D., and S. E. Hobbie. 2005. Spatial and temporal variation in islands of fertility in the Sonoran Desert. Biogeochemistry 73:541–553.

Schade, J. D., J. R. Welter, E. Martí, and N. B. Grimm. 2005. Hydrologic exchange and N uptake by riparian vegetation in an arid-land stream Hydrologic exchange and N uptake by riparian vegetation in an arid-land stream. Journal of the North American Benthological Society 24:19–28.

von Schiller, D., E. Martí, J. L. Riera, and F. Sabater. 2007. Effects of nutrients and light on periphyton biomass and nitrogen uptake in Mediterranean streams with contrasting land uses. Freshwater Biology 52:891–906.

von Schiller, D., S. Bernal, and E. Martí. 2011. A comparison of two empirical approaches to estimate in-stream net nutrient uptake. Biogeosciences 8:875–882.

von Schiller, D., S. Bernal, F. Sabater, and E. Martí. 2015. A round-trip ticket: the importance of release processes for in-stream nutrient spiraling. Freshwater Science 34.

Schilling, K. E. 2007. Water table fluctuations under three riparian land covers, Iowa (USA). Hydrological Processes 21:2415–2424.

Schimel, J. P., T. C. Balser, and M. D. Wallenstein. 2007. Microbial stress-response physiology and its implications for ecosystem function. Ecology 88:1386–1394.

Schlesinger, W. H. 2009. On the fate of anthropogenic nitrogen. Proceedings of the National Academy of Sciences of the United States of America 106:203–8.

Scholefield, D., T. Le Goff, J. Braven, L. Ebdon, T. Long, and M. Butler. 2005. Concerted diurnal patterns in riverine nutrient concentrations and physical conditions. The Science of the Total Environment 344:201–210.

Schütt, M., W. Borken, O. Spott, C. F. Stange, and E. Matzner. 2014. Temperature sensitivity of C and N mineralization in temperate forest soils at low temperatures. Soil Biology and Biochemistry 69:320–327.

Seibert, J., and M. J. P. Vis. 2012. Teaching hydrological modeling with a user-friendly catchment-runoff-model software package. Hydrology and Earth System Sciences 16:3315–3325.

Serrasolses, I. 1999. Soil nitrogen dynamics. Pages 223–235 in F. Rodà, J. Retana, C. Gracia, and J. Bellot, editors. Ecological Studies 137: Ecology of Mediterranean Evergreen Oak Forests. Springer–Verlag Berlin Heidelberg, New York, NJ, USA.

Sleutel, S., B. Moeskops, W. Huybrechts, A. Vandenbossche, J. Salomez, S. Bolle, D. Buchan, and S. Neve. 2008. Modeling soil moisture effects on net nitrogen mineralization in loamy wetland soils. Wetlands 28:724–734.

Smith, M., P. Conte, A. E. Berns, J. R. Thomson, and T. R. Cavagnaro. 2012. Spatial patterns of, and environmental controls on, soil properties at a riparian-paddock interface. Soil Biology and Biochemistry 49:38–45.

Snyder, K. A., and D. G. Williams. 2000. Water sources used by riparian trees varies among stream types on the San Pedro River, Arizona. Agricultural and Forest Meteorology 105:227–240.

Sponseller, R. A. 2007. Precipitation pulses and soil CO_2 flux in a Sonoran desert ecosystem. Global Change Biology 13:426–436.

Springer, A. E., M. A. Amentt, T. E. Kolb, and R. M. Mullen. 2006. Evapotranspiration of two vegetation communities in a high-elevation riparian meadow at Hart Prairie, Arizona. Water Resources Research 42:1–11.

Stark, J. M., and S. C. Hart. 1997. High rates of nitrification and nitrate turnover in undisturbed coniferous forests. Nature 385:61–64.

Starry, O. S., H. M. Valett, and M. E. Schreiber. 2005. Nitrification rates in a headwater stream: influences of seasonal variation in C and N supply. Journal of the North American Benthological Society 24:753–768.

Sterner, R. W., and J. J. Elser. 2002. Ecological stoichiometry: The biology of elements from molecules to the biosphere. Princetion University Press, Princeton, NJ, USA.

Stock, W. D., K. T. Wienand, and A. C. Baker. 1995. Impacts of invading N_2-fixing Acacia species on patterns of nutrient cycling in two Cape ecosystems: evidence from soil incubation studies and ^{15}N natural abundance values. Oecologia 101:375–382.

Strauss, E. A., and G. A. Lamberti. 2000. Regulation of nitrification in aquatic sediments by organic carbon. Limnology and Oceanography 45:1854–1859.

Strayer, D. L., M. E. Power, W. F. Fagan, S. T. A. Pickett, and J. Belnap. 2003. A Classification of Ecological Boundaries. BioScience 53:723.

Sudduth, E. B., S. S. Perakis, and E. S. Bernhardt. 2013. Nitrate in watersheds: Straight from soils to streams? Journal of Geophysical Research: Biogeosciences 118:291–302.

Suseela, V., R. T. Conant, M. Wallenstein, and J. S. Dukes. 2012. Effects of soil moisture on the temperature sensitivity of heterotrophic respiration vary seasonally in an old-field climate change experiment. Global Change Biology 18:336–348.

Sutton, M. A., O. Oenema, J. W. Erisman, A. Leip, H. van Grinsven, and W. Winiwarter. 2011. Too much of a good thing. Nature 472:159–61.

Tabacchi, E., D. L. Correll, R. Hauer, G. Pinay, A. M. Planty-Tabacchi, and R. C. Wissmar. 1998. Development, maintenance and role of riparian vegetation in the river landscape. Freshwater Biology 40:497–516.

Tabacchi, E., L. Lambs, H. Guilloy, A.-M. Planty-Tabacchi, E. Muller, and H. Décamps. 2000. Impacts of riparian vegetation on hydrological processes. Hydrological Processes 14:2959–2976.

Tank, J. L., E. J. Rosi-Marshall, M. A. Baker, and R. O. Hall, Jr. 2008. Are rivers just big streams? A pulse method to quantify nitrogen demand in a large river. Ecology 89:2935–2945.

Technicon. 1976. Technicon Instrument System. Technicon Method Guide. Technicon, Tarrytown, NY, USA.

Templer, P. H., M. A. Arthur, G. M. Lovett, and K. C. Weathers. 2007. Plant and soil natural abundance delta (15)N: indicators of relative rates of nitrogen cycling in temperate forest ecosystems. Oecologia 153:399–406.

Tiemann, L. K., and S. A. Billings. 2012. Tracking C and N flows through microbial biomass with increased soil moisture variability. Soil Biology and Biochemistry 49:11–22.

Tockner, K., and J. A. Stanford. 2002. Riverine flood plains: present state and future trends. Environmental Conservation 29:308–330.

Trap, J., F. Bureau, M. Akpa-Vinceslas, T. Decaens, and M. Aubert. 2011. Changes in humus forms and soil N pathways along a 130-year-old pure beech forest chronosequence. Annals of Forest Science 68:595–606.

Uehlinger, U. 2000. Resistance and resilience of ecosystem metabolism in a ood-prone river system. Science 45:319–332.

United Nations Environtment Programme (UNEP). 1992. World Atlas of Desertification. Edward Arnorld Press, London, UK.

Valett, H. M., J. A. Morrice, C. N. Dahm, and M. E. Campana. 1996. Parent lithology, surface-groundwater exchange, and nitrate retention in headwater streams. Limnology and Oceanography 41:333–345.

Valett, H. M., S. A. Thomas, P. J. Mulholland, J. R. Webster, C. N. Dahm, C. S. Fellows, C. L. Crenshaw, and C. G. Peterson. 2008. Endogenous and exogenous control of ecosystem function: N cycling in headwater streams. Ecology 89:3515–3527.

Vannote, R. L., G. W. Minshall, K. W. Cummins, J. R. Sedell, and C. E. Cushing. 1980. The river continuum concept. Canadian Journal of Fisheries and Aquatic Sciences 37:130–137.

Venterea, R. T., G. M. Lovett, P. M. Groffman, and P. A. Schwarz. 2003. Landscape patterns of net nitrification in a northern hardwood-conifer forest. Soil Biology and Biochemistry:527–539.

Verburg, P. S. J., D. W. Johnson, D. E. Schorran, L. L. Wallace, Y. Luo, and J. A. Arnone III. 2009. Impacts of an anomalously warm year on soil nitrogen availability in experimentally manipulated intact tallgrass prairie ecosystems. Global Change Biology 15:888–900.

Vidon, P. G. F., and A. R. Hill. 2004a. Landscape controls on the hydrology of stream riparian zones. Journal of Hydrology 292:210–228.

Vidon, P., and A. R. Hill. 2004b. Denitrification and patterns of electron donors and acceptors in eight riparian zones with contrasting hydrogeology. Biogeochemistry 71:259–283.

Vidon, P., C. J. Allan, D. Burns, T. P. Duval, N. Gurwick, S. Inamdar, R. Lowrance, J. Okay, D. Scott, and S. Sebestyen. 2010. Hot spots and hot moments in riparian zones: Potential for improved water quality management. Journal of the American Water Resources Association 46:278–298.

Volkmar, E. C., S. S. Henson, R. A. Dahlgren, A. T. O'Geen, and E. E. van Nieuwenhuyse. 2011. Diel patterns of algae and water quality constituents in the San Joaquin River, California, USA. Chemical Geology 283:56–67.

Wade, A. J., P. Durand, V. Beaujouan, W. W. Wessel, K. J. Raat, G. Whitehead, D. Butterfield, K. Rankinen, A. Lepisto, A. J. Wade, P. Durand, V. Beaujouan, W. W. Wessel, and K. J. Raat. 2002. A nitrogen model for European catchments : INCA , new model structure and equations. Hydrology and Earth System Sciences Discussions, 6(3):559-582.

Walling, D. E., and B. W. Webb. 1986. Solutes in river systems. Pages 251–327 in S. T. Trudgill, editor. Solute Processes. Willey Press, Chichester, UK.

Welter, J. R., S. G. Fisher, and N. B. Grimm. 2005. Nitrogen transport and retention in an arid land watershed: Influence of storm characteristics on terrestrial–aquatic linkages. Biogeochemistry 76:421–440.

Wine, M. L., and C. B. Zou. 2012. Long-term streamflow relations with riparian gallery forest expansion into tallgrass prairie in the Southern Great Plains, USA. Forest Ecology and Management 266:170–179.

White, W. N. 1932. A method of estimating ground-water supplies based on discharge by plants and evaporation from soil: Results of investigations in Escalante Valley, Utah. US Government Printing Office 659.

Wollheim, W. M., C. J. Vörösmarty, B. J. Peterson, S. P. Seitzinger, and C. S. Hopkinson. 2006. Relationship between river size and nutrient removal. Geophysical Research Letters 33:2–5.

Wu, H., M. Wiesmeier, Q. Yu, M. Steffens, X. Han, and I. Kögel-Knabner. 2012. Labile organic C and N mineralization of soil aggregate size classes in semiarid grasslands as affected by grazing management. Biology and Fertility of Soils 48:305–313.

Xu, L., D. D. Baldocchi, and J. Tang. 2004. How soil moisture, rain pulses, and growth alter the response of ecosystem respiration to temperature. Global Biogeochemical Cycles 18:GB4002.

Yahdjian, L., and O. E. Sala. 2010. Size of precipitation pulses controls nitrogen transformation and losses in an arid Patagonian ecosystem. Ecosystems 13:575–585.

Young, R. G., and A. D. Huryn. 1998. Comment: Improvements to the diurnal upstream-downstream dissolved oxygen change technique for determining whole-stream metabolism in small streams. Canadian Journal of Fisheries and Aquatic Sciences 55:1784–1785.

Zar, J. H. 2010. Biostatistical analysis. Prentice-Hall/Pearson Press, Upper Saddle River, NJ, USA.

SUPPORTING INFORMATION

This section comprises supporting information for Chapter 4, Chapter 6, Chapter 7, and Chapter 8.

Appendix A provides further information about the contribution of riparian groundwater inputs to day-night variations in stream nitrate concentration (Chapter 6), and comprises 2 pages and 1 figure.

Appendix B provides all references used for performing Figure 8.1 and Fugire 8.3, and comprises 8 pages and 2 tables.

Appendix C provides further information about the calibration of daily stream discharge with PERSiST model (Chapter 8), and comprises 2 pages and 1 table.

Appendix D provides the original publications of Chapter 4 and Chapter 7, as well as the editor acceptance letter of Chapter 6.

APPENDIX A. CONTRIBUTION OF RIPARIAN GROUNDWATER INPUTS TO DAY-NIGHT VARIATIONS IN STREAM NITRATE CONCENTRATION

We considered the possibility that day-night fluctuations in riparian groundwater inputs suffice to explain the observed diel variations in stream nitrate (NO_3^-) concentration during spring 2012 at the down-stream site. We used a mass balance approach to calculate midnight NO_3^- concentrations based solely on hydrological mixing. For each day:

$$[NO_3]_{sw\,(0h)} = \frac{[NO_3]_{sw\,(12h)} * Q_{sw\,(12h)} + [NO_3]_{gw} * Q_{sw\,(0h\text{-}12h)}}{Q_{sw\,(0h)}} \quad (A.1)$$

where $[NO_3]_{sw}$ is stream NO_3^- concentration and $[NO_3]_{gw}$ is the average of riparian groundwater NO_3^- concentration between midnight and noon (all in mg N L^{-1}). Q_{sw} is stream discharge and $Q_{sw\,(0h\text{-}12h)}$ is riparian groundwater input estimated as the difference in Q_{sw} between midnight and noon (all in L s^{-1}). The subscripts (0h) and (12h) denote time of the day, midnight and noon respectively. We calculated the relative difference between midnight NO_3^- concentrations predicted from hydrological mixing and those observed at noon ($\Delta_{NO3,}$ in %) (Equation 6.1). Moreover, we used a Wilcoxon paired rank sum test to examine whether differences between NO_3^- concentrations observed at noon and those predicted for midnight were statistically significant.

During spring 2012, midnight stream NO_3^- concentration predicted from hydrological mixing were similar to those observed at noon (for each week from March to June: $Z > Z_{0.05}$, df = 6, $p > 0.1$). The average Δ_{NO3} calculated from predicted midnight NO_3^- concentrations was 0.6% (Figure A.1, white circles). This value was 20 fold lower than the Δ_{NO3} obtained from observed midnight and noon NO_3^- concentrations (13%) (Figure A.1, black circles). Similar results were obtained when using midnight rather than average riparian groundwater NO_3^- concentration. These findings, together with the fact that no simultaneous diel variations in discharge, riparian groundwater level and N concentrations were observed, support the idea that terrestrial processes did not control diel variations in NO_3^- concentrations at the study site.

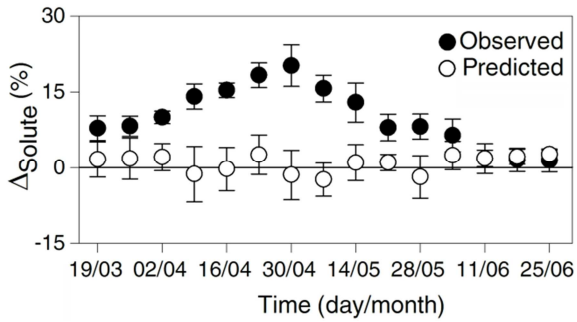

Figure A.1 Temporal pattern of the relative difference between midnight and noon stream nitrate concentrations (Δ_{NO3}) during spring 2012 at the down-stream site. The Δ_{NO3} is shown for observed values and for values predicted from hydrological mixing (black and white circles, respectively). Symbols are the median of $\Delta_{NO3}$for each week and whiskers denote the 25th and 75th percentiles. The black line indicates no differences between midnight and noon nitrate concentrations.

References

Zar, J. H. 2010. *Biostatistical analysis in* Prentice-Hall/Pearson, *editors*. Upper Saddle River, NJ.

APPENDIX B. PUBLISHED STUDIES COLLECTED FOR DISCUSSION FIGURES

Table B.1 Net nitrification rates (NN) and mean annual precipitation (MAP) of riparian and upland systems in arid/semiarid, Mediterranean, and temperate regions.

Climate	System	NN (mg N kg^{-1} d^{-1})	MAP (mm yr^{-1})	Source
Arid/Semiarid	**Riparian**	0.1	200	Adair et al. 2004
		0.05	280	Adair et al. 2004
		0.37	500	Bechtold Naiman 2006
		0.17	500	Bechtold Naiman 2006
		0.5	500	Follstad Dahm
		0.35	500	Follstad et al. 2009
		0.03	500	Harms and Grimm 2010
		0.25	500	Heffernan and Sponseller 2004
		0.2	400	Kauffman et al. 2004
		0.71	500	Schaede and Hobbie 2005
Arid/Semiarid	**Upland**	0.13	500	Bechtold Naiman 2006
		0.14	310	Booth et al. 2003
		0.03	340	Dijkstra et al. 2012
		0.15	500	Heffernan and Sponseller 2004
		0.36	500	Mathers et al. 2006
		0.4	500	Schaede and Hobbie 2005
		0.6	280	Stark and Norton 2015
		0.09	380	Wu et al. 2012
		-0.1	200	Yahdjian and Sala 2010
		0.1	200	Yahdjian and Sala 2010

Table B.1 Continuation.

Climate	System	NN (mg N kg^{-1} d^{-1})	MAP (mm yr^{-1})	Source
Mediterranean	**Riparian**	1.5	800	Castro-Diez et al. 2012
		1.1	800	Evans et al. 2011
		0.3	880	Hefting et al. 2004
		0.9	885	Hefting et al. 2004
		0.2	580	Hefting et al. 2004
		0.95	950	Lohse et al. 2010
		0.44	950	Lohse et al. 2010
		1.18	880	Lupon 2014
		2	750	Pinay et al. 1995
		0.8	750	Smith et al. 2012
Mediterranean	**Upland**	0.05	700	Bonilla &Roda 1992
		0.2	455	Emmett et al. 2004
		0.26	950	Lohse et al. 2010
		0.13	950	Lohse et al. 2010
		0.05	880	Lupon et al. 2015
		0.15	880	Lupon et al. 2015
		0.05	670	Miller et al. 2005
		0.38	660	Perakis et al. 2007
		0.51	660	Perakis et al. 2007
		0.01	918	Rosenkranz et al. 2001
		0.2	700	Serrasolses 1999
		0.5	700	Serrasolses 1999

Table B.1 Continuation.

Climate	System	NN (mg N kg^{-1} d^{-1})	MAP (mm yr^{-1})	Source
Temperate	**Riparian**	0.53	1200	Clément et al. 2002
		0.23	1200	Clément et al. 2002
		0.36	1200	Clément et al. 2002
		0.7	1000	Frank and Groffman 1998
		0.03	1000	Groffman et al. 1992
		0.2	1100	Hanson et al. 1994
		0.35	1000	Harris & Riha 1991
		0.4	1050	Hefting et al. 2004
		0.1	1740	Hefting et al. 2004
		0.3	1100	Hefting et al. 2004
		0.36	1600	Merril and Benning 2006
Temperate	**Upland**	1.45	1400	Andrianarisoa et al. 2009
		0.9	1000	Emmett et al. 2004
		1.5	1400	Guilliam et al. 1996
		0.43	1000	Harris & Riha 1991
		0.12	1400	Kaiser et al. 2011
		2.79	1000	Kelly et al. 2011
		0.71	1000	Kelly et al. 2011
		2.5	1120	Lovett et al. 2004
		3	1100	Malchair and Carnol 2009
		3	1500	Ross et al. 2009
		1.8	1150	Templer et al. 2007
		2.2	1400	Venterea et al. 2003

Table B.2 Precipitation (P), potential evapotranspiration rates (PET), Aridity Index (AI) and riparian water depletions (RWD) for different catchments located worldwide.

Climate	P (mm yr^{-1})	PET (mm yr^{-1})	AI	RWD (%)	Source
Arid	250	2280	0.11	33	Dahm et al. 2002
Arid	300	1800	0.17	36	Doble et al. 2006
Arid	400	1400	0.29	22	Contreras et al. 2011
Arid	255	693	0.37	20	Goodrick 2000
Arid	570	900	0.63	13	Springer et al. 2006
Mediterranean	1296	1911	0.68	9	Scott 1996
Mediterranean	780	1055	0.72	12	Folch and Ferrer 2015
Mediterranean	850	1170	0.73	7	Wine and Zou 2012
Mediterranean	750	990	0.77	5	Bernal and Sabater 2012
Mediterranean	925	1100	0.84	3.6	Lupon 2015
Temperate	1780	1400	1.27	4	Dunford and Fletcher 1947
Temperate	858	590	1.45	3	Petrone 2007
Mediterranean	1523	1011	1.51	2.5	Salami et al. 2013
Temperate	1800	900	2.00	1.2	Dunford and Fletcher 1947
Tropical	4370	1825	2.39	1.4	Cadol et al. 2012

References

Adair, E. C., D. Binkley, and D. C. Andersen. 2004. Patterns of nitrogen accumulation and cycling in riparian floodplain ecosystems along the Green and Yampa rivers. Oecologia 139:108–116.

Andrianarisoa, K. S., B. Zeller, J. L. Dupouey, and E. Dambrine. 2009. Comparing indicators of N status of 50 beech stands (Fagus sylvatica L.) in northeastern France. Forest Ecology and Management 257:2241–2253.

Bechtold, J. S., and R. J. Naiman. 2006. Soil texture and nitrogen mineralization potential across a riparian toposequence in a semi-arid savanna. Soil Biology and Biochemistry 38:1325–1333.

Bonilla, D., and F. Rodà. 1992. Soil nitrogen dynamics in a holm oak forest. Vegetatio 99-100:247–257.

Booth, M. S., J. M. Stark, and M. M. Caldwell. 2003. Inorganic N turnover and availability in annual- and perennial-dominated soils in a northern Utah shrub-steppe ecosystem. Biogeochemistry 66:311–330.

Cadol, D., S. Kampf, and E. Wohl. 2012. Effects of evapotranspiration on baseflow in a tropical headwater catchment. Journal of Hydrology 462-463:4–14.

Castro-Díez, P., N. Fierro-Brunnenmeister, N. González-Muñoz, and A. Gallardo. 2012. Effects of exotic and native tree leaf litter on soil properties of two contrasting sites in the Iberian Peninsula. Plant and Soil 350:179–191.

Clément, J.C., G. Pinay, and P. Marmonier. 2002. Seasonal dynamics of denitrification along topohydrosequences in three different riparian wetlands. Journal of Environment Quality 31:1025–1037.

Contreras, S., E. G. Jobbágy, P. E. Villagra, M. D. Nosetto, and J. Puigdefábregas. 2011. Remote sensing estimates of supplementary water consumption by arid ecosystems of central Argentina. Journal of Hydrology 397:10–22.

Dahm, C. N., J. R. Cleverly, J. Coonrod, E. Allred, J. R. Thibault, D. E. McDonnell, and D. J. Gilroy. 2002. Evapotranspiration at the land/ water interface in a semi-arid drainage basin. Freshwater Biology 47:831–844.

Dijkstra, F. A., D. J. Augustine, P. Brewer, and J. C. von Fischer. 2012. Nitrogen cycling and water pulses in semiarid grasslands: are microbial and plant processes temporally asynchronous? Oecologia 170:799–808.

Doble, R., C. Simmons, I. Jolly, and G. Walker. 2006. Spatial relationships between vegetation cover and irrigation-induced groundwater discharge on a semi-arid floodplain, Australia. Journal of Hydrology 329:75–97.

Dunford, E. G., and P. W. Fletcher. 1947. Effect of removal of stream-bank vegetation upon water yield. American Geophysics Union 28:105–110.

Emmett, B. A., C. Beier, M. Estiarte, A. Tietema, H. L. Kristensen, D. Williams, J. Peñuelas, I. Schmidt, and A. Sowerby. 2004. The response of soil processes to climate change: results from manipulation studies of shrublands across an environmental gradient. Ecosystems 7:625–637.

Evans, D. M., and S. H. Schoenholtz. 2011. Nitrogen mineralization in riparian soils along a river continuum within a Multi-Land-Use basin. Soil Science Society of America Journal 75:719–728.

Folch, A., and N. Ferrer. 2015. The impact of poplar tree plantations for biomass production on the aquifer water budget and base flow in a Mediterranean basin. The Science of the Total Environment 524-525:213–24.

Follstad Shah, J, J., and C. N. Dahm. 2008. Flood regime and leaf fall determine soil inorganic nitrogen dynamics in semiarid riparian forests. Ecological Applications 18:771–788.

Frank, D. A., and P. M. Groffman. 1998. Ungulate vs. landscape control of soil C and N processes in grasslands of Yellowstone National Park. Ecology 79:2229–2241.

Gilliam, F. S., B. M. Yurish, and M. B. Adams. 2001. Temporal and spatial variation of nitrogen transformations in nitrogen-saturated soils of a central Appalachian hardwood forest. Canadian Journal of Forest Research 31:1768–1785.

Goodrich, D. C., R. Scott, J. Qi, B. Goff, C. L. Unkrich, M. S. Moran, D. Williams, S. Schaeffer, K. Snyder, R. MacNish, T. Maddock, D. Pool, A. Chehbouni, D. I. Cooper, W. E. Eichinger, W. J. Shuttleworth, Y. Kerr, R. Marsett, and W. Ni. 2000. Seasonal estimates of riparian evapotranspiration using remote and in situ measurements. Agricultural and Forest Meteorology 105:281–309.

Groffman, P. M., A. J. Gold, and R. C. Simmons. 1992. Nitrate dynamics in riparian forests: Microbial studies. Journal of Environment Quality 21:666.

Hanson, G. C., P. M. Groffman, and A. J. Gold. 1994. Symtoms of nitrogen saturation in a riparian wetland. Ecological Applications 4:750–756.

Harms, T. K., and N. B. Grimm. 2008. Hot spots and hot moments of carbon and nitrogen dynamics in a semiarid riparian zone. Journal of Geophysical Research: Biogeoscience 113:1–14.

Harris, M. M., and S. J. Riha. 1991. Carbon and nitrigen dynamics in forest floor during short-term. Soil Biology and Biochemistry 23:1035–1041.

Heffernan, J. B., and R. A. Sponseller. 2004. Nutrient mobilization and processing in Sonoran desert riparian soils following artificial re-wetting. Biogeochemistry 70:117–134.

Hefting, M. M., J.C. Clément, D. J. Dowrick, A. C. Cosandey, S. Bernal, C. Cimpian, A. Tatur, T. P. Burt, and G. Pinay. 2004. Water table elevation controls on soil nitrogen cycling in riparian wetlands along a European climatic gradient. Biogeochemistry 67:113–134.

Kaiser, C., L. Fuchslueger, M. Koranda, M. Gorfer, C. F. Stange, B. Kitzler, F. Rasche, J. Strauss, A. Sessitsch, S. Zechmeister-Boltenstern, and A. Richter. 2011. Plants control the seasonal dynamics of microbial N cycling in a beech forest soil by belowground C allocation. Ecology 92:1036–51.

Kauffman, J. B., A. S. Thorpe, and E. N. J. Brookshire. 2004. Livestock exclusion and belowground ecosystem responses in riparian meadows of eastern Oregon. Ecological Applications 14:1671–1679.

Kelly, C. N., S. H. Schoenholtz, and M. B. Adams. 2011. Soil properties associated with net nitrification following watershed conversion from Appalachian hardwoods to Norway spruce. Plant and Soil 344:361–376.

Lohse, K. A., J. Sanderman, and R. Amundson. 2013. Identifying sources and processes influencing nitrogen export to a small stream using dual isotopes of nitrate. Water Resources Research 49: 5715–5731.

Lovett, G. M., K. C. Weathers, M. A. Arthur, and J. C. Schultz. 2004. Nitrogen cycling in a northern hardwood forest: Do species matter? Biogeochemistry 67:289–308.

Malchair, S., and M. Carnol. 2009. Microbial biomass and C and N transformations in forest floors under European beech, sessile oak, Norway spruce and Douglas-fir at four temperate forest sites. Soil Biology and Biochemistry 41:831–839.

Mathers, N. J., B. Harms, and R. C. Dalal. 2006. Impacts of land-use change on nitrogen status and mineralization in the Mulga Lands of Southern Queensland. Austral Ecology 31:708–718.

Merrill, A. G., and T. L. Benning. 2006. Ecosystem type differences in nitrogen process rates and controls in the riparian zone of a montane landscape. Forest Ecology and Management 222:145–161.

Miller, A. E., J. P. Schimel, T. Meixner, J. O. Sickman, and J. M. Melack. 2005. Episodic rewetting enhances carbon and nitrogen release from chaparral soils. Soil Biology and Biochemistry 37:2195–2204.

Perakis, S. S., and C. H. Kellogg. 2007. Imprint of oaks on nitrogen availability and δ15N in California grassland-savanna: a case of enhanced N inputs? Plant Ecology 191:209–220.

Petrone, K., I. Buffam, and H. Laudon. 2007. Hydrologic and biotic control of nitrogen export during snowmelt: A combined conservative and reactive tracer approach. Water Resources Research 43: W06420.

Rosenkranz, P., N. Brüggemann, H. Papen, Z. Xu, G. Seufert, and K. Butterbach-Bahl. 2006. N_2O, NO and CH_4 exchange, and microbial N turnover over a Mediterranean pine forest soil. Biogeosciences 3:121–133.

Ross, D. S., B. C. Wemple, A. E. Jamison, G. Fredriksen, J. B. Shanley, G. B. Lawrence, S. W. Bailey, and J. L. Campbell. 2009. A cross-site comparison of factors influencing soil nitrification rates in northeastern USA forested watersheds. Ecosystems 12:158–178.

Sabater, F., and S. Bernal. 2011. Keeping healthy riparian and aquatic ecosystems in the Mediterranean: challenges and solutions through riparian forest management. Pages 151–155 in Y. Boirot, C. Gracia, and M. Palahí, editors. Water for Forests and People

in the Mediterranean Region: A challenging Balanc. European Forest Institute, Joensuu, Finland.

Salemi, L. F., J. D. Groppo, R. Trevisan, J. Marcos de Moraes, W. de Paula Lima, and L. A. Martinelli. 2012. Riparian vegetation and water yield: A synthesis. Journal of Hydrology 454-455:195–202.

Schade, J. D., and S. E. Hobbie. 2005. Spatial and temporal variation in islands of fertility in the Sonoran Desert. Biogeochemistry 73:541–553.

Scott, D. F. 1999. Managing riparian zone vegetation to sustain streamflow: results of paired catchment experiments in South Africa. Canadian Journal of Forest Research 29:1149–1157.

Serrasolses, I. 1999. Soil nitrogen dynamics. Pages 223–235 in F. Rodà, J. Retana, C. Gracia, and J. Bellot, editors. Ecological Studies 137: Ecology of Mediterranean Evergreen Oak Forests. Springer–Verlag Berlin Heidelberg, New York, NJ, USA.

Smith, M., P. Conte, A. E. Berns, J. R. Thomson, and T. R. Cavagnaro. 2012. Spatial patterns of, and environmental controls on, soil properties at a riparian-paddock interface. Soil Biology and Biochemistry 49:38–45.

Springer, A. E., M. A. Amentt, T. E. Kolb, and R. M. Mullen. 2006. Evapotranspiration of two vegetation communities in a high-elevation riparian meadow at Hart Prairie, Arizona. Water Resources Research 42:1–11.

Stark, J. M., and J. M. Norton. 2015. The invasive annual cheatgrass increases nitrogen availability in 24-year-old replicated field plots. Oecologia 177:799–809.

Templer, P. H., M. A. Arthur, G. M. Lovett, and K. C. Weathers. 2007. Plant and soil natural abundance delta (15)N: indicators of relative rates of nitrogen cycling in temperate forest ecosystems. Oecologia 153:399–406.

Venterea, R. T., G. M. Lovett, P. M. Groffman, and P. A. Schwarz. 2003. Landscape patterns of net nitrification in a northern hardwood-conifer forest. Soil Biology and Biochemistry:527–539.

Wine, M. L., and C. B. Zou. 2012. Long-term streamflow relations with riparian gallery forest expansion into tallgrass prairie in the Southern Great Plains, USA. Forest Ecology and Management 266:170–179.

Wu, H., M. Wiesmeier, Q. Yu, M. Steffens, X. Han, and I. Kögel-Knabner. 2012. Labile organic C and N mineralization of soil aggregate size classes in semiarid grasslands as affected by grazing management. Biology and Fertility of Soils 48:305–313.

Yahdjian, L., and O. E. Sala. 2010. Size of precipitation pulses controls nitrogen transformation and losses in an arid Patagonian ecosystem. Ecosystems 13:575–585.

APPENDIX C. CALIBRATION OF STREAM DISCHARGE WITH THE PERSIST MODEL

To explore the influence of riparian evapotranspiration (ET) on the seasonal variation of stream discharge at Font del Regàs, we used the PERSiST model (Precipitation, Evapotranspiration and Runoff Simulator for Solute Transport). The PERSiST model is a conceptual, daily time step, semi-distributed model designed primarily for generating hydrologic inputs for the Integrated Catchments INCA family models (Futter et al. 2013) (http://www.reading.ac.uk/geographyandenvironmentalscience/research/INCA). Among other key model features, the PERSiST model includes the option of differentiating the riparian compartment from the other catchment water pools generating stream runoff. The riparian water fluxes represented in the model are subsurface flow, evapotranspiration, inundation and infiltration (Futter et al. 2013).

We calibrated the PERSiST model for two complete water years (2010-2012) using the time series of precipitation and air temperature obtained at the meteorological station installed within the catchment, and stream discharge measured at the up-, mid- and down-stream sites. The parameterization of both upland and riparian ET was adjusted to obtain values of water demand within the range reported for evergreen oak, beech and riparian forests at Montseny Mountains (Àvila et al. 1996, Llorens and Domingo 2007, Nadal-Sala et al. 2013). Residence water times were estimated empirically by tracer additions similar to Bernal et al. (2004). Other parameters, such as the base flow index or time constant for quick flow, soil flow and groundwater flow were adjusted manually against the peaks of the hydrograph.

To explore whether riparian ET was contributing to the temporal pattern of stream discharge at Font del Regàs along the stream continuum, we considered two scenarios: with and without including the riparian compartment into the model structure. During the two year period, the classic approach of PERSiST model (i.e., without including the riparian compartment) was capable to successfully reproduce the temporal pattern of stream discharge at the three sampling sites as indicated by the high Nash-Sutcliffe (E) coefficients (Table C.1 and Figure 8.4). However, the relative error (RE) associated with the model-data fusion was 30 fold greater for the down- than for the up-stream site, mainly due to mismatches between simulated and measured values during summer low flow conditions (Table C.1 and Figure 8.4). The consideration of the riparian compartment was essential to improve the model-data agreement, especially at the mid- and down-stream sites as indicated by both higher E and lower RE values (Table C.1). In this case, the model captured both the magnitude and seasonal pattern exhibited by

stream discharge even during low discharge periods (Figure 8.4). This first exploration of our hydrological time series with the PERSiST model together with the results obtained in Chapter 5, suggest that riparian ET was shaping the temporal pattern of stream discharge especially in the downstream reaches with well-developed riparian forests.

Table C.1 Nash-Sutcliffe model efficiency coefficient and relative error between observed and simulated stream discharge at the up-, mid- and down-stream sites during the September 2010- August 2012 period.

	Nash-Sutcliffe (E)		**Relative Error (%)**	
	No riparian zone	**Riparian zone**	**No riparian zone**	**Riparian zone**
Up-stream	0.91	0.91	1.17	1.17
Mid-stream	0.92	0.93	-7.23	-0.39
Down-stream	0.87	0.9	-33.69	-5.21

References

Àvila, A., C. Neal, and J. Terradas. 1996. Climate change implications for streamflow and streamwater. Journal of Hydrology 177:99–116.

Bernal, S., A. Butturini, J. L. Riera, E. Vázquez, and F. Sabater. 2004. Calibration of the INCA model in a Mediterranean forested catchment: the effect of hydrological inter-annual variability in an intermittent stream. Hydrology and Earth System Sciences 8:729–741.

Futter, M. N., M. a. Erlandsson, D. Butterfield, P. G. Whitehead, S. K. Oni, and a. J. Wade. 2013. PERSiST: the precipitation, evapotranspiration and runoff simulator for solute transport. Hydrology and Earth System Sciences Discussions 10:8635–8681.

Llorens, P., and F. Domingo. 2007. Rainfall partitioning by vegetation under Mediterranean conditions. A review of studies in Europe. Journal of Hydrology 335:37–54.

Nadal-Sala, D., S. Sabaté, E. Sánchez-Costa, A. Boumghar, and C. A. Gracia. 2013. Different responses to water availability and evaporative demand of four co-occurring riparian tree species in NE Iberian Peninsula. Temporal and spatial sap flow patterns. Acta Horticulturae 991:215–222.

APPENDIX D. PUBLICATIONS OF THE PRESENT DISSERTATION

This Appendix provides the original publications of:

Chapter 4: Lupon, A., S. Gerber, F. Sabater and S. Bernal. 2015. Climate response of the soil nitrogen cycle in three forest types of a headwater Mediterranean catchment, Journal of Geophysical Research – Biogeosciences, 120: 859-875.

Chapter 7: Bernal, S., A. Lupon, M. Ribot, F. Sabater, E. Martí. 2015. Riparian and in-stream controls on nutrient concentrations and fluxes in a headwater forested stream. Biogeosciences 12:1941–1954.

This Appendix also provides the editor acceptance letter of:

Chapter 6: Lupon, A., E. Martí, F. Sabater and S. Bernal. 2015. Green light: Gross primary production influences seasonal stream nitrogen exports by controlling fine-scale nitrogen dynamics, Ecology (in press).

AGU PUBLICATIONS

JGR

Journal of Geophysical Research: Biogeosciences

RESEARCH ARTICLE
10.1002/2014JG002791

Key Points:
- Model-data fusion of N cycle elicits climate response in Mediterranean soils
- Moisture drives soil N cycle in upland forests but not in riparian forest
- Positive effects of warming on soil N cycle may be offset by increased drought

Correspondence to:
A. Lupon,
alupon@ub.edu

Citation:
Lupon, A., S. Gerber, F. Sabater, and S. Bernal (2015), Climate response of the soil nitrogen cycle in three forest types of a headwater Mediterranean catchment, *J. Geophys. Res. Biogeosci.*, *120*, doi:10.1002/2014JG002791.

Received 2 SEP 2014
Accepted 15 MAR 2015
Accepted article online 26 MAR 2015

Climate response of the soil nitrogen cycle in three forest types of a headwater Mediterranean catchment

Anna Lupon[1], Stefan Gerber[2], Francesc Sabater[1], and Susana Bernal[1,3]

[1]Department d'Ecologia, Universitat de Barcelona, Barcelona, Spain, [2]Soil and Water Science Department, University of Florida, Gainesville, Florida, USA, [3]Center of Advanced Studies of Blanes (CEAB-CSIC), Blanes, Spain

Abstract Future changes in climate may affect soil nitrogen (N) transformations, and consequently, plant nutrition and N losses from terrestrial to stream ecosystems. We investigated the response of soil N cycling to changes in soil moisture, soil temperature, and precipitation across three Mediterranean forest types (evergreen oak, beech, and riparian) by fusing a simple process-based model (which included climate modifiers for key soil N processes) with measurements of soil organic N content, mineralization, nitrification, and concentration of ammonium and nitrate. The model describes sources (atmospheric deposition and net N mineralization) and sinks (plant uptake and hydrological losses) of inorganic N from and to the 0–10 cm soil pool as well as net nitrification. For the three forest types, the model successfully recreated the magnitude and temporal pattern of soil N processes and N concentrations (Nash-Sutcliffe coefficient = 0.49–0.96). Changes in soil water availability drove net N mineralization and net nitrification at the oak and beech forests, while temperature and precipitation were the strongest climatic factors for riparian soil N processes. In most cases, net N mineralization and net nitrification showed a different sensitivity to climatic drivers (temperature, soil moisture, and precipitation). Our model suggests that future climate change may have a minimal effect on the soil N cycle of these forests (<10% change in mean annual rates) because positive warming and negative drying effects on the soil N cycle may counterbalance each other.

1. Introduction

Global climate is anticipated to become significantly warmer over the next decades, accompanied with shifts in the water cycle, which in turn can compromise both terrestrial and aquatic nutrient cycles and budgets [*Pendall et al.*, 2008; *Luo et al.*, 2011]. Among other things, climate affects soil nitrogen (N) dynamics through changing soil N mineralization and nitrification rates, influencing plant nutrition and formation of soil organic matter. Furthermore, changes in the terrestrial N cycle could affect N losses from soils to streams and thus influence headwater stream N loads, in-stream N retention, and downstream water quality [*Goodale and Aber*, 2001; *Rogora*, 2007; *Brookshire et al.*, 2009].

Soil moisture, temperature, and precipitation pulses are important drivers of key steps of the soil N cycling [*Miller et al.*, 2007; *Bell et al.*, 2008], although each of these climatic variables may impact differently on the various soil processes. Warming can stimulate soil mineralization and increase soil nutrient availability [*Rustad et al.*, 2001; *Emmett et al.*, 2004], while decreased water availability can reduce mineralization and nutrient availability in the soil pool [*Niboyet et al.*, 2011; *Manzoni et al.*, 2012]. The magnitude of this climatic response is likely ecosystem specific. Cold climate ecosystems tend to be more sensitive to changes in temperature than warmer ecosystems [*Rustad et al.*, 2001; *Dessureault-Rompré et al.*, 2010], while arid ecosystems tend to be more sensitive to increases in soil moisture than mesic ecosystems [*Borken and Matzner*, 2009]. Less clear is the response of soil nutrient cycles to precipitation pulses; yet most of studies suggest that it increases with dryness and substrate availability [*Collins et al.*, 2008; *Borken and Matzner*, 2009].

Furthermore, changes in water availability and temperature can promote shifts in vegetation and drive tree species ranges toward higher elevations in headwater catchments [*Peñuelas and Boada*, 2003; *Colwell et al.*, 2008; *Chen et al.*, 2011]. The impact of species substitution on the soil N cycle and catchment N losses is difficult to assess empirically, and it is largely unknown. Soil organic matter, litter quality, and soil microbial population can vary widely among forest types [*Lovett et al.*, 2004; *Booth et al.*, 2005], and thus, changes in vegetation together with forest type specific responses to climate may both contribute to shifts in N

cycling patterns at the landscape level. Therefore, understanding the response of the soil N cycle to changes in climate in different forest types coexisting within catchments is central for evaluating present and future characteristics of N cycling in these ecosystems, but it still remains a major challenge of ecological research.

Most of studies analyzing the climate sensitivity of the soil N cycle are based on manipulation experiments [*Rustad et al*., 2001; *Borken and Matzner*, 2009]. However, field observations that consider natural climate variability are complementary tools that add to our understanding of how ecosystems work, especially when combined with process-based models that allow to explicitly link the response of biogeochemical processes to climate variability [e.g., *Ise and Moorcroft*, 2006; *Brookshire et al*., 2011]. Another appealing feature of process-based models is that they allow testing the sensitivity of ecosystem processes to specific environmental drivers in isolation and thus provide the opportunity to separate the simultaneous effect of different environmental drivers on biogeochemical processes [*Luo et al*., 2011].

The aim of this study was to investigate the response of soil N cycling to changes in soil moisture, soil temperature, and precipitation across three forest types (evergreen oak, beech, and riparian) that coexist in Mediterranean catchments by using a simple process-based model. To do so, we analyzed a detailed empirical data set of soil N cycling rates from a headwater catchment in the Montseny Mountains Natural Park (NE, Spain) with a simple ad hoc model that represents the interrelated processes of N mineralization, nitrification, and removal of ammonium and nitrate from the soil pool. We hypothesized that the sensitivity of the soil N cycle to climate variables will differ among the three forest types because these forests differ in ecosystem properties (e.g., species composition and C and N stocks) and microclimatic conditions, which both of them are strong drivers of soil N processes. The evergreen oak and beech forests are Mediterranean and cold-temperate ecosystems, respectively, that grow in steep upland areas with poorly developed soils and fast water drainage toward the stream channel [*Peñuelas and Boada*, 2003]. In contrast, riparian forests are settled in flatter and lower areas with stable groundwater tables, higher moisture content, and organic N-rich soils [*Bernal et al*., 2015]. Therefore, we expected that (i) N cycling rates in the oak and beech forests will show strong responses to soil moisture and precipitation compared to the riparian forest because the formers are water-limited ecosystems and (ii) N cycling in the beech forest will be more sensitive to soil temperature than in the oak and riparian forests because beech forests typically grow in colder environments.

Currently, little is known about the combined effect of future changes in temperature and soil water availability on soil N dynamics in seasonally dry forests [*Bai et al*., 2013; *Cameron et al*., 2013]. In scenarios of medium to severe climate change, Mediterranean regions will experience a year-round decrease in soil moisture and increase in temperature and decreased precipitation in summer [*Intergovernmental Panel on Climate Change* (*IPCC*), 2013]. We hypothesized that any positive effect of temperature on the soil N cycle will be reduced by the simultaneous negative effect of dryness, at least in the oak and beech forests, which commonly exhibit severe dry conditions in Mediterranean regions [*Peñuelas and Boada*, 2003]. Further, Mediterranean mountains are experiencing a progressive climate-induced beech-by-oak substitution at medium altitudes (800–1400 m) that may result in a complete replacement by the end of this century [*Peñuelas and Boada*, 2003]. Thus, we additionally considered the hypothesis that this shift in species composition will affect future soil N cycle in these catchments.

2. Materials and Methods

2.1. Study Site and Empirical Data Set

Font del Regàs is a headwater catchment (14.2 km^2) located in the Montseny Natural Park, NE Spain (41°50′N, 2°30′E). The climate is subhumid Mediterranean, with an annual precipitation of 925 ± 151 mm (mean ± standard deviation) and a mean annual temperature of 12.1 ± 2.5°C (values for the period of 1940–2000; Catalan Meteorological Service: http://www.meteo.cat/servmet/index.html). Total inorganic N deposition is ~15 kg N ha^{-1} yr^{-1}, with wet and dry deposition fractions being about equally important (45% versus 55%) [*Àvila et al*., 2009; *Àvila and Rodà*, 2012].

The catchment is dominated by biotitic granite, and its altitude ranges from 300 to 1200 m above sea level [*Institut Cartografic de Catalunya*, 2010]. Evergreen oak (*Quercus ilex*) and beech (*Fagus sylvatica*) forests cover 54% (500–1000 m above sea level (asl)) and 38% (800–1400 m asl) of the catchment, respectively.

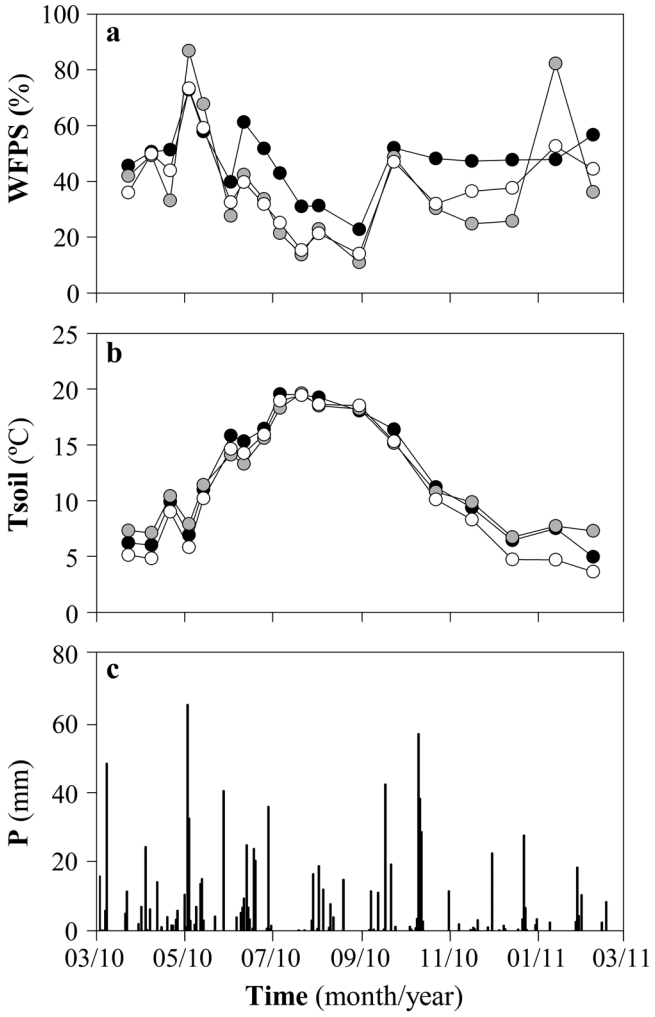

Figure 1. Temporal pattern of (a) soil water-filled pore space (*WFPS*), (b) soil temperature (*Tsoil*), and (c) precipitation (*P*) during the study period. For both *WFPS* and *Tsoil*, mean values for each incubation period are shown for the riparian (black), oak (grey), and beech (white) forest.

Hillslope soils (pH~6) are sandy and have a 3 cm deep organic layer followed by 10 cm deep A horizon. Soil bulk density is 1.40 and 1.35 g cm^{-3} at the oak and beech forests, respectively. The riparian zone covers the remaining 6% of the catchment area, and it consists mainly of alder (*Alnus glutinosa*), black locust (*Robinea pseudoacacia*), ash (*Fraxinus excelsior*), sycamore (*Platanus hydrida*), and poplar (*Populus nigra*). Riparian soils (pH~7) are sandy loam and have a 5 cm deep organic layer followed by a 30 cm deep A horizon. Soil bulk density in the riparian forest is 1.09 g cm^{-3}. During base flow conditions, the riparian groundwater table is located 50 ± 10 cm below the soil surface, and thus, it is disconnected from organic soil layers most of the time.

In order to explore the climatic sensitivity of soil microbial N processes, we took advantage of a preexisting empirical data set of soil N processes and concentrations at the upper soil layer (0–10 cm depth) collected every 2–4 weeks during the period of 2010–2011 (18 sampling dates) at three sites (~1 ha each), one for each dominant forest type (evergreen oak, beech, and riparian). For each forest type, the data set included mean values (from 12 averaged plots, sample size 1 dm^2) of soil organic nitrogen (SON), ammonium (NH_4^+), and nitrate (NO_3^-) concentrations. Moreover, it incorporated mean rates of net N mineralization (NNM) and net nitrification (NN) measured with in situ soil incubations by using the polyethylene bag technique [*Eno*, 1960]. At each sampling date, soil was buried into the soil for 12–15 days and then removed from the soil. The polyethylene bags prevented leaching but allowed temperature and gas exchange, and thus, measured NNM and NN were the net result between either gross N mineralization or gross nitrification and microbial N immobilization and denitrification. In addition, the data set included mean rates of potential NO_3^- losses from the soil pool (PNL, in μg N g $soil^{-1}$ d^{-1}) measured with ion exchange resins, which were buried into the soil close to each polyethylene bag during each incubation period (which started at each sampling date). The NO_3^- content in resin bags was used as a proxy of NO_3^- leaching, infiltration, and uptake expressed as N content per bag weight [*Lovett et al*., 2004; *Berger et al*., 2009]. Following *Berger et al*. [2009], we expressed resin bags data as N content per soil weight by taking into account the bag volume and the soil bulk density. Although this is a rough transformation, it is useful for our purposes because it allows comparing PNL to other soil N processing rates.

The data set further included environmental variables such as mean values of soil moisture (expressed as water-filled pore space (*WFPS*)) and soil temperature (*Tsoil*) for each sampling date and forest type

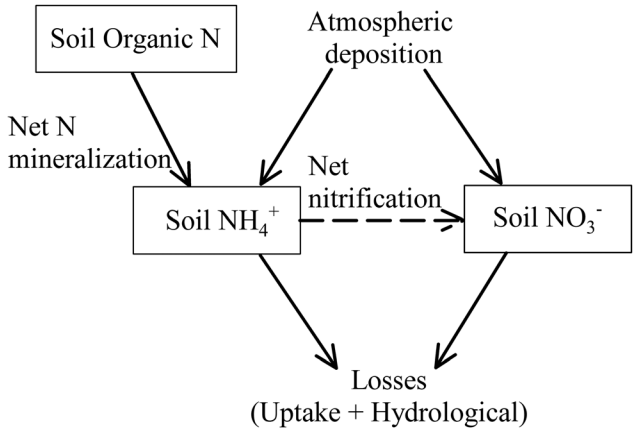

Figure 2. The model presented here concerns soil inorganic nitrogen (N) at the upper soil layer (0–10 cm) and the fluxes into and out of this pool (solid arrows). Inputs of soil inorganic N pool are atmospheric deposition and net N mineralization from soil organic matter. The proportion of ammonium (NH_4^+) and nitrate (NO_3^-) in the soil depends on net nitrification (dashed line). Outputs from the soil inorganic N pool are plant and microbial uptake (uptake) and infiltration and leaching (hydrological losses).

(Figures 1a and 1b). *WFPS* was calculated from soil volumetric moisture content measured at 10 cm depth (four replicates per plot) with a time domain reflectometry sensor (HH2 Delta-T Devices Moisture Meter). *Tsoil* was recorded at 10 cm depth (two replicates per plot) by using a temperature sensor (CRISON 25). In addition, we recorded daily precipitation (*P*), which showed the expected seasonal pattern for this region with higher values in spring than in summer and winter (Figure 1c). More details can be found in A. Lupon et al., Contribution of pulses of soil nitrogen mineralization and nitrification to soil nitrogen availability in three Mediterranean forests, *European Journal of Soil Sicence*, in review (2015).

2.2. Model Development and Climatic Modifiers

We developed an ad hoc ecosystem model similar to *Brookshire et al*. [2011] to evaluate soil N dynamics at the upper soil layer (0–10 cm) over time (Figure 2). This model describes sources and sinks of soil inorganic N and therefore incorporates key mechanisms to link the different measured variables. In our model, inorganic N enters to the system from atmospheric deposition (D_{NH4} and D_{NO3}, in $\mu g\,N\,g\,soil^{-1}\,d^{-1}$) and net N mineralization (NNM, in $\mu g\,N\,g\,soil^{-1}\,d^{-1}$), which depends on the amount of soil organic N (SON, in $\mu g\,N\,g\,soil^{-1}$). In turn, inorganic N losses are plant and microbial uptake (U_{NH4} and U_{NO3}, in $\mu g\,N\,g\,soil^{-1}\,d^{-1}$) and hydrological leaching (H_{NH4} and H_{NO3}, in $\mu g\,N\,g\,soil^{-1}\,d^{-1}$). Simulated concentrations of both ammonium (NH_4^+) and nitrate (NO_3^-) (in $\mu g\,N\,g\,soil^{-1}$) change over time as a result of changes in input and output fluxes of inorganic N to and from the soil pool, and as a consequence of net nitrification (NN, in $\mu g\,N\,g\,soil^{-1}\,d^{-1}$), which transforms NH_4^+ to NO_3^-. For each forest type, changes of soil N concentration over time were described as

$$dNH_4/dt = SON \times k_{NNM} + D_{NH4} - NH_4 \times k_{NN} - NH_4 \times k_{UNH4} - NH_4 \times k_{HNH4} \quad (1)$$

$$dNO_3/dt = NH_4 \times k_{NN} + D_{NO3} - NO_3 \times k_{UNO3} - NO_3 \times k_{HNO3} \quad (2)$$

where k_{NNM} is the first-order rate for net N mineralization, k_{NN} is the rate for net nitrification, and k_U and k_H are the first-order rates of NH_4^+ and NO_3^- biological uptake and hydrological losses, respectively (all rates in d^{-1}). Following *Brookshire et al*. [2011], the model assumed that plants are N limited, and thus, plant uptake was scaled to available N. In our case, this assumption can be justified by the strong N limitation usually reported in these Mediterranean forests [*Àvila and Rodà*, 2012]. Note that our model considers biological uptake and hydrological losses separately; however, disentangling these two processes is difficult as we do not have independent empirical data to constrain each of them. Thus, we considered that the assumption of N limitation is adequate if there is a fast turnover of mineral N and strong sink strength (high values of $k_U + k_H$) for the inorganic N pool, NH_4^+, and NO_3^-. Finally, the possible nitrogen fixed by symbionts in riparian tree roots is often directly incorporated into biota, and thus, it is implicit in the model in the form of SON mineralization. As such, higher levels of SON and N mineralization in the riparian forest (see below) may be at least partly attributable to N_2 fixation.

We assumed that SON was invariant over time, because soil organic matter changes relatively slowly compared to soil N fluxes and inorganic N concentrations [*Lawrence et al*., 2000]. Our empirical data set supports this assumption because the variation of soil organic matter content and soil C:N ratios (CV < 15%) was consistently lower than the variation of soil microbial processes (CV~50–200%) for the three forests

(Lupon et al., in review, 2015). Based on available data of soil N content at Font del Regàs soils, SON in the model was fixed to 120, 54, and 60 μg N g soil^{-1} for the riparian, oak, and beech forests, respectively.

D_{NH4} and D_{NO3} were calculated as the sum of wet and dry deposition values for each day by assuming constant dry and wet deposition over time. We used published values of annual N deposition at the Montseny Mountains as a reference (dry deposition values are 4.12 and 4.04 kg N ha^{-1} yr^{-1} and wet deposition value is 3.36 kg N ha^{-1} yr^{-1} for NH_4^+ and NO_3^-, respectively) [*Àvila et al*., 2009; *Àvila and Rodà*, 2012]. Deposition rates were divided by soil depth (in cm) and bulk density (in g cm^{-3}) to obtain deposition values per soil weight (μg N g soil^{-1} d^{-1}).

Finally, we approximated soil concentrations of NH_4^+ and NO_3^- to be in equilibrium with respect to environmental drivers and inputs from mineralization and deposition. This assumption is based on the observation that turnover times of mineral forms of N in soils are fast (approximately 1 day) and thus equilibrate rapidly compared to changes in the driving variables [*Stark and Hart*, 1997; *Gerber and Brookshire*, 2014]. For each forest type, we estimated inorganic N concentrations in the soil as (equations (1) and (2) equal 0)

$$NH_4 = (SON \times k_{NNM} + D_{NH4})/(k_{UNH4} + k_{HNH4} + k_{NN}) \quad (3)$$

$$NO_3 = (NH_4 \times k_{NN} + D_{NO3})/(k_{UNO3} + k_{HNO3}) \quad (4)$$

Most of existing models have formulated climate dependency of soil N processes [*Raich et al*., 1991; *Rastetter et al*., 1997; *Brookshire et al*., 2011]. Here the first-order rates k_{NNM}, k_{NN}, k_U, and k_H for each forest type were multiplied by factors that parameterize soil moisture (r_θ and r'_θ), soil temperature (r_T), and precipitation (r_P) [*Raich et al*., 1991; *Brookshire et al*., 2011], such that

$$k_n = k_{0,n} \times r_{\theta,n} \times r_{T,n} \times r_{P,n} \quad (5)$$

where k_n is the first-order rate for the process n (n = NNM, NN, uptake, or leaching); $k_{0,n}$ is a constant base rate; and $r_{\theta,n}$, $r_{T,n}$, and $r_{P,n}$ are the moisture, temperature, and rainfall modifier for each process.

The moisture modifier (r_θ) was used as a proxy of the effect of soil water availability on k_{NNM} and k_{NN}, and thus, it relies on the combined effect of precipitation, evapotranspiration, and groundwater level. Following *Brookshire et al*. [2011], r_θ was parameterized as a Gaussian function for both NNM and NN mimicking moisture limitation at low soil moisture levels and possible oxygen limitation at high levels of soil wetness. Yet rather than inferring soil moisture from stream discharge time series as in *Brookshire et al*. [2011], we calculated r_θ from empirically measured values of *WFPS* with

$$r_\theta = 1/\sigma\sqrt{2\pi} \times \exp^{-(WFPS-\mu)^2/2\sigma^2} \quad (6)$$

where *WFPS* is the water-filled pore space in percent measured at the beginning of each incubation period, μ is a parameter indicating the optimal *WFPS* value for each soil N process, and σ is a parameter that indicates the sensitivity to changes in *WFPS* of each process. Values of μ close to 0 imply an overall negative effect of soil moisture on soil N processes, whereas values close to 100 indicate that soil N processes may be limited by low soil wetness for the measured moisture range. In turn, values of σ close to 0 indicate a narrow range of moisture conditions under which a given soil N process occurs, whereas large values (up to 100) indicate little sensitivity to soil moisture. r_θ is assumed to be 1 for k_U.

The rate of hydrological N losses, k_H, was modified by using a potential function to simulate an increase in leaching and infiltration during high soil moisture conditions:

$$r'_\theta = WFPS^x \quad (7)$$

where x is the exponent representing soil moisture sensitivity. The r'_θ replaces r_θ in equation (5). Values of x close to 0 indicate that hydrological N losses do not depend on soil moisture, whereas larger values (>0.5) indicate that leaching and infiltration increase substantially during wet periods.

We used a Q_{10} function to estimate the temperature dependence (r_T) for k_{NNM}, k_{NN}, and k_U:

$$r_T = Q_{10}^{(Tsoil - \overline{Tsoil})/10} \quad (8)$$

where *Tsoil* is the average of the soil temperature measured empirically at the beginning and at the end of each incubation period, $\overline{Tsoil}$ is the mean annual soil temperature, and Q_{10} is the factor by which soil N

processes are multiplied when temperature increases by 10°C. Typically, Q_{10} values are close to 2, and thus, deviation of Q_{10} values indicates either oversensitivity or undersensitivity of soil N processes to temperature [*Emmett et al.*, 2004]. The r_T is assumed to be 1 for k_H.

We further explored the influence of hydrological conditions on k_{NNM} and k_{NN}, by considering a precipitation modifier (r_P), that was used to consider the typical pulse behavior reported for microbial activity during rewetting in Mediterranean systems [*Borken and Matzner*, 2009]. The r_P was parameterized as a linear function for both NNM and NN, because empirical soil N processes increased linearly with precipitation in our data set:

$$r_P = a \times P + b \tag{9}$$

where P is the precipitation accumulated during 24 h before each incubation period, a is the slope representing precipitation sensitivity, and b is the modifier value if no precipitation occurs. Large values of a indicate that soil N processing rates sharply increase after precipitation, whereas a values close to 0 indicate that precipitation affects soil N processes only marginally. In turn, b can be interpreted as the baseline rate in absence of any precipitation pulse in the system. The r_P is assumed to be 1 for k_H and k_U.

2.3. Model Analysis

The model was fitted to empirical observations obtained at the study site using maximum-likelihood estimation [*Edwards*, 1992]. According to the present SON and climate data (year 2010), we optimized the parameter set for obtaining the best possible fit between simulated and observed values for NNM, NN, and between simulated NO_3^- sinks (uptake + hydrological losses) and empirical PNL on the timeframe of the 18 incubation periods (12 months).

The likelihood (L) for the processes (j) in each incubation period (i) was calculated as follows:

$$L_{(j,i)} = \frac{d_{j,i}^{a_j-1}}{b^{a_j}\Gamma(a_j)} \exp\left(\frac{d_{j,i}}{b_j}\right) \tag{10}$$

where a_j and b_j are the parameters for the gamma function (Γ), which allow for nonnormal error distribution [*Ise and Moorcroft*, 2006]. The $d_{j,i}$ is the absolute difference between the simulated and the observed values of each process (i.e., NNM, NN, and PNL) for each incubation period ($n = 18$) ($\left| j_i^{\text{modeled}} - j_i^{\text{observed}} \right|$). The best model fit is achieved when the sum of the log-transformed likelihoods ($l = \Sigma(\log(L_{j,i}))$ is maximized. To estimate model and gamma distribution parameters for optimization, we used GNU Octave functions *bfgsmin* and *gamfit*, respectively. Since optimization procedure with GNU Octave depends on the first guess of the parameters, we performed a Monte Carlo simulation with 500 random draws, where the first guess was randomly chosen within a large a priori range for the whole suite of parameters (k_n: from 10^{-6} to 100 d^{-1}; σ, μ: from 10^{-6} to 100%; x: from 0 to 1; Q_{10}: from 10^{-6} to 5; and a,b: from 0 to 1).

To investigate the sensitivity of NNM and NN to climate factors at each forest type, base models that included all climatic modifiers were compared with reduced versions, which discount the effect of moisture, temperature, or precipitation by setting the relevant modifiers to 1. To quantitatively compare these nested model versions, we used Akaike information criterion (AIC) [*Akaike*, 1974], where $AIC = 2p - 2l$, with p being the number of parameters and l is the sum of the log-transformed likelihoods (see above). Following *Burnham and Anderson* [2002], we considered that the nested model with minimum AIC was the best one, that is the simplest model minimizing the loss of information. In order to compare the nested models against each other, we rescaled the AIC value ($\Delta_m = AIC_m - AIC_{best}$, where the subscripts m and *best* denote a particular and the best model, respectively) and calculated the relative likelihood ($L_r = L_m/L_{best}$, with L_m and L_{best} being the product of the likelihoods across variables and incubation periods; equation (10)) to assess which climatic modifier contributed the most to the best fit of the temporal pattern of either NNM or NN for each forest type [*Burnham and Anderson*, 2002]. Large values of Δ_m and small values of L_r indicate that the nested model lost significant information relative to the best model, and thus, it can be interpreted that the discounted climatic variable was a major driver of the temporal dynamics of the soil N cycle.

In order to understand the predictive power of our model, we explored the uncertainty of the parameters by assuming that the more curved the likelihood function is, the more certainty we have that we have estimated

the right parameter [*Burnham and Anderson*, 2002]. The standard error (S) of each parameter (p_i) was calculated as follows:

$$s(p_i) = \sqrt{\left[\frac{\partial^2 L}{dp_i^2}\right]^{-1}} \tag{11}$$

where L again is the product of the likelihoods across incubation periods and variables. Since the analytical form of the likelihood function (L) is not known, we estimated the second derivative by perturbing each parameter by an arbitrary ± 10% to obtain slopes around the maximum likelihood.

Further, we evaluated the goodness of fit between empirical and simulated values of NNM and NN and between empirical PNL and simulated NO_3^- losses (uptake + hydrological) with the Nash-Sutcliffe model efficiency coefficient (E):

$$E = 1 - \frac{\sum_{i=1}^{n}(O_i - M_i)^2}{\sum_{i=1}^{n}(O_i - \overline{O})^2} \tag{12}$$

where O_i is the empirical value of a particular process at the incubation period i, M_i is the simulated value, and $\overline{O}$ is the mean empirical value over the entire period of length n. The E coefficient is an important determinant of the predictive power of biogeochemical models [*Moriasi et al*., 2007]. An $E = 1$ corresponds to a perfect match of simulated to observed data, whereas an $E = 0$ indicates that the simple mean of the data has the same predictive power as the model. Finally, we validated the performance of our model by comparing an independent empirical data set of soil inorganic N concentrations with simulated values. We used mean seasonal concentrations for both NH_4^+ and NO_3^- because soil N concentrations were empirically measured at the beginning of each incubation period, while our model simulated mean soil N concentration between sampling dates (average of 15 days of incubation).

2.4. Climate Change Scenarios

In order to understand how climate change may affect soil N dynamics in Mediterranean forests, we calculated future soil N dynamics given the predicted changes in climate for the period of 2081–2100. We assumed that climatic conditions during the study period (2010–2011) were representative for the period of 1986–2005 because they fall within the annual precipitation and temperature long-term average. We based our simulations on the Representative Concentration Pathway 4.5 (RCP4.5) projections for Mediterranean zones [*IPCC*, 2013], which reported a mean annual decrease in soil moisture of 0.8 mm at 10 cm depth, and an increase in air temperature of 1.25 °C and 2.5 °C from December to May and from June to November, respectively. We considered that soil moisture will decrease equally in the three forest types because we cannot reliably estimate future effects of groundwater level on soil moisture at the riparian site. In turn, we constructed future *Tsoil* based on the air temperature Intergovernmental Panel on Climate Change (IPCC) projections and then, we inferred *Tsoil* values from the linear regression between observed mean daily air and soil temperature during the study period ($R^2 > 0.90$, $n = 18$). According to RCP4.5 projections, future precipitation may not significantly differ from today for winter time (October–March) and may decrease 5% during summer (April–September). Finally, we considered that atmospheric N deposition would not change in the future as both empirical and modeling studies indicate no significant trend for this region [*Àvila and Rodà,* 2012; *Lamarque et al*., 2013].

Our model is not able of addressing the larger plant-soil cycle, and we therefore do not have the means to predict future levels of soil organic matter and mineralization per se. We therefore developed two scenarios which bracket potential alterations of the plant-soil cycle. In our first scenario (i.e., transition), we assumed that due to climate change, the terrestrial N cycle would be in transition toward a future equilibrium, and thus, the SON stock would be similar to the present stock. This transition scenario can be justified by the small temporal variation of soil organic matter stocks over time [*Lawrence et al*., 2000]. In our second scenario (i.e., equilibrium), we assumed that the terrestrial N cycle would be in equilibrium with the new climate regime, and thus, mean annual NNM rate would revert to present mean rates, provided that overall productivity does not change. Clearly, these assumptions are afflicted with uncertainty, but the two scenarios (transition and equilibrium) help bracket the effects from rapid and long-term adjustments of the N cycle to climate change.

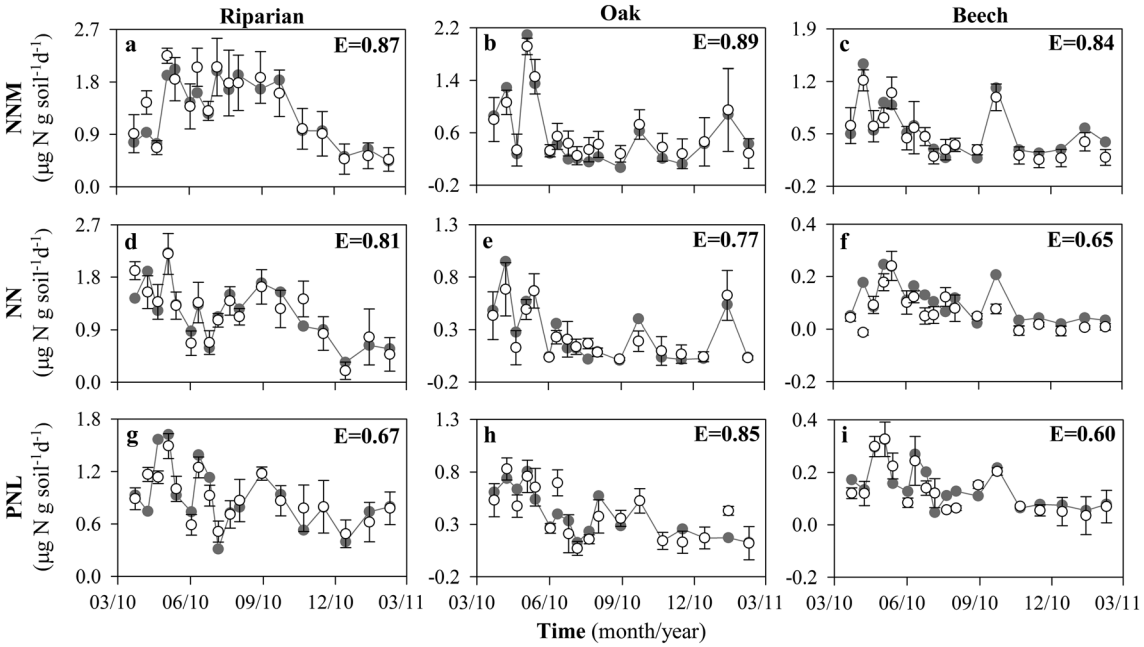

Figure 3. (a–c) Net N mineralization (NNM), (d–f) net nitrification (NN), and (g–i) potential nitrate losses (PNL) at the (left) riparian, (middle) oak, and (right) beech forests. Circles are mean values of measured soil N processing rates, and error bars standard deviations. Gray circles are simulated values. The Nash-Sutcliffe model efficiency coefficient (*E*) is shown in each panel.

To understand how climate-induced changes in vegetation may affect future soil N budgets and soil N export, we compared the contribution of soil N dynamics of each forest to the overall catchment response according to the areal extent of each forest type for both the present and expected future scenario. Based on *Peñuelas and Boada* [2003], we considered complete beech-by-oak substitution by the end of this century and that future riparian forest area remains the same.

Future scenarios were based on the same 18 incubation periods as the present-day simulations but with adjusted soil organic N concentrations and climate drivers. In order to compare present and future soil N dynamics among forests, we estimated mean daily rates of both soil N processing rates and soil inorganic N concentrations. The average rates of the simulated soil N dynamics allowed us to explore the central tendency of soil N cycling. We multiplied daily soil N processing rates and mean soil inorganic N concentrations by soil bulk density (in g cm^{-3}) and soil depth (in cm) to obtain areal estimates. We then aggregated the areal values into annual averages and multiplied simulated mean annual soil N processing rates and NO_3^- concentrations of each forest type (and taking into account the changing extent of forest types in the beech-by-oak substitution scenario).

3. Results

3.1. Data-Model Fusion and Model Evaluation

The empirical data set showed substantial differences in mean daily rates of soil N processing and PNL among forests. At the oak and beech forests, mean daily rates of NNM (0.625 and 0.495 μg N g $soil^{-1}$ d^{-1}), NN (0.240 and 0.067 μg N g $soil^{-1}$ d^{-1}), and PNL (0.383 and 0.135 μg N g $soil^{-1}$ d^{-1}) were low compared to rates measured at the riparian forest (1.352, 1.178, and 0.892 μg N g $soil^{-1}$ d^{-1} for NNM, NN, and PNL, respectively). Moreover, the oak and beech forests showed minimum soil N processing rates in summer, contrasting with the high rates measured at the riparian forest (Figure 3). Consideration of climatic modifiers was essential to model-data agreement (Table 1), which allowed the model to capture both the magnitude and the seasonal pattern exhibited by NNM, NN, and PNL for the three forest types as indicated by the high Nash-Sutcliffe (*E*) coefficients (Figure 3).

Table 1. Akaike Index Criterion (AIC), Distance Between AIC_m and AIC_{best} (Δ_m), and Model Likelihood (L_m) for the Best Model (Best), the Null Model (No Climate Sensitivity, Null), the Base Model Including the Three Climatic Modifiers (Base), and the Reduced Versions of the Base Model With No Sensitivity to Moisture ($r_\theta = 1$), Temperature ($r_T = 1$), or Precipitation ($r_P = 1$) for Net N Mineralization (NNM) and Net Nitrification (NN)[a]

	Riparian			Oak			Beech		
Model	AIC	Δ_m	L_m	AIC	Δ_m	L_m	AIC	Δ_m	L_m
Best	20.25	0.000	1.000	41.908	0.000	1.000	−17.896	0.000	1.000
Null	41.989	21.742	$<10^{-3}$	49.304	7.396	0.025	−0.844	17.052	$<10^{-3}$
Base model	28.670	8.423	0.015	41.908	0.000	1.000	−17.896	0.000	1.000
Base − r_θ NNM	24.904	4.657	0.097	60.319	18.411	$<10^{-3}$	4.125	22.021	$<10^{-3}$
Base − r_T NNM	52.653	32.406	$<10^{-3}$	50.860	8.952	0.011	−4.847	13.049	0.001
Base − r_P NNM	43.342	23.095	$<10^{-3}$	57.114	15.206	$<10^{-3}$	−5.306	12.590	0.002
Base − r_θ NN	25.343	5.096	0.078	50.842	8.934	0.011	−11.666	6.230	0.044
Base − r_T NN	36.721	16.474	$<10^{-3}$	47.952	6.044	0.049	−7.472	10.424	0.005
Base − r_P NN	49.048	28.801	$<10^{-3}$	45.450	3.542	0.170	−7.410	10.486	0.005

[a]Data are shown separately for each forest type.

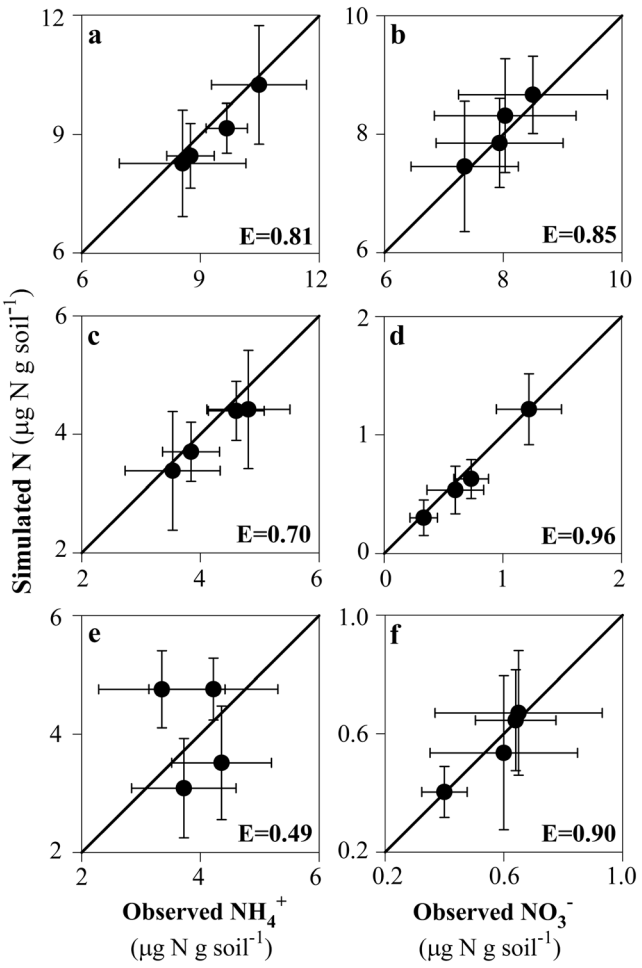

Figure 4. Relationship between observed and simulated soil nitrogen concentrations in the (a and b) riparian, (c and d) oak, and (e and f) beech forests. (left) Ammonium (NH_4^+) and (right) nitrate (NO_3^-) concentrations, respectively, are shown. Circles are mean seasonal concentrations, and error bars show the standard deviation. The 1:1 relation and the Nash-Sutcliffe model efficiency coefficient (E) are shown in each panel.

The good fit obtained through the data-model fusion was corroborated by the model validation process: simulated and independently measured soil inorganic N concentrations across seasons and forests yielded a high E, except for NH_4^+ at the beech site (Figure 4). In all forests, simulated mean daily concentrations differed from empirical data <10% and <5% for NH_4^+ and NO_3^-, respectively.

We calculated mean first-order rates ($\overline{k_n}$) by averaging each k_n over the 18 incubation periods (Tables 2 and 3). The model-data analysis yielded distinct mean first-order rates for NNM ($\overline{k}_{NNM}$) and NN ($\overline{k}_{NN}$), being tenfold lower for the former than for the latter. Mean $\overline{k}_{NNM}$ and $\overline{k}_{NN}$ were 40–60% lower at the beech than at the oak and riparian forests (Table 2). Mean NO_3^- removal rates from the mineral pool ($\overline{k}_U + \overline{k}_H$) showed small differences among forests and were threefold to fivefold higher than those for NH_4^+ (Table 3). In turn, mean $\overline{k}_U + \overline{k}_H$ for NH_4^+ were 15% higher for the beech than for the riparian and oak forests, indicating that NH_4^+ was more efficiently removed from the soil pool at the former than at the latter (Table 3).

3.2. Climate Sensitivity of Soil N Processes

The AIC model evaluation indicated that climatic modifiers contributed

Table 2. Best Fit Model Parameters of Soil Moisture Sensitivity (μ, σ), Temperature Sensitivity (Q_{10}), Precipitation Sensitivity (a, b), and Mean First-Order Rates ($\bar{k}$) for Net N Mineralization (NNM) and Net Nitrification (NN) for Each Forest Type[a]

	Riparian		Oak		Beech	
	NNM	NN	NNM	NN	NNM	NN
Moisture						
μ (%)	-	-	100 ± 7	72 ± 5	66 ± 4	100 ± 5
σ (%)	-	-	62 ± 13	21 ± 11	25 ± 5	37 ± 8
Temperature						
Q_{10}	2.9 ± 0.3	1.7 ± 0.1	1.6 ± 0.4	2.3 ± 0.3	1.7 ± 0.3	2.9 ± 0.3
Precipitation						
a	0.05 ± 0.01	0.10 ± 0.01	0.01 ± 0.01	0.07 ± 0.02	0.01 ± 0.01	0.05 ± 0.01
b	0.92 ± 0.58	0.94 ± 0.1	0.45 ± 0.32	0.81 ± 1.00	0.56 ± 0.34	0.80 ± 0.1
Constants						
$\bar{k}$ (d^{-1})	0.011 ± 0.007	0.114 ± 0.058	0.012 ± 0.009	0.121 ± 0.024	0.008 ± 0.006	0.077 ± 0.021

[a]Data are average ± standard deviation.

significantly to improve the model fitness (Table 1). For the oak and beech forests, the best fit models required all three climatic modifiers (r_θ, r_T, and r_P). However, inclusion of soil moisture did not improve riparian NNM and NN to pass the AIC test. We tested the effect of individual climate modifiers by omitting one at a time from the all-inclusive base model (Table 1). The optimization of climatic modifiers generally yielded a bigger effect on likelihood estimation (i.e., higher values of Δ_m and lower values of L_m) for NNM than for NN, likely because model errors in NNM propagated into NN. For the riparian forest model, r_T had the strongest effect on NNM, while r_P was the most important environmental driver for NN. For the oak forest, the fitness of the model notably decreased when we excluded r_θ for both NNM and NN, whereas the effect of r_P on NN rates was small. For the beech forest model, r_θ was the dominant driver for NNM, whereas r_T and r_P were critical to improve NN.

In Figure 5, we illustrate the sensitivity of each rate to individual climate variables. The model analysis revealed that the response of soil N processes to changes in *WFPS* differed between NNM and NN as well as among forest types (Table 2). The lack of response of riparian soil N processes to soil moisture contrasted with the pattern exhibited by both NNM and NN at the oak and beech forests, which were sensitive to a narrow range of moisture conditions ($\sigma < 40$) in most cases (Table 2). The model-data fusion yielded a sustained increase in oak NNM and beech NN for the whole range of *WFPS* values. In contrast, oak NN and beech NNM showed a strong reduction at *WFPS* < 20% and at *WFPS* > 66% and >75%, respectively. Yet there were only few data points at *WFPS* < 20% and >60% (Table 2 and Figure 5a). Soil moisture had a positive effect on hydrological losses, being higher for NO_3^- ($x > 0.5$) than for NH_4^+ ($x < 0.05$) (Table 3).

The results indicate distinct temperature sensitivity among processes and forest types, being the highest for riparian NNM and for beech NN, which showed a $Q_{10} = 2.9$ (Table 2). For the oak and beech forests, NN ($Q_{10} > 2$)

Table 3. Best Fit Model Parameters of Soil Moisture Sensitivity (x), Temperature Sensitivity (Q_{10}), and Mean First-Order Rates of N Losses From the Soil Pool ($\bar{k}_U + \bar{k}_H$) for Both Ammonium (NH_4^+) and Nitrate (NO_3^-) for Each Forest[a]

	Riparian		Oak		Beech	
	NH_4^+	NO_3^-	NH_4^+	NO_3^-	NH_4^+	NO_3^-
Moisture						
x	0.01 ± 0.02	0.71 ± 0.4	0.05 ± 0.07	0.80 ± 0.5	0.05 ± 0.04	0.62 ± 0.5
Temperature						
Q_{10}	1.9 ± 0.4	2.5 ± 0.5	1.8 ± 0.4	1.5 ± 0.4	1.5 ± 0.4	1.8 ± 0.3
Constants						
$\bar{k}_U + \bar{k}_H$ (d^{-1})	0.049 ± 0.013	0.223 ± 0.065	0.054 ± 0.022	0.248 ± 0.104	0.059 ± 0.029	0.209 ± 0.072

[a]N losses are the sum of mean rates of biological uptake and hydrological losses. Data are average ± standard deviation.

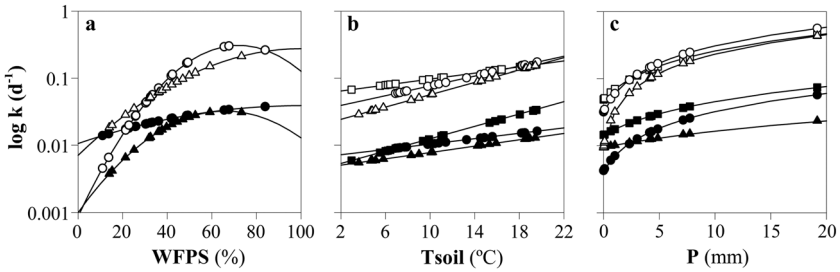

Figure 5. Sensitivity of first-order rates (k_n) for net mineralization (black) and net nitrification (white) to (a) soil moisture (*WFPS*), (b) soil temperature (*Tsoil*), and (c) precipitation (*P*) at the riparian (squares), oak (circles), and beech (triangles) forests. Symbols are data for each incubation period, and lines represent the considered function (Gaussian, Q_{10}, and linear for moisture, temperature, and precipitation, respectively). Note that first-order rates are log transformed. The response of k_n to changes in a particular climatic variable was examined by setting the value of the other two climatic variables to its mean. For example, in Figure 5a, *Tsoil* and *P* equaled the average of the 18 sampling dates.

was more sensitive to changes in temperature than NNM ($Q_{10} < 2$), whereas Q_{10} values for NN and NNM showed the opposite pattern at the riparian forest (Table 2 and slope in Figure 5b). The model fit also suggested a stronger effect of temperature on NO_3^- uptake by biota at the riparian forest ($Q_{10} = 2.5$) compared to the oak and beech forests (Q_{10}~1.8) (Table 3).

Pulses of precipitation had a larger influence on microbial activity at the three forest types but especially for NN at the riparian and oak forests (slope $a > 0.07$) (Table 2 and Figure 5c). Both oak and beech NNM appeared to be little responsive to rewetting events (slope $a = 0.01$) (Table 2). Responses of NNM and NN to rewetting were relatively high at the riparian forest compare to upland forests (Figure 5c).

3.3. Soil N Dynamics Under Climate Change Scenarios

The application of our model projections of soil N dynamics for the period of 2081–2100 revealed a distinct change for NNM and NN because each soil N process showed a different moisture and temperature sensitivity at each forest type. In the transition scenario, where we held SON constant (see Method section), changes in mean daily NNM rates were small but differed among forest types (+8%, −12%, and −8% for the riparian, oak, and beech forests, respectively) (Table 4). Changes in mean daily NN rates were similar or even smaller than for NNM (+6%, −8%, and −8% for the riparian, oak, and beech forests, respectively). While all forest types experienced the positive effect of warming, the negative effect of drying on soil transformation rates offsets the positive effect of temperature in the two upland forest types. In the equilibrium scenario, where mean NNM rates revert to the present value, the response of NN to climate change became diminishingly small for all forest types (+2%, −4%, and −1% for the

Table 4. Simulated Mean Annual Rates of Net N Mineralization (NNM), Net Nitrification (NN), and Soil Nitrate Concentration (NO_3) for the Present Climate, the Transition Phase (Increased Mean NNM), and the Future Equilibrium (Mean NNM Reverts to Present Value) Scenarios[a]

	Riparian	Oak	Beech
NNM ($\mu g\ N\ g\ soil^{-1}\ d^{-1}$)			
Present	1.311 ± 0.460	0.596 ± 0.531	0.502 ± 0.374
Transition	1.421 ± 0.552	0.526 ± 0.633	0.462 ± 0.459
Equilibrium	1.311 ± 0.460	0.596 ± 0.531	0.502 ± 0.374
NN ($\mu g\ N\ g\ soil^{-1}\ d^{-1}$)			
Present	1.188 ± 0.458	0.264 ± 0.496	0.074 ± 0.242
Transition	1.268 ± 0.476	0.244 ± 0.530	0.068 ± 0.295
Equilibrium	1.208 ± 0.503	0.254 ± 0.586	0.073 ± 0.310
NO_3 ($\mu g\ N\ g\ soil^{-1}$)			
Present	8.10 ± 3.19	0.90 ± 1.66	0.60 ± 1.05
Transition	8.50 ± 3.54	0.80 ± 1.55	0.57 ± 1.10
Equilibrium	8.21 ± 3.85	0.81 ± 1.40	0.58 ± 1.04

[a]Data are shown as average ± standard deviation for each forest type.

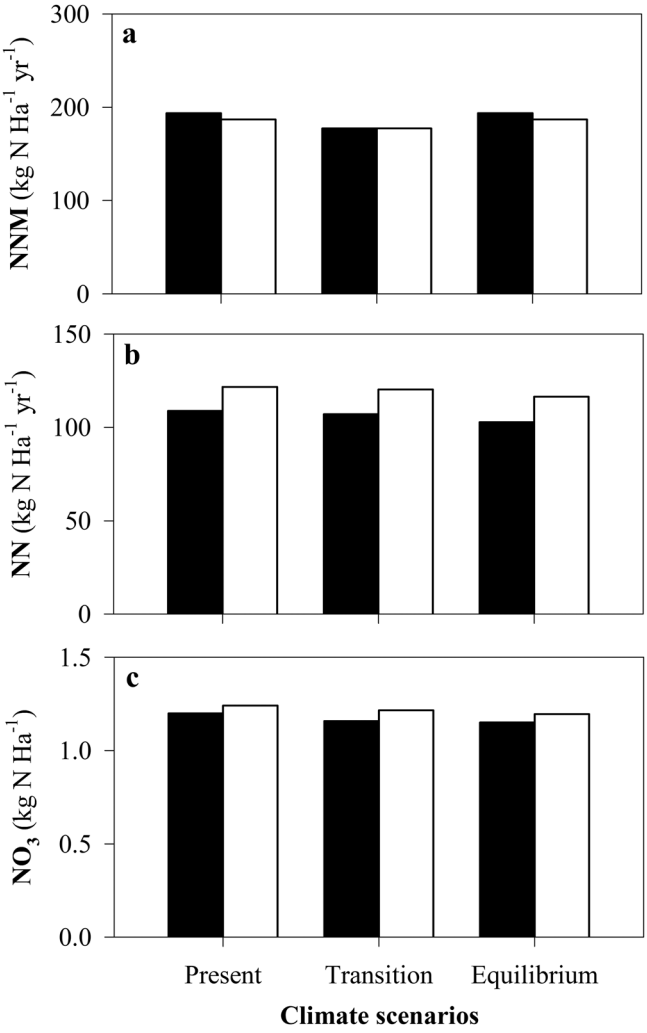

Figure 6. Simulated mean annual (a) net nitrogen mineralization (NNM), (b) net nitrification (NN), and (c) soil nitrate concentration (NO_3) in Font del Regàs catchment for the present climate, the transition phase (increased mean NNM), and the future equilibrium (mean NNM reverts to present value). Two vegetation cover scenarios were considered: present tree species composition (black) and a complete beech-by-oak substitution (white).

riparian, oak, and beech forests, respectively). In accordance with change in NNM and NN, simulated soil NO_3^- concentration slightly increased by +5% (transition) and +1% (equilibrium) in the riparian forest, while it declined by −11% and −4% at the oak and beech forests, respectively (Table 4).

At the catchment scale, our model projections indicated that the expected changes in climate could induce relatively small decreases in mean annual rates of NNM (−8%) and NN (−5%) and minimal changes in the soil NO_3^- pool (−4%) (black bars in Figure 6). This reduction is mainly caused by the negative effect of dryness in the upland forests. According to our model results, the beech-by-oak substitution expected by the end of this century could lead to small decreases in mean annual NNM (−4%) but could increase mean annual NN by +13%. As a result, modeled soil NO_3^- concentration increased slightly (+5%; white bars in Figure 6). The changes in NN and soil NO_3^- concentrations caused by this species substitution were similar for both the transition and the equilibrium scenarios.

4. Discussion

4.1. Data-Model Fusion

This study aimed to understand the impact of climate drivers on crucial steps in the N cycle, which are mineralization, nitrification, and removal of bioavailable N (NO_3^- and NH_4^+). To this end, we fused empirical data with a simple mechanistic model of the soil N cycle to evaluate and quantify the sensitivities of Mediterranean forest ecosystems to different environmental drivers simultaneously. Our framework recreated the temporal variation in soil NO_3^- and NH_4^+ concentrations over the course of a year in three forest types. The consideration of climatic modifiers into the model improved the goodness of fit between simulated and empirical data for NNM, NN, and PNL during most of the year, which support the idea that environmental variables are crucial to understand the seasonal behavior of soil N cycling [*Miller et al.*, 2007; *Bell et al.*, 2008]. Further, the good fit between simulated and empirical data indicates that our model was able to capture the net result of the main processes determining net rates of mineralization and nitrification. However, mismatches were observed, especially for soil NH_4^+ concentrations and NN rates at the beech forest, which possibly reflect aspects of NH_4^+ uptake not captured in our model such as transient microbial immobilization, biological NN inhibition, or sorption-desorption processes [*Matschonat and Matzner*, 1995; *Trap et al.*, 2011]. We did not consider denitrification fluxes nor were we able to constrain this process with the available empirical data. Denitrification (and the absence of this process in

the model) could skew the empirical estimate of NN rates as incubation bags allow for gas exchange. However, rates of denitrification in these Mediterranean forests are low (by 10 times or even more) compared to nitrification rates [*Bernal et al.*, 2007; Poblador, personal communication], and thus, the effect of denitrification on NN signal is likely small.

Our analysis further supports the idea that processes involved in soil N cycling have a rapid response to climate because the model-data fusion yielded short residence time (~3–4 days) for both NH_4^+ and NO_3^-. This result justifies the equilibrium assumption made for soil N concentrations [*Stark and Hart*, 1997; *Gerber and Brookshire*, 2014]. However, our results did not fully justify the assumption of chronic N limitation, at least in the riparian forest, because this forest showed weak sink strength (low $\bar{k}_U + \bar{k}_H$) for soil NH_4^+ and NO_3^- pools compared to upland soils. Such high N availability at the riparian forest could be partially explained by symbiotic N_2 fixation, a process that was not explicitly included in our model conceptualization, but that could supply extra NH_4^+ to riparian trees, increase soil organic nitrogen, and ultimately enhance both riparian NNM and NN [*Booth et al.*, 2005; *Rennenberg et al.*, 2009]. Nevertheless, the good matches obtained indicate that the consideration of a first-order N removal rate was not incompatible with the data.

4.2. Response of Soil N Dynamics to Climate Variation

As expected, we found that moisture dependence of N processing rates was key to improving the data-model fit at the oak and beech forests. These findings agree with previous empirical studies performed across semiarid biomes and provide further evidence that the seasonality of soil N dynamics can strongly rely on the temporal pattern of soil moisture [*Niboyet et al.*, 2011; *Manzoni et al.*, 2012]. Our results showed increases in soil N processes with increasing water availability, as well as strong decreases during severe dry conditions (i.e., $WFPS < 20\%$), suggesting that extended drought periods may lead to reduced inorganic N turnover in Mediterranean biomes [*Larsen et al.*, 2011]. Similar to previous studies, we found that sensitivity to dryness and wetness differed between NNM and NN [*Manzoni et al.*, 2012; *Björsne et al.*, 2014], and further, that high moisture content (>60%) could reduce soil mineralization in some forest types [*Linn and Doran*, 1984].

In contrast to upland forests, soil moisture did not improve the model fit for the riparian forest, which suggests that water availability was not a limiting factor which was expected for riparian zones [*Sleutel et al.*, 2008]. The absence of soil moisture sensitivity was likely due to perennial moist conditions, as riparian soils kept relatively moist even in summer ($WFPS > 30\%$), when precipitation was low and evapotranspiration rates were the highest. At our study site, riparian groundwater usually flowed well below the soil surface, and thus, hydraulic lift by fine roots was likely responsible for keeping topsoil layers wet in summer [*Tabacchi et al.*, 2000]. As a consequence, riparian systems may be less vulnerable to drought than upland forests. Overall, this contrasting sensitivity to soil moisture highlights that distinct hydrologic dynamics in upland versus riparian sites ultimately lead to marked differences in soil N processing.

Temperature dependence applied for soil NNM and NN was crucial to improve the model's fitness at the three forest types, supporting the well-established idea that warming enhances microbial activity [*Emmett et al.*, 2004; *Butler et al.*, 2012]. The obtained Q_{10} values were within the range of other observations carried out in Mediterranean and temperate systems [*Emmett et al.*, 2004; *Dessureault-Rompré et al.*, 2010; *Novem-Auyeung et al.*, 2013]. Yet our results did not support the hypothesis that microbes adapted to cold climates would be more sensitive to changes in soil temperature because the highest temperature sensitive (Q_{10}~3) was exhibited by both riparian NNM and beech NN. This finding suggests that other site-specific features can influence the temperature sensitivity of soil N cycling. For instance, NNM at the oak and beech forests was less responsive to increases in temperature than riparian NNM, which could be explained by the higher moisture stress experienced by upland forests [*Suseela et al.*, 2012; *Novem-Auyeung et al.*, 2013]. Additionally, SON availability was twofold higher at the riparian than at the upland soils, which could further contribute to enhance riparian soil mineralization during warm periods compared to upland soils that could be substrate limited [*von Lützow and Kögel-Knabner*, 2009; *Schütt et al.*, 2014].

Our results further suggest that the response to changes in temperature can substantially differ between NNM and NN. We found that NN was more responsive to increases in temperature than NNM at the oak and beech forests, in line with previous empirical studies showing that warming enhances NN in forest soils by reducing both NH_4^+ and NO_3^- immobilization [*Emmett et al.*, 2004; *Rennenberg et al.*, 2009; *Butler*

et al., 2012]. However, this pattern was not observed in the riparian forest, which showed lower Q_{10} values for NN compared to NNM. Overall, our model supports the idea that the various processes involved in soil N cycling can respond differently to warming [*Emmett et al*., 2004; *Bai et al*., 2013]. Further, our results point out that interaction between temperature and other site-specific features such as water and substrate availability is essential to understand future responses of ecosystem biogeochemical cycles to warming.

Finally, our results showed that including precipitation pulses into the model improved the goodness of fit at the three forest types. These results support the idea that rewetting episodes are essential to understand soil N cycling likely because they stimulate soil microbial activity through mobilizing soil N, the release of intracellular osmolites, and the enhancement of metabolic rates [*Schimel et al*., 2007; *Borken and Matzner*, 2009]. In contrast to our expectation, the highest response to rewetting ($a > 0.5$) was shown by soil N processing rates in the riparian forest, which were expected to be less sensitive to increases in water availability than those in the upland soils. This seemingly counterintuitive result may be partly a modeling artifact and stems from the fact that part of a small but not model-relevant moisture effect has spilled over to a precipitation response in the riparian zone, as moisture and precipitation are somewhat correlated. As observed for soil moisture and temperature, our results point to a differential sensitivity of NNM and NN to rewetting events, being NN more responsive than NNM (as indicated by the steeper *a* slopes). The higher sensitivity of NN to increases in soil water availability has been previously observed and suggests that soil NO_3^- availability may be vulnerable to changes in the amount and timing of precipitation [*Groffman et al*., 2009; *Larsen et al*., 2011]. Our findings showed that rewetting episodes can be crucial to predict temporal patterns of soil N cycling, and therefore, the incorporation of water pulse dynamics within terrestrial models could help to our understanding of temporal patterns of nutrient biogeochemistry in Mediterranean systems.

4.3. Effect of Climate Change on Soil N Cycling

We developed climate change scenarios for our sites using broad IPCC model evaluations that suggest year-round decrease in soil moisture (−0.8 mm), year-round temperature increase (+2°C), and decreased precipitation in summer (−5%) when applying the RCP4.5 scenario. While the temperature increase would be similar to or lower than in other systems, Mediterranean forest systems are expected to experience a reduction in precipitation during summer months, which renders these regions more vulnerable to drought compared to other forested regions worldwide [*IPCC*, 2013]. Our model approximation allowed us to evaluate the effect of the expected climate change on the overall soil N cycle as the combination of simultaneous changes in the climatic drivers (soil moisture, temperature, and precipitation) and the sensitivity of the different soil N processes to these drivers.

Our model calculations were based on seasonal data obtained over 1 year. The model was designed to specifically address the short-term responses of the considered soil N processes to climate variability in presence of soil organic N. Therefore, we cannot predict future levels of soil organic matter, long-term mineralization rates, nor future changes in the climatic sensitivity of soil N cycling. However, given the derived sensitivity to climate drivers, the modeling framework allows us to explore how the interactive effect of moisture and temperature could affect soil N cycle in the future. The consideration of two future states of the long-term N cycle (a transition phase with fixed SON versus a steady state equilibrium with fixed mean mineralization fluxes) helps bracketing potential alterations of the long-term plant-soil cycle. Both states showed similar results under future climate scenarios, giving some consistency to the model predictions.

According to our model and our assumptions therein, the climate change projected for later in this century may have a relatively small effect on mean daily rates of soil N cycling. Our results indicate that mean NNM and NN at the riparian forest could increase by up to +8% from today's rates as a consequence of warmer temperatures, as observed for temperate systems [*Rustad et al*., 2001; *Bai et al*., 2013]. Contrarily, mean daily NNM and NN in upland forests may slightly decline in the future because the negative effect of decreases in water availability will likely outweigh the positive temperature effect. Our model simulations agree with the hypothesis that future warming and drying may have an antagonistic effect on soil N cycling and ultimately lead to minimal changes in mean NNM, NN, and soil NO_3^- concentrations in these Mediterranean upland forests. Similar antagonistic effects between temperature and soil moisture have

been recently reported in manipulative warming experiments in grassland systems [*Liu et al*., 2009; *Verburg et al*., 2009]. Our study adds a novel piece of knowledge to the growing evidence that terrestrial ecosystems can show a complex response to climate change and that the interaction between different climatic drivers can eventually lead to less pronounced responses than previously expected [*Rustad et al*., 2001; *Bai et al*., 2013].

When projected to the catchment scale, our results suggest that expected future changes in soil N cycling would not be enough to alter soil N concentration in this Mediterranean system. Moreover, we found that future climate-induced shifts in vegetation would have a relatively small effect on both soil N fluxes and pools because oak and beech forests may respond similar to climate. Our results differ from previous studies in temperate systems that have related long-term increases in hydrological N export to warming-induced increases in mineralization [*Rogora*, 2007; *Brookshire et al*., 2011]. In those mesic regions, extrapolation of past climatic trends did not reveal future changes in soil moisture, and therefore, moisture did not affect function cycling rates. Yet our findings revealed that soil water availability can play a pivotal role in driving soil N cycling. Although our results have to be considered with caution, our study and method provide insights into how interaction among direct and indirect climatic drivers affects soil N processing in Mediterranean catchments and stresses that future response of soil N cycle to climate change cannot be generalized among biomes or forest types.

5. Conclusions

Our study adds to the growing evidence demonstrating the effects of changes in climate on soil N cycling in forests ecosystems [*Rustad et al*., 2001; *Larsen et al*., 2011]. To explore climate sensitivity of key soil N processes, we use a relatively short-term data set (18 sampling dates over 1 year) but take advantage of suite of detailed soil N cycle measurements (soil organic and inorganic N concentrations, net N mineralization, net nitrification, and potential N losses from the soil pool). We showed that the inclusion of climatic modifiers improves the model, supporting the idea that they are important drivers of the dynamics of the N cycle in Mediterranean systems. Soil moisture, temperature, and precipitation generally have a positive effect on soil N cycling rates, although sensitivity to climatic factors differed among processes and forests. Soil moisture was the major driver of soil N cycle at oak and beech forests, but temperature and precipitation shifted soil N dynamics at the riparian forest. In most cases, net nitrification was more sensitive to changes in climate than net N mineralization; yet the response of soil N processes to climate change was often masked by antagonistic effects of moisture availability and temperature. As a consequence of this interaction between warming and drying, we found that future climate may have a small influence on mean daily soil N processing rates, which would ultimately lead to minimal variation in mean annual soil NO_3^- concentration in these Mediterranean catchments. Together, our analyses provide mechanistic insights into the sensitivity of the soil N cycle to climate variation and add to our understanding of how future changes in climate may shape soil N cycling in Mediterranean regions.

Acknowledgments
We thank S. Poblador for the field and laboratory assistance. Financial support was provided by the Spanish Government through the projects MONTES-Consolider (CSD2008-00040-MONTES) and MEDFORESTREAM (CGL2011-30590). A.L. was funded by the Spanish Ministry of Education, Culture and Sport (MECD) with a FPU grant (AP-2009-3711). S.B. was supported by the Spanish Ministry of Economy and Competitiveness (MINECO) with a Juan de la Cierva contract (JCI-2010-594 06397). S.B. received additional funds from the Spanish Research Council (CSIC) with the contract JAEDOC027. The Vichy Catalan Company, the Regàs family, and the Catalan Water Agency (ACA) graciously gave us permission for at the Font del Regàs catchment. The data for this paper are available by contacting the corresponding author.

References

Akaike, H. (1974), A new look at the statistical model identification, *IEEE Trans. Autom. Control*, *19*, 716–723.
Àvila, A., and F. Rodà (2012), Changes in atmospheric deposition and streamwater chemistry over 25 years in undisturbed catchments in a Mediterranean mountain environment, *Sci. Total Environ.*, *434*, 18–27, doi:10.1016/j.scitotenv.2011.11.062.
Àvila, A., R. Molowny-Horas, B. S. Gimeno, and J. Peñuelas (2009), Analysis of decadal time series in wet N concentrations at five rural sites in NE Spain, *Water Air Soil Pollut.*, *207*(1-4), 123–138, doi:10.1007/s11270-009-0124-7.
Bai, E., S. Li, W. Xu, W. Li, W. Dai, and P. Jiang (2013), A meta-analysis of experimental warming effects on terrestrial nitrogen pools and dynamics, *New Phytol.*, *199*(2), 431–40, doi:10.1111/nph.12252.
Bell, C., N. McIntyre, S. Cox, D. Tissue, and J. Zak (2008), Soil microbial responses to temporal variations of moisture and temperature in a Chihuahuan Desert grassland, *Microb. Ecol.*, *56*, 153–167.
Berger, T. W., E. Inselsbacher, F. Mutsch, and M. Pfeffer (2009), Nutrient cycling and soil leaching in eighteen pure and mixed stands of beech (*Fagus sylvatica*) and spruce (*Picea abies*), *For. Ecol. Manage.*, *258*(11), 2578–2592, doi:10.1016/j.foreco.2009.09.014.
Bernal, S., F. Sabater, A. Butturini, E. Nin, and S. Sabater (2007), Factors limiting denitrification in a Mediterranean riparian forest, *Soil Biol. Biogeochem.*, *39*(10), 2685–2688.
Bernal, S., A. Lupon, M. Ribot, F. Sabater, and E. Martí (2015), Riparian and in-stream controls on nutrient concentrations along a headwater forested stream, *Biogeosciences*, *12*, 1941–1954, doi:10.5194/bg-12-1941-2015.
Björsne, A. K., T. Rütting, and P. Ambus (2014), Combined climate factors alleviate changes in gross soil nitrogen dynamics in heathlands, *Biogeochemistry*, *120*(1-3), 191–201, doi:10.1007/s10533-014-9990-1.

Booth, M. S., J. M. Stark, and E. Rastertter (2005), Controls on nitrogen cycling in terrestrial ecosystems: A synthetic analysis of literature data, *Ecol. Monogr.*, *75*(2), 139–157.
Borken, W., and E. Matzner (2009), Reappraisal of drying and wetting effects on C and N mineralization and fluxes in soils, *Global Change Biol.*, *15*(4), 808–824, doi:10.1111/j.1365-2486.2008.01681.x.
Brookshire, J. E. N., H. M. Valett, and S. Gerber (2009), Maintenance of terrestrial nutrient loss signatures during in-stream transport, *Ecology*, *90*, 293–299.
Brookshire, J. E. N., S. Gerber, J. R. Webster, J. M. Vose, and W. T. Swank (2011), Direct effects of temperature on forest nitrogen cycling revealed through analysis of long-term watershed records, *Global Change Biol.*, *17*(1), 297–308, doi:10.1111/j.1365-2486.2010.02245.x.
Burnham, K. P., and D. R. Anderson (2002), *Model Selection and Multimodel Inference: A Practical Information-Theoretic Approach*, 2nd ed., Springer, New York.
Butler, S. M. J., et al. (2012), Soil warming alters nitrogen cycling in a New England forest: Implications for ecosystem function and structure, *Oecologia*, *168*(3), 819–28, doi:10.1007/s00442-011-2133-7.
Cameron, D. R., et al. (2013), Environmental change impacts on the C- and N-cycle of European forests: A model comparison study, *Biogeosciences*, *10*(3), 1751–1773, doi:10.5194/bg-10-1751-2013.
Chen, I. C., J. K. Hill, R. Ohlemüller, D. B. Roy, and C. D. Thomas (2011), Rapid range shifts of species associated with high levels of climate warming, *Science*, *333*(6045), 1024–1026.
Collins, S. L., R. L. Sinsabaugh, C. Crenshaw, L. Green, A. Porras-Alfaro, M. Stursova, and L. H. Zeglin (2008), Pulse dynamics and microbial processes in arid land ecosystems, *J. Ecol.*, *96*, 413–420.
Colwell, R. K., G. Brehm, C. L. Cardelús, A. C. Gilman, and J. T. Longino (2008), Global warming, elevational range shifts, and lowland biotic attrition in the wet tropics, *Science*, *322*, 258–261.
Dessureault-Rompré, J., B. J. Zebarth, A. Georgallas, D. L. Burton, C. A. Grant, and C. F. Drury (2010), Temperature dependence of soil nitrogen mineralization rate: Comparison of mathematical models, reference temperatures and origin of the soils, *Geoderma*, *157*(3), 97–108, doi:10.1016/j.geoderma.2010.04.001.
Edwards, A. (1992), *Likelihood*, John Hopkins Univ. Press, Baltimore, Md.
Emmett, B. A., C. Beier, M. Estiarte, A. Tietema, H. L. Kristensen, D. Williams, J. Peñuelas, I. Schmidt, and A. Sowerby (2004), The response of soil processes to climate change: Results from manipulation studies of shrublands across an environmental gradient, *Ecosystems*, *7*(6), 625–637, doi:10.1007/s10021-004-0220-x.
Eno, C. F. (1960), Nitrate production in the field by incubating the soil in polyethylene bags, *Soil Sci. Soc. Am. J.*, *24*, 277–279.
Gerber, S., and E. N. J. Brookshire (2014), Scaling of physical constraints at the root-soil interface to macroscopic patterns of nutrient retention in ecosystems, *Am. Nat.*, *183*(3), 418–30, doi:10.1086/674907.
Goodale, C. L., and J. D. Aber (2001), The long-term effects of land-use history on nitrogen cycling in northern hardwood forests, *Ecol. Appl.*, *11*(1), 253–267.
Groffman, P. M., J. P. Hardy, M. C. Fisk, T. J. Fahey, and C. T. Driscoll (2009), Climate variation and soil carbon and nitrogen cycling processes in a northern hardwood forest, *Ecosystems*, *12*(6), 927–943, doi:10.1007/s10021-009-9268-y.
Institut Cartografic de Catalunya (2010), Orthophotomap of Catalunya 1:25 000 Departament de Política Territorial i Obres Públiques, Generalitat de Catalunya.
Intergovernmental Panel on Climate Change (IPCC) (2013), Summary for policymakers, in *Climate Change 2013: The Physical Science Basis*, edited by V. B. Stocker et al., Cambridge Univ. Press, Cambridge, U. K.
Ise, T., and P. R. Moorcroft (2006), The global-scale temperature and moisture dependencies of soil organic carbon decomposition: An analysis using a mechanistic decomposition model, *Biogeochemistry*, *80*(3), 217–231, doi:10.1007/s10533-006-9019-5.
Lamarque, J. F., et al. (2013), Multi-model mean nitrogen and sulfur deposition from the Atmospheric Chemistry and Climate Model Intercomparison Project (ACCMIP): Evaluation historical and projected changes, *Atmos. Chem. Phys. Discuss.*, *13*(3), 6247–6294, doi:10.5194/acpd-13-6247-2013.
Larsen, K. S., et al. (2011), Reduced N cycling in response to elevated CO_2, warming, and drought in a Danish heathland: Synthesizing results of the CLIMAITE project after two years of treatments, *Global Change Biol.*, *17*(5), 1884–1899, doi:10.1111/j.1365-2486.2010.02351.x.
Lawrence, G. B., G. M. Lovett, and H. Yvonne (2000), Atmospheric deposition and watershed nitrogen export along an elevational gradient in the Catskill Mountains, New York, *Biogeochemistry*, *50*(1), 21–43.
Linn, D. M., and J. W. Doran (1984), Effect of water-filled pore space on carbon dioxide and nitrous oxide production in tilled and nontilled soils, *Soil Sci. Soc. Am. J.*, *48*(6), 1267–1272.
Liu, W., Z. H. E. Zhang, and S. Wan (2009), Predominant role of water in regulating soil and microbial respiration and their responses to climate change in a semiarid grassland, *Global Change Biol.*, *15*(1), 184–195.
Lovett, G. M., K. C. Weathers, M. A. Arthur, and J. C. Schultz (2004), Nitrogen cycling in a northern hardwood forest: Do species matter?, *Biogeochemistry*, *67*(3), 289–308, doi:10.1023/B:BIOG.0000015786.65466.f5.
Luo, Y., et al. (2011), Coordinated approaches to quantify long-term ecosystem dynamics in response to global change, *Global Change Biol.*, *17*(2), 843–854, doi:10.1111/j.1365-2486.2010.02265.x.
Manzoni, S., J. P. Schimel, and A. Porporato (2012), Responses of soil microbial communities to water stress: Results from a meta-analysis, *Ecology*, *93*(4), 930–8.
Matschonat, G., and E. Matzner (1995), Quantification of ammonium sorption in acid forest soils by sorption isotherms, *Plant Soil*, *168-169*(1), 95–101.
Miller, A. E., J. P. Schimel, J. O. Sickman, T. Meixner, A. P. Doyle, and J. M. Melack (2007), Mineralization responses at near-zero temperatures in three alpine soils, *Biogeochemistry*, *84*(3), 233–245, doi:10.1007/s10533-007-9112-4.
Moriasi, D. N., J. G. Arnold, M. W. Van Liew, R. L. Bingner, R. D. Harmel, and T. L. Veith (2007), Model evaluation guidelines for systematic quantification of accuracy in watershed simulations, *Am. Soc. Agric. Biol. Eng.*, *50*(3), 885–900.
Niboyet, A., X. Le Roux, P. Dijkstra, B. A. Hungate, L. Barthes, J. C. Blankinship, J. R. Brown, C. B. Field, and P. W. Leadley (2011), Testing interactive effects of global environmental changes on soil nitrogen cycling, *Ecosphere*, *2*(5), 1–24, doi:10.1890/ES10-00148.1.
Novem-Auyeung, D. S., V. Suseela, and J. S. Dukes (2013), Warming and drought reduce temperature sensitivity of nitrogen transformations, *Global Change Biol.*, *19*(2), 662–76, doi:10.1111/gcb.12063.
Pendall, E., L. Rustad, and J. Schimel (2008), Towards a predictive understanding of belowground process responses to climate change: Have we moved any closer?, *Funct. Ecol.*, *22*(6), 937–940, doi:10.1111/j.1365-2435.2008.01506.x.
Peñuelas, J., and M. Boada (2003), A global change-induced biome shift in the Montseny mountains (NE Spain), *Global Change Biol.*, *9*, 131–140.
Raich, A. J. W., et al. (1991), Potential net primary productivity in South America: Application of a global model, *Ecol. Appl.*, *1*(4), 399–429.

Rastetter, E. B., G. I. Ågren, and G. R. Shaver (1997), Responses of N-limited ecosystems to increased CO_2: A balanced-nutrition, coupled-element-cycles model, *Ecol. Appl.*, *7*(2), 444–460.

Rennenberg, H., M. Dannenmann, A. Gessler, J. Kreuzwieser, J. Simon, and H. Papen (2009), Nitrogen balance in forest soils: Nutritional limitation of plants under climate change stresses, *Plant Biol.*, *11*(s1), 4–23.

Rogora, M. (2007), Synchronous trends in $N–NO_3$ export from N-saturated river catchments in relation to climate, *Biogeochemistry*, *86*(3), 251–268, doi:10.1007/s10533-007-9157-4.

Rustad, L., J. L. Campbell, G. Marion, R. J. Norby, M. J. Mitchell, A. Hartley, J. Cornelissen, and J. Gurevitch (2001), A meta-analysis of the response of soil respiration, net nitrogen mineralization, and aboveground plant growth to experimental ecosystem warming, *Oecologia*, *126*(4), 543–562, doi:10.1007/s004420000544.

Schimel, J., T. C. Balser, and M. Wallenstein (2007), Microbial stress-response physiology and its implications for ecosystem function, *Ecology*, *88*(6), 1386–1394.

Schütt, M., W. Borken, O. Spott, C. F. Stange, and E. Matzner (2014), Temperature sensitivity of C and N mineralization in temperate forest soils at low temperatures, *Soil Biol. Biochem.*, *69*, 320–327, doi:10.1016/j.soilbio.2013.11.014.

Sleutel, S., B. Moeskops, W. Huybrechts, A. Vandenbossche, J. Salomez, S. Bolle, D. Buchan, and S. Neve (2008), Modeling soil moisture effects on net nitrogen mineralization in loamy wetland soils, *Wetlands*, *28*(3), 724–734, doi:10.1672/07-105.1.

Stark, J. M., and S. C. Hart (1997), High rates of nitrification and nitrate turnover in undisturbed coniferous forests, *Nature*, *385*, 61–64.

Suseela, V., R. T. Conant, M. D. Wallenstein, and J. S. Dukes (2012), Effects of soil moisture on the temperature sensitivity of heterotrophic respiration vary seasonally in an old-field climate change experiment, *Global Change Biol.*, *18*(1), 336–348.

Tabacchi, E., L. Lambs, H. Guilloy, A. M. Planty-Tabacchi, E. Muller, and H. Decamps (2000), Impacts of riparian vegetation on hydrological processes, *Hydrol. Processes*, *14*(16-17), 2959–2976.

Trap, J., F. Bureau, M. Akpa-Vinceslas, T. Decaens, and M. Aubert (2011), Changes in humus forms and soil N pathways along a 130-year-old pure beech forest chronosequence, *Ann. Forest Sci.*, *68*(3), 595–606, doi:10.1007/s13595-011-0063-5.

Verburg, P. S., D. W. Johnson, D. E. Schorran, L. L. Wallace, Y. Luo, and J. A. Arnone III (2009), Impacts of an anomalously warm year on soil nitrogen availability in experimentally manipulated intact tallgrass prairie ecosystems, *Global Change Biol.*, *15*(4), 888–900.

von Lützow, M., and I. Kögel-Knabner (2009), Temperature sensitivity of soil organic matter decomposition: What do we know?, *Biol. Fertil. Soils*, *46*(1), 1–15, doi:10.1007/s00374-009-0413-8.

Biogeosciences, 12, 1941–1954, 2015
www.biogeosciences.net/12/1941/2015/
doi:10.5194/bg-12-1941-2015

Biogeosciences Open Access

Riparian and in-stream controls on nutrient concentrations and fluxes in a headwater forested stream

S. Bernal[1,2], A. Lupon[2], M. Ribot[1], F. Sabater[2], and E. Martí[1]

[1]Center for Advanced Studies of Blanes (CEAB-CSIC), Accés a la Cala Sant Francesc 14, 17300, Blanes, Girona, Spain
[2]Departament d'Ecologia, Facultat de Biologia, Universitat de Barcelona, Av. Diagonal 643, 08028, Barcelona, Spain

Correspondence to: S. Bernal (sbernal@ceab.csic.es)

Received: 16 June 2014 – Published in Biogeosciences Discuss.: 29 July 2014
Revised: 29 December 2014 – Accepted: 1 March 2015 – Published: 24 March 2015

Abstract. Headwater streams are recipients of water sources draining through terrestrial ecosystems. At the same time, stream biota can transform and retain nutrients dissolved in stream water. Yet studies considering simultaneously these two sources of variation in stream nutrient chemistry are rare. To fill this gap of knowledge, we analyzed stream water and riparian groundwater concentrations and fluxes as well as in-stream net uptake rates for nitrate (NO_3^-), ammonium (NH_4^+), and soluble reactive phosphorus (SRP) along a 3.7 km reach on an annual basis. Chloride concentrations (used as conservative tracer) indicated a strong hydrological connection at the riparian–stream interface. However, stream and riparian groundwater nutrient concentrations showed a moderate to null correlation, suggesting high in-stream biogeochemical processing. In-stream net nutrient uptake (F_{sw}) was highly variable across contiguous segments and over time, but its temporal variation was not related to the vegetative period of the riparian forest. For NH_4^+, the occurrence of $F_{sw} > 0$ µg N m^{-1} s^{-1} (gross uptake > release) was high along the reach, while for NO_3^-, the occurrence of $F_{sw} < 0$ µg N m^{-1} s^{-1} (gross uptake < release) increased along the reach. Within segments and dates, F_{sw}, whether negative or positive, accounted for a median of 6, 18, and 20 % of the inputs of NO_3^-, NH_4^+, and SRP, respectively. Whole-reach mass balance calculations indicated that in-stream net uptake reduced stream NH_4^+ flux up to 90 %, while the stream acted mostly as a source of NO_3^- and SRP. During the dormant period, concentrations decreased along the reach for NO_3^-, but increased for NH_4^+ and SRP. During the vegetative period, NH_4^+ decreased, SRP increased, and NO_3^- showed a U-shaped pattern along the reach. These longitudinal trends resulted from the combination of hydrological mixing with terrestrial inputs and in-stream nutrient processing. Therefore, the assessment of these two sources of variation in stream water chemistry is crucial to understand the contribution of in-stream processes to stream nutrient dynamics at relevant ecological scales.

1 Introduction

Stream water chemistry integrates hydrological and biogeochemical processes occurring within its drainage area, and thus the temporal variation in stream solute concentrations at the catchment outlet is considered a good indicator of the response of terrestrial and aquatic ecosystems to environmental drivers (Bormann and Likens, 1967; Bernhardt et al., 2003; Houlton et al., 2003). Less attention has been paid to the spatial variation in water chemistry along the stream, though it can be considerably important because stream nutrient concentrations are influenced by changes in hydrological flow paths, vegetation cover, and soil characteristics (Dent and Grimm, 1999; Likens and Buso, 2006). For instance, spatial variation in nutrient concentration along the stream has been attributed to changes in soil nitrification rates (Bohlen et al., 2001), soil organic carbon availability (Johnson et al., 2000), and organic soil depth across altitudinal gradients (Lawrence et al., 2000). Moreover, nutrient cycling within the riparian zone can strongly influence stream nutrient concentrations along the stream because these ecosystems are hot spots of biogeochemical processing (McClain et al., 2003; Vidon et al., 2010). In addition, processes occurring at the riparian–stream interface have a larger influence on stream water chemistry than those occurring at catchment locations further

from the stream (Ross et al., 2012). Finally, stream ecosystems have a strong capacity to transform and retain nutrients; thus, in-stream biogeochemical processes can further influence nutrient chemistry along the stream (Peterson et al., 2001; Dent et al., 2007). Therefore, consideration of these multiple sources of variation in stream water chemistry is important to understand drivers of stream nutrient dynamics.

Our understanding of nutrient biogeochemistry within riparian zones and streams is mainly based on field studies performed at the plot scale or in small stream reaches (a few hundred meters) (Lowrance et al., 1997; Peterson et al., 2001; Sabater et al., 2003; Mayer et al., 2007; von Schiller et al., 2015). These empirical studies have widely demonstrated the potential of riparian and stream ecosystems as either sinks or sources of nutrients, which ultimately influence the transport of nutrients to downstream ecosystems. Riparian and stream biota are capable of decreasing the concentration of essential nutrients, such as dissolved inorganic nitrogen (DIN) and phosphate, especially with increasing water storage and residence time (Valett et al., 1996; Hedin et al., 1998; Peterson et al., 2001; Vidon and Hill, 2004). Conversely, riparian forests can become sources rather than sinks of nutrients when N_2-fixing species predominate (Helfield and Naiman, 2002; Compton et al., 2003), and in-stream nutrient release can be important during some periods (Bernhardt et al., 2002; von Schiller et al., 2015). Moreover, there is an intimate hydrological linkage between riparian and stream ecosystems that can result in strong biogeochemical feedbacks between these two compartments (e.g., Morrice et al., 1997; Martí et al., 2000; Bernal and Sabater, 2012). However, studies integrating biogeochemical processes of these two nearby ecosystems are rare (but see Dent et al., 2007), and the exchange of water and nutrients between stream and groundwater is unknown in most studies assessing in-stream gross and net nutrient uptake (Roberts and Mulholland, 2007; Covino et al., 2010; von Schiller et al., 2011).

There is a wide body of knowledge showing the potential of riparian and stream ecosystems to modify either groundwater or stream nutrient concentrations. However, a comprehensive view of the influence of riparian and in-stream processes on stream water chemistry at the catchment scale is still lacking (but see Meyer and Likens, 1979). This gap of knowledge mostly exists because hydrological and biogeochemical processes can vary substantially along the stream (Covino and McGlynn, 2007; Jencso et al., 2010), which limits our ability to extrapolate small plot- and reach-scale measurements to larger spatial scales. Some authors have proposed that nutrient concentrations should decline along the stream if in-stream net uptake is high enough and riparian groundwater inputs are relatively small (Brookshire et al., 2009). This declining pattern is not systematically observed in reach-scale studies, which could bring us to the conclusion that terrestrial inputs are the major driver of stream water chemistry because in-stream gross uptake and release counterbalance each other most of the time (Brookshire et al., 2009). However, synoptic studies have revealed that nutrient concentrations are patchy and highly variable along the stream as a result of spatial patterns in upwelling and in-stream nutrient processing (Dent and Grimm, 1999). Thus, in-stream nutrient cycling could be substantial, but it might not necessarily lead to longitudinal increases or declines in nutrient concentration, a question that probably needs to be addressed at spatial scales larger than a few hundred meters.

The goal of this study was to gain a better understanding of the influence of riparian groundwater inputs and in-stream biogeochemical processing on stream nutrient chemistry and fluxes in a headwater forested catchment. To approach this question, we explored the longitudinal pattern of stream nutrient (nitrate, ammonium, and phosphate) concentration along a 3.7 km reach over 1.5 years. We chose a headwater catchment as a model system to investigate drivers of spatial patterns in stream water chemistry because they typically show pronounced changes in riparian and stream features across relatively short distances (Uehlinger, 2000). First, we evaluated riparian groundwater inputs and in-stream nutrient processing as sources of variation in stream nutrient concentration along the reach. We expected stream and riparian groundwater nutrient concentrations to be similar and strongly correlated if riparian groundwater is a major source of nutrients to the stream. In addition, we estimated the in-stream nutrient-processing capacity for 14 contiguous segments along the reach with a mass balance approach. Second, we evaluated the relative contribution of riparian groundwater inputs and in-stream biogeochemical processing to stream nutrient fluxes at the whole-reach scale by applying a mass balance approach that included all hydrological input and output fluxes along the reach.

2 Study site

The research was conducted in the Font del Regàs catchment (14.2 km^2) (Fig. 1), located in the Montseny Natural Park, NE Spain (41°50′ N, 2°30′ E; 300–1200 m a.s.l.) during the period 2010–2011. Total inorganic N deposition in this area oscillates between 15 and 30 kg N ha^{-1} yr^{-1} (Àvila and Rodà, 2012). The climate at the Montseny Mountains is subhumid Mediterranean. The long-term mean annual precipitation is 925 ± 151 mm and the long-term mean annual air temperature is 12.1 ± 2.5 °C (mean $\pm$ SD, period: 1940–2000; Catalan Meteorological Service: http://www.meteo.cat/observacions/xema/). During the study period, mean annual precipitation (975 mm) and temperature (12.9 °C) fell within the long-term average (data from a meteorological station within the study catchment). In this period, summer 2010 was the driest season (140 mm), while most of the precipitation occurred in winter 2010 (370 mm) and autumn 2011 (555 mm) (Fig. 2a).

The catchment is dominated by biotitic granite (ICC, 2010) and it has steep slopes (28 %). Evergreen oak (*Quercus*

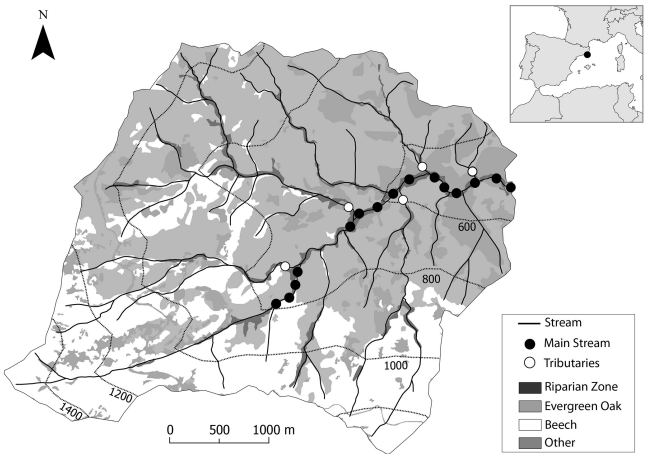

Figure 1. Map of the Font del Regàs catchment within the Montseny Natural Park (NE, Spain). The vegetation cover and the main stream sampling stations along the 3.7 km reach are indicated. There were 5 and 10 sampling stations along the second- and third-order sections, respectively. Four permanent tributaries discharged to the main stream from the upstream- to the downstream-most site (white circles). Additional water samples were collected from a small tributary draining through the inhabited area at the lowest part of the reach. The remaining tributaries were dry during the study period.

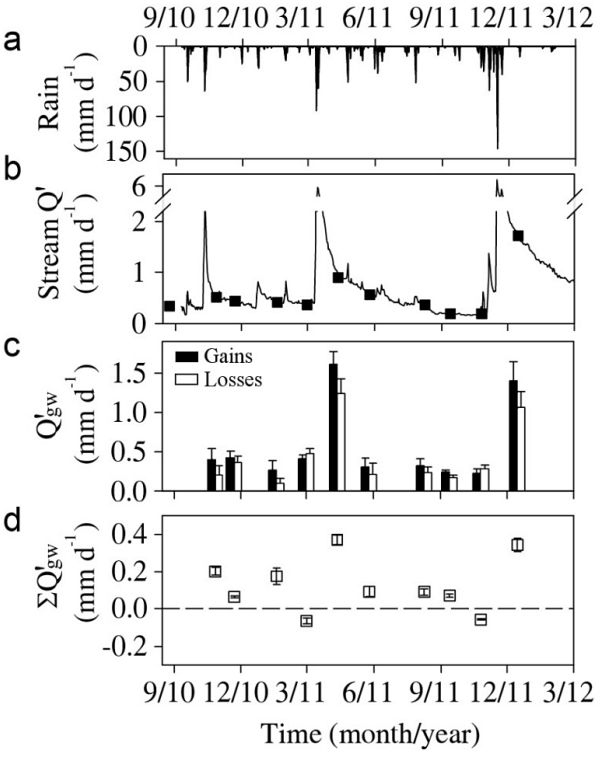

Figure 2. Temporal pattern of area-specific **(a)** rainfall, **(b)** stream discharge, **(c)** whole-reach gross hydrological gains and losses, and **(d)** cumulative net groundwater inputs at the downstream-most site. Black squares in **(b)** are dates of field campaigns. Error bars in **(c)** and **(d)** show the uncertainty associated with the empirical estimation of Q from tracer slug additions. Error bars in **(b)** are smaller than the symbol size.

ilex) and beech (*Fagus sylvatica*) forests cover 54 and 38 % of the catchment area, respectively (Fig. 1). The upper part of the catchment (2 %) is covered by heathlands and grasslands (ICC, 2010). The catchment has a low population density (< 1 person km^{-2}) which is concentrated in the valley bottom. Hillslope soils (pH ~ 6) are sandy, with a high content of rocks (33–36 %). Soils at the hillslopes have a 3 cm depth O horizon and a 5 to 15 cm depth A horizon (averaged from 10 soil profiles).

The riparian zone is relatively flat (slope < 10 %), and it covers 6 % of the catchment area. Riparian soils (pH ~ 7) are sandy loam with low rock content (13 %) and a 5 cm depth organic layer followed by a 30 cm depth A horizon (averaged from five soil profiles). Along the 3.7 km reach, the width of the riparian zone increases from 6 to 32 m, whereas the total basal area of riparian trees increases 12-fold (based on forest inventories of 30 m plots every ca. 150 m) (Fig. S1 in the Supplement). *Alnus glutinosa*, *Robinia pseudoacacia*, *Platanus hybrida*, and *Fraxinus excelsior* are the most abundant riparian tree species followed by *Corylus avellana*, *Populus tremula*, *Populus nigra*, and *Sambucus nigra*. The abundance of N_2-fixing species (*A. glutinosa* and *R. pseudoacacia*) increases from 0 to > 60 % along the longitudinal profile (Fig. S1). During base flow conditions, riparian groundwater (< 1.5 m from the stream channel) flows well below the soil surface (0.5 ± 0.1 m), and thus the interaction with the riparian organic soil is minimal (averaged from 15 piezometers, $n = 165$) (Fig. S1). During the period of study, riparian groundwater temperature ranged from 5 to 19.5 °C.

The 3.7 km study reach is a second-order stream along the first 1.5 km and a third-order stream for the remaining 63 % of its length. The geomorphology of the stream bed changes substantially with stream order. The stream bed along the second-order section is mainly composed of rocks and cobbles (70 %) with a small contribution of sand (~ 10 %). At the valley bottom, sands and gravels represent 44 % of the stream substrate and the presence of rocks is minor (14 %). Mean wetted width and water velocity increase between the second- and third-order section (from 1.6 to 2.7 m and from 0.24 to 0.35 m s^{-1}, respectively) (Fig. S1). During the study period, stream water temperature ranged from 5 to 18 °C. Stream discharge was low in summer (0.33 mm) and peaked in spring (0.79 mm).

3 Materials and methods

3.1 Field sampling and laboratory analysis

We selected 15 sampling sites along the 3.7 km study reach. The distance between consecutive sampling sites ranged from 110 to 600 m (Fig. 1). At each sampling site, we installed a 1 m long PVC piezometer (3 cm ∅) in the riparian zone at ∼ 1.5 m from the stream channel.

For each sampling site, we sampled stream water (from the thalweg) and riparian groundwater every 2 months from August 2010 to December 2011. We used pre-acid-washed polyethylene bottles to collect water samples after triple-rinsing them with either stream or groundwater. On each sampling date, we also measured dissolved oxygen concentration (DO, in $mg\,L^{-1}$) and water temperature (in °C) with a YSI ProODO device in both stream water and riparian groundwater. We avoided sampling soon after storms to ensure that our measurements were representative of low-flow conditions, when the influence of in-stream biogeochemical processes on stream nutrient concentrations and fluxes is expected to be the highest. All field campaigns were performed at least 9 days after storm events, except in October 2011 (Fig. 2b, black squares). On each sampling date and at each sampling site, we measured groundwater table elevation (in meters below soil surface) with a water level sensor (Eijkelkamp 11.03.30) as well as wetted width (in m), stream discharge (Q, in $L\,s^{-1}$), and water velocity ($m\,s^{-1}$). Q and water velocity were estimated with the slug-addition technique by adding 1 L of NaCl-enriched solution to the stream (electrical conductivity $= 75 - 90\,mS\,cm^{-1}$, $n = 11$) (Gordon et al., 2004). The uncertainty associated with Q measurements was calculated as the relative difference in Q between pairs of tracer additions under equal water depth conditions (difference < 1 mm). The pairs of data were selected from a set of 126 slug additions and water level measurements obtained from the permanent field stations at Font del Regàs (Lupon, unpublished). The measured uncertainty was relatively small (1.9 %, $n = 11$). On each sampling date, we also collected stream water and measured Q at the four permanent tributaries discharging to Font del Regàs stream, which drained 1.9, 3.2, 1.8, and 1.1 km^2, respectively (Fig. 1). These data were used for mass balance calculations (see below). Additional stream water samples were collected from a small permanent tributary that drained through an area (< 0.4 km^2) with few residences and crop fields for personal consumption.

Water samples were filtered through pre-ashed GF / F filters (Whatman®) and kept cold (< 4 °C) until laboratory analysis (< 24 h after collection). Chloride (Cl^-) was used as a conservative hydrological tracer and analyzed by ionic chromatography (Compact IC-761, Methrom). Nitrate (NO_3^-) was analyzed by the cadmium reduction method (Keeney and Nelson, 1982) using a Technicon autoanalyzer (Technicon, 1976). Ammonium (NH_4^+) was manually analyzed via the salicylate–nitroprusside method (Baethgen and Alley, 1989) using a spectrophotometer (PharmaSpec UV-1700 SHIMADZU). Soluble reactive phosphorus (SRP) was manually analyzed via the acidic molybdate method (Murphy and Riley, 1962) using a spectrophotometer (PharmaSpec UV-1700 SHIMADZU).

3.2 Data analysis

The seasonality of biological activity can strongly affect both riparian groundwater chemistry and in-stream biogeochemical processes (Groffman et al., 1992; Hill et al., 2001). Therefore, the data set was separated into two groups based on sampling dates during the vegetative and dormant period (seven and four sampling dates, respectively). As a reference, we considered the vegetative period starting at the beginning of riparian leaf-out (April) and ending at the peak of leaf-litter fall (October), coinciding with the onset and offset of riparian tree evapotranspiration, respectively (Nadal-Sala et al., 2013). During the study period, rainfall was similar between the vegetative and dormant period (775 and 876 mm, respectively).

3.2.1 Patterns of stream discharge, riparian groundwater inputs, and stream solute concentrations

For each period, we examined the longitudinal pattern of stream discharge, riparian groundwater inputs, and stream solute concentrations along the reach. On each sampling date, we calculated area-specific stream discharge by dividing instantaneous discharge by catchment area (Q', in $mm\,d^{-1}$) at each sampling site. We used Q' rather than Q to be able to compare water fluxes from the 15 nested catchments along the reach. We examined the longitudinal patterns of Q' and stream solute concentration (C_{sw}) by applying regression models (linear, exponential, potential, and logarithmic). Model selection was performed by ordinary least squares (Zar, 2010). We referred only to the best-fit model in each case.

The contribution of net riparian groundwater inputs to surface water along each stream segment (Q_{gw}) was estimated as the difference in Q between consecutive sampling sites (Covino et al., 2010). The empirical uncertainty associated with Q was used to calculate a lower and upper limit of Q_{gw}. We considered that Q_{gw} was representative of the net riparian groundwater flux draining to the stream within each stream segment. We acknowledge that this approach oversimplifies the complex hydrological interactions at the riparian–stream interface because it does not consider concurrent hydrological gains and losses within each segment (Payn et al., 2009), but we consider that it provides a representative estimate at the scale of this study. To investigate the longitudinal pattern of riparian groundwater inputs, we calculated the cumulative area-specific net riparian groundwater input ($\Sigma Q'_{gw}$, in

mm d^{-1}) by summing up Q_{gw} from the upstream-most site to each of the downstream segments and dividing it by the cumulative catchment area.

For each sampling date, we examined whether the 3.7 km reach was either net gaining or net losing water by comparing concurrent gross hydrological gains and losses over the entire reach (Payn et al., 2009). For this spatial scale, we considered that stream segments exhibiting $Q_{gw} > 0$ contributed to gross hydrological gains ($\Sigma Q_{gw} > 0$), while segments with $Q_{gw} < 0$ contributed to gross hydrological losses ($\Sigma Q_{gw} < 0$). Note that gross riparian groundwater fluxes divided by the total catchment area are equal to $\Sigma Q'_{gw}$ at the downstream-most site. For each sampling date, we calculated the relative contribution of different water sources to stream discharge at the downstream-most site (Q_{bot}), with Q_{top} / Q_{bot}, ΣQ_{ef} / Q_{bot}, and ΣQ_{gw} / Q_{bot} for upstream, tributaries and riparian groundwater, respectively.

3.2.2 Sources of variation in stream nutrient concentration along the reach riparian groundwater inputs

We investigated whether longitudinal patterns in stream solute concentration were driven by riparian groundwater inputs by comparing solute concentrations between stream water and riparian groundwater with a Wilcoxon paired rank sum test. A non-parametric test was used because solute concentrations were not normally distributed (Shapiro–Wilk test, $p < 0.01$ for all study solutes) (Zar, 2010).

Moreover, we examined the degree of hydrological interaction at the riparian–stream interface by exploring the relationship between stream and riparian groundwater Cl^- concentrations with a Spearman correlation. For each period, we quantified the difference between Cl^- concentrations in the two water bodies by calculating divergences from the 1 : 1 line with the relative root-mean-square error (RRMSE, in %):

$$\mathrm{RRMSE} = \frac{\sqrt{\sum_{i=1}^{n}\left(C_{sw} - C_{gw}\right)^2}}{n \times \overline{C_{gw}}} \times 100, \quad (1)$$

where C_{sw} and C_{gw} are stream and riparian groundwater solute concentrations, respectively, n is the total number of observations, and $\overline{C_{gw}}$ is the average of C_{gw}. A strong correlation and a low RRMSE between stream and riparian groundwater Cl^- concentrations indicate a strong hydrological connection between the two water bodies. Similarly, we examined the correlation between stream and riparian groundwater nutrient concentrations. We expected a weak correlation and a high RRMSE value between nutrient concentrations measured at the two water bodies if the stream has a high nutrient processing capacity and in-stream gross uptake and release do not counterbalance each other.

In-stream nutrient processing. We investigated the influence of in-stream biogeochemical processes on the longitudinal pattern of stream nutrient concentrations by applying a mass balance approach for each individual segment (Roberts and Mulholland, 2007). For each nutrient, we calculated changes in stream flux between contiguous sampling sites (F_{sw}, in µg m^{-1} s^{-1}), with F_{sw} being the net flux resulting from in-stream gross uptake and release along a particular stream segment (von Schiller et al., 2011). We expressed F_{sw} by unit of stream length in order to compare net changes in stream flux between segments differing in length. For each sampling date and for each nutrient, F_{sw} was approximated with

$$F_{sw} = (F_{top} + F_{ef} + F_{gw} - F_{bot})/x, \quad (2)$$

where F_{top} and F_{bot} are the nutrient flux at the top and at the bottom of each stream segment, F_{gw} is the nutrient flux from net riparian groundwater inputs, and F_{ef} is the nutrient flux from tributary inputs for those reaches including a tributary (all in µg s^{-1}) (Fig. 3). F_{top} and F_{bot} were calculated by multiplying Q by C_{sw} at the top and at the bottom of the segment, respectively. F_{gw} was estimated by multiplying net groundwater inputs (Q_{gw}) by nutrient concentration in either riparian groundwater or stream water. For net gaining segments ($Q_{gw} > 0$), we assumed that the chemistry of net water inputs was similar to that measured in riparian

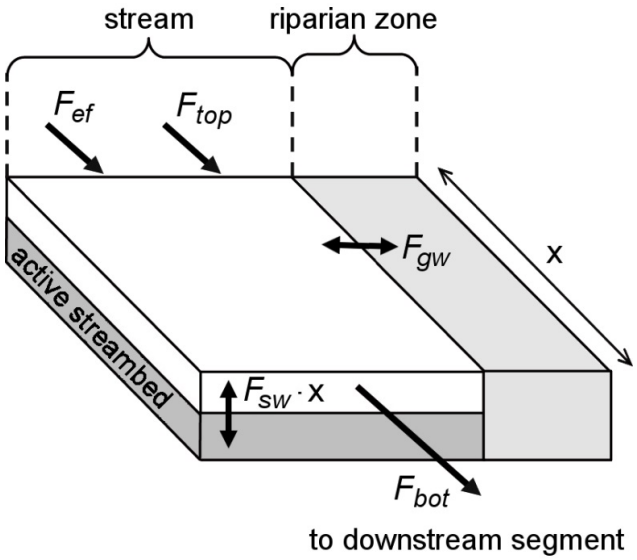

Figure 3. Conceptual representation of nutrient fluxes considered to estimate in-stream net nutrient uptake for each stream segment ($F_{sw} \times x$, Eq. 2). For each segment of length x, the considered nutrient input fluxes were upstream (F_{top}) and tributaries (F_{ef}). Nutrient fluxes exiting the stream segment (F_{bot}) were F_{top} for the contiguous downstream segment. Riparian groundwater nutrient fluxes could either enter ($F_{gw} > 0$) or exit ($F_{gw} < 0$) the stream. Nutrient fluxes for each component were estimated by multiplying its water flux (Q) by its nutrient concentration (C). In-stream net nutrient uptake ($F_{sw} \times x$) is the result of gross nutrient uptake and release by the active streambed. $F_{sw} \times x$ can be positive (gross uptake > release), negative (gross uptake < release), or zero (gross uptake ∼ release). See text for details.

groundwater, and thus C_{gw} was the average between riparian groundwater nutrient concentration at the top and bottom of the reach. For net losing segments ($Q_{gw} < 0$), we assumed that the chemistry of net water losses was similar to that measured in stream water and thus, C_{gw} averaged stream water concentration at the top and at the bottom of each reach segment (C_{top} and C_{bot}, respectively). For those cases in which stream segments received water from a tributary, F_{ef} was calculated by multiplying Q and C at the outlet of the tributary. We calculated an upper and lower limit of F_{sw} based on the empirical uncertainty associated with water fluxes (Q and Q_{gw}). Finally, x (in m) is the length of the segment between two consecutive sampling sites. The same approach was applied for Cl^-, a conservative tracer that was used as a hydrological reference. For Cl^-, we expected $F_{sw} \sim 0$ if inputs from upstream, tributaries, and riparian groundwater account for most of the stream Cl^- flux. For nutrients, F_{sw} can be positive (gross uptake > release), negative (gross uptake < release), or zero (gross uptake ∼ release). Therefore, we expected $F_{sw} \neq 0$ if in-stream gross uptake and release processes do not fully counterbalance each other (von Schiller et al., 2011). To investigate whether stream segments were consistently acting as net sinks or net sources of nutrients along the stream during the study period, we calculated the frequency of $F_{sw} > 0$, $F_{sw} < 0$, and $F_{sw} = 0$ for each nutrient and for each segment. We assumed that F_{sw} was undistinguishable from 0 when its upper and lower limit contained zero.

Since in-stream nutrient cycling can substantially vary with reach length (Meyer and Likens, 1979; Ensign and Doyle, 2006), we also calculated F_{sw} for the whole 3.7 km reach by including all hydrological input and output fluxes (solute fluxes from the upstream-most site, tributaries, and riparian groundwater gross gains and losses) in a mass balance at the whole-reach scale. For the two spatial scales (segment and whole reach), we examined whether F_{sw} differed among nutrients with a Mann–Whitney test.

3.2.3 Relative contribution of riparian groundwater and in-stream nutrient processing to stream nutrient fluxes

To assess the relevance of F_{sw} compared to input solute fluxes, we calculated the ratio between $F_{sw} \times x$ (absolute value) and the total input flux (F_{in}) for each solute and sampling date. For the two spatial scales (segment and whole reach), F_{in} was the sum of upstream (F_{top}), tributaries (F_{ef}), and net riparian groundwater inputs (F_{gw}). The latter was included when $Q_{gw} > 0$. We interpreted a high $|F_{sw} \times x / F_{in}|$ ratio as a strong potential of in-stream processes to modify input fluxes (either as a consequence of gross uptake or release). For each spatial scale, we explored whether $|F_{sw} \times x / F_{in}|$ differed among nutrients with a Mann–Whitney test.

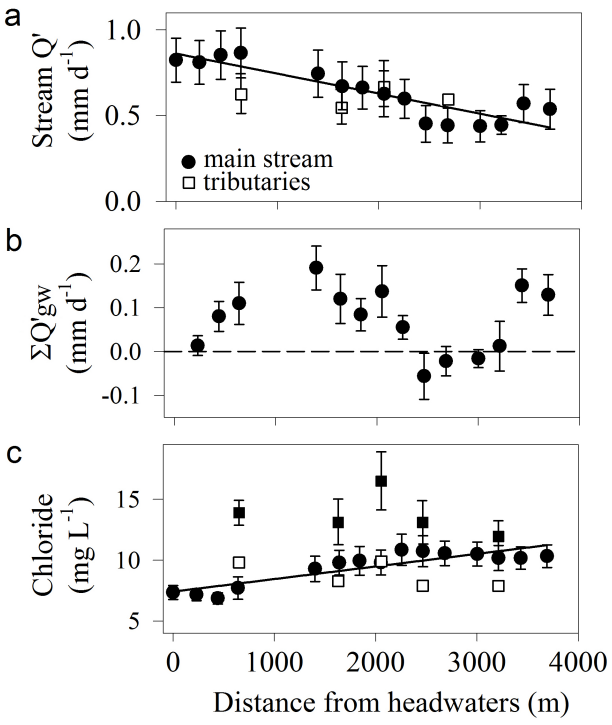

Figure 4. Longitudinal pattern of **(a)** area-specific stream discharge, **(b)** cumulative area-specific net groundwater inputs along the reach, and **(c)** stream chloride concentration. Symbols are average and standard error (whiskers) for the main stream (circles) and tributaries (squares). Stream chloride concentration in tributaries is shown separately for the dormant (white) and vegetative (black) period. Tributaries showed no differences in discharge between the two periods. Model regressions are indicated with a solid line only when significant (tributaries not included in the model).

We used a whole-reach mass balance approach to assess the relative contribution of net riparian groundwater inputs $\left(\left(F_{gw} > 0\right)/F_{in}\right)$ to stream solute fluxes. In addition, we calculated the contribution of upstream (F_{top}/F_{in}) and tributary inputs (F_{ef}/F_{in}) to stream solute fluxes. For each solute, we analyzed differences in the relative contribution of different sources to stream input fluxes with a Mann–Whitney test. Finally, when the whole reach was acting as a net sink for a particular nutrient ($F_{sw} > 0$), we calculated the relative contribution of in-stream net uptake to reduce stream nutrient fluxes along the 3.7 km reach with $F_{sw} \times x / F_{in}$.

4 Results

4.1 Hydrological characterization of the stream reach

During the study period, mean Q' decreased from 0.82 ± 0.13 [mean ± SE] to 0.54 ± 0.11 mm d^{-1} along the reach (linear regression [l.reg], $r^2 = 0.79$, degrees of freedom [df] = 14, $F = 51.4$, $p < 0.0001$) (Fig. 4a). This pat-

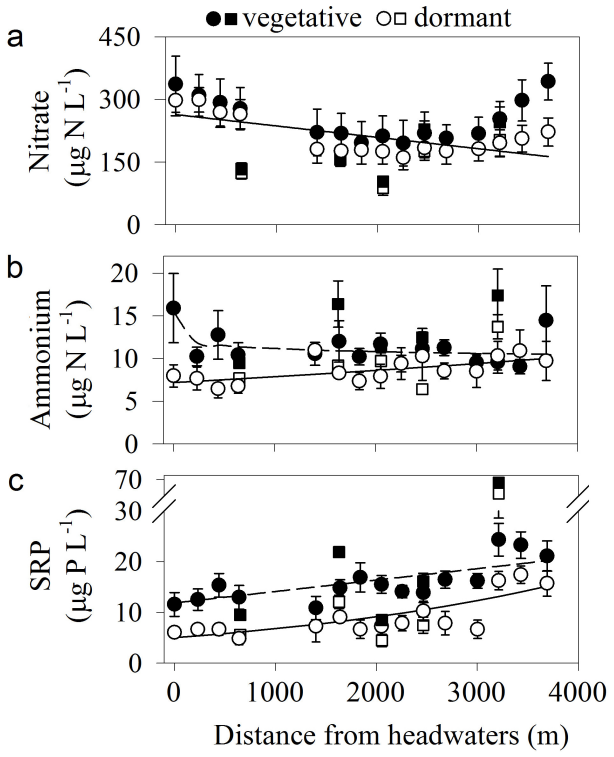

Figure 5. Longitudinal pattern of stream nutrient concentrations for **(a)** nitrate, **(b)** ammonium, and **(c)** solute reactive phosphorus at Font del Regàs. Symbols are average and standard error (whiskers) for the main stream (circles) and tributaries (squares). Lines indicate significant longitudinal trends for the dormant (solid) and vegetative (dashed) period (tributaries not included in the model).

tern hold for the two seasonal periods considered (dormant and vegetative; Wilcoxon rank sum test, $p > 0.05$).

On average, the stream had net water gain along the 3.7 km reach, though the hydrological interaction between the riparian zone and the stream was highly variable across contiguous segments (Fig. 4b). The stream was consistently gaining water along the first 1.5 km and the last 0.5 km, while hydrological losses were evident along the intermediate 2 km (Fig. 4b). At the whole-reach scale, gross hydrological gains exceed gross losses in 8 out of 10 field dates (Fig. 2c and d). This was especially noticeable in April and December 2011, the two sampling dates most influenced by storm events. In contrast, the whole reach was acting as net hydrological losing in March and October 2011.

Stream Cl^- concentrations showed a 40 % increase along the reach (l.reg, $r^2 = 0.88$, $df = 14$, $F = 44.6$, $p < 0.0001$), which contrasted with the longitudinal pattern exhibited by stream discharge (Fig. 4c). The two periods showed a similar longitudinal pattern, though stream Cl^- concentration was lower during the dormant than during the vegetative period (Wilcoxon rank sum test, $Z = -6.4$, $p < 0.0001$) (Table 1). The same seasonal pattern was exhibited by the five permanent tributaries (Fig. 4c). There was a strong correlation between stream and riparian groundwater Cl^- concentrations, which fitted well to the 1 : 1 line (low RRMSE for the two periods) (Table 2 and Fig. S2).

The median net change in Cl^- flux within individual segments was $6\,\mu g\,m^{-1}\,s^{-1}$, which represented a small fraction of the Cl^- input flux ($|F_{sw} \times x / F_{in}| = 3\,\%$). Similar results were obtained when calculating Cl^- budgets for the whole-reach approach (Table 3). The stream Cl^- flux was mainly explained by inputs from tributaries followed by riparian groundwater and upstream. Similar results were obtained when calculating the relative contribution of different water sources to stream discharge at the whole-reach scale (Table 4).

4.2 Longitudinal pattern of stream nutrient concentration

The longitudinal pattern of stream concentration differed between nutrients and periods. During the dormant period, stream NO_3^- concentration decreased along the reach especially within the first 1.5 km (l.reg, $r^2 = 0.47$, $df = 15$, $F = 11.4$, $p < 0.005$) (Fig. 5a). During the vegetative period, stream NO_3^- concentration showed a U-shaped pattern: it decreased along the first 1.5 km, remained constant along the following 1 km, and increased by 60 % along the last kilometer of the reach (Fig. 5a). Despite these differences, stream NO_3^- concentration was similar between the dormant and vegetative period for both the main stream and tributaries (Wilcoxon rank sum test: $p > 0.05$ in al cases) (Table 1).

Stream NH_4^+ concentration showed an increasing longitudinal pattern during the dormant period (exponential regression [e.reg], $r^2 = 0.45$, $df = 15$, $F = 10.5$, $p < 0.01$), while concentration decreased during the vegetative period (logarithmic regression [lg.reg], $r^2 = 0.42$, $df = 15$, $F = 9.6$, $p < 0.01$) (Fig. 5b). The main stream showed higher NH_4^+ concentration during the vegetative than during the dormant period (Wilcoxon rank sum test, $Z = -3.5$, $p < 0.001$) (Table 1). For the tributaries, NH_4^+ concentration was similar between the two periods (Wilcoxon rank sum test: $p > 0.01$ in all cases).

Stream SRP concentration increased along the reach during both the dormant (e.reg, $r^2 = 0.59$, $F = 18.5$, $df = 14$, $p < 0.01$) and vegetative period (l.reg, $r^2 = 0.49$, $F = 12.4$, $df = 14$, $p < 0.01$) (Fig. 5c). Similar to NH_4^+, the main stream showed higher SRP concentration during the vegetative than during the dormant period (Wilcoxon rank sum test, $Z = -6.6$, $p < 0.001$) (Table 1). For the tributaries, SRP concentration was similar between the two periods (Wilcoxon rank sum test: $p > 0.01$ in all cases).

4.3 Sources of variation in stream nutrient concentration

Riparian groundwater inputs. The relationship between stream and riparian groundwater concentrations differed be-

Table 1. Median and interquartile range [25th, 75th percentiles] of stream and riparian groundwater solute concentrations for the dormant and vegetative period. The number of cases is shown in parentheses for each group. For each variable, the asterisk indicates statistically significant differences between the two water bodies (Wilcoxon paired rank sum test, * $p < 0.01$).

		Stream	Riparian groundwater
Dormant	Cl^- (mg L^{-1})	7.6 [6.5, 8] (60)	7.7 [7.2, 8.8] (57)*
	$N\text{-}NO_3^-$ (µg L^{-1})	192 [159, 262] (60)	194 [109, 298] (56)
	$N\text{-}NH_4^+$ (µg L^{-1})	8.9 [6.5, 10.3] (60)	19 [13.8, 34.2] (56)*
	SRP (µg L^{-1})	7.6 [4.5, 11.7] (60)	8 [6, 20] (51)
	DO (mg L^{-1})	12.9 [11.5, 16] (60)	3.5 [1.5, 4.6] (54)*
Vegetative	Cl^- (mg L^{-1})	8.8 [7.9, 13.5] (100)	10.1 [8.6, 15] (98)*
	$N\text{-}NO_3^-$ (µg L^{-1})	223 [155, 282] (102)	168 [77, 264] (98)*
	$N\text{-}NH_4^+$ (µg L^{-1})	10 [8.7, 12.8] (103)	27 [18.2, 37.1] (101)*
	SRP (µg L^{-1})	16.5 [11.7, 21.3] (103)	14.1 [9.3, 23.3] (97)
	DO (mg L^{-1})	9.9 [9.1, 11.1] (84)	1.7 [0.8, 2.5] (98)*

Table 2. Spearman ρ coefficient between stream water and riparian groundwater solute concentrations for each period and for the whole data set collected at the Font del Regàs during the study period. The relative root-mean-square error (RRMSE) indicates divergences from the 1 : 1 line. n = number of cases. * $p < 0.01$. ns: not significant.

	Dormant			Vegetative			All data		
	ρ	RRMSE (%)	n	ρ	RRMSE (%)	n	ρ	RRMSE (%)	n
Cl^-	0.78*	2.1	53	0.8*	2.9	98	0.84*	2.8	151
$N\text{-}NO_3^-$	0.48*	8.1	57	0.34*	8.3	101	0.37*	6	158
$N\text{-}NH_4^+$	ns	11.7	57	ns	9.1	101	ns	7.3	158
SRP	ns	17.9	57	0.43*	5.5	101	0.41*	7.3	158

Table 3. Median and interquartile range [25th, 75th percentile] of in-stream net nutrient uptake flux (F_{sw}) and the potential of F_{sw} to modify solute input fluxes ($|F_{sw} \times x/F_{in}|$) for the two spatial scales considered (stream segment and whole reach) during the study period. $n = 150$ and 10 for segments and whole-reach data sets, respectively.

		By segment	By whole reach
F_{sw} (µg m^{-1} s^{-1})	Cl^-	6 [−37, 80]	12 [2, 33]
	$N\text{-}NO_3^-$	−0.43 [−4.4, 1.3]	−0.97 [−3.4, 1.6]
	$N\text{-}NH_4^+$	0.17 [−0.06, 0.63]	0.2 [−0.02, 1.1]
	SRP	0 [−0.6, 0.21]	−0.06 [−0.21, 0.01]
$\lvert F_{sw} \times x/F_{in} \rvert$ (%)	Cl^-	3 [1, 10]	4 [2, 9]
	$N\text{-}NO_3^-$	6 [2, 14]	24 [8, 67]
	$N\text{-}NH_4^+$	18 [9.5, 35]	48 [25, 71]
	SRP	20.5 [3.4, 41]	15.5 [6, 66]

tween nutrients and periods. During the dormant period, stream and riparian groundwater NO_3^- concentrations were similar, while the stream showed higher concentration during the vegetative period (Table 1). During the two periods, stream and riparian groundwater NO_3^- concentrations were positively correlated and showed relatively small RRMSE (Table 2 and Fig. S2). NH_4^+ concentration in stream water was 2–3 times lower than in riparian groundwater (Table 1), and stream and groundwater concentrations were no correlated either during the dormant or vegetative periods (Table 2). Stream and riparian groundwater SRP concentrations were similar in the two periods (Table 1). During the dormant period, SRP concentration showed a significant correlation between the two water bodies, while no correlation and relatively high RRMSE occurred during the vegetative period (Table 2). The differences in nutrient concentrations between stream and riparian groundwater in the two study periods were accompanied by consistently higher DO concentrations in the stream than in riparian groundwater (Table 1).

In-stream nutrient processing. The influence of in-stream nutrient processing on stream water chemistry differed among nutrients. During the study period, median F_{sw} was negative for NO_3^-, positive for NH_4^+, and close to 0 for SRP (Table 3). However, between-nutrient differences in F_{sw} were not statistically significant for either the vegetative or dormant period (for both periods: Mann–Whitney test with post hoc Tukey test, $p > 0.05$). Similar F_{sw} values were obtained when calculating nutrient budgets either by segment or whole reach (Table 3).

The frequency of an individual segment to act either as a nutrient sink or source differed among nutrients and along the reach. For NO_3^-, the frequency of $F_{sw,NO_3} < 0$ (gross uptake < release) increased from 9 to > 50 % along

Table 4. Median and interquartile range [25th, 75th percentile] of the relative contribution of inputs from upstream (F_{top}/F_{in}), net riparian groundwater ($(F_{gw} > 0)/F_{in}$), tributaries (F_{ef}/F_{in}), and in-stream release ($(F_{sw} < 0)/F_{in}$) to stream solute fluxes at the whole-reach scale. Note that relative contributions from different sources do not add up to 100 % because they are medians rather than means. For each solute, different letters indicate statistically significant differences between sources (Mann–Whitney test with post hoc Tukey test, $p < 0.01$). $n = 10$ for the four solutes.

Relative contribution (%)	Cl^-	$N\text{-}NO_3^-$	$N\text{-}NH_4^+$	SRP
Upstream	15 [12, 17]^{B}	22 [20, 35]^{A}	8 [6, 13]^{BC}	11 [6, 17]^{B}
Riparian groundwater	28 [14, 38]^{B}	17 [5, 47]^{A}	63 [43, 75]^{A}	21 [7, 38]^{AB}
Tributaries	59 [46, 69]^{A}	22 [19, 24]^{A}	21 [17, 30]^{B}	34 [26, 50]^{A}
In-stream release	0 [0, 0.3]^{C}	22 [0, 50]^{A}	0 [0, 6]^{C}	19 [0, 55]^{B}

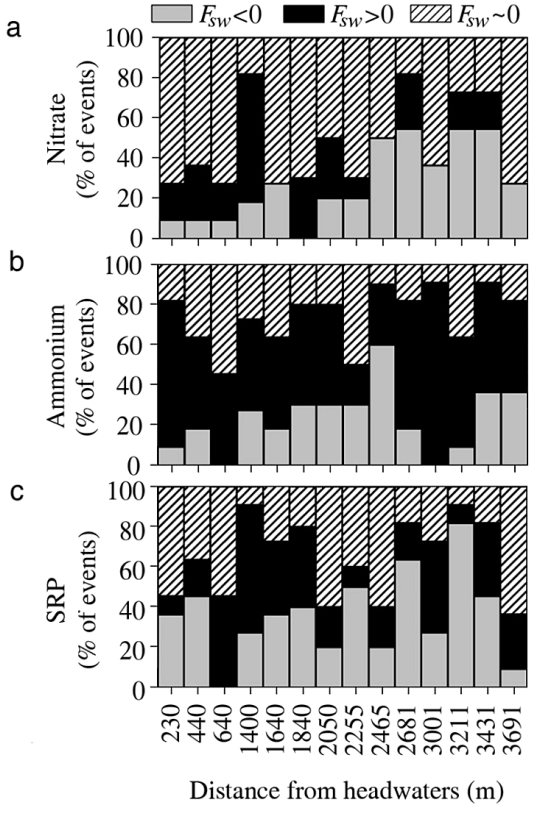

Figure 6. Frequency of dates for which $F_{sw} < 0$ (gross uptake < release), $F_{sw} > 0$ (gross uptake > release), and $F_{sw} \sim 0$ (gross uptake ∼ release) for **(a)** nitrate, **(b)** ammonium, and **(c)** soluble reactive phosphorus for the 14 contiguous segments along the study reach from August 2010 to December 2011 ($n = 11$). The frequency is expressed as number of events in relative terms.

the reach (l.reg, $r^2 = 0.55$, $df = 13$, $F = 14.67$, $p < 0.01$) (Fig. 6a). For NH_4^+, the frequency of $F_{sw,\,NH_4} > 0$ (gross uptake > release) was high across individual segments, ranging from 20 to 90 % (Fig. 6b). For SRP, the frequency of $F_{sw,\,SRP} < 0$, > 0, or ~ 0 did not show any consistent longitudinal pattern (Fig. 6c). Overall, the frequency of sampling dates for which in-stream biogeochemical processes were imbalanced ($F_{sw} \neq 0$) was lower for NO_3^- (36 %) than for NH_4^+ (80 %) and SRP (68 %) (Fig. 6).

4.4 Relative contribution of riparian groundwater and in-stream processing to stream nutrient fluxes at the segment and whole-reach scale

The capacity of in-stream processes to modify stream input fluxes differed between nutrients and spatial scales. For individual segments, $|F_{sw} \times x/F_{in}|$ was smaller for NO_3^- (6 %) than for NH_4^+ and SRP (∼ 20 %) (Mann–Whitney test with post hoc Tukey test, $p < 0.01$, Table 3). However, $|F_{sw} \times x/F_{in}|$ increased substantially for NO_3^- and NH_4^+ when nutrient budgets were calculated at the whole-reach scale (Table 3).

According to whole-reach mass balance calculations, the stream acted as a net source of NO_3^- on 7 out of the 10 sampling dates for which whole-reach budgets were calculated. The contribution of in-stream release to stream NO_3^- fluxes was as important as that of riparian groundwater and upstream fluxes (Table 4). In-stream net NO_3^- retention at the whole-reach scale was observed only in spring (March and April 2011) and December 2011 (Fig. 7a).

In contrast to NO_3^-, the stream generally acted as a net sink of NH_4^+, and it retained up to 90 % of the input fluxes in spring and autumn (Fig. 7b). The stream acted as a source of NH_4^+ in summer (Fig. 7b), though the contribution of in-stream release to stream NH_4^+ fluxes was minimal compared to that from riparian groundwater (Table 4).

The stream acted as a net source of SRP in 6 out of the 10 sampling dates. The contribution of in-stream release to stream SRP fluxes was as important as that of riparian groundwater (Table 4). In-stream net SRP retention was minimal, except in autumn 2011 (October and December 2011) (Fig. 7c).

5 Discussion

In terms of hydrology, the study headwater stream was a net gaining reach, though the hydrological interaction between the riparian zone and the stream was complex as in-

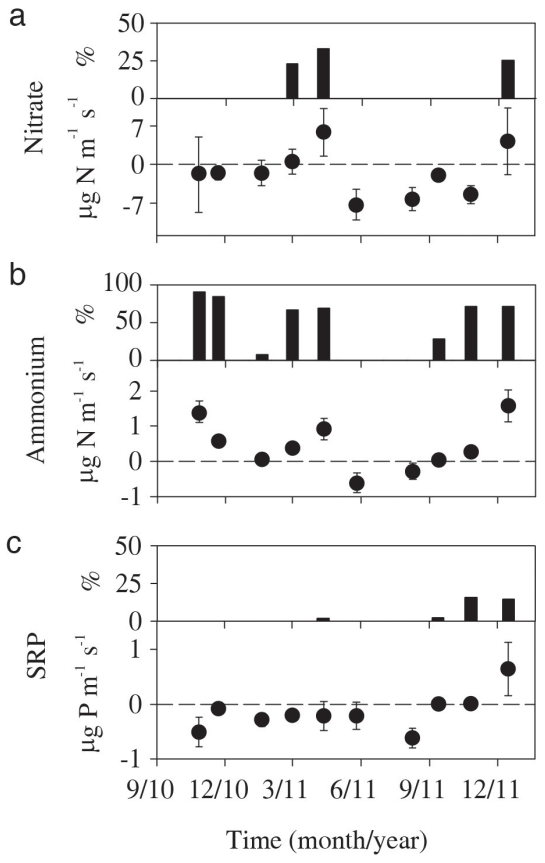

Figure 7. Temporal pattern of in-stream net nutrient uptake (F_{sw}, in $\mu g\,m^{-1}\,s^{-1}$) for **(a)** nitrate, **(b)** ammonium, and **(c)** soluble reactive phosphorus at the whole-reach scale. Whiskers are the uncertainty associated with the estimation of stream discharge from slug tracer additions. $F_{sw} > 0$ indicates that gross uptake prevailed over release, while $F_{sw} < 0$ indicates the opposite. For those cases for which $F_{sw} > 0$, the contribution of in-stream net nutrient uptake to reduce stream nutrient fluxes ($F_{sw} \times x/F_{in}$, in %) is shown (black bars).

dicated by the longitudinal variation in net riparian groundwater inputs. Moreover, the longitudinal decrease in area-specific discharge suggests that hydrological retention increased at the valley bottom compared to upstream segments as reported in previous studies (Covino et al., 2010). Despite the complex hydrological processes along the reach, the strong positive correlation between stream and riparian groundwater Cl^- concentration suggests high hydrological connectivity at the riparian–stream interface (Butturini et al., 2003). In addition, we found that the permanent tributaries, which comprised ~ 50 % of the catchment area, contributed 56 % of stream discharge, and thus were an essential component for understanding stream nutrient chemistry and loads. Hydrological mixing of stream water with water from tributaries could partially explain the longitudinal increase in Cl^- because its concentration was higher at the tributaries than at the main stream, especially during the vegetative period. In addition, riparian groundwater inputs to the stream could further contribute to the longitudinal increase in stream Cl^- concentration because they contributed 26 % of stream discharge and also exhibited higher Cl^- concentration than stream water.

Based on the strong hydrological connectivity between the stream and the riparian groundwater and the large contribution of tributaries to stream discharge, one would expect a strong influence of these water sources on the longitudinal variation in stream nutrient chemistry. However, the relationship between stream and riparian groundwater nutrient concentration was from moderate to weak for NO_3^- and SRP, and zero for NH_4^+. Further, the contribution of tributaries to stream nutrient fluxes was relatively small (from 21 to 34 %) compared to their contribution to stream Cl^- and water fluxes (> 50 %). Together these data suggest that longitudinal patterns of stream nutrient concentration could not be explained by hydrological mixing alone, thus pointing to in-stream biogeochemical processing as a likely mechanism to modify nutrient concentrations along the study reach. In fact, the estimates of in-stream net nutrient uptake (F_{sw}) at the different stream segments supported this idea and agreed with previous studies showing that in-stream processes can mediate stream nutrient chemistry and downstream nutrient export (McClain et al., 2003; Harms and Grimm, 2008).

Our results revealed an extremely high variability in F_{sw}, which could range by up to one order of magnitude, across individual segments and over time, which agrees with findings from other headwater streams (von Schiller et al., 2011). However, some general trends appeared when comparing patterns for the different studied nutrients. For instance, the frequency of dates for which in-stream gross uptake and release were imbalanced ($F_{sw} \neq 0$) was higher for NH_4^+ (80 %) and SRP (68 %) than for NO_3^- (37 %). Further, the potential of in-stream processes to modify stream fluxes within stream segments ($|F_{sw} \times x/F_{in}|$) was 3-fold higher for NH_4^+ and SRP than for NO_3^-. Our findings are concordant with studies performed at short stream reaches (< 300 m) worldwide, which show that in-stream gross uptake velocity (as a proxy of nutrient demand) is typically higher for NH_4^+ and SRP than for NO_3^- (Ensign and Doyle, 2006). This difference among nutrients is commonly attributed to the higher biological demand for NH_4^+ and SRP than for NO_3^-. However, we found that F_{sw} was similar among nutrients; thus, differences in $|F_{sw} \times x/F_{in}|$ were mainly associated with differences in the concentration of the inputs, which tend to be 20-fold lower for NH_4^+ and SRP than for NO_3^-. Divergences between F_{sw} and $|F_{sw} \times x/F_{in}|$ were even more remarkable when nutrient budgets were considered at the whole-reach scale, especially for DIN forms. NO_3^- and NH_4^+ showed no differences in F_{sw} between the two scales of observation; however, they showed a substantial increase in $|F_{sw} \times x/F_{in}|$ at the whole-reach scale (length of kilometers) compared to the segment scale (length of hundreds of meters). Similarly, previous nutrient

spiraling studies have reported an increase in the proportion of nutrient removal with stream order despite no changes in gross uptake rates among stream reaches (Ensign and Doyle, 2006; Wollheim et al., 2006). This pattern has been attributed to variation in intrinsic stream characteristics, such as stream nutrient concentration, discharge, stream width, and the size of the hyporheic zone (Wollheim et al., 2006; Alexander et al., 2009), which may also hold for our study since these characteristics varied along the 3.7 km reach. However, our results also indicate that the assessment of riparian groundwater inputs is crucial to understand the contribution of in-stream processes to stream nutrient fluxes. Overall, our findings add to the growing evidence that streams are hot spots of nutrient processing (Peterson et al., 2001; Dent et al., 2007), and that in-stream processes can substantially modify stream nutrient fluxes at the catchment scale (Ensign and Doyle, 2006; Bernal et al., 2012).

The potential of in-stream processes to regulate stream nutrient fluxes was especially remarkable for NH_4^+. There was no relationship between stream and riparian groundwater NH_4^+ concentrations; further, whole-reach budgets indicated that in-stream net uptake could reduce the flux of NH_4^+ up to 90 % along the reach. This high in-stream bioreactive capacity could be favored by the sharp increase in redox conditions from riparian groundwater to stream water (Hill et al., 1998; Dent et al., 2007). Concordantly, NH_4^+ concentrations were higher in riparian groundwater than in the stream, while the opposite occurred for NO_3^- (although only during the vegetative period). These results suggest fast nitrification of groundwater inputs within the stream as environmental conditions become well oxygenated (Jones et al., 1995). However, the marked increase in stream NO_3^- concentration observed along the last 700 m of the reach during the vegetative period could not be explained entirely by nitrification of riparian groundwater NH_4^+ because this flux ($F_{\mathrm{gw,\,NH_4}} \sim 2$ µg N m^{-1} s^{-1}) was not large enough to sustain in-stream NO_3^- release ($|F_{\mathrm{sw,\,NO_3}} < 0|$ (~ 10 µg N m^{-1} s^{-1}). This finding suggests an additional source of N at the valley bottom. Previous studies have shown that leaf litter from riparian trees, and especially from N_2-fixing species, can enhance in-stream nutrient cycling because of its high quality and degradability (Starry et al., 2005; Mineau et al., 2011). Thus, the increase in NO_3^- and SRP concentrations and in-stream NO_3^- release observed at the lowest part of the catchment during the vegetative period could result from the combination of warmer temperatures and the mineralization of large stocks of alder and black locust leaf litter stored in the stream bed (Strauss and Lamberti, 2000; Bernhardt et al., 2002; Starry et al., 2005). Alternatively, increases in stream NO_3^- and SRP concentration could result from human activities, which were concentrated at the lowest part of the catchment. However, regarding NO_3^-, anthropogenic sources seem unlikely because DIN concentrations at the tributary draining through the inhabited area were low. In contrast, this tributary showed high SRP concentrations (from 2- to 6-fold higher than in the main stream), though its discharge would have had to be ca. 4 times higher than expected for its drainage area (< 0.4 km^2) to explain the observed changes in concentration. Another possible explanation for the increase in stream N concentration at the valley bottom could be increased N fixation by stream algae (Finlay et al., 2011). However, in-stream DIN release (NO_3^- and NH_4^+) peaked in late spring and summer (May and August 2011), when light penetration was limited by riparian canopy and in-stream photoautotrophic activity was low (Lupon et al., 2015). Altogether, these data suggest that the sharp increase in nutrient availability along the last 700 m of the reach was likely related to the massive presence of the invasive black locust at the valley bottom. Black locust is becoming widespread throughout riparian floodplains in the Iberian Peninsula (Castro-Díez et al., 2014), and its potential to subsidize N to stream ecosystems via root exudates and leaf litter could dramatically alter in-stream nutrient processing and downstream nutrient export (e.g., Stock et al., 1995; Mineau et al., 2011). However, further research is needed to test the hypothesis that this invasive species can alter stream nutrient dynamics in riparian floodplains.

It is worth noting that longitudinal trends in stream nutrient concentrations showed no simple relationship to in-stream processes. This finding evidenced that other sources of variation in stream water chemistry were counterbalancing the influence of in-stream processes on stream nutrient fluxes. In this sense, results from NH_4^+ were paradigmatic. The mass balance approach clearly showed that in-stream gross uptake of NH_4^+ exceeded release; concordantly, NH_4^+ concentration was consistently lower in the stream than in riparian groundwater. However, stream NH_4^+ concentration showed small longitudinal variation likely because in-stream net uptake balanced the elevated inputs from riparian groundwater. Therefore, our results challenge the idea that stream nutrient concentration should decrease in the downstream direction when in-stream processes are efficient in taking up nutrients from receiving waters (Brookshire et al., 2009). Conversely, our findings convincingly show that in-stream processes can strongly affect stream nutrient chemistry and downstream nutrient export even in the absence of consistent longitudinal gradients in nutrient concentration. For NO_3^-, our data suggest that the marked increase in concentration along the last 700 m could be a consequence of in-stream mineralization of N-rich leaf-litter stocks. However, the observed decrease in NO_3^- concentration along the first 1.5 km of the reach could barely be explained by in-stream processing alone because its contribution to reduce stream NO_3^- fluxes was too low, even when the whole-reach budget was recalculated excluding the last 700 m of the reach ($F_{\mathrm{sw}} = 0.61$ µg N m^{-1} s^{-1} and $(F_{\mathrm{sw}} > 0)/F_{\mathrm{in}} = 10$ %). Therefore, the declining pattern was likely a combination of both in-stream nutrient processing and hydrological mixing with riparian groundwater and tributary inputs. For SRP, the longitudinal increase in concentration could neither be fully ex-

plained by in-stream release because $F_{sw,\,SRP} < 0$ was not widespread along the reach and the stream only contributed to input fluxes by 19 % (6 % when excluding the last 700 m). Again, stream nutrient chemistry along the reach was the combination of both in-stream nutrient processing and hydrological mixing as indicated by our whole-reach mass balance. Recent studies have concluded that riparian groundwater is a major driver of longitudinal patterns in stream nutrient concentration in headwater streams (Bernhardt et al., 2002; Asano et al., 2009; Scanlon et al., 2010). Our study adds to our knowledge of catchment biogeochemistry by showing that stream nutrient chemistry results from the combination of both hydrological mixing from the riparian zone and in-stream nutrient processing, which can play a pivotal role in shaping stream nutrient concentrations and fluxes at the catchment scale.

6 Conclusions

The synoptic approach adopted in this study highlighted that the Font del Regàs stream had a strong potential to transform nutrients. The longitudinal pattern in stream nutrient concentrations could not be explained solely by hydrological mixing with riparian groundwater and tributary sources because dissolved nutrients underwent biogeochemical transformation while traveling along the stream channel. Our results revealed that in-stream processes were highly variable over time and space, though in most cases this variability could not be associated with either physical longitudinal gradients or shifts in environmental conditions between the dormant and vegetative period. Nevertheless, results from a mass balance approach showed that in-stream processes contributed substantially to modify stream nutrient fluxes and that the stream could act either as a net nutrient sink (for NH_4^+) or as a net nutrient source (for SRP and NO_3^-) at the catchment scale. These results add to the growing evidence that in-stream biogeochemical processes need to be taken into consideration in either empirical or modeling approaches if we are to understand drivers of stream nutrient chemistry within catchments.

Recent studies have proposed that riparian groundwater is a major control of longitudinal patterns of nutrient concentration because in-stream gross nutrient uptake and release tend to counterbalance each other most of the time (Brookshire et al., 2009; Scanlon et al., 2010). Conversely, our study showed that in-stream processes can influence stream nutrient chemistry and downstream exports without generating longitudinal gradients in concentration and flux because changes in stream nutrient chemistry are the combination of both in-stream processing and nutrient inputs from terrestrial sources. Our results imply that the assessment of these two sources of variation in stream nutrient chemistry is crucial to understand the contribution of in-stream processes to stream nutrient dynamics at relevant ecological scales.

Reliable measurements of riparian groundwater inputs are difficult to obtain because spatial variability can be high (Lewis et al., 2006) and determination of the chemical signature of the groundwater that really enters the stream is still a great challenge (Brookshire et al., 2009). In this study, we installed 15 piezometers along the reach (one per sampling site), which may not be representative enough of the variation in riparian groundwater chemistry. However, and despite its limitations, riparian groundwater sampling near the stream can help to constrain the uncertainty associated with this water source and provide more reliable estimations of in-stream net nutrient uptake for both nutrient mass balance and spiraling empirical approaches (von Schiller et al., 2011).

The Supplement related to this article is available online at doi:10.5194/bg-12-1941-2015-supplement.

Author contributions. S. Bernal, F. Sabater, and E. Martí designed the experiment. S. Bernal, A. Lupon, M. Ribot, and F. Sabater carried it out. A. Lupon performed all laboratory analysis. S. Bernal analyzed the data set and prepared the manuscript with contributions from A. Lupon, M. Ribot, and E. Martí.

Acknowledgements. We are grateful to the three anonymous reviewers for their helpful comments on an earlier version of the manuscript, and in particular to one of them for their constructive and meaningful suggestions. We thank A. Oltra for assisting with GIS, and S. Poblador, E. Martín, and C. Romero for field assistance. S. Bernal and A. Lupon were funded by the Spanish Ministry of Economy and Competitiveness (MINECO) with a Juan de la Cierva contract (JCI-2010-06397) and an FPU grant (AP-2009-3711). S. Bernal received additional funds from the Spanish Research Council (CSIC) (JAEDOC027) and the MICECO-funded project MED_FORESTREAM (CGL2011-30590). M. Ribot was funded through a technical training contract from the MINECO-funded project ISONEF (CGL2008-05504-C02-02/BOS) and MED_FORESTREAM. Additional financial support was provided by the European Union-funded project REFRESH (FP7-ENV-2009-1-244121) and the MINECO-funded project MONTES-Consolider (CSD 2008-00040). The Vichy Catalan Company, the Regàs family, and the Catalan Water Agency (ACA) graciously gave us access to the Font del Regàs catchment.

Edited by: T. J. Battin

References

Alexander, R. B., Böhlke, J. K., Boyer, E. W., David, M. B., Harvey, J. W., Mulholland, P. J., Seitzinger, S. P., Tobias, C. R., Tonitto, C., and Wollheim, W. M.:Dynamic modeling of nitrogen losses in river networks unravels the coupled effects of hydrological and biogeochemical processes, Biogeochemistry, 93, 91–116, 2009.

Asano, Y., Uchida, T. M., Mimasu, Y., and Ohte, N.: Spatial patterns of stream solute concentrations in a steep mountainous catchment with a homogeneous landscape, Water Resour. Res., 45, W10432, doi:10.1029/2008WR007466, 2009.

Àvila, A. and Rodà, F.: Changes in atmospheric deposition and streamwater chemistry over 25 years in undisturbed catchments in a Mediterranean mountain environment, Sci. Total Environ., 434, 18–27, 2012.

Baethgen, W. and Alley, M.: A manual volorimetric procedure for ammonium nitrogen in soil and plant Kjeldahl Digests, Commun. Soil Sci. Plan., 20, 961–969, 1989.

Bernal, S. and Sabater, F. Changes in stream discharge and solute dynamics between hillslope and valley-bottom intermittent streams, Hydrol. Earth Syst. Sci., 16, 1595–1605, 2012, http://www.hydrol-earth-syst-sci.net/16/1595/2012/.

Bernal, S., von Schiller, D., Martí, E., and Sabater, F.: In-stream net uptake regulates inorganic nitrogen export from catchment under base flow conditions, J. Geophys. Res., 117, G00N05, doi:10.1029/2012JG001985, 2012.

Bernhardt, E. S., Hall, R. O., and Likens, G. E.: Whole-system estimates of nitrification and nitrate uptake in streams of the Hubbard Brook experimental forest, Ecosystems, 5, 419–430, 2002.

Bernhardt, E. S., Likens, G. E., Buso, D. C., and Driscoll, C. T.: In-stream uptake dampens effects of major forest disturbance on watershed nitrogen export, P. Natl. Acad. Sci. USA, 100, 10304–10308, 2003.

Bohlen, P. J., Groffman, P. M., Driscoll, C. T., Fahey, T. J., and Siccama, T. G.: Plant-soil-microbial interactions in a northern hardwood forest, Ecology, 82, 965–978, 2001.

Bormann, F. H. and Likens, G. E.: Nutrient cycling, Science, 155, 424-429, 1967.

Brookshire, E. N. J., Valett, H. M., and Gerber, S. G.: Maintenance of terrestrial nutrient loss signatures during in-stream transport, Ecology, 90, 293–299, 2009.

Butturini, A., Bernal, S., Nin, E., Hellín, C., Rivero, L., Sabater, S., and Sabater, F.: Influences of stream groundwater hydrology on nitrate concentration in unsaturated riparian area bounded by an intermittent Mediterranean stream, Water Resour. Res., 39, 1110, doi:10.1029/2001WR001260, 2003.

Castro-Díez, P., Valle, G., González-Muñoz, N., and Alonso, A.: Can the life-history strategy explain the success of the exotic trees *Ailanthus altissima* and *Robinia pseudoacacia* in Iberian floodplain forests?, PLOS One, 9, 1–12, doi:10.1371/journal.pone.0100254, 2014.

Compton, J. E., Robbin Church, M., Larned S. T., and Hogsett, W. E.: Nitrogen export from forested watershed in the Oregon Coast Range: the role of N_2-fixing red alder, Ecosystems, 6, 773–785, 2003.

Covino, T. P. and McGlynn, B. L.: Stream gains and losses across a mountain-to-valley transition: impacts on watershed hydrology and stream water chemistry, Water Resour. Res., 43, W10431, doi:10.1029/2006WR005544, 2007.

Covino, T. P., McGlynn, B. L., and Baker, M.: Separating physical and biological nutrient retention and quantifying uptake kinetics from ambient to saturation in successive mountain stream reaches, J. Geophys. Res., 115, G04010, doi:10.1029/2009/JG001263, 2010.

Dent, C. L. and Grimm, N. B.: Spatial heterogeneity of stream water nutrient concentrations over successional time, Ecology, 80, 2283–2298, 1999.

Dent, C. L., Grimm, N. B. Martí, E., Edmonds, J. W., Henry, J. C., and Welter, J. R.: Variability in surface-subsurface hydrologic interactions and implications for nutrient retention in an arid-land stream, J. Geophys. Res., 112, G04004, doi:10.1029/2007JG000467, 2007.

Ensign, S. H. and Doyle, M. W.: Nutrient spiraling in streams and river networks,. J. Geophys. Res., 111, G04009, doi:10.1029/2005JG00114, 2006.

Finlay, J. C., Hood, J. M., Limm, M. P., Power, M. E., Schade, J. D., and Welter, J. R.: Light-mediated thresholds in stream-water nutrient composition in a river network, Ecology, 92, 140–150, 2011.

Gordon N. D., McMahon T. A., Finlayson B. L., Gippel, C. J., and Nathan, R. J.: Stream hydrology: an introduction for ecologists, Wiley, West Sussex, UK, 2004.

Groffman, P. M., Gold, A. J., and Simmons, R. C.: Nitrate dynamics in riparian forests: microbial studies, J. Environ. Qual., 21, 666–671, 1992.

Harms, T. K. and Grimm, N. B.: Hot spots and hot moments of carbon and nitrogen dynamics in a semiarid riparian zone, J. Geophys. Res., 113, G01020, doi:10.1029/2007JG000588, 2008.

Hedin, L. O., von Fisher, J. C., Ostrom, N. E., Kennedy, B. P., Brown, M. G., and Robertson, G. P.: Thermodynamic constraints on nitrogen transformations and other biogeochemical processes at soil-stream interfaces, Ecology, 79, 684–703, 1998.

Helfield, J. M. and Naiman, R. J.: Salmon and alder as nitrogen sources to riparian forests in a boreal Alaskan watershed, Oecologia, 133, 573–582, 2002.

Hill, A. R., Labadia, C. F., and Sanmugadas, K.: Hyporheic zone hydrology and nitrogen dynamics in relation to the streambed topography of a N-rich stream, Biogeochemistry, 42, 285–310, 1998.

Hill, W. R., Mulholland, P. J., and Marzolf, E. R.: Stream ecosystem response to forest leaf emergence in spring, Ecology, 82, 2306–2319, 2001.

Houlton, B. Z., Driscoll, C. T., Fahey, T. J., Likens, G. E., Groffman, P. M., Bernhardt, E. S., and Buso, D. C.: Nitrogen dynamics in ice-storm-damaged forest ecosystems: implications for nitrogen limitation theory, Ecosystems, 6, 431–443, 2003.

Institut Cartografic de Catalunya (ICC): Orthophotomap of Catalunya 1 : 25 000, Generalitat de Catalunya. Departament de Política Territorial i Obres, 2010.

Jencso, K. G., McGlynn, B. L., Gooseff, M. N., Bencala, K. E., and Wondzell, S. M.: Hillslope hydrologic connectivity controls riparian groundwater turnover: implications of catchment structure for riparian buffering and stream water sources, Water Resour. Res., 46, W10524, doi:10.1029/2009WR008818, 2010.

Johnson, C. E., Driscoll, C. T., Siccama, T. G., and Likens, G. E.: Element fluxes and landscape position in a northern hardwood forest watershed ecosystem, Ecosystems, 3, 159–184, 2000.

Jones Jr., J. B., Fisher, S. G., and Grimm, N. B.: Nitrification in the hyporheic zone of a desert stream ecosystem, J. North Am. Benthological Soc., 14, 249–258, 1995.

Keeney D. R. and Nelson D. W.: Nitrogen-inorganic forms. Methods of soil analysis, Part 2, in: Agronomy Monography 9, ASA and SSSA. Madison, WI, 643–698, 1982.

Lawrence, G. B., Lovett, G. M., and Baevsky, Y. H.: Atmospheric deposition and watershed nitrogen export along an elevational gradient in the Castkills Mountains, New York, Biogeochemistry, 50, 21–43, 2000.

Lewis, D. B., Schade, J. D., Huth, A. K., and Grimm, N. B. The spatial structure of variability in a semi-arid, fluvial ecosystem, Ecosystems, 9, 386–397, 2006.

Likens, G. E. and Buso, D. C.: Variation in streamwater chemistry throughout the Hubbard Brook Valley, Biogeochemistry, 78, 1–30, doi:10.1007/s10533-005-2024-2, 2006.

Lowrance, R., Altier, L. S., Newbold, J. D., Schnabel, R. R., Groffman, P. M., Denver, J. M., Correl. D. L., Gilliam, J. W., Robinson, J. L., Brinsfield, R. B., Staver, K. W., Locas, W., and Todd, A. H. Water quality functions of riparian forest buffers in Chesapeake Bay watersheds, Environ. Manag., 21, 687–712, 1997.

Lupon, A., Martí, E., Sabater, F., and Bernal, S. Green light: gross primary production influences seasonal stream N export by controlling fine-scale N dynamics, Ecology, in review, 2015.

Martí, E., Fisher, S. G., Schade, J. D., and Grimm, N. B.: Flood-frequency and stream-riparian linkages in arid lands, in: Streams and ground waters, edietd by: Jones, J. B. and Mulholland, P. J., Academic Press, London, UK, 111–136, 2000.

Mayer, P. M., Reynolds Jr., S. K., McCutchen, M. D., and Canfield, T. J.: Meta-Analysis of nitrogen removal in riparian buffers, J. Environ. Qual., 36, 1172–1180, 2007.

McClain, M. E., Boyer, E. W., Dent, C. L., Gergel, S. E., Grimm, N. B., Groffman, P. M., Hart, S. C., Harvey, J. W., Johnston, C. A., Mayorga, E., McDowell, W. H., and Pinay, G.: Biogeochemical hot spots and hot moments at the interface of terrestrial and aquatic ecosystems, Ecosystems, 6, 301–312, 2003.

Meyer, J. L. and Likens, G. E.: Transport and transformation of phosphorus in a forest stream ecosystem, Ecology, 60, 1255–1269, 1979.

Mineau, M. M., Baxter, C. V., and Marcarelli, A. M.: A non-native riparian tree (*Elaeagnus angustifolia*) changes nutrient dynamics in streams, Ecosystems, 14, 353–365, 2011.

Morrice, J. A., Valett, H. M., Dahm, C. N., and Campana, M. E.: Alluvial characteristics, groundwater-surface water exchange and hydrological retention in headwaters streams, Hydrol. Process., 11, 253–267, 1997.

Murphy, J. and Riley, J. P.: A modified single solution method for determination of phosphate in natural waters, Anal. Chim. Acta, 27, 31–36, 1962.

Nadal-Sala, D, Sabaté, S., Sánchez-Costa, E., Boumghar, A., and Gracia, C. A.: Different responses to water availability and evaporative demand of four co-occurring riparian tree species in N Iberian Peninsula. Temporal and spatial sap flow patterns, Acta Hortic, 991, 215–222, 2013.

Payn, R. A., Gooseff, M. N., McGlynn, B. L., Bencala, K. E., and Wondzell, S. M.: Channel water balance and exchange with subsurface flow along a mountain headwater stream in Montana, United States, Water Resour. Res., 45, W11427, doi:10.1029/2008WR007644, 2009.

Peterson, B. J., Wollheim, W. M., Mulholland, P. J., Webster J. R., Meyer, J. L., Tank, J. L., Martí, E., Bowden, W. B., Valett, H. M., Hershey, A. E., McDowell, W. H., Dodds, W. K., Hamilton, S. K., Gregory, S., and Morrall, D. D. Control of nitrogen export from watersheds by headwater streams, Science, 292, 86–90, 2001.

Roberts, B. J. and Mulholland, P. J.: In-stream biotic control on nutrient biogeochemistry in a forested stream, West Fork of Walker Branch, J. Geophys. Res., 112, G04002, doi:10.1029/2007JG000422, 2007.

Ross, D. S., Shanley, J. B., Campbell, J. L., Lawrence, G. B., Bailey, S. W., Likens, G. E., Wemple, B. C., Fredriksen, G., and Jamison, A. E.: Spatial patterns of soil nitrification and nitrate export from forested headwaters in the northeastern United States, J. Geophys. Res., 117, G01009, doi:10.1029/2011JG001740, 2012.

Sabater, S., Butturini, A., Clement, J. C., Burt, T., Dowrick, D., Hefting, M., Maître, V., Pinay, G., Postolache, C., Rzepecki, M., and Sabater, F.: Nitrogen removal by riparian buffers along a European climatic gradient: patterns and factors of variation, Ecosystems, 6, 20–30, 2003.

Scanlon, T. M., Ingram, S. P., and Riscassi, A. L.: Terrestrial and in-stream influences on the spatial variability of nitrate in a forested headwater catchment, J. Geophys. Res., 115, G02022, doi:10.1029/2009JG001091, 2010.

Starry, O. S., Valett, H. M., and Schreiber, M. E.: Nitrification rates in a headwater stream: influences of seasonal variation in C and N supply, J. North Am. Benthological Soc., 24, 753–768, 2005.

Stock, W. D., Wienand, K. T., and Baer, A. C.: Impacts of invading N_2-fixing acacia species on patterns of nutrient cycling in two Cape ecosystems: evidence from soil incubation studies and ^{15}N natural abundance values, Oecologia, 101, 375–382, 1995.

Strauss, E. A. and Lamberti, G. A.: Regulation of nitrification in aquatic sediments by organic carbon, Limnol. Oceanogr., 45, 1854–1859, 2000.

Technicon: Technicon Instrument System, in: Technicon Method Guide, Technicon, ed.Tarrytown, New York, 1976.

Uehlinger, U. Resistance and resilience of ecosystem metabolism in a flood-prone river system, Freshwater Biol., 45, 319–332, 2000.

Valett, H. M., Morrice, J. A., Dahm, C. N., and Campana, M. E.: Parent lithology, surface-groundwater exchange and nitrate retention in headwater streams, Limnol. Oceanogr., 41, 333–345, 1996.

Vidon, P. and Hill, A. R.: Landscape controls in nitrate removal in stream riparian zones, Water Resour. Res., 40, W03201, doi:10.1029/2003WR002473, 2004.

Vidon, P. G. F., Craig, A., Burns, D., Duval, T. P., Gurwick, N., Inamdar, S., Lowrance, R., Okay, J., Scott, D., and Sebestyen, S.: Hot spots and hot moments in riparian zones: potential for improved water quality management, J. Am. Water Resour. Assoc., 46, 278–298, 2010.

von Schiller, D., Bernal, S., and Martí, E.: Technical Note: A comparison of two empirical approaches to estimate in-stream net nutrient uptake, Biogeosciences, 8, 875–882, doi:10.5194/bg-8-875-2011, 2011.

von Schiller, D., Bernal, S., Sabater, S., and Martí, E.: A round-trip ticket: the importance of release processes for in-stream nutrient spiraling, Freshwater Sci., 34, 20–30, doi:10.1086/679015, 2015.

Wollheim, W. M., Vörösmarty, C. J., Peterson, B. J., Seitzinger, S. P., and Hopkinson, C. S.: Relationship between river size and nutrient removal, Geophys. Res. Lett., 33, L06410, doi:10.1029/2006GL025845, 2006.

Zar, J. H.: Biostatistical analysis. Prentice-Hall/Pearson, 5th Edn., Upper Saddle River, NJ, 2010.

Dear Mrs. Lupon,

I am pleased to learn that your paper "Green light: gross primary production influences seasonal stream N export by controlling fine-scale N dynamics" (MS# 14-2296R3) has been accepted for publication in Ecology by a member of our Board of Editors. Congratulations!

Included with this email are three attachments:

- Publication Agreement
- Author Billing Information Form
- Financial Arrangements for Publication

Publication Agreement

Before the paper is published, we will need to complete the attached Publication Agreement. **All** authors are required to sign the agreement.

It is acceptable to provide emailed (digital) signatures by creating PDF scans of signed forms. To accomplish this, you are welcome to forward the attached Publication Agreement form to your co-authors (if any).

Each co-author should print that form, add their signature, and scan the document, creating a digital version of the signed form to return to you.

After receiving signed copies from each co-author, the completed forms must be submitted in a single transmission (whether by hard copy or digitally in PDF format) to the ESA Business Office to facilitate handling.

Electronic copies should be attached to a single email message, not sent separately in succession. Whenever possible, all signature pages should be combined into a single PDF.

Author Billing Information

At this time we also need to resolve financial arrangements for publication. ESA policies on page charges and other publication costs are outlined in the attached sheet, "Financial Arrangements for Publication."

Please complete the attached Author Billing Information Form and submit it with the executed

Publication Agreement.

Send the completed Publication Agreement and Author Billing Information Forms, either via hard copy or electronic copy, to the ESA Business Office in Washington DC:

Postal mail:
ATTN: Author Agreements
Business Office
The Ecological Society of America
1990 M Street NW, Suite 700
Washington, DC 20036

Email:
agreements@esa.org

If you have any billing questions or wish to further discuss financial matters, please contact the ESA Business Office by phone (202-833-8773) or email (agreements@esa.org).

Any other questions regarding the publication process should continue to be addressed to the ESA Publications Office (esa_journals@cornell.edu).

Sincerely,

Regina Przygocki
Interim Associate Manager
Ecological Society of America